PRESSURIZED WATER REACTOR OWNERS GROUP

PWROG-15109-NP-A
Revision 0

WESTINGHOUSE NON-PROPRIETARY CLASS 3

PWR Pressure Vessel Nozzle Appendix G Evaluation

Materials Committee

PA-MSC-1091, Revision 5

January 2020

Westinghouse framatome

PWROG-15109-NP-A, Revision 0

PWR Pressure Vessel Nozzle Appendix G Evaluation

PA-MSC-1091, Revision 5

January 2020

J. Brian Hall*
Churchill Laboratory Services

Verifier: **Justin Webb***
Structural Design & Analysis

Verifier: **Benjamin E. Mays***
License Renewal, Radiation Analysis & Nuclear Operations

Verifier: **Anees Udyawar***
Reactor Vessel / Containment Vessel Design & Analysis

Reviewer: **Jianwei Chen***
Nuclear Operations & Radiation Analysis

Approved: **James P. Molkenthin***,
Program Director, PWR Owners Group PMO

Approved: **David B. Love***
Manager, Churchill Laboratory Services

Approved: **Stephen P. Rigby***
Manager, Structural Design & Analysis

Approved: **Lynn A. Patterson***
Manager,
Reactor Vessel / Containment Vessel Design & Analysis

*Electronically approved records are authenticated in the electronic document management system

Westinghouse Electric Company LLC
1000 Westinghouse Drive
Cranberry Township, PA 16066, USA

CONTENTS

Cover Letter for the Final Safety Evaluation for the Topical Report PWROG-15109-NP, Revision 0, "PWR Pressure Vessel Nozzle Appendix G Evaluation," (EPID L-2018-TOP-0009), October 31, 2019 iv

Final Safety Evaluation by the Office of Nuclear Reactor Regulation for Pressurized Water Reactor Owners Group Topical Report PWROG-15109-NP, Revision 0, "PWR Pressure Vessel Nozzle Appendix G Evaluation," EPID L-2018-TOP-0009, October 2019 vii

PWR Owners Group Transmittal of PWROG-15109-NP, Revision 0, "PWR Pressure Vessel Nozzle Appendix G Evaluation," PA-MSC-1091R4, OG-18-55, March 5, 2018 xxviii

PWROG-15109-NP, Revision 0, "PWR Pressure Vessel Nozzle Appendix G Evaluation," PA-MSC-1091R4, February 2018 xxxii

PWR Owners Group Transmittal of the Response to Request for Additional Information, RAIs 1-6 Associated with PWROG-15109-NP, Revision 0, "PWR Pressure Vessel Nozzle Appendix G Evaluation," PA-MSC-1091, OG-19-65, March 2019 ..... A-2

Responses to the U.S. NRC Request for Additional Information on PWROG-15109-NP, "PWR Pressure Vessel Nozzle Appendix G Evaluation," RT-LTR-19-2, Rev. 0, March 2019 ..... A-4

UNITED STATES
NUCLEAR REGULATORY COMMISSION
WASHINGTON, D.C. 20555-0001

October 31, 2019

Mr. W. Anthony Nowinowski,
Executive Director
PWR Owners Group;
Program Management Office
Westinghouse Electric Company
1000 Westinghouse Drive, Suite 380
Cranberry Township, PA 16066

SUBJECT: FINAL SAFETY EVALUATION BY THE OFFICE OF NUCLEAR REACTOR REGULATION TOPICAL REPORT PWROG-15109-NP, REVISION 0, "PWR PRESSURE VESSEL NOZZLE APPENDIX G EVALUATION" (EPID: L-2018-TOP-0009)

Dear Mr. Nowinowski:

By letter dated March 5, 2018 (Agencywide Documents and Access Management System (ADAMS) Accession No. ML18067A228), the Pressurized Water Reactor (PWR) Owners Group (PWROG) submitted for U.S. Nuclear Regulatory Commission (NRC) review and approval Topical Report (TR) PWROG-15109-NP, Revision 0, "PWR Pressure Vessel Nozzle Appendix G Evaluation" (ADAMS Package Accession No. ML118067A229). By letter dated March 27, 2019, the PWROG submitted a supplement to PWROG-15109-NP, "Response to Requests for Additional Information, RAIs 1-6 Associated with on PWROG-15109-NP, Revision 0" (ADAMS Package Accession No. ML19091A089) and requested that the NRC prepare the final safety evaluation (SE) for PWROG-15109-NP against Revision 0.

The NRC staff has reviewed the TR and its supplemental information, and based on the evaluation in Section 4 of the enclosed SE, finds that the TR, as modified by the SE, provides an acceptable means for addressing the potential for pressure-temperature (P-T) limit curves for inlet or outlet nozzle corners of U.S. PWRs to be more limiting than the current NRC-approved P-T limits (as of the time of issuance of this SE) of the shell (and associated welds) in the traditional beltline region of the reactor pressure vessel Accordingly, the TR, as modified by the SE, is acceptable for referencing to satisfy the fracture toughness requirements in Appendix G to Title 10 of the *Code of Federal Regulations* Part 50 for U.S. PWR inlet and outlet nozzles only, which provide adequate margins of safety during any condition of normal operation, including anticipated operational occurrences and system hydrostatic tests, to which the pressure boundary may be subjected over its service lifetime. Applicants who utilize the TR will be required to adhere to the conditions that the NRC staff imposed in the SE and shall be subject to NRC staff review and approval on a case-by-case basis.

By letter dated June 25, 2019 (ADAMS Accession No. ML19158A266), the NRC staff provided the draft SE to the PWROG for review and comment. By letter dated August 22, 2019 (ADAMS Accession No. ML19239A119), the PWROG provided comments on the draft SE. In accordance with the guidance provided on the NRC website, we request that the PWROG publish approved versions of PWROG-15109-NP, Revision 0 within 3 months of receipt of this letter. The approved version shall incorporate this letter and the enclosed final SE after the title

page. Also, the approved versions must contain historical review information, including NRC requests for additional information (RAIs) and the responses. The approved versions shall include an "-A" (designating approved) following the TR identification symbol. As an alternative to including the request for RAIs and RAI responses behind the title page, if changes to the TR were provided to the NRC staff to support the resolution of RAI responses, and if the NRC staff reviewed and approved those changes as described in the RAI responses, there are two ways that the accepted version can capture the RAIs:

1. The RAIs and RAI responses can be included as an Appendix to the accepted version.
2. The RAIs and RAI responses can be captured in the form of a table (inserted after the final SE) which summarizes the changes as shown in the approved version of the TR. The table should reference the specific RAIs and RAI responses which resulted in any changes, as shown in the accepted version of the TR.

If future changes to the NRC's regulatory requirements affect the acceptability of these TRs, PWROG will be expected to revise the TRs appropriately or justify their continued applicability for subsequent referencing. Licensees referencing these TRs would be expected to justify their continued applicability or evaluate their plant using the revised TRs.

If you have any questions, please contact Leslie Fields at 301-415-1186.

Sincerely,

Dennis C. Morey, Chief
Licensing Processes Branch
Division of Operating Reactor Licensing
Office of Nuclear Reactor Regulation

Docket No. 99902037

Enclosure:
Final SE (Nonproprietary)

W. Nowinowski - 3 -

SUBJECT: FINAL SAFETY EVALUATION BY THE OFFICE OF NUCLEAR REACTOR REGULATION TOPICAL REPORT PWROG-15109-NP, REVISION 0, "PWR PRESSURE VESSEL NOZZLE APPENDIX G EVALUATION" (EPID L-2018-TOP-0009) DATED OCTOBER 31, 2019

DISTRIBUTION:

PUBLIC	DMorey, NRR	LFields, NRR
RidsResOd	RidsOgcMailCenter	RidsACRS_MailCTR
RidsNrrDorl	RidsNrrDorlLlpb	RidsNrrDnrlNvib
RidsNrrLADHarrison	DDijamco, NRR	HGonzalez, NRR
OYee, NRR		

ADAMS Accession Nos.
ML19301D191 (Package)
ML19301D063 (Cover Letter)
ML19301D160 (Enclosure)

OFFICE	NRR/DORL/LLPB/PM	NRR/DORL/LLPB/LA	NRR/DNLR/NVIB/BC	NRR/DORL/LLPB/BC
NAME	LFields	DHarrison	HGonzalez	DMorey
DATE	10/29/19	10/31/19	10/31/19	10/31/19

OFFICIAL RECORD COPY

UNITED STATES
NUCLEAR REGULATORY COMMISSION
WASHINGTON, D.C. 20555-0001

FINAL SAFETY EVALUATION

BY THE OFFICE OF NUCLEAR REACTOR REGULATION

FOR PRESSURIZED WATER REACTOR OWNERS GROUP TOPICAL REPORT

PWROG-15109-NP, REVISION 0,

"PWR PRESSURE VESSEL NOZZLE APPENDIX G EVALUATION"

EPID L-2018-TOP-0009

1.0 INTRODUCTION

By letter dated March 5, 2018 (Agencywide Documents Access and Management System (ADAMS) Accession No. ML18067A228), as supplemented by letter dated March 27, 2019 (ADAMS Accession No. ML19091A089), the Pressurized Water Reactor (PWR) Owners Group (PWROG) submitted to the U.S. Nuclear Regulatory Commission (NRC) topical report (TR) PWROG-15109-NP, Revision 0, "PWR Pressure Vessel Nozzle Appendix G Evaluation," (ADAMS Accession No. ML18067A229) for review and approval.

The TR addresses the potential for pressure-temperature (P-T) limit curves (or P-T limits) for inlet or outlet nozzle corners of pressurized water reactors (PWRs) to be more limiting than those of the shell (and associated welds) of the "traditional" beltline region of the reactor pressure vessel (RPV) and closure flange regions. The PWROG developed the TR to demonstrate that the RPV nozzle corner P-T limits are bounded by the NRC-approved P-T limits of the shell (and associated welds) in the RPV traditional beltline region for a 60-year license for U.S. PWRs. Specifically, the TR presented generic PWR fracture mechanics analyses of RPV inlet and outlet nozzle corners to show that P-T limits for nozzles corners, developed in accordance with the requirements of Appendix G, "Fracture Toughness Requirements," to Title 10 of the *Code of Federal Regulations* (10 CFR) Part 50, are bounded by the P-T limits of the shell (and associated welds) in the RPV traditional beltline region.

2.0 REGULATORY EVALUATION

The NRC has established requirements in 10 CFR Part 50 to protect the integrity of the reactor coolant pressure boundary in nuclear power plants. The NRC staff (the staff) evaluates the acceptability of a facility's proposed P-T limits based on the following NRC regulations and guidance:

- Section 50 60 of 10 CFR, "Acceptance criteria for fracture prevention measures for lightwater nuclear power reactors for normal operation," imposes fracture toughness and

Enclosure

material surveillance program requirements, which are set forth in 10 CFR Part 50, Appendices G and H, "Reactor Vessel Material Surveillance Program Requirements."

- Appendix G to 10 CFR Part 50 requires that a facility's P-T limits for the RPV be at least as conservative as those obtained by following the methods of analysis and the margins of safety in Appendix G to Section XI of the American Society of Mechanical Engineers *Boiler and Pressure Vessel Code* (ASME Code).

The most recent version of Appendix G to Section XI of the ASME Code which has been endorsed in 10 CFR 50.55a, and therefore by reference in 10 CFR Part 50, Appendix G, is the 2013 Edition of the ASME Code. Calculations of P-T limits are based, in part, on the nil-ductility reference temperature (RT_{NDT}) for the material, as specified in the ASME Code, Section XI, Appendix G. The RT_{NDT} is the critical parameter for determining the critical or reference stress intensity factor (fracture toughness, K_{IC}) for the material. As required by 10 CFR Part 50, Appendix G, RT_{NDT} values for materials in the RPV beltline region shall be adjusted to account for the effects of neutron irradiation. Regulatory Guide (RG) 1.99, Revision 2, "Radiation Embrittlement of Reactor Vessel Materials," contains methodologies for calculating the adjusted RT_{NDT} (ART) due to neutron irradiation.

Appendix G to 10 CFR Part 50 defines the beltline or beltline region of the reactor vessel as the region of the RPV (shell material including welds, heat affected zones, and plates or forgings) that directly surrounds the effective height of the active core and adjacent regions of the RPV that are predicted to experience sufficient neutron irradiation damage to be considered in the selection of the most limiting material with regard to radiation damage.

Determination of the P-T limits for a plant in accordance with the requirements of Appendix G to 10 CFR Part 50 considers several factors, which include the initial properties and chemical composition of the RPV materials, the accumulated neutron fluence for each material, the stress levels applied to the materials resulting from heatup and cooldown transients (which include internal pressure and thermal gradient loads), and structural discontinuities such as nozzles. Development of P-T limits for the beltline region of the RPV considers not only the RPV shell material but also other RPV materials with structural discontinuities such as nozzles.

3.0 SUMMARY OF THE TOPICAL REPORT

The TR is organized as follows:

Section 1, "Background" – provides a background of why nozzle corners must be considered in evaluations of P-T limits, a summary of the NRC-approved methodologies for development of P-T limits for Westinghouse Electric Company (Westinghouse), Combustion Engineering, Inc., and Babcock & Wilcox Company (B&W) PWR designs, a summary of reports that inform nozzle corner analyses, and a summary of low-temperature overpressure protection.

Section 2, "Flaw Size" – describes the basis for postulating a smaller than quarter-thickness (1/4T) flaw and describes the small flaw size models postulated in the inlet and outlet nozzles.

Section 3, "Fracture Toughness" – provides details of the determination of generic nozzle fracture toughness using the master curve approach and generic embrittlement trend curve.

Section 4, "Stress Intensity Factor Calculation" – provides details of the determining stress intensity factors (SIFs) using the finite element method for the small flaw size models in Section 2 of the TR.

Section 5, "Pressure-Temperature Limit Curves" – describes determination of the P-T limits for nozzle corners with a small flaw (using information from Sections 3 and 4 of the TR) and 1/4T beltline size flaw; compares P-T limits for nozzles corners with those from NRC-approved P-T limits for shell (and associated welds) in the RPV beltline region and for the closure flange regions.

Section 6, "Conclusion" – concludes that the generic P-T limits for nozzles corners developed in the TR in accordance with the requirements of Appendix G to 10 CFR Part 50 are bounded by the P-T limits of the shell (and associated welds) in the RPV beltline region and closure flange regions in the U.S. PWR fleet.

4.0 TECHNICAL EVALUATION

The staff reviewed the TR to determine whether the PWROG's evaluation to demonstrate the P-T limits of shell (and associated welds) in the RPV traditional beltline region bound those of inlet and outlet nozzle corners is acceptable. The staff also reviewed the TR to determine that the technical bases are consistent with the requirements of 10 CFR 50.60.

The staff evaluated eleven major topics of the TR. Each topic is addressed in the subsections of the safety evaluation (SE) that follow. Within each major topic, the staff summarized the relevant content of a subsection of the TR or described the relevant information in the subsection that falls under each major topic. Then the staff provided its findings or determinations on the TR subsection or on the major topic.

4.1 Postulated Flaw Size

In Section 2 of the TR, the PWROG explained that a traditionally postulated 1/4T flaw in the nozzle corner region can result in a depth of approximately 4 to 5 inches as measured at a 45-degree angle from the nozzle corner to the RPV outside surface since the nozzle and RPV are thicker in the vicinity of nozzles per the ASME Code design requirements. Crack driving forces for a postulated 1/4T flaw could lead to overly conservative P-T limits. Therefore, the PWROG opted to postulate smaller flaws as allowed in the 2008 edition of the ASME Code, Section XI, Appendix G, Subarticle G-2120, "Maximum Postulated Defect," which states that flaws less than 1/4T may be used on an individual case basis if a smaller size of maximum postulated defect can be ensured. Additionally, the 2008 edition of the ASME Code, Section XI, Appendix G, Paragraph G-2223(a), "Toughness Requirements for Nozzles," states that examination methods "shall be sufficiently reliable and sensitive to detect these smaller defects." The PWROG created finite element models (FEMs) with a small postulated flaw in the nozzle corner (the flaw penetrates 0.5 inch into the low alloy steel (LAS) from the clad-to-LAS interface) to determine SIFs since closed-form SIF solutions for nozzle corners are typically for 1/4T flaws. Additionally, the PWROG created FEMs with a postulated flaw that penetrates 0.05 inch into the LAS to address the effect of the difference in coefficient of thermal expansion (CTE) between the clad and the LAS.

The PWROG showed a probability of detection (POD) plot for vessels that indicates a POD of 100 percent for a 0.5-inch flaw into the LAS and stated that crack growth analyses have been performed for postulated flaws smaller than 0.5 inch based on their high POD. Although a similar POD for nozzle corners does not exist, the PWROG qualitatively concluded that the POD for nozzle corners would be high because pre-service examination through ultrasonic testing (UT) was performed from the inside surface and presented a conclusion by the Electric Power

Research Institute (EPRI) Nondestructive Examination Center that detecting flaws as small as 0.25 inch by UT located in RPV nozzles is excellent.

The staff reviewed the POD information for vessels in the TR, which the PWROG obtained from Performance Demonstration Initiative (PDI) data from UT performed in accordance with ASME Code, Section XI, Appendix VIII. The staff also reviewed the ASME Code, Section XI, examination requirements for nozzle corners, which requires nozzle corners to be examined by UT through PDI in accordance with ASME Code, Section XI, Appendix VIII. Accordingly, the staff determined that the PWROG's qualitative evaluation of high POD for nozzle corners to be reasonable. Thus, the staff determined that the postulated flaw size of 0.5 inch into the LAS meets the detectability criterion of Paragraph G-2223(a) of the 2013 edition of ASME Code, Section XI, which is the latest NRC-approved version of the ASME Code.

The staff noted that the ASME Code, Section XI, examination volume requirement for nozzle corners specifies a maximum depth of 0.5 inch into the LAS. Thus, the staff determined that the postulated flaw size of 0.5 inch into the LAS meets the required examination volume.

The staff noted that Paragraph G-2223(a) in the 2008 edition is different than in the 2013 edition. In addition to the detectability criterion described in Section 4.1 of this SE, Paragraph G-2223(a) of the 2013 edition states that the postulated smaller flaw must appropriately consider the combined effects of internal pressure, external loading, thermal stresses, and flaw shape, and the postulated smaller flaw shall be no smaller than the applicable inservice inspection criteria in Table IWB-3410-1 of ASME Code, Section XI. The staff reviewed Section 4.7, "Loads," of the TR and determined that the PWROG applied the appropriate loads and flaw shape (evaluated in Section 4.6 of this SE). The staff also reviewed the flaw size requirements in Table IWB-3410-1 of the ASME Code, Section XI, and determined that the flaw size of 0.5 inch into the LAS region that the PWROG postulated meets the requirements of the table. Based on this and the POD information the PWROG provided, the staff finds that a postulated flaw of 0.5 inch into the LAS is acceptable and meets the criteria of Subarticle G-2120 and Paragraph G-2223(a) of the 2013 edition of ASME Code, Section XI.

4.2 Fracture Toughness

Generic Nozzle Forging Master Curve Reference Temperature

In Section 3.1, "Generic Nozzle Forging Master Curve Reference Temperature" of the TR, the PWROG stated that the use of the lower bound plane-strain, static fracture toughness (K_{IC}) curve has inherent margin since RT_{NDT} is a conservative method for locating the K_{IC} curve. RT_{NDT} is based on drop weight testing, which is a crack arrest transition temperature measurement, and the Charpy impact test, which is a blunt notch impact test. These data are conservatively bounded by the K_{IC} curve, which is a lower bound crack initiation fracture toughness curve.

In contrast, the PWROG stated that the master curve method is based on an initiation transition temperature true fracture toughness test technique and the master curve index temperature (T_0) provides a much more accurate measure of the material fracture toughness. The PWROG explained that existing master curve fracture toughness data for A-508 Class 2 type forgings was gathered to establish a generic mean and standard deviation for alternate RT_{NDT} for the U.S. PWR inlet and outlet nozzles. Specifically, the master curve fracture toughness data is used with ASME Section XI Code Case N-629, "Use of Fracture Toughness Test Data to Establish Reference Temperature for Pressure Retaining Materials, Section XI, Division 1,"

which is endorsed by RG 1.147 and incorporated by reference in 10 CFR 50.55a as an alternative to RT_{NDT}.

The staff noted that the 2013 edition of ASME Code Section XI (i.e., the latest edition endorsed by 10 CFR 50.55a) permits the use of an alternate RT_{NDT}, which is consistent with Code Case N-629. Specifically, Subarticle G-2110 in the 2013 edition of ASME Code Section XI states, in part, that if material-specific temperature value, T_0, for ferritic steels in the transition range is available then a reference temperature, RT_{T0}, may be used in place of RT_{NDT}.

Since Code Case N-629 is incorporated by reference (e.g., RG 1.147) in 10 CFR 50.55a, and the use of RT_{T0} in lieu of RT_{NDT} is permitted by ASME Code Section XI, the staff finds the use of a fracture-toughness-based reference temperature, RT_{T0}, acceptable and that an exemption to Appendix G to 10 CFR Part 50 by the licensees is not required.

Master Curve Data Search

In Section 3.1.1, "Master Curve Data Search," of the TR, the PWROG described the approach it used for searching and gathering master curve data relevant to RPV nozzle forgings in U.S. PWRs. The PWROG explained that relevant data was gathered from open literature, the Electric Power Research Institute (EPRI) fracture toughness database, and internal Westinghouse references. Specifically, the PWROG considered thick sections of A-508 Class 2 or similar forgings that were used in RPV fabrication or are representative of the materials used to construct U.S. PWR inlet and outlet nozzles. The purpose was to capture all available transition temperature fracture toughness data to establish a generic master curve transition reference temperature for A-508 Class 2 type forgings. The PWROG explained in its supplement that "representative" means that the forging heats from which master curve data were obtained had material specifications similar to A-508 Class 2 forgings used in U.S. PWR inlet and outlet nozzles. Specifically, the staff noted that the PWROG's selection included alternate forging alloys—22NiMoCr37, 20NiMoCr26, and SFVQ2A (the staff's review regarding the applicability of these alternate forging alloys to U.S. PWR inlet and outlet nozzles is discussed below). The PWROG also stated that the meaning of "bounding" is explained in Section 3.1.2.2 of the TR. The staff noted that the master curve data is considered bounding because it included irradiated materials, fracture toughness data based on K_{IC}, one material with RT_{NDT} greater than 60°F, and a diversity of relevant forgings (as evidenced by the large standard deviation presented in Section 3.1.2.2 of the TR), all of which conservatively impact fracture toughness. Based on its review, the staff finds the scope of materials that the PWROG considered and included into the master curve data is representative and reasonably bounds the fracture toughness of RPV inlet and outlet nozzle forgings in U.S. PWRs.

The PWROG explained that the nozzle forgings used in U.S. PWRs are all ASME SA-508 Class 2 or ASTM A-508 Class 2 with the following exceptions: Prairie Island Nuclear Generating Station Units 1 and 2 nozzles, which are SA-508 Class 3, Palo Verde Nuclear Generating Station Units 2 and 3 nozzles (which are a combination of SA-508 Classes 2 and 3), and R.E. Ginna Nuclear Power Plant nozzles (which are SA-336). The PWROG noted that the Ginna nozzles meet the A-508 Class 2 specification requirements per the Ginna Certified Material Test Reports (CMTRs). With regard to the nozzles forgings that are SA-508 Class 3, the PWROG stated that master curve data was assessed for A-508 Class 3 and showed that the fracture toughness properties were better than A-508 Class 2. Based on its review of the master curve data for A-508 Class 3 materials referenced by the PWROG, the staff finds it reasonable that the A-508 Class 2 generic RT_{T0} developed in this TR is conservative compared to A-508 Class 3 forgings. In addition, the staff finds that the A-508 Class 2 generic RT_{T0}

developed in the TR is appropriate for the SA-336 forgings because plant-specific CMTRs demonstrate that these forgings meet the A-508 Class 2 specification requirements.

The PWROG provided a description of the materials relevant to the U.S. PWR nozzle forgings that were included in its master curve data search. Specifically, the PWROG included in its supplement available master curve data, chemical composition, and mechanical properties of the following materials: 22NiMoCr37, ASTM A-508-64 Class 2, SA-508 Class 2 (1971), SA-508 Grade 2 Class 1 (2007), 20NiMoCr26, and SFVQ2A. The staff reviewed the chemical composition and mechanical properties listed for the different forgings and noted that the differences in the chemical composition limits and mechanical properties between all the different alloys are very minor when compared to the alloys used in U.S. PWR nozzle forgings. The PWROG confirmed that each of these forgings in the master curve dataset was quenched and tempered steel for pressure vessels, and that a similar heat treatment was used to produce the required properties. The PWROG also confirmed that the master curve data was produced from specimens taken from thick section forgings except for the 20NiMoCr26 forging, which was thinner. For this particular forging that was thinner, the PWROG indicated that consideration of the forging in the dataset is conservative (i.e., increases the average generic RT_{T0} in the TR). Based on the impact of the 20NiMoCr26 forging to the average generic RT_{T0} determined in the TR, the staff finds its inclusion into the master curve dataset to be conservative.

Based on its review, the staff considers A-508 and SA-508, Class 2, 22NiMoCr37, 20NiMoCr26, and SFVQ2A forgings are essentially the same alloy because of the minor differences in the chemical composition and mechanical properties, and the PWROG's confirmation regarding the methods used to produce these forgings. Thus, the staff finds the PWROG's inclusion of A-508 and SA-508, Class 2, 22NiMoCr37, 20NiMoCr26, and SFVQ2A materials in its master curve dataset to be acceptable and representative of U.S. PWR nozzle forgings.

Based on its review, the staff finds the scope of materials considered by the PWROG and included into the master curve data is representative and reasonably bounds the fracture toughness of the RPV inlet and outlet nozzle forgings in U.S. PWRs.

Results from Master Curve Data Search

Section 3.1.2, "Results from Master Curve Data Search," of the TR states that master curve data for 22 distinct forgings were identified, and in all cases the heats selected are representative of the forgings used in commercial PWRs and boiling water reactors (BWRs) from Japanese, Swedish, German, and U.S. RPVs. The PWROG confirmed that the references were checked to ensure that all the data collected for the TR was from unique forgings.

The PWROG explained that in some cases the references only reported K_{IC} values; nevertheless, the master curve reference temperature can conservatively be developed from these K_{IC} values. The PWROG stated that the K_{IC} values are always the same or lower than the cleavage-onset fracture toughness (K_{JC}) values from the same test; thus, the T_0 value developed from these K_{IC} values would be conservative. The staff noted that where K_{IC} is used instead of K_{JC}, K_{IC} is defined by ASTM E399, "Standard Test Method for Linear-Elastic Plane-Strain Fracture Toughness K_{IC} of Metallic Materials," and is the applied SIF (K) where the load displacement trace deviates from linearity by 5 percent. Whereas in ASTM E1921, "Standard Test Method for Determination of Reference Temperature, T_0, for Ferritic Steels in the Transition Region," K_{JC} is K converted from the applied J-integral at cleavage. The staff noted that the K_{IC} curve was established using only data deemed to be "valid" by linear elastic fracture mechanics criteria per ASTM E399; thus, only the lower range of cleavage fracture toughness values were used, whereas K_{JC} is determined from data from specimens in a temperature range where either

cleavage cracking or crack pop-in develops during the loading of specimens and is not limited to the lower range values. Thus, the staff finds it acceptable and conservative that the PWROG included relevant K_{IC} values in determining the master curve reference temperature because these values only include the lower range of cleavage fracture toughness data.

Table 3-2 "All Available Master Curve Data on A-508 Class 2 Type Forgings," of the TR presents the results from the master curve data search performed by the PWROG. The PWROG stated that the range of RT_{NDT} values in Table 3-2 of the TR exceeds the range (i.e., more conservative) of the RT_{NDT} values generally observed in U.S. PWR nozzle forgings utilizing the criteria in NB-2300 of Section III of ASME Code, which typically fall between -34°C and -12°C. Additionally, the PWROG stated that the average RT_{NDT} (-11°C) of the 22 forgings in Table 3-2 of the TR falls above (i.e., more conservative) this typical range of RT_{NDT} values observed for U.S. PWR nozzle forgings based on measured data and ASME Code NB-2300 criteria. The PWROG summarized in its supplement NB-2300-compliant measured RT_{NDT} values for U.S. PWR nozzle forgings developed from a review of original CMTRs. The staff noted that this information is not intended to be a complete list of all U.S. PWR nozzle RT_{NDT} values but contains those readily available to the PWROG, which are representative of approximately half of the U.S. PWR nozzle forgings.

The staff reviewed these NB-2300-compliant RT_{NDT} values and noted an average value of -10.5°F (-23.6°C). The staff noted the average value from the reported RT_{NDT} values in the master curve data search (i.e., Table 3-2 in the TR) is 12.2°F (-11°C). Based on the readily available data from U.S. PWR nozzle forgings and the master data search in the TR, the staff finds the forgings included in the master curve data used to develop the A-508 Class 2 generic RT_{T0} in the TR, on average, is not as tough as the nozzle material in U.S. PWRs and, therefore, conservatively represents the fracture toughness of U.S. PWR nozzle forgings.

Based on the discussion above, the staff finds the PWROG demonstrated that the master curve data presented in the TR is conservatively representative with respect to fracture toughness of U.S. PWR nozzle forgings. Specifically, since RT_{T0} is an acceptable alternate to RT_{NDT}, the staff finds the A-508 Class 2 generic RT_{T0} developed in this TR is also considered conservatively representative of the U.S. PWR fleet of nozzle forgings.

Specimen Geometry Constraint Adjustment

Table 3-2 of the TR provides the details of the specimen geometry of the forgings that were used to determine generic nozzle forging master curve reference temperature. Section 3.1.2.1, "Specimen Geometry Constraint Adjustment," of the TR indicates that, as observed by Tregoning and Joyce (Ref. 45 of the TR), there is a systematic, non-conservative bias toward the Single Edge Notched Bend (SE(B)) specimen of generally 5°C to 10°C relative to the compact tension (CT) specimen geometry due to its lower constraint. Thus, the PWROG elected to address this by adding a 10°C bias to the SE(B) T_0 values to adjust for the lower constraint SE(B) geometry, as shown in Table 3-2 of the TR.

By letter dated August 4, 2005 (ADAMS Accession No. ML052070408), the staff approved the use of a 10°C bias for the lower constraint SE(B) geometry in its SE of BAW-2308, Revision 1. In addition, the staff noted that recent editions of ASTM E1921 included an average difference between the CT and SE(B) of 10°C.

The staff finds the PWROG's use of a 10°C bias to the SE(B) T_0 values acceptable because it is consistent with (1) the data and information available on the differences between SE(B)

specimen and CT specimen test result, and (2) the previous approval of a 10°C bias for the lower constraint SE(B) geometry.

Surface Effect

Section 3.2, "Surface Effect," of the TR describes improved toughness near the surface of a forging material compared to a location deeper in the forging. The PWROG cited references that illustrated the improved toughness near the surface and presented transition temperature data for 24 longitudinal (LT) specimens and seven transverse (TL) specimens. The data consisted of shifts in transition temperature at the surface relative to the 1/4T location and were determined from Charpy V-Notch (CVN) or the master curve measurements. The PWROG stated that specimens without a reported orientation were included in the LT data set. Table 3-3, "Summary of Transition Temperature Shifts for LT and TL Specimens," of the TR showed the average and standard deviation of the transition temperature shifts for the LT and TL data sets. The PWROG selected the conservative set of average and standard deviation (i.e., the LT data set) to take credit for improved fracture toughness for the small flaw models described in Section 4.1 of this SE.

The staff reviewed the information in Section 3.2 of the TR and verified the average and standard deviation of the transition temperature shifts in Table 3-3 of the TR. The staff noted these observations in the LT measurements: five of the measurements were taken at less than the assumed flaw size of 0.5 inch and two measurements had only a small difference in the depths that they were taken. The staff recalculated the average and standard deviation without these LT measurements and determined that they caused a negligible change. Therefore, the staff finds the average and standard deviation of the temperature shifts shown in Table 3-3 of the TR to be acceptable. The staff noted that the inherent scatter in CVN measurements tend to increase the standard deviation in the transition temperature shifts, which is conservative; thus, the staff also finds including CVN measurements to be acceptable.

The PWROG addressed in its supplement the specimens without a reported orientation being included in the LT data set in two aspects. First, the PWROG confirmed that the ten B&W forgings, the Westinghouse Four-Loop Inlet Nozzle, Westinghouse Four-Loop Outlet Nozzle #1, and Westinghouse Four-Loop Outlet Nozzle #2 have CMTRs dated from 1969 and 1970. The PWROG stated that testing of TL specimens was not required until after the issuance of the Summer 1972 Addenda of the 1971 Edition of the ASME Code Section III. Although the staff is unable to confirm that these forgings produced prior to 1972 were tested in the LT direction, the second aspect of how the PWROG addressed specimens with unknown orientation is reasonable. The PWROG stated that in addition to the forgings discussed above, the orientation was not reported for the BethForge forging ID, BethForge forging OD, Forging M1, Forging I, and the French forging. For all of the forgings with unknown orientation identified above, the PWROG illustrated the breakdown of the LT dataset measured transition temperature surface shift between those with a reported LT orientation and those with an *assumed* LT orientation. The PWROG explained that the addition of the assumed LT orientation data biases the average shift value in the conservative direction compared to the dataset with only known LT orientation. Specifically, the staff noted that the "known" LT dataset provides an average shift of 44.7°F; whereas, the "unknown" LT dataset in this second category would only provide an average shift of 33.8°F. Thus, when the "known" and "unknown" LT datasets are both included, the average shift and standard deviation values in the TR (36.5°F and 28.9°F, respectively) result in a more conservative ART compared to the ART value based only on known LT data.

In summary, the staff finds that the PWROG adequately addressed the forgings without a reported orientation and their inclusion with the known LT data is appropriate and conservative, as described above. Thus, the staff finds that the PWROG has selected a conservative dataset set to determine the improved fracture toughness near the surface of a forging material and finds it acceptable when addressing the small flaw models described in the TR.

Underclad Heat-Affected Zone Toughness

Section 3.3, "Underclad HAZ Toughness," of the TR states that a significant portion of the small postulated flaw in this TR would be in the underclad heat-affected zone (HAZ); therefore, the properties of the HAZ relative to the adjoining base metal must be considered. The staff's evaluation of the small postulated flaw is documented in Section 4.1 of this SE.

The PWROG provided information from Oak Ridge National Laboratory (ORNL), in which ORNL conducted Charpy impact testing on a stainless steel cladded plate to determine the effect of clad on the propagation of small surface flaws. This plate was specifically heat treated to produce a high transition temperature but was not quenched and only slightly tempered. The testing performed by ORNL showed that the clad HAZ had significantly better properties (i.e., lower transition temperature) than the 1/4T location in the plate. The PWROG stated that since the plate was not quenched, the improved HAZ transition temperature would not be due to a faster cooling rate from quenching, but the tempering of the cladding operation.

The staff noted that HAZ test results from surveillance specimens have revealed the inhomogeneous nature of the HAZ material, which also resulted in significant scatter of the HAZ Charpy test data. As discussed in "Irradiation Embrittlement of Reactor Pressure Vessels (RPVs) in Nuclear Power Plants" (Soneda, N. ed., 2015), the weld HAZ has been shown to exhibit superior fracture toughness compared to the plate or forging. In addition, the staff also noted that the continued need to include HAZ material in RPV material surveillance programs was more recently investigated in a paper by Koichi Masaki, Jinya Katsuyama, and Kunio Onizawa, "Study on the Structural Integrity of RPV Using PFM (Probabilistic Fracture Mechanics) Analysis Concerning Inhomogeneity of the Heat-Affected Zone." This paper investigated the features of HAZ inhomogeneity in RPV steels to determine the need for surveillance test specimens of HAZ materials in Japan. The authors examined the inhomogeneous distribution of fracture toughness for HAZ materials using a PFM code and determined that the high-toughness coarse grain HAZ caused arrest of postulated cracks. This outcome is expected metallurgically, because the HAZ is a tempered version of the plate or forging and, as such, it should exhibit superior fracture toughness compared to the plate or forging.

Thus, the staff finds that the PWROG has adequately addressed the properties of the HAZ relative to the adjoining base metal and finds the PWROG's conclusion that underclad HAZ in nozzles is as tough, or tougher than, the adjacent forging base metal to be acceptable.

4.3 Neutron Embrittlement

Section 3.4, "Neutron Embrittlement," of the TR states that the copper (Cu) content was not measured for all the nozzles manufactured for the U.S. PWR fleet, however it was measured for a substantial number covering nearly the full range of manufacturing dates and all major U.S. RPV fabricators. Cu measurements were averaged for 178 inlet and outlet nozzles yielding an average of 0.0947 percent with a standard deviation of 0.0319 percent, yielding a best-estimate value, as defined by RG 1.99, Revision 2, of average plus one standard deviation of 0.127 percent. The PWROG explained that for nickel (Ni) content, the upper limit of the SA-508

Class 2 specification during the fabrication time period is used, which was 0.90 percent. The PWROG stated that the Cu and Ni contents discussed above are appropriate for the U.S. PWR nozzles, since the database was established from Cu measurements from PWR nozzle forgings only.

The staff reviewed the information in Section 3.4 of the TR and RG 1.99, Revision 2, regarding the Cu and Ni content. The staff finds the PWROG appropriately determined Cu and Ni contents that are representative of U.S. PWR nozzle forgings consistent with the guidance in RG 1.99, Revision 2.

Using the Cu and Ni contents discussed above and RG 1.99, Revision 2, the PWROG developed an embrittlement trend curve (ETC) that shows the shift in RT_{NDT} (ΔRT_{NDT}) as a function of neutron fluence, applicable to U.S. PWR nozzles. The PWROG then determined the fluence value of 4.28×10^{17} n/cm^2 for a ΔRT_{NDT} of 25°F. The PWROG cited NRC Technical Letter Report TLR-RES/DE/CIB-2013-01, "Evaluation of the Beltline Region for Nuclear Reactor Pressure Vessels," Office of Nuclear Regulatory Research (RES), dated November 14, 2014 (ADAMS Accession No. ML14318A177), as a basis for not considering the shift due to irradiation of RPV beltline materials (including nozzles) if ΔRT_{NDT} is less than 25°F. The PWROG used the fluence value at ΔRT_{NDT} of 25°F as a screening threshold below which embrittlement due to irradiation may be neglected in the calculation of ART (as discussed in Section 4.4 of this SE). Section 3.4.5, "Future Increased Nozzle Fluence Projections," of the TR indicates that as long as the nozzle fluence projections are less than the fluence screening threshold, the nozzle P-T limits developed in the TR is applicable (if the new fluence is greater than the threshold, a plant-specific ΔRT_{NDT} or ART shall be calculated).

The PWROG provided additional justification in its supplement that supports the recommendation in TLR-RES/DE/CIB-2013-01 related to ΔRT_{NDT} of 25°F. The PWROG stated that predictions of ΔRT_{NDT} have inherent scatter due to uncertainty in ΔRT_{NDT} data measurement and uncertainty in ΔRT_{NDT} prediction models. The PWROG's premise is that a ΔRT_{NDT} of 25 °F does not have to be considered because 25°F is a reasonable value that represents the scatter in ΔRT_{NDT} due to these uncertainties. To demonstrate this, the PWROG compared the standard deviation (a measure of scatter) of the ΔRT_{NDT} data in TLR-RES/DE/CIB-2013-01 and from the embrittlement database used to develop the ASTM E900 ETC, which included data from welds, plates, and forgings from tested surveillance capsules. The PWROG determined a standard deviation of ΔRT_{NDT} of 23 °F from the data in TLR-RES/DE/CIB-2013-01 and a standard deviation of ΔRT_{NDT} of 18.6 °F from the ASTM E900 ETC data. The standard deviation from the ASTM E900 ETC data included fluence levels up to 4.28×10^{17} n/cm^2, which is the fluence corresponding to a ΔRT_{NDT} of 25 °F and the fluence threshold the PWROG is proposing in the TR below which embrittlement shifts for nozzles do not have to be considered. The PWROG noted that 18.6 °F is slightly less than 23°F but is consistent with the standard deviation of ΔRT_{NDT} from other ETCs, which included ETCs based on RG 1.99, Revision 2 and 10 CFR 50.61a.

To further demonstrate that 25°F is a reasonable value below which embrittlement shifts do not have to be considered, the PWROG, using the ETC from RG 1.99, Revision 2, determined ΔRT_{NDT} values of 24.5°F, 25.4°F, and 29.6°F—all comparable to 25°F–for RPV materials that have hypothetically high Cu content (i.e., highly embrittled) at a fluence level of 0.99×10^{17} n/cm^2. This fluence level is slightly less than the 1×10^{17} n/cm^2 threshold established in Appendix H to 10 CFR Part 50 for monitoring changes in the fracture toughness properties of ferritic materials in the reactor vessel beltline region. Since 0.99×10^{17} n/cm^2 is less than 1×10^{17} n/cm^2, these ΔRT_{NDT} values for RPV materials having hypothetically high Cu content would not have been considered. Based on the discussion above, the PWROG concluded that

25°F is a reasonable value below which embrittlement shifts do not have to be considered. The staff reviewed the PWROG's justification for using the recommendation in TLR-RES/DE/CIB-2013-01 for not having to consider a ΔRT_{NDT} of 25°F. The staff noted that the ΔRT_{NDT} data from the ASTM E900 embrittlement trend curve (Figure 1 in the supplement) have more positive shifts than negative shifts and shifts could be up to 60°F. However, the staff recognizes that the effect of embrittlement is difficult to distinguish from the data scatter for shifts less than 25°F. Therefore, given the safety significance of RPV components, the staff does not find the justification sufficient to demonstrate generically that embrittlement shifts less than 25°F do not have to be considered. In order to determine whether the recommendation in TLR-RES/DE/CIB-2013-01 of excluding 25°F embrittlement is acceptable specifically for this TR, the staff evaluated the safety significance of the recommendation by identifying if there are any U.S. PWRs in which the nozzles are the limiting material for P-T limits when accounting for an embrittlement shift of 25°F.
For this independent assessment to be focused on those U.S. PWRs in which the nozzle material is more limiting than the traditional beltline for P-T limits, the following criteria were used to screen out U.S. PWRs as not needing any additional review:

- Plants that are already shutdown or not pursuing a renewed operating license
- Plant-specific license amendment requests have been reviewed and approved by the NRC to address irradiation embrittlement of the nozzles
- Plant-specific Pressure-Temperature Limits Report (PTLR) demonstrates that the NRC-approved P-T limit curves are limiting
- Neutron fluence at the nozzle region is less than 1×10^{17} n/cm^2 (E > 1 MeV) at the end of 60-years of plant operation (neutron fluence information is publicly available in plant-specific license renewal applications, license amendment requests, or PTLR)
- Reactors with traditional beltline materials with Cu ≥ 0.2 wt. % (information is publicly available in Reactor Vessel Integrity Database (RVID) Version 2.0.1)

The staff determined that reactors with a neutron fluence at the nozzle region less than 1×10^{17} n/cm^2 (E > 1 MeV) at the end of 60 years of plant operation are screened out consistent with the threshold established in Appendix H to 10 CFR Part 50 for monitoring changes in the fracture toughness properties of ferritic materials in the RPV beltline region. Furthermore, the staff determined that it is reasonable that U.S. PWRs with traditional beltline materials with Cu ≥ 0.2 wt. % are screened out because this level of Cu content would cause a significant shift due to embrittlement in the P-T limits such that it will continue being the limiting material through the license renewal period (i.e., 40 to 60 years of operation).

Following this initial screening, the staff reviewed the information available in RVID 2.0.1 to identify "candidate" U.S. PWRs based on the following criteria:

- Reactors with a traditional beltline material with low Cu content (i.e., ≤ 0.03 wt. %)
- Reactors with NRC-approved P-T limits based on a limiting material with low Cu content
- Nozzle material information (e.g., initial RT_{NDT}, Cu, Ni, and neutron fluence) is available in ADAMS to generate P-T limit curves

The staff noted that reactors meeting these criteria, particularly those reactors with good beltline material properties (i.e., low initial RT_{NDT}), have the highest likelihood that a shift due to embrittlement of the nozzle could lead to nozzle P-T limits being more limiting than the NRC-approved P-T limits based on a traditional beltline material. Since a data search was being performed for nozzle material property information for the "candidate" reactors, the staff opted to also include any additional reactors at the site since the information was already

available in the source documents (e.g., license renewal application). This resulted in a total of nine U.S. PWRs that the staff further investigated by generating P-T limit curves for the limiting nozzle forging using ART values based on an effective full power year (EFPY) that was available from the appropriate source document or data. These nozzle P-T limit curves are based on a 100°F per hour cooldown rate and a postulated inside corner flaw of depth 1/4T.

For the independent assessment, the staff determined applied SIFs for nozzles due to pressure loading (K_{IP}) and thermal gradients (K_{IT}) consistent with those published in the ORNL study, ORNL/TM-2010/246, "Stress and Fracture Mechanics Analyses of Boiling Water Reactor and Pressurized Water Reactor Pressure Vessel Nozzles -Revision 1, June 2012." The staff noted that these SIF solutions are also consistent with those in the 2013 edition of the ASME Code, Section XI, Paragraph G-2223(c), which are applicable to postulated nozzle corner flaws, regardless of plant design. The staff used the limiting nozzle location from ORNL/TM-2010/246 (i.e., the nozzle location with the highest stresses) in its independent assessment. As such, the staff finds that the use of the SIF solutions in ORNL/TM-2010/246 for calculating the K_{IP} and K_{IT} values for the nozzles are acceptable and appropriate for use in its independent assessment.

The nozzle P-T limit curves generated by the staff for these "candidate" U.S. PWRs were then compared to their respective NRC-approved P-T limit curves, both of which were based on ART values calculated at the same EFPY. Based on this comparison, the staff determined that for these nine "candidate" reactors, the limiting traditional beltline NRC-approved P-T limit curves were bounding compared to the nozzle P-T limit curves generated by the staff.

For the remaining U.S. PWRs, the staff noted that nozzle material information (e.g., initial RT_{NDT}, Cu, Ni, and neutron fluence) was not readily available. Thus, for the staff to determine if the nozzle P-T limit curve is limiting, a generic screening ART value for the nozzle was calculated and then compared against the ART values from the traditional beltline. The staff noted that if the ART value for the traditional beltline materials (information available in RVID 2.0.1) is less than this screening generic nozzle ART value, there is a potential that the nozzle P-T limit curve may be more limiting. Since the plant-specific nozzle information was not available, the staff used the generic mean alternate RT_{NDT} value determined in the TR for U.S. PWR nozzle forgings. As discussed in Sections 4.2 and 4.4 of this document, the staff determined the generic mean alternate RT_{NDT} value (i.e., RT_{T0}) in the TR is relevant and conservatively representative of U.S. PWR nozzle forgings.

The generic screening nozzle ART value was determined in the following manner:

- Generic Nozzle $ART_{screening} = RT_{T0\ Intial} + \Delta RT_{NDT\ Stress} + \Delta RT_{NDT\ Embrittle} + margin_{Embrittle}$
- $margin_{Embrittle} = 2(\sigma_I^2+\sigma_\Delta^2)^{½}$ – Per RG 1.99, Revision 2
- $RT_{T0\ Intial}$ = -66.4°F – Per Section 3.5 of the TR
- $\Delta RT_{NDT\ Stress}$ = 25°F – Bounding shift due to stress based on review of P-T limit curves
- $\Delta RT_{NDT\ Embrittle}$ = 25°F – Maximum shift due to embrittlement
- σ_I = 54.5°F – Per Section 3.5 of the TR
- σ_Δ = 12.5°F – Per RG 1.99, Revision 2, σ_Δ cannot be more than ½ of $\Delta RT_{NDT\ Embrittle}$
- Generic Nozzle $ART_{screening}$ = 95.4°F

As noted above, $\Delta RT_{NDT\ Stress}$ represents the shift of the nozzle P-T limit curve resulting from the stress levels due to the structural discontinuities in the nozzle region as compared to the P-T limits curve generated for the traditional beltline. Based on its observations and previous reviews of License Amendment Requests for P-T limits curves, the staff noted that a value of 25°F is appropriate and bounding to account for the increased stress levels due to the structural

discontinuity in the nozzle. Based on this screening generic nozzle ART value, the staff identified four U.S. PWRs that needed a detailed assessment. The staff determined that two of these U.S. PWRs are governed by the P-T limit curve from the bounding unit at the site, which was previously screened out because the ART value for a traditional beltline material was greater than the screening generic nozzle ART value. For the remaining two PWRs, the staff generated P-T limit curves for a generic nozzle ART value, consistent with the methods described above, for comparison with the traditional beltline NRC-approved P-T limit curves. However, to generate these nozzle P-T limit curves, $\Delta RT_{NDT\ Stress} = 25°F$ was not included in the ART value because $\Delta RT_{NDT\ Stress}$ was only for the purpose of screening in PWRs for assessment. The resulting generic nozzle ART value used for generating the P-T limit curves is 70.4°F.
The staff generated nozzle P-T limit curves for the two remaining PWRs using the generic ART value of 70.4 °F and compared them to the NRC-approved P-T limit curves. Based on this comparison for the two U.S. PWRs, the staff noted the following:

- The NRC-approved P-T limit curve was limiting for one reactor
- The NRC-approved P-T limit curve coincided with the P-T limit curve generated with the generic nozzle ART value of 70.4 °F for the other reactor

For the case in which the two curves coincided, the staff noted that the NRC-approved P-T limit curve was based on 36 EFPY (i.e., 40 years of plant operation); whereas, the generic nozzle ART value is based on a neutron fluence in the nozzle region that is conservatively expected after 60-years of plant operation. The staff noted that if the comparison of the NRC-approved P-T limit curve and the P-T limit curve generated with the generic nozzle ART value for the subject reactor was at the same EFPY, the nozzle material would not be limiting. In addition, as discussed in Section 4.2 of this document, the generic nozzle ART value, which is based on RT_{T0} and σ_I developed in the TR, is conservatively representative of the U.S. PWR nozzle forgings. The staff noted that the generic screening nozzle ART value included the shift of 25°F due to embrittlement and that the nozzle-specific shift can be less than this value. Thus, the staff noted that if the plant-specific nozzle material properties for the subject reactor are used, it is reasonable to expect that the nozzle would be tougher than the "generic nozzle" addressed in this TR and would make the NRC-approved P-T limit curve more limiting than the nozzle P-T limit curve.

In summary, based on its assessment of the PWROG's justification and the staff's independent assessment, as described above, the staff finds that for a neutron fluence less than 4.28×10^{17} n/cm^2 (E > 1 MeV) in the nozzle region, the NRC-approved P-T limit curves are limiting for 60 years of plant-operation when compared to the nozzle P-T limit curves. In addition, even though the PWROG did not consider the shift due to irradiation of the nozzles if ΔRT_{NDT} is less than 25°F, the staff demonstrated in its independent assessment that this assumption is unlikely to cause the P-T limit curves for inlet or outlet nozzle corners of U.S. PWRs to be more limiting than those of the shell (and associated welds) of the traditional beltline region (and closure flange regions, as applicable) of the RPV for a neutron fluence less than 4.28×10^{17} n/cm^2 (E > 1 MeV) in the nozzle region.

Fluence Location Relative to the Postulated Flaw Location and Fluence Methodology

Section 3.4.1, "Calculated Fluence Location Relative to the Postulated Flaw Location," of the TR states that nozzle fluence values are typically assumed to be equal to the RPV upper-shell-to-nozzle forging weld fluence value or the lowest extent of the nozzle forging, and thus the nozzle fluence values are conservative. The PWROG stated that since the postulated flaws in the TR are at the nozzle corners, which are at a higher elevation and therefore further away from the

active core, the fluence value is expected to be significantly lower than the fluence at the lowest extent of the nozzle forging or weld. The staff reviewed the discussion of fluence location relative to the postulated flaw location in Section 3.4.1 of the TR and finds it acceptable.

Section 3.4.2, "Fluence Calculational Methodology," of the TR states the use of new fluence evaluation methods can more accurately determine the nozzle fluence reducing the needed conservatisms. The PWROG showed a comparison of nozzle fluence values between three methods of fluence evaluations. The staff reviewed the information in Section 3.4.2 of the TR and noted that the fluence methods approved by the NRC staff are unique to the individual licensee's current licensing basis. Thus, plant-specific fluence calculations performed by the individual licensee in a manner consistent with the NRC-approved methodology will be necessary to determine whether the use of the TR is applicable.

Neutron Streaming

Section 3.4.3, "Neutron Streaming," of the TR states that neutron streaming up the cavity to the nozzle region from the beltline region is an existing phenomenon. As such, the traditional fluence attenuation equation used in the beltline (i.e., in RG 1.99, Revision 2) is not appropriate in the nozzle region when only considering fluence calculated at the inside surface. The PWROG indicated that the fluence at the outside diameter lowest extent of the nozzles can be higher than the fluence at the lowest extent of the nozzle forging at the RPV inside surface due to cavity neutron streaming. The PWROG investigated the stresses at the inlet and outlet nozzles due to pressure and the thermal cooldown transient. The stresses are shown in Section 4.8 "Stresses at Limiting Locations" of the TR, specifically in the figures from the 3D finite element analysis. The PWROG states that these figures demonstrate that the stresses at the lowest extent outside diameter of the nozzles are significantly lower than at the nozzle inside corner, and when pressure stress and thermal stress are considered together, the combined stress is likely compressive. As is discussed in Section 4.8 of the TR, the flaw is postulated at the nozzle inside surface corner at a geometric discontinuity where the highest stresses exist. As a result, the nozzle inside corner is the limiting location, and this location is where the fluence is considered for embrittlement.

Based on its review, the staff finds the neutron streaming effect is applicable to the 3/4T postulated flaw and that the PWROG's exclusion of the 3/4T postulated flaw in the development of the P-T limits in the TR for the nozzles is appropriate, as described below. Specifically, the staff noted that the pressure stress decreases as a function of distance from the inside corner along the through-wall nozzle corner path, as shown in Figure 24 of ORNL/TM-2010/246. Therefore, the applied SIF due to pressure for a 3/4T postulated flaw at the outside corner of the nozzle would be lower than that for the 1/4T flaw postulated for the inside corner region. The linear elastic fracture mechanics analyses in ORNL/TM-2010/246 do not address 3/4T postulated flaws for this reason. It should be noted that, based on the analysis of the 1/4T location and the smaller postulated flaw from the inside corner region, the nozzle P-T limits for a heatup transient would be less restrictive than those calculated for a cooldown transient because the thermal stresses for a postulated inside corner flaw are compressive for heatup. Therefore, the staff determined that analyses of the 1/4T location and the smaller postulated flaw at the nozzle inside corner during a cooldown transient generates the most bounding P-T limits for the nozzles.

4.4 Calculation of ART

In Section 3.1.2.2, "Calculation of Generic Mean Alternate RT_{NDT}," and Section 3.5, "Adjusted Reference Temperature," of the TR, the PWROG calculated ART with and without the surface effect using the RT_{T0} (evaluated in Section 4.2 of this SE) as the initial reference temperature. The ART value with the surface effect is to be used for the postulated small flaw and the ART

value without the surface effect is to be used for the traditional, postulated 1/4T flaw in the nozzle P-T limits developed in Section 5.1, "Generation of Nozzle P-T Limit Curves," of the TR (evaluated in Section 4.10 of this SE). Both ART calculations do not consider an embrittlement shift of 25°F (which the staff evaluated in Section 4.3 of this SE) since the PWROG developed a fluence threshold screening criterion of 4.28×10^{17} n/cm^2. The staff noted that this fluence threshold screening criterion corresponds to a ΔRT_{NDT} of 25°F below which embrittlement shifts may be neglected.

The staff verified the ART calculations in Sections 3.1.2.2 and 3.5 of the TR consistent with the guidance in RG 1.99, Revision 2, and finds the ART values of 43°F for the 1/4T flaw and 21°F for the shallow flaw are acceptable for the A-508 Class 2 generic RT_{T0} developed in this TR.

4.5 Selection of Inlet and Outlet Nozzle Model Geometry

In Section 4.1 of the TR, the PWROG considered several geometric parameters that affect the stress due to pressure and thermal transient in the nozzle corner region. The PWROG stated that "important characteristics that affect nozzle corner stress and SIF were assessed to ensure representative or bounding models were chosen for the whole U.S. PWR fleet." The PWROG considered nozzle radius-to-thickness (R/t) ratio, nozzle diameter, nozzle corner geometry, and clad thickness as the important geometric parameters that affect the nozzle corner stress and SIF. Table 4-1, "Model Geometry Comparison," pictorially depicted in Figure 4-3, "Diversity of Nozzle Geometries Modeled," of the TR summarizes the inlet and outlet geometries that were modeled.

The staff finds the PWROG's approach for selecting nozzle model geometries acceptable since it is not practical to model the unique geometry of each inlet and outlet nozzle design in the U.S. PWR fleet. It is reasonable to consider only the parameters that are most relevant, with respect to the stress that can extend a postulated flaw in the nozzle corner. The staff considers that the thickness of the nozzle section and the sharpness of the nozzle corner radius are the most relevant parameters that can extend a postulated flaw in the nozzle corner. The staff finds that the PWROG adequately addressed the effects of these two parameters by considering the nozzle R/t ratio, nozzle diameter, nozzle corner geometry, and clad thickness. Considering the nozzle R/t ratio (and nozzle diameter which accounts for the radius) addresses the section thickness effect on stress. Considering the nozzle corner geometry addresses the effect of the nozzle corner radius, which causes high stresses on the inside surface of the corner. Considering the clad thickness addresses the effects of clad welding residual stress on the small flaw models described in Section 2.

Furthermore, the staff determined that selecting a nozzle section thickness that bounds all U.S. PWR fleet inlet and outlet nozzle is challenging for two reasons: (1) the effect of thickness on stress due to internal pressure counterbalances the effect of thickness on stress due to thermal transients: a thinner section would generate a higher stress due to internal pressure, but a lower stress due to thermal transient; and (2) the time at which the maximum stress due to internal pressure occurs does not occur at the same time the maximum stress due to thermal transient occurs. Therefore, the staff determined that the PWROG's selection of a nozzle geometry for modeling that is representative of the U.S. PWR fleet nozzle geometry is a practical and reasonable approach.

Based on the discussion above, the staff finds the four nozzle geometries listed in Table 4-1 of the TR acceptable for representing the inlet and outlet nozzle designs in the U.S. PWR fleet.

4.6 Finite Element Model and Analyses

Model Creation

The PWROG described the FEMs of the inlet and outlet nozzles in Section 4 2, "Model/Mesh," Section 4.3, "Flaw Modeling Methodology," and Section 4.6, "Material Properties," of the TR. The three-dimensional FEMs of the inlet and outlet nozzles included flaws in the nozzle corner with depths of 0.05 inch and 0.5 inch into the LAS and with length-to-depth aspect ratios of 2:1 and 6:1. The mesh in the vicinity of the modeled flaws included very fine elements that have features for handling the sharp edges around the flaw tip. The PWROG summarized the FEM cases in Table 4-2, "Flaw Case List," of the TR.

The staff reviewed the descriptions of the FEMs in Sections 4.2, 4.3, and 4.6 of the TR and finds the methods (selection of element types, meshing, and definition of material properties) acceptable.

Boundary Conditions

The PWROG described the boundary conditions applied to FEMs of the inlet and outlet nozzles in Section 4.4, "Thermal Boundary Conditions," and Section 4.5, "Structural Boundary Conditions," of the TR. Thermal boundary conditions included temperature coupling of the coincident nodes of the modeled flaw, an assumption of infinite heat transfer coefficient on the wetted surfaces, and insulated conditions on the surfaces of the FEMs where the models are "cut" from the un-modeled structure. The structural boundary conditions included displacement restraints, internal pressure on the wetted surface and on the crack face, end-cap pressure loads on the modeled RPV shell and nozzle safe-end, and mechanical loads on the modeled nozzle safe-end. Additionally, the temperature field from the thermal FEMs are applied to the structural FEMs.

The staff reviewed the descriptions of the thermal and structural boundary conditions in Sections 4.4 and 4.5 of the TR. One thermal boundary condition of the note is the assumption of infinite heat transfer coefficient on the wetted surface. The staff determined that this assumption produces a large temperature gradient across the nozzle section thickness due to a cooldown transient, which generates conservative tensile stresses on the inside surface of the nozzle corner. The staff, therefore, finds the assumption acceptable. The staff noted that the application of the temperature field from the thermal FEMs into the structural FEMs is actually a structural load in the structural FEMs and is therefore acceptable.

Based on the discussion above, the staff finds that the PWROG applied the proper boundary conditions to the inlet and outlet nozzle FEMs, and therefore finds the boundary conditions acceptable.

Loads

The PWROG described the loads applied to FEMs of the inlet and outlet nozzles in Section 4.7, "Loads," of the TR. The applied loads are the residual stress due to clad welding (clad residual stress), mechanical piping loads, and cooldown transient. The internal pressure load is treated as a boundary condition, which the staff evaluated in the "Boundary Conditions" section.

The staff reviewed the descriptions of the applied loads in Sections 4.7 of the TR. One applied load of note is the clad residual stress. The staff reviewed the PWROG's modeling approach that accounts for clad residual stress. The PWROG cited the review of the Sweden Nuclear Power Inspectorate of programs that measured the effects of cladding on structural integrity of cladded RPVs. Specifically, the PWROG referenced the residual stress profile measured across the cladding of an RPV specimen. Then, using this residual stress profile as a reference

stress distribution and the FEM described in Section 4.2 of the TR, the PWROG determined, through an iterative process, the average stress in the clad by adjusting the CTE reference temperature of the clad material that would produce a similar effect at the flaw tip as the measured clad residual stress profile. Given that the availability of residual stress measurements due to clad welding is limited, the staff determined that this approach to address the effect of clad residual stress is reasonable since the reference residual stress is based on measured data. The staff also reviewed open literature and verified that the method of adjusting the CTE reference temperature is a common approach to simulate a stress between two adjacent materials. The staff, therefore finds the load due to clad residual stress acceptable.

The piping loads included those due to deadweight and thermal expansion loads at normal operating conditions. The staff finds the piping loads acceptable. The cooldown transient included one with composite rates (100°F/hour, then 50°F/hour, then 20°F/hour) and one with 100°F/hour for the limiting outlet nozzle FEM. The staff reviewed PWR systems manuals and previous P-T limit curves for cooldown and determined that both cooldown transients are acceptable.

Based on the discussion above, the staff finds the loads applied to the FEMs of the inlet and outlet nozzle acceptable.

4.7 Stresses

The PWROG presented stresses for the inlet and outlet nozzle in Section 4.8, "Stresses at Limiting Locations," of the TR. The staff reviewed the stress contour plots due to internal pressure and cooldown transient for the inlet and outlet nozzle FEMs and determined that the stress values are within the expected values for these nozzles.

4.8 Stress Intensity Factors

The PWROG presented SIFs for the outlet nozzle in Section 4.9, "Stress Intensity Factor Results," of the TR and stated that it performed evaluations for both inlet and outlet nozzles, but showed SIF results only for the outlet nozzle in the TR. The staff determined that showing SIF results only for the outlet nozzle is sufficient for its review since the SIF results for the inlet nozzle would show similar trends because it was subject to the same loads as the outlet nozzle. The staff reviewed the SIF plots due to internal pressure and cooldown transient (which includes the effect of clad residual stress) and determined that the SIF values are reasonable compared to those calculated from a closed-form SIF solution for a nozzle corner crack.

4.9 Constraint and Cladding Effect

The staff reviewed the discussion of T-stress in Section 4.10.1, "Constraint," of the TR, which is commonly used as a measure of constraint and is correlated to toughness. The staff determined that not taking credit for the increased toughness for a nozzle corner flaw (due to lower constraint compared to the constraint on an SE(B) specimen, the data from which fracture toughness is determined) is acceptable.

The staff also reviewed the discussion of cracking restraint due to cladding in Section 4.10.2, "Cladding," of the TR and determined that not taking credit for the ability of cladding to restrain crack growth is acceptable.

4.10 Generic Nozzle P-T Limit Curves

The PWROG developed generic nozzle P-T limit curves in Section 5.1.1, "Generation of Nozzle P-T Limit Curves with Postulated Small Flaw," and Section 5.1.2, "Generation of Nozzle P-T Limit Curves with Postulated with 1/4T Beltline Thickness Size Flaw," of the TR based on the methodology in Appendix G to Section XI of the ASME Code.

The PWROG presented the nozzle P-T limits for the postulated small flaws in Section 5.1.1 of the TR with the ART determined in Section 3.5 of the TR, and the nozzle P-T limits for the postulated 1/4T flaws in Section 5.1.2 of the TR with the ART determined in Section 3.1.2.2 of the TR. The nozzle P-T limits for the small postulated flaws were based on SIFs developed in Section 4 of the TR and included the effect of clad residual stress. The nozzle P-T limits for the 1/4T flaws were based on stresses determined from unflawed nozzle FEMs and SIFs from ORNL/TM-2010/246 (Ref. 18 of the TR).

The staff reviewed the nozzle P-T limit curves in Sections 5.1.1 and 5.1.2 of the TR and compared the limiting curves with known nozzle P-T limit curves. The staff finds the nozzle P-T limit curves in the TR acceptable.

4.11 Comparison of Generic Nozzle P-T Limit Curves to RPV Shell P-T Limit Curves

In Section 5.2, "Comparison of Nozzle to Traditional NRC Approved Pressure-Temperature Limit Curves," the PWROG selected the limiting nozzle P-T limit curves developed in Sections 5.1.1 and 5.1.2 of the TR and compared them to the NRC-approved P-T limits of the shell (and associated welds) in the RPV beltline region. The PWROG determined that eleven NRC-approved P-T limits of Westinghouse plants (identified in the TR as A through K) do not bound the generic limiting nozzle P-T limits developed in this TR and evaluated them separately in Figures 5-10 through 5-14 of the TR. For these eleven plants, plant-specific nozzle RT_{NDT} values were used instead of the generic nozzle RT_{TO} value developed in the TR, using the P-T limit methodologies in Sections 4 and 5.1.2 of the TR. The staff reviewed the generic bounding nozzle P-T limit curves compared to the NRC-approved P-T limit curves to determine whether the PWROG adequately addressed that the NRC-approved P-T limit curves are bounding when compared to bounding generic nozzle P-T limit curves. The PWROG provided additional information in its supplement that aided the staff's review of the eleven plants in which the NRC-approved P-T limit curves did not bound the generic bounding nozzle P-T limits developed in the TR.

The staff reviewed Figure 5-15 of the TR, which provided a comparison of the bounding nozzle P-T limit curves compared to NRC-approved P-T limit curves for CE and B&W PWRs. Based on this comparison, the staff finds the PWROG adequately addressed that the NRC-approved P-T limit curves for CE and B&W PWRs bounds the generic nozzle P-T limit curves developed in this TR, as shown in Figure 5-9 of the TR. The staff reviewed Figure 5-9 of the TR, which provided a comparison of the Westinghouse bounding generic nozzle P-T limit curves compared to the NRC-approved P-T limit curves for Westinghouse PWRs, except for the eleven plant-specific cases which are further discussed below (i.e., Plants "A" through "K"). Based on this comparison, the staff finds the PWROG adequately addressed that the NRC-approved P-T limit curves for Westinghouse PWRs (except for Plants "A" through "K") bound the generic Westinghouse nozzle P-T limit curves developed in this TR, as shown in Figure 5-9 of the TR. The staff's review of Plants "A" through "K" identified in the TR is provided below.

For Plant "A," the PWROG explained in its supplement that WCAP-18191-NP, which was previously submitted to the NRC, contains a calculation of nozzle P-T limit curves using the standard 1/4T nozzle corner flaw and the methods in ORNL/TM-2010/246, as well as the determination of the initial RT_{NDT} values for the nozzle forgings. The staff reviewed WCAP-

18191-NP, Appendix B, and verified that the licensee performed confirmatory P-T limit curve calculations of the RPV inlet and outlet nozzles. The staff noted that the Cu and Ni contents of the nozzles were based on plant-specific CMTRs and that the unirradiated RT_{NDT} values are based on drop-weight data, TL CVN test data and NUREG-0800 Branch Technical Position (BTP) 5-3, "Fracture Toughness Requirements," Positions 1.1(3)(a) and (b), with the more limiting unirradiated RT_{NDT} value being selected. The staff noted that the methodology in BTP 5-3 paragraph 1.1(3)(b) was determined to be acceptable in closure memorandum dated April 2017 (ADAMS Accession No. ML16364A285). The staff noted that the licensee performed these nozzle calculations solely to verify that the P-T limits for the RPV "traditional" beltline is bounding compared to any P-T limit curves for the RPV inlet and outlet nozzles. The staff verified that the licensee used the staff-developed methodology in ORNL/TM-2010/246 to generate the P-T limits of the nozzles. Based on its review of the pertinent information in WCAP-18191-NP, for the purposes of this TR, the staff finds the PWROG adequately addressed that the NRC-approved P-T limit curve for Plant "A" bounds the nozzle P-T limit curves, as shown in Figure 5-14 of the TR.

For Plant "B," the PWROG confirmed that the NRC-approved P-T limit curves were previously shown to not be impacted by the nozzle P-T limits curves using the 1/4T flaw, as documented in letter dated January 22, 2015 (ADAMS Accession No. ML15029A417). The staff's review of this comparison is documented in SE dated April 29, 2016 (ADAMS Accession No. ML16081A333). The staff finds the PWROG has adequately addressed that the NRC-approved P-T limit curve for Plant "B" is bounding.

For Plant "C" through Plant "H," the staff noted the nozzle RT_{NDT} values were measured to the requirements of post-1973 ASME Subarticle NB-2300, and the uncertainty associated with an RT_{NDT} estimation method does not affect these RT_{NDT} values. The staff also noted that the PWROG used the FEM with postulated flaws in the TR to generate the nozzle P-T limit curves. The staff's review of the FEM with postulated flaws in the TR are documented in Sections 4.5 through 4.9 of this SE. Based on its review, the staff finds it acceptable that the PWROG used plant-specific nozzle RT_{NDT} values instead of the A-508 Class 2 generic RT_{T0} developed in this TR, along with the FEM with postulated flaws in the TR to generate the nozzle P-T limit curves. Thus, the staff finds the PWROG has adequately addressed that the NRC-approved P-T limit curves for Plant "C" though Plant "H" bound the nozzle P-T limit curve, as shown in Figures 5-10, 5-11, and 5-12 of the TR.

For Plant "I," the PWROG indicated in its supplement that the actual design dimension of the cladding (5/8 inch after machining) was utilized with the postulated 0.5-inch deep LAS flaw, which resulted in a flaw depth of 0.99 inch from the wetted surface. The SIFs for this 0.99-inch flaw in the FEM were developed using the same methodologies that were used for the other nozzle flaws in the TR. The staff's review of the FEM with postulated flaws in the TR are documented in Sections 4.5 through 4.9 of this SE. For Plant "I," the staff noted the nozzle RT_{NDT} values were measured to the requirements of post-1973 ASME Subarticle NB-2300, and the uncertainty associated with an RT_{NDT} estimation method does not affect these RT_{NDT} values. The staff finds it acceptable that the PWROG used plant-specific nozzle RT_{NDT} values instead of the A-508 Class 2 generic RT_{T0} developed in this TR, to generate the nozzle P-T limit curves. Based on the use of the plant-specific nozzle RT_{NDT} values and the PWROG's confirmation that the flaw size for Plant "I" is based on the plant-specific design dimension of the cladding thickness, the staff finds the PWROG adequately addressed that the NRC-approved P-T limits curve for Plant "I" bounds the nozzle P-T limit curve, as shown in Figure 5-13 of the TR.

For Plants "J" and "K," the PWROG confirmed in its supplement the initial RT_{NDT} values for the reactor vessel nozzle forging materials were determined using the methodology in BTP 5-3

paragraph 1.1(3)(b). The staff noted that the methodology in BTP 5-3 paragraph 1.1(3)(b) was determined to be acceptable in closure memorandum dated April 2017 (ADAMS Accession No. ML16364A285). Based on the PWROG's confirmation regarding the source of the initial RT_{NDT} values for Plants "J" and "K," the staff finds the PWROG adequately addressed that the NRC-approved P-T limits curve for Plants "J" and "K" bounds their respective nozzle P-T limit curve, as shown in Figure 5-11 of the TR.

Based on the staff's review of the comparison for the NRC-approved P-T limit curves and the nozzle P-T limits developed in this TR, as described above, the staff finds that the PWROG has adequately demonstrated that the nozzle P-T limit curves developed in the TR are bounded by the NRC-approved P-T limit curves for U.S. PWRs.

5.0 USE AND REFERENCING OF THE TR

As addressed in the TR and in this SE, the use and referencing of this TR is only applicable to U.S. PWR inlet and outlet nozzles with a projected nozzle corner neutron fluence, as calculated by an NRC-approved method of fluence evaluation consistent with the plant licensing basis, or another NRC-approved method of fluence evaluation, of less than 4.28×10^{17} n/cm^2 (E > 1 MeV). As noted in the TR, if the nozzle fluence is greater than 4.28×10^{17} n/cm^2 (E > 1 MeV), the shift (ΔRT_{NDT}) may be calculated for those nozzles on a plant-specific basis using an NRC-approved method; as long as the shift remains below 25°F or the plant-specific ART values remain below the ART determined in the TR, then the analysis in the TR is applicable.

6.0 CONCLUSION

The staff has reviewed the TR including the supplemental information, and based on the evaluation in Section 4 of this SE, finds the TR as modified by this SE, provides an acceptable means for addressing the potential for P-T limit curves for inlet or outlet nozzle corners of U.S. PWRs to be more limiting than the current NRC-approved P-T limits (as of the time of issuance of this SE) of the shell (and associated welds) in the traditional beltline region (and closure flange regions, as applicable) of the RPV. The staff's independent safety assessment in Section 4.3 of this SE of the TR's use of the recommendation in TLR-RES/DE/CIB-2013-01 of excluding 25°F embrittlement is specific only to the TR, and as such, should not be construed as a generic safety assessment. Thus, other applications that use the recommendation in TLR-RES/DE/CIB-2013-01 must be sufficiently justified and shall be subject to NRC review and approval on a case-by-case basis. Accordingly, PWROG-15109-NP, as modified by this SE, is acceptable for referencing to satisfy the fracture toughness requirements in Appendix G to 10 CFR Part 50 for U.S. PWR inlet and outlet nozzles only, which provide adequate margins of safety during any condition of normal operation, including anticipated operational occurrences and system hydrostatic tests, to which the pressure boundary may be subjected over its service lifetime.

Attachment: Comment Resolution Table

Principal Contributors: On Yee
David Dijamco

Date: October 31, 2019

TOPICAL REPORT PWROG-15109-NP, REVISION 0					
Comment #	**DSE Page No.**	**DSE Line No.**	**Comment Type**	**PWROG Comment**	**NRC Response**
1	1	20	Editorial comment	Please revise the text to add: "and closure flange regions" after "(RPV)"	Comment acceptable
2	2	47	Editorial comment	Please revise the text to add: "beltline size" after "1/4T"	Comment acceptable
3	2	49	Editorial comment	Please revise the text to add: "and closure flange regions" after "region"	Comment acceptable
4	3	1	Editorial comment	Please revise the text to add: "and closure flange regions" after "region"	Comment acceptable
5	8	23	Clarification; the PWROG data and experience show that this conclusion is reasonable.	Please revise the text: "Although the staff does not find it reasonable that these forgings…" to: "Although the staff is unable to confirm that these forgings…"	Comment acceptable
6	8	50	Revises text to reflect correct section in the DSE	Please revise the text from: "Section 2" to "Section 4.1"	Comment acceptable
7	12	28, 38, 46	No change is being requested; this is only a comment	The value of the $\Delta RT_{NDT\ Stress}$ = 25°F has not been verified by the PWROG.	Comment noted
8	13	31	Editorial comment	After "beltline region" please add "(and closure flange regions, as applicable)".	Comment acceptable
9	16	4	Revises text to reflect correct section in the TR	Please revise the text from: "Section 4.3" to "Section 4.4" and "Section 4.4" to "Section 4.5".	Comment acceptable
10	16	15	Revises text to reflect correct section in the TR	Please revise the text: "Sections 4.3 and 4.4" to "Sections 4.4 and 4.5".	Comment acceptable
11	20	5	Clarification; this change makes it consistent with the text on DSE page 13, lines 48-52	Please revise the text after "NRC-approved method of fluence evaluation" adding "consistent with the plant licensing basis, or another NRC-approved method of fluence evaluation".	Comment acceptable
12	20	9	Editorial comment	Please add the text "then" after "TR,"	Comment acceptable
13	20	17	Editorial comment	Please add the text "(and closure flange regions, as applicable)" after "beltline region".	Comment acceptable

Program Management Office
20 International Drive
Windsor, Connecticut 06095

March 5, 2018

OG-18-55

Document Control Desk
U.S. Nuclear Regulatory Commission
11555 Rockville Pike
Rockville, MD 20852-2738

Subject: PWR Owners Group
Transmittal of PWROG-15109-NP, Revision 0, "PWR Pressure Vessel Nozzle Appendix G Evaluation," PA-MSC-1091R4

Reference: **NRC Regulatory Issue Summary 2014-11, "Information on Licensing Applications for Fracture Toughness Requirements for Ferritic Reactor Coolant Pressure Boundary Components," October 2014**

The purpose of this letter is to transmit Pressurized Water Reactor Owners Group (PWROG) Topical Report (TR), PWROG-15109-NP, Revision 0, "PWR Pressure Vessel Nozzle Appendix G Evaluation," in accordance with the Nuclear Regulatory Commission (NRC) TR program for review and acceptance for referencing in regulatory actions (Enclosure 1).

Background

The NRC has issued Requests for Additional Information (RAIs) on License Amendment Requests (LARs) on proposed revisions to the 10 CFR Part 50 Appendix G P-T limit curves. The RAIs asked whether the submitted P-T limit curves based on the beltline region of the Reactor Pressure Vessel (RPV) and the closure head flange bound the RPV inlet and outlet nozzles.

Additionally, NRC Regulatory Information Summary (RIS) 2014-11 was issued to clarify what information should be included in submittals associated with reactor vessel fracture toughness and associated pressure-temperature limits. Specifically, the RIS clarifies that ASME Section XI, Appendix G evaluations should address structural discontinuities such as the RPV nozzles. PWROG-15109-NP contains generic PWR fracture mechanics analyses of the RPV inlet and outlet nozzle corners in accordance with the requirements of 10 CFR Part 50 Appendix G to generically address the issue discussed in RIS 2014-11.

Topical Report Summary

PWROG-15109-NP contains generic PWR nozzle Appendix G P-T limit curves that were developed and compared to the existing NRC approved Appendix G P-T limit curves for

all the operating U.S. PWRs. The comparison confirms that the nozzle P-T limit curves are bounded in every case by the existing U.S. PWR P-T limit curves.

Licensees will reference PWROG-15109-NP to demonstrate compliance with 10 CFR Part 50 Appendix G and RIS 2014-11 for RPV nozzles in future LARs.

Limits of Applicability

PWROG-15109-NP is applicable to all U.S PWRs.

Intended Application

PWROG-15109-NP is being submitted for NRC review and approval. Licensees will utilize the TR to demonstrate that P-T limits derived using the existing approved methodologies (WCAP-14040-A, Rev. 4, CE NPSD-683-A, Rev. 06 and BAW-10046A, Rev. 2) bound RPV inlet and outlet nozzle corners P-T limits.

Industry Implementation

WCAP-15109-NP may be implemented by all U. S. PWRs.

Specialized Resource Availability

This TR is being submitted to the NRC for review and approval so that the NRC approved version can be utilized by licensees to demonstrate existing NRC approved P-T limits and future LARs using existing approved methodologies (WCAP-14040-A, Rev. 4, CE NPSD-683-A, Rev. 06 and BAW-10046A, Rev. 2) bound RPV inlet and outlet nozzle corner P-T limits which is the issue identified in RIS 2014-11. NRC approval of the generic TR will reduce the impact on both licensee and NRC resources by eliminating the need for the preparation of and NRC review of plant specific evaluations to confirm that the traditional P-T limits bound RPV inlet and outlet nozzle corners P-T limits.

NRC Review Schedule

The PWROG requests that the NRC complete their review of the TR by February 2019.

Request for Review Fee Waiver

The PWROG will be requesting that a fee waiver for the NRC review of PWROG-15109-NP, Revision 0 pursuant to the provisions of 10 CFR 170.11(a)(1)(ii). PWROG-15109-NP contains a generic evaluation that can be utilized by all U. S. PWR licensees to confirm compliance with 10 CFR 50 Appendix G. NRC approval of the generic TR will reduce the impact on both licensee and NRC resources by eliminating licensee specific RPV nozzle evaluations and the NRC review associated with those evaluations. Therefore, the review of this TR will support ongoing NRC generic regulatory improvements/efforts associated with RIS 2014-11.

During the fee waiver decision period, the PWROG respectfully requests the NRC Staff to perform its acceptance review of PWROG-15109-NP. The PWROG will assume the responsibility of payment of the NRC review fees accrued both during the acceptance review, and during the review, if the fee waiver is not approved.

This letter transmits one copy of PWROG-15109-NP, Revision 0 (Enclosure 1).

Correspondence related to this transmittal should be addressed to:

Mr. W. Anthony Nowinowski, Program Manager
PWR Owners Group, Program Management Office
Westinghouse Electric Company
1000 Westinghouse Drive
Suite 380
Cranberry Township, Pennsylvania, 16066

If you have any questions, please do not hesitate to contact me at (205) 992-7037 or Mr. W. Anthony Nowinowski, Program Manager of the PWR Owners Group, Program Management Office at (412) 374-6855.

Sincerely yours,

Ken J Schrader

Ken Schrader, Chief Operating Officer and Chairman
PWR Owners Group

KS:WAN:am

Enclosure 1: One copy of PWROG-15109-NP, Revision 0

cc: PWROG Management Committee
PWROG Analysis Committee
PWROG Steering Committee
PWROG Licensing Committee
PWROG PMO
J. Andrachek, Westinghouse
B. Benney, US NRC
B. Hall, Westinghouse
B. Mays, Westinghouse
A. Udyawar, Westinghouse
J. Chen, Westinghouse
D. Love, Westinghouse
S. Rigby, Westinghouse
L. Patterson, Westinghouse
M. DeVan, Framatome
A. Nana, Framatome

ACKNOWLEDGEMENTS

This report was prepared for and funded by the PWR Owners Group under the leadership of the participating utility representatives of the Materials Committee. The author would like to thank the following people and/or organizations for their valuable contributions to this report:

- Warren Bamford for his overall support and advice,
- Dan Denis, Amy Freed, Alley Carolan, and Andy Ruminski for author/verification of the supporting materials and fracture mechanics calculations,
- Rick Rishel for his verification of the non-destructive examination flaw size section,
- Ramin M. Rafatpanah, Gordon Hall, Sarah Lax, and Thomas E. Demers for their extensive effort and expertise with the three-dimensional finite element analysis,
- Ben Amiri, Greg Fischer, and Arzu Alpan for fluence advice,
- Jim Andrachek for his licensing input and overall review,
- Matt DeVan and Ashok Nana (both from Framatome) for providing the B&W materials information and overall review,
- Gary Stevens (SIA) and Nathan Palm (EPRI) for providing constructive comments which yielded an improved analysis and report,
- Mo Dingler (Wolf Creek), Tim Wells (Southern), Chris Wax (APS), Bernie Rudell (Exelon), Heather Malikowski (Exelon) and Scott Boggs (FP&L) for their review from the utility perspective.

WESTINGHOUSE ELECTRIC COMPANY LLC

LEGAL NOTICE

This report was prepared as an account of work performed by Westinghouse Electric Company LLC. Neither Westinghouse Electric Company LLC, nor any person acting on its behalf:

1. Makes any warranty or representation, express or implied including the warranties of fitness for a particular purpose or merchantability, with respect to the accuracy, completeness, or usefulness of the information contained in this report, or that the use of any information, apparatus, method, or process disclosed in this report may not infringe privately owned rights; or
2. Assumes any liabilities with respect to the use of, or for damages resulting from the use of, any information, apparatus, method, or process disclosed in this report.

COPYRIGHT NOTICE

DISTRIBUTION NOTICE

This report was prepared for the PWR Owners Group. This Distribution Notice is intended to establish guidance for access to this information. This report (including proprietary and non-proprietary versions) is not to be provided to any individual or organization outside of the PWR Owners Group program participants without prior written approval of the PWR Owners Group Program Management Office. However, prior written approval is not required for program participants to provide copies of Class 3 Non-Proprietary reports to third parties that are supporting implementation at their plant, or for submittals to the USNRC.

PWR Owners Group
United States Member Participation* for PA-MSC-1091, Revision 5

Utility Member	Plant Site(s)	Participant	
		Yes	No
Ameren Missouri	Callaway (W)	X	
American Electric Power	D.C. Cook 1 & 2 (W)	X	
Arizona Public Service	Palo Verde Unit 1, 2, & 3 (CE)	X	
Dominion Connecticut	Millstone 2 (CE)	X	
	Millstone 3 (W)	X	
Dominion VA	North Anna 1 & 2 (W)	X	
	Surry 1 & 2 (W)	X	
Duke Energy Carolinas	Catawba 1 & 2 (W)	X	
	McGuire 1 & 2 (W)	X	
	Oconee 1, 2, & 3 (B&W)	X	
Duke Energy Progress	Robinson 2 (W)	X	
	Shearon Harris (W)	X	
Entergy Palisades	Palisades (CE)	X	
Entergy Nuclear Northeast	Indian Point 2 & 3 (W)	X	
Entergy Operations South	Arkansas 1 (B&W)	X	
	Arkansas 2 (CE)	X	
	Waterford 3 (CE)	X	
Exelon Generation Co LLC	Braidwood 1 & 2 (W)	X	
	Byron 1 & 2 (W)	X	
	TMI 1 (B&W)	X	
	Calvert Cliffs 1 & 2 (CE)	X	
	Ginna (W)	X	
FirstEnergy Nuclear Operating Co.	Beaver Valley 1 & 2 (W)	X	
	Davis-Besse (B&W)	X	
Florida Power & Light \ NextEra	St Lucie 1 & 2 (CE)	X	
	Turkey Point 3 & 4 (W)	X	
	Seabrook (W)	X	
	Pt. Beach 1 & 2 (W)	X	
Luminant Power	Comanche Peak 1 & 2 (W)	X	

PWR Owners Group
United States Member Participation* for PA-MSC-1091, Revision 5

Utility Member	Plant Site(s)	Participant	
		Yes	No
Pacific Gas & Electric	Diablo Canyon 1 & 2 (W)	X	
PSEG – Nuclear	Salem 1 & 2 (W)	X	
South Carolina Electric & Gas	V C. Summer (W)	X	
So. Texas Project Nuclear Operating Co.	South Texas Project 1 & 2 (W)	X	
Southern Nuclear Operating Co.	Farley 1 & 2 (W)	X	
	Vogtle 1 & 2 (W)	X	
Tennessee Valley Authority	Sequoyah 1 & 2 (W)	X	
	Watts Bar 1 & 2 (W)	X	
Wolf Creek Nuclear Operating Co.	Wolf Creek (W)	X	
Xcel Energy	Prairie Island 1 & 2 (W)	X	

* **Project participants as of the date the final deliverable was completed. On occasion, additional members will join a project. Please contact the PWR Owners Group Program Management Office to verify participation before sending this document to participants not listed above.**

PWR Owners Group
International Member Participation* for PA-MSC-1091, Revision 5

Utility Member	Plant Site(s)	Participant	
		Yes	No
AXPO AG	Beznau 1 & 2 (W)	X	
EDF Energy	Sizewell B (W)	X	
Electrabel (Belgian Utilities)	Doel 1, 2 & 4, Tihange 1 & 3 (W)	X	
Electricite de France	58 Units	X	
Electronuclear ETN	ANGRA 1 (W)	X	
Emirates Nuclear Energy Corporation	Barakah 1 & 2	X	
EPZ	Borssele	X	
Eskom	Koeberg 1 & 2	X	
Hokkaido	Tomari 1, 2 & 3 (MHI)	X	
Japan Atomic Power Company	Tsuruga 2 (MHI)	X	
Kansai Electric Co., Ltd	Mihama 3, Ohi 1, 2, 3 & 4, Takahama 1, 2, 3 & 4 (W & MHI)	X	
Korea Hydro and Nuclear Power Corp	Kori 1, 2, 3, & 4 (W) Hanbit 1 & 2 (W)	X	
	Hanbit 3, 4, 5 & 6 (CE) Hanul 3, 4, 5, & 6 (CE)	X	
Kyushu	Genkai 2, 3 & 4, Sendai 1 & 2 (MHI)	X	
Nuklearna Elektrarna KRSKO	Krsko (W)	X	
Ringhals AB	Ringhals 2, 3 & 4 (W)	X	
Shikoku	Ikata 1, 2 & 3 (MHI)	X	
Spanish Utilities	Asco 1 & 2, Vandellos 2, Almaraz 1 & 2 (W)	X	
Taiwan Power Co.	Maanshan 1 & 2 (W)	X	

* **Project participants as of the date the final deliverable was completed. On occasion, additional members will join a project. Please contact the PWR Owners Group Program Management Office to verify participation before sending this document to participants not listed above.**

TABLE OF CONTENTS

LIST OF TABLES xxxix

LIST OF FIGURES xl

EXECUTIVE SUMMARY xiv

1 BACKGROUND 1-1
1.1 ORNL PWR RPV NOZZLE REPORT 1-2
1.2 OTHER PWR RPV NOZZLE EVALUATIONS 1-2
1.3 PRESSURE-TEMPERATURE LIMIT PROTECTIONS 1-2
2 FLAW SIZE 2-1
3 FRACTURE TOUGHNESS 3-1
3.1 GENERIC NOZZLE FORGING MASTER CURVE REFERENCE TEMPERATURE 3-1
3.1.1 Master Curve Data Search 3-2
3.1.2 Results from Master Curve Data Search 3-3
3.2 SURFACE EFFECT 3-10
3.3 UNDERCLAD HAZ TOUGHNESS 3-16
3.4 NEUTRON EMBRITTLEMENT 3-16
3.4.1 The Calculated Fluence Location Relative to the Postulated Flaw Location 3-20
3.4.2 Fluence Calculational Methodology 3-20
3.4.3 Neutron Streaming 3-22
3.4.4 Nozzle Neutron Embrittlement Conclusion 3-23
3.4.5 Future Increased Nozzle Fluence Projections 3-23
3.5 ADJUSTED REFERENCE TEMPERATURE 3-24
4 STRESS INTENSITY FACTOR CALCULATION 4-1
4.1 NOZZLE GEOMETRIES MODELED 4-1
4.2 MODEL/MESH 4-6
4.3 FLAW MODELING METHODOLOGY 4-7
4.4 THERMAL BOUNDARY CONDITIONS 4-9
4.5 STRUCTURAL BOUNDARY CONDITIONS 4-10
4.5.1 Displacement Restraints 4-10
4.5.2 System Pressure 4-13
4.5.3 Nozzle Mechanical Loads 4-14
4.5.4 Body Temperature 4-14
4.6 MATERIAL PROPERTIES 4-15
4.7 LOADS 4-15
4.7.1 Clad Residual Stress 4-15
4.7.2 Pipe loads 4-18
4.7.3 Cooldown Rate 4-18
4.8 STRESSES AT LIMITING LOCATIONS 4-20
4.9 STRESS INTENSITY FACTOR RESULTS 4-22
4.9.1 Static Load Cases 4-22
4.9.2 Cooldown Transient 4-26

4.10 CONSTRAINT AND CLADDING EFFECT 4-29
4.10.1 Constraint 4-29
4.10.2 Cladding 4-31
5 PRESSURE-TEMPERATURE LIMIT CURVES 5-1
5.1 GENERATION OF NOZZLE P-T LIMIT CURVES 5-1
5.1.1 Generation of Nozzle P-T Limit Curves with Postulated Small Flaw 5-1
5.1.2 Generation of Nozzle P-T Limit Curves with Postulated ¼T Beltline Thickness Size Flaw 5-6
5.2 COMPARISON OF NOZZLE TO TRADITIONAL NRC APPROVED PRESSURE-TEMPERATURE LIMIT CURVES 5-8
6 CONCLUSION 6-1
7 REFERENCES 7-1

LIST OF TABLES

Table 3-1 Specifications for A-508 Class 2 Type Forgings....3-3
Table 3-2 All Available Master Curve Data on A-508 Class 2 Type Forgings....3-5
Table 3-3 Summary of Transition Temperature Shifts for LT and TL Specimens....3-13
Table 3-4 Generic Material Properties and T_{cold} for the U.S. PWR Fleet Nozzles....3-18
Table 3-5 Comparison of a Representative Westinghouse 4-Loop Plant 54 EFPY Fluence Values using DORT, TORT, and RAPTOR-M3G....3-21
Table 4-1 Model Geometry Comparison....4-2
Table 4-2 Flaw Case List....4-7

LIST OF FIGURES

Figure 2-1 Probability of Detection and Correct Rejection for Vessels 2-2
Figure 2-2 Postulated Flaw for Outlet Nozzle Corner (example shown) 2-3
Figure 2-3 Postulated Flaws Used for Finite Element Analysis of the Nozzle Corner 2-4
Figure 3-1 Cumulative Distribution Showing the Difference between Unirradiated T_0 and RT_{NDT} 3-9
Figure 3-2 A-508 Class 2 Type Forging Cumulative Distribution Showing the Difference between RTT_0 and RT_{NDT} 3-9
Figure 3-3 Variation of Master Curve Reference Temperature through Thickness for a SA-508 Class 2 Forging 3-10
Figure 3-4 Difference of Charpy Impact Energy Near-Surface versus ¼T for a PWR Outlet Nozzle Forging 3-11
Figure 3-5 Transition Temperature Shifts for LT Specimens 3-14
Figure 3-6 Transition Temperature Shifts for TL Specimens 3-15
Figure 3-7 Transition Temperature Shift versus Fluence for Best-Estimate Chemistry 3-19
Figure 3-8 Location of the Top Support Plug Relative to the Top of the Active Fuel and the Reactor Vessel Nozzles 3-22
Figure 4-1 FEM with Inlet Nozzle, Shell, and Cladding 4-3
Figure 4-2 FEM with Outlet Nozzle, Shell, and Cladding 4-3
Figure 4-3 Diversity of Nozzle Geometries Modeled 4-4
Figure 4-4 Comparison of Modeled Baseline and Bounding Westinghouse 4-Loop Nozzle Designs 4-5
Figure 4-5 Example Cross-section View of Flaw 4-8
Figure 4-6 Example Flaw Region Mesh 4-8
Figure 4-7 Example Flaw Tip Mesh 4-9
Figure 4-8 Wetted Surface for Bulk Temperature 4-10
Figure 4-9 Full Model Boundary Conditions 4-11
Figure 4-10 Quarter-symmetry Model Boundary Conditions 4-11
Figure 4-11 Coupled Node Restraint on Top of RPV Shell 4-12
Figure 4-12 Pressure Surface 4-13
Figure 4-13 Mechanical Load Application Point 4-14
Figure 4-14 Clad Residual Stress Profile through Thickness 4-16

Figure 4-15 SIF Result Comparison for Explicit Method and Reference Temperature Method 4-18

Figure 4-16 Bounding Normal Cooldown Transient 4-19

Figure 4-17 Inlet Model without Crack – Stress for 1,000 psi Pressure 4-20

Figure 4-18 Inlet Model without Crack – Maximum Stress during Cooldown 4-21

Figure 4-19 Outlet Model without Crack – Stress for 1,000 psi Pressure 4-21

Figure 4-20 Outlet Model without Crack – Maximum Stress during Cooldown 4-22

Figure 4-21 SIF Output Location Definition 4-23

Figure 4-22 Pressure SIF along Crack Front for Baseline Outlet Nozzle with a = 1.18 Inch, L = 2.36 Inch Flaw for 1,000 psi 4-24

Figure 4-23 Pressure SIF along Crack Front for Baseline Outlet Nozzle with a = 1.18 Inch, L = 7.08 Inch Flaw for 1,000 psi 4-25

Figure 4-24 SIF for Baseline Outlet Nozzle along Crack Front with a = 1.18 Inch, L = 7.08 Inch Flaw for Deadweight + Normal Operating Thermal Mechanical Load 4-25

Figure 4-25 Pressure SIF along Crack Front for Outlet Nozzle for Different Modeled Geometries using Limiting LAS Flaw Size of 6:1 Ratio, 0.5-Inch Depth 4-26

Figure 4-26 SIF Time-history for Baseline Outlet Nozzle with a = 1.18 Inch, L = 7.08 Inch Flaw at Various Locations along the LAS Crack Front during Cooldown (Thermal and Residual) 4-27

Figure 4-27 SIF for Baseline Outlet Nozzle with a = 1.18 Inch, L = 7.08 Inch Flaw at t = 16,092 Seconds of Cooldown (Thermal and Residual) 4-28

Figure 4-28 SIF Cooldown Time-history for Outlet Nozzle for Different Modeled Geometries using Limiting LAS Flaw Size of 6:1 Ratio, 0.5 Inch Depth 4-28

Figure 4-29 T-stress/σ_y versus T_0 Dependency 4-30

Figure 5-1 Inlet Nozzle Cooldown P-T Limit Curves with Flaw Depth of 0.3 Inch (ART = 21°F) 5-2

Figure 5-2 Inlet Nozzle Cooldown P-T Limit Curves with Flaw Depth of 0.75 Inch (ART = 21°F) 5-3

Figure 5-3 Outlet Nozzle Cooldown P-T Limit Curves with Flaw Depth of 0.9 Inch (ART = 21°F) 5-3

Figure 5-4 Outlet Nozzle Cooldown P-T Limit Curves with Flaw Depth of 1.18 Inch (ART = 21°F) 5-4

Figure 5-5 Outlet Nozzle 100°F/hour Cooldown P-T Limit Curves Comparing Four Models with Limiting Flaw Geometry/Location (Surface Tip, Aspect Ratio = 6:1, 0.5-Inch Flaw in LAS) 5-5

Figure 5-6 Nozzle Corner Stress Path for Pressure and Thermal Stress Analysis (Inlet Nozzle Shown) 5-6

Figure 5-7 Nozzle Cooldown P-T Limit Curves with Flaw Depth Comparable to ¼T Beltline..5-7

Figure 5-8 U.S. PWR 10 CFR 50 Appendix G NRC Approved P-T Limit Curves..... 5-8

Figure 5-9 Westinghouse 4-Loop Bounding Nozzle P-T Limit Curves Compared to U.S. PWR NRC Approved Appendix G P-T Limit Curves (See Figure 5-10 through Figure 5-14 for Plant-Specific Cases not included) 5-9

Figure 5-10 Westinghouse 4-Loop Bounding Nozzle P-T Limit Curves Compared to Flange-Exempt Plant C NRC Approved Appendix G P-T Limit Curves 5-10

Figure 5-11 Westinghouse 4-Loop Bounding Nozzle P-T Limit Curves Compared to Flange-Exempt Plants D, E, J, and K NRC Approved Appendix G P-T Limit Curves... 5-11

Figure 5-12 Westinghouse 4-Loop Bounding Nozzle P-T Limit Curves Compared to Flange-Exempt Plants F, G and H NRC Approved Appendix G P-T Limit Curves..... 5-11

Figure 5-13 Westinghouse 4-Loop Bounding Nozzle P-T Limit Curves Compared to Flange-Exempt Plant I NRC Approved Appendix G P-T Limit Curves..... 5-12

Figure 5-14 Plant-Specific Large Flaw Nozzle P-T Limit Curves Compared to Plant A NRC Approved Appendix G P-T Limit Curves..... 5-12

Figure 5-15 CE System-80 Nozzle P-T Limit Curves Compared to U.S. CE and B&W Design NRC Approved Appendix G P-T Limit Curves 5-13

EXECUTIVE SUMMARY

Since the implementation of pressure-temperature (P-T) limit curves in the 1960s for light water reactors, the P-T limit curves have been based on the limiting locations in the reactor coolant system, which are typically the irradiated reactor pressure vessel (RPV) region adjacent to the core (beltline) and the closure head flange. Recently, it has been questioned as to whether the inlet or outlet nozzle corners could be more limiting due to the stress concentration at these locations. The work presented herein conclusively demonstrates that the RPV nozzle corner P-T limit curves are bounded by the NRC approved traditional P-T limit curves for the U.S. pressurized water reactors (PWRs).

The Nuclear Regulatory Commission (NRC) has issued Requests for Additional Information (RAIs) for License Amendment Requests (LARs) that proposed revisions to the 10 CFR 50 Appendix G P-T limit curves. The RAIs inquired as to whether the beltline region of the RPV bounds the inlet and outlet nozzle corners. NRC Regulatory Information Summary (RIS) 2014-11 was also issued clarifying that ASME Section XI, Appendix G evaluations must address the RPV nozzles. To address this issue, this report presents generic PWR fracture mechanics analyses of the RPV inlet and outlet nozzle corners in accordance with the requirements of Appendix G.

A generic fracture toughness transition reference temperature was established for the PWR nozzle forgings near the surface at the postulated flaw location as allowed by ASME Section III, Subparagraph NB-2223.2. A generic ¼ thickness fracture toughness was established based on conservative measurements of 22 representative forgings with a margin of two standard deviations to ensure a conservative lower bound toughness using NRC approved ASME Section XI Code Case N-629. The near-surface forging toughness was conservatively determined through evaluation of 31 near-surface toughness measurements. The fluence effect at the nozzle corner region was considered and was determined to have an insignificant effect on the fracture toughness at the postulated flaw location.

Detailed three-dimensional finite element analyses of postulated reliably detectable ½ inch (excluding clad thickness) and smaller surface breaking flaws in the high stress RPV inlet and outlet nozzle corners were performed. Four typical U.S. PWR plant nozzle designs were modeled to ensure the analyses bound all the U.S. PWR designs. The finite element models were used to generate stresses and stress intensity factors considering all the applicable loads, including clad residual stress, pressure, mechanical pipe loads and thermal stress for a bounding normal cooldown transient. In addition, a flaw size comparable to the beltline ¼-thickness flaw (~2.1 inch) that is considered in the traditional P-T curves was postulated in the nozzle using stresses from unflawed finite element models and the ASME Section XI, Appendix G closed form stress intensity factor solution.

The generic PWR nozzle Appendix G P-T limit curves that were developed were compared to the NRC approved Appendix G P-T limit curves for the operating U.S. PWR fleet. The results demonstrated that the nozzle P-T limit curves were bounded in every case by the current NRC approved U.S. PWR P-T limit curves. The PWR nozzle P-T limit curves are applicable through 60 years of operation. With licensee evaluation of subsequent license renewal (SLR) or other changes to nozzle fluence projections, new fluence projections can be compared to the values used in this work for applicability as discussed in the conclusion section.

Based on the results of this detailed and conservative assessment, the current operating U.S. PWR fleet P-T limit curves which have used NRC approved methodologies bound the nozzle P-T limit curves.

1 BACKGROUND

Plant-specific fracture mechanics analyses of the reactor pressure vessel (RPV) inlet and outlet nozzle corners have been performed per the requirements of ASME Section XI, Appendix G [1] to address Nuclear Regulatory Commission (NRC) issued Requests for Additional Information (RAIs) for License Amendment Requests (LARs) related to 10 CFR 50, Appendix G [2] pressure-temperature (P-T) limit curves. NRC Regulatory Information Summary (RIS) 2014-11 [3] was issued clarifying that ASME Section XI, Appendix G evaluations must address the RPV nozzles. Eleven units have been evaluated using the traditionally postulated ¼ thickness flaw for the nozzle corners, confirming that the nozzles are bounded by P-T limits based on the RPV beltline region and flange in each case. All of these evaluations were approved by the NRC:

- Seabrook Unit 1 [4]
- Farley Units 1 and 2 [5]
- Indian Point Units 2 and 3 [6 and 7]
- Point Beach Units 1 and 2 [8]
- Catawba Unit 1 [9]
- McGuire Units 1 and 2 [10]
- H. B. Robinson Unit 2 [11]

RIS 2014-11 clarified that acceptable P-T limit curve submittals must address RPV structural discontinuities (such as nozzles), not just the limiting adjusted reference temperature values in the cylindrical portion of the RPV.

The Westinghouse NRC approved methodology used to develop reactor coolant system (RCS) heatup and cooldown P-T limit curves [12] does not explicitly address the nozzles. An analysis done in 1975 using an upper bound nil-ductility reference temperature (RT_{NDT}) of 60°F for nozzles and a 1.25-inch flaw was postulated for the nozzle and it showed that the nozzles were not limiting relative to the larger RT_{NDT} and larger postulated flaw in the beltline [13]. Therefore, the nozzles were not considered limiting in the Westinghouse Appendix G P-T limit curve methodology and have not been specifically addressed in subsequent methodology updates.

Over the course of the Combustion Engineering (CE) fabrication history, the inlet and outlet nozzles were considered, but not necessarily specifically evaluated, in the analysis to establish brittle fracture limits for a CE plant as stated in the NRC approved methodology [14]. As part of RPV design and fabrication of the CE RPV, a P-T limit evaluation in accordance with ASME Section III, Appendix G requirements was performed for some or all of the RPV, as appropriate. The results of those evaluations were used to establish an initial set of P-T limits for plant operation. Per the CE methodology, the P-T limit evaluations for the regions outside of the RPV beltline, once established, do not change significantly due to exposure to neutron flux unless they are updated through regulation or more recent advances in the technology.

Framatome's NRC approved Appendix G P-T limit curve methodology considers the nozzles [15]. The limiting nozzle considered is the outlet nozzle with a 3-inch deep postulated nozzle corner flaw. The nozzle stress intensity factor (SIF) used is from Welding Research Council Bulletin, WRC-175 [16]. In Revision 4 of BAW-10046 [17], it is noted that when using a

0.1T postulated flaw the nozzle corner flaw is always bounded by the beltline P-T limit. However, this approach [17] was never used in any subsequent P-T limits submittals. Instead, consistent with Appendix G of the applicable ASME Section XI Code and Framatome's NRC approved methodology [15], a 3-inch deep postulated flaw was used to construct the limiting composite P-T limit curve in all submittals to date.

1.1 ORNL PWR RPV NOZZLE REPORT

A separate PWR and BWR RPV nozzle corner analysis performed by Oak Ridge National Laboratory (ORNL), as reported in ORNL/TM-2010/246, Revision 1 [18], was used as a comparison to the fracture mechanics evaluation performed herein. The ORNL work was performed to gain a better understanding of nozzle stress and fracture mechanics solutions as they apply to P-T limit curves. The analysis in Reference [18] investigated a 4-loop PWR outlet and inlet nozzle having generally consistent geometry to that of one of the models considered in this report. The ORNL PWR and BWR RPV analysis considered a ¼ thickness (¼T) circular corner crack and an approximated shallower 0.1T corner crack. The three-dimensional (3D) SIF analysis results and conclusions from ORNL analysis are considered and compared to the evaluations performed in this report.

1.2 OTHER PWR RPV NOZZLE EVALUATIONS

Stevens, et al. performed a probabilistic evaluation of the RPV nozzles using a modified version of the FAVOR Code [19]. For normal operational cooldown transients it was stated that the "analysis demonstrates that, given the range of material properties for nozzles in the fleet, it is highly unlikely that the nozzle will ever be the limiting condition for this loading/flaw combination." The conclusion was: "Neglecting nozzles in FAVOR calculations for flaws of sizes expected in PWR RPVs is reasonable." However, the analysis demonstrated that for low embrittled PWRs using deterministic evaluations with the larger ¼T postulated nozzle flaw, that the nozzles can produce more limiting P-T limits than the beltline ¼T flaw.

Using a detailed 3D finite element analysis (FEA), Siegele, et al. [20], demonstrated for various flaw sizes and both loss of coolant accident scenarios and normal operating transients that crack initiation would not occur in the nozzle in a German 1300 MW PWR.

1.3 PRESSURE-TEMPERATURE LIMIT PROTECTIONS

At RCS temperatures lower than approximately 350°F, the RPV becomes more vulnerable to non-ductile failure. The P-T limit curves protect against pressures that might lead to failure. To provide further protection, all plants are required to have a low-temperature overpressure protection (LTOP) system. The LTOP system protects against brittle fracture of the RPV ferritic steel components such as the beltline and the nozzles during an unanticipated event when the system pressure might reach the P-T limit curve. LTOP may also be referred to as cold overpressure protection system (COPS) or cold overpressure mitigating system (COMS).

Depending upon the plant design and operations, LTOP is ensured by one or a combination of the following types of plant system components:

- Westinghouse residual heat removal (RHR) system relief valves,
- CE shutdown cooling (SDC) relief valves,
- B&W plants are equipped with either: (1) a dual setpoint pilot-operated relief valve that is set below the LTOP limit, or (2) an additional relief valve (e.g., decay heat removal system relief valve) that is also set below the LTOP limit [17],
- Pressurizer power-operated relief valves (PORVs).

With RHR (SDC for CE plants or B&W decay heat removal system) in operation, the RHR, SDC or decay heat removal system relief valves provide overpressure protection via their pressure setpoints. Some plants may have an additional or supplemental line of protection against overpressure provided by the pressurizer PORVs, which have pressure setpoints that are in service at the enable temperature.

For Westinghouse-designed plants, the RHR system design pressure is 600 psig, while the RHR relief valve setpoint is nominally set at 450 psig. The LTOP system, which uses the pressurizer PORVs with reduced lift settings, is designed to protect the lower of the P-T limit curve or the PORV discharge piping limit of 800 psig. Depending on the plant design basis, one or both of these systems are capable of maintaining pressures below the nozzle and beltline P-T limit curves at temperatures below the LTOP enable temperature.

2 FLAW SIZE

The nozzle corner region is examined at various times in the manufacturing process, during the pre-service inspection, and during periodic in-service inspections (ISI). Such pre-service examinations (consisting of surface and volumetric methods) were intended to preclude the existence of inside diameter surface planar flaws (cladding surface origin) and underclad (clad/base metal interface origin) planar flaws prior to plant operation. In addition, volumetric examinations have been conducted of the inlet and outlet nozzle inner regions since the inception of ASME Section XI in 1970 through 2003 when the NRC approved [21] ASME Code Case N-648-1. Since then, some licensee examinations have elected to apply enhanced visual examinations using a 0.001-inch width wire resolution on these same nozzle inner region surfaces in lieu of the volumetric examinations. To date, no flaws have been found in PWR inlet and outlet nozzle corner regions using volumetric or visual exams.

A postulated ¼T flaw in the nozzle corner region can result in a depth of approximately 4 to 5 inches as measured at a 45° angle from the nozzle corner to the RPV outside. The nozzle and RPV are thicker in the vicinity of nozzles per the ASME design requirements. The reference postulated flaw for the ASME Section XI, Appendix G, Subsubarticle G-2120, "Maximum Postulated Defect," flaw evaluation may be less than 25% of the section thickness [1]:

> *"Smaller defect sizes may be used on an individual case basis if a smaller size of maximum postulated defect can be ensured."*

Such sizes are permissible as long as the reference flaw satisfies the following statement, which was taken from paragraph 5.C.(2) of Welding Research Council bulletin WRC-175 [16]:

> *"...examination methods must be able to assure smaller defects in those locations (are detectable)."*

Magnetic particle examination of the nozzle forging was performed at the time of fabrication in accordance with ASME Code Section III, Paragraph NB-2545. Indications greater in length than 1/16 inch were considered relevant. The postulated flaw size must be greater than the smallest indication that can be detected.

The postulated flaw size must also be detectable by ISI, and this can be demonstrated using Performance Demonstration Initiative (PDI) data obtained in 2001 by the Electric Power Research Institute (EPRI) Nondestructive Evaluation (NDE) Center, as shown in Figure 2-1. This figure depicts the expected rejection probability as a function of flaw depth. The probability of correct rejection considers both the detection capability and sizing capability for flaws. For example, Figure 2-1 shows that the probability of correctly detecting and rejecting a flaw with a depth of 0.25 inches is 90%. ASME Code Section XI, Appendix VIII PDI demonstrations were initiated in 1994, for Supplements 4 and 6. Five inspection vendors and more than 50 personnel have completed Appendix VIII Supplement 4, clad-to-base-metal demonstrations per the 2001 Reference [22]. In this time no individual, even those who failed the test, failed to detect cracks deeper than approximately 0.25 inch.

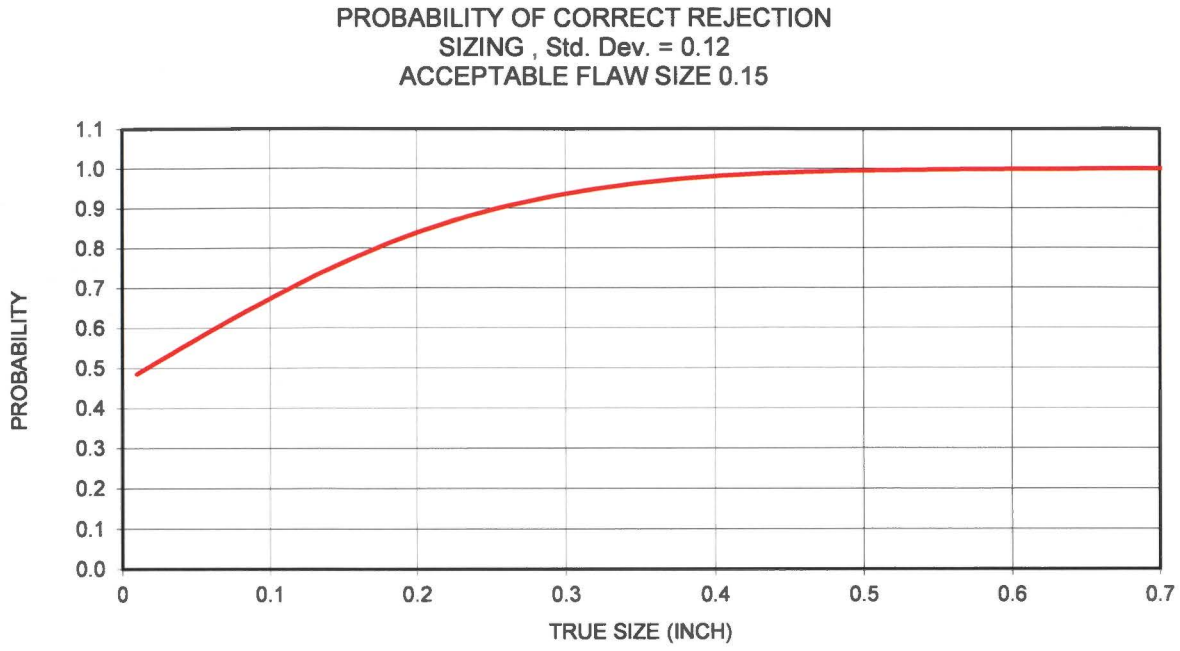

Figure 2-1 Probability of Detection and Correct Rejection for Vessels [23]

The results shown in Figure 2-1 are based on ultrasonic test (UT) qualification tests for the RPV shell regions. The probability of detection for the more complicated nozzle corner would also be high since the pre-service UT inspection was performed from both the inside of the RPV shell and the inside surface of the nozzle bore, so there is more opportunity to find reflectors.

EPRI NDE Center concluded the following regarding boiling water reactor (BWR) Nozzle Blend Radii [23]:

> *"Performance capabilities of ultrasonic techniques for examination of the reactor pressure vessel shell nozzles and shell welds have improved substantially since 1985. Analysis of the PDI database has provided valuable insight into the effectiveness of these ultrasonic examinations. Evaluations presented herein demonstrate that the probability of detecting and sizing flaws equal to and greater than 0.25 inches in depth, located at the inside surface and the clad-to-base metal interface, is excellent."*

A 0.25-inch initial flaw size is used for BWR feedwater nozzle crack growth analyses based on the ability of modern ultrasonic testing techniques to accurately locate and size cracks as small as 0.25 inch in depth [24].

In light of the capability to reliably detect a 0.25-inch flaw, a 0.5-inch postulated flaw was conservatively chosen for assessment. The 0.5-inch flaw depth was postulated from the clad low-alloy steel (LAS) interface to the deepest point of the flaw. The total depth of the postulated flaw considering the cladding thickness can be substantially larger, as shown in Figure 2-2. For example, in Figure 2-2, the total depth of the flaw from the wetted surface is 1.18 inches for the

outlet nozzle corner, but the depth in the LAS nozzle forging is 0.5 inches due to the relatively thick cladding on the outlet nozzle corner. The flaw depth defined from the clad-LAS interface into the LAS is consistent with the required examination volume in Figure IWB-2500-7(a) and (b) and the Section XI, Appendix G, Figure 2223-1 definition. Since the flaw sizes postulated for both the inlet and outlet nozzle corners are larger than those which can be detected with high certainty, the requirements of ASME Section XI, Appendix G, Subsubarticle G-2120 are met. Therefore, such postulated flaw sizes are acceptable in regards to the requirements of 10 CFR 50, Appendix G.

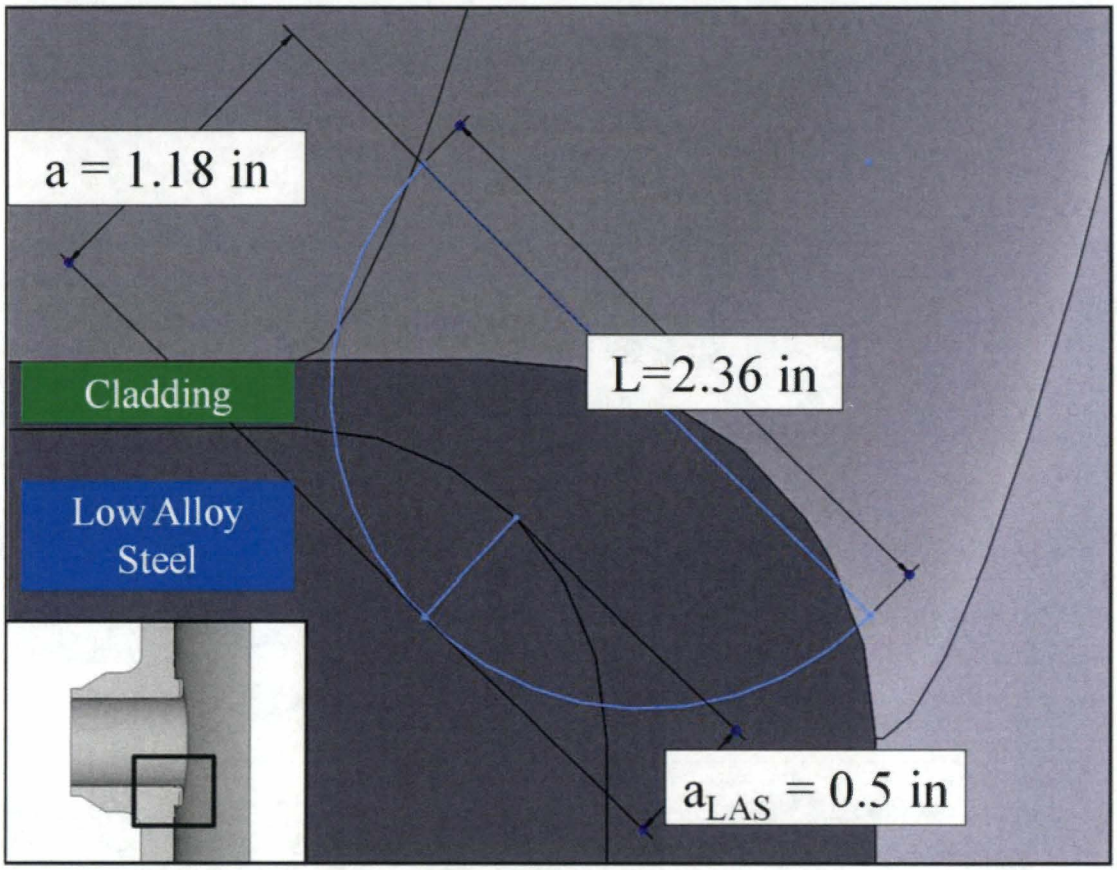

Figure 2-2 Postulated Flaw for Outlet Nozzle Corner (example shown)

In addition to the postulated flaw that extends 0.5 inch into LAS, a smaller flaw (0.05 inch) was postulated to address the high stress imparted near the clad-LAS interface due to clad-LAS differential coefficients of thermal expansion (CTE). Two flaw aspect ratios were also postulated for each postulated flaw size. A circular flaw with a/L = ½ and a semi-ellipse with a/L = 1/6 were postulated. Figure 2-3 graphically shows the eight postulated flaws. The use of the smaller flaw sizes and the two different aspect ratios were also evaluated by ORNL [18].

There are three principal margins inherent in the non-ductile failure rules of the ASME Code. These are the postulated flaws, the lower bound fracture toughness, and the required factor of safety of 2.0 on the mechanical stresses. Therefore, the reduction of one of these margins (i.e.

flaw size) in discontinuity regions was deemed to be acceptable by the original authors of Appendix G, and its basis document, Welding Research Council bulletin WRC-175 [16].

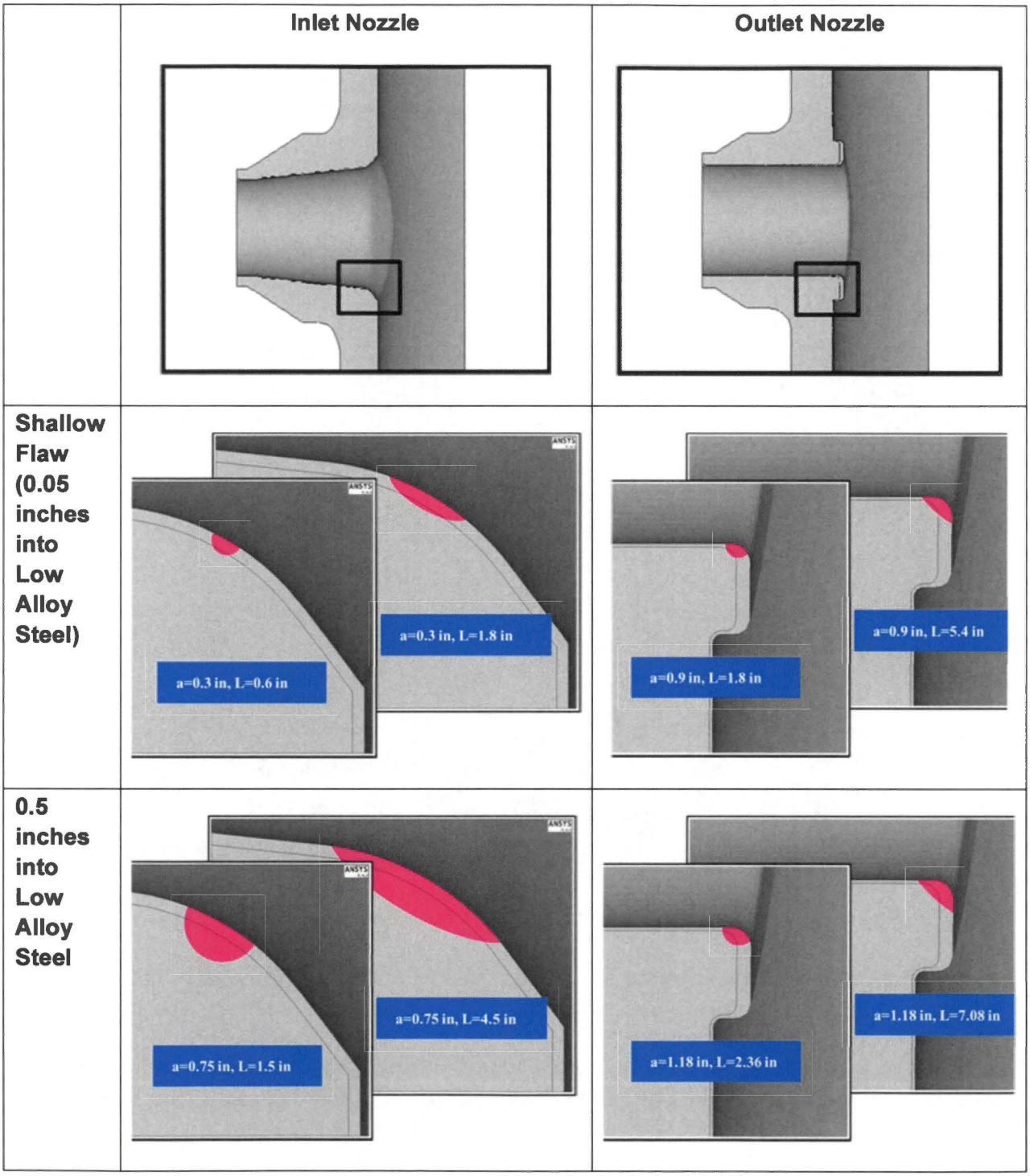

Figure 2-3 Postulated Flaws Used for Finite Element Analysis of the Nozzle Corner

3 FRACTURE TOUGHNESS

The fracture toughness is generically established for the U.S. PWR fleet of nozzle forgings from test data of typical representative forgings using the master curve method. Then, since the postulated flaws are relatively small, the toughness is adjusted to account for the improved near-surface properties using a database of measurements. The potential effect of neutron embrittlement on the fracture toughness is evaluated. Finally, a generic bounding adjusted reference temperature (ART) is established for the nozzles, which is then used with the applied SIF for the P-T limit curve calculations.

The master curve method for locating the ductile-brittle transition reference temperature is more accurate than RT_{NDT} since it is based on fracture toughness data as described in Section 3.1. Another significant advantage to using a generically established master curve reference temperature is the avoidance for the need to estimate RT_{NDT}. Many of the RPVs in the U.S. PWR fleet were fabricated to ASME Code years prior to 1972, the first year in which the definition RT_{NDT} was codified in Subarticle NB-2300. Therefore, methods were developed, such as NRC Branch Technical Position 5-3, to estimate RT_{NDT} from material test data which was available from RPVs fabricated in prior years. The conservatism of this estimation method was called into question [25], therefore use of a generically established master curve reference temperature does not have this potential non-conservatism.

3.1 GENERIC NOZZLE FORGING MASTER CURVE REFERENCE TEMPERATURE

The use of the lower bound K_{IC} curve has inherent margin since RT_{NDT} is a conservative method for locating the K_{IC} curve [26 and 27]. The temperature index, RT_{NDT}, is based on drop weight testing, which is a crack arrest transition temperature measurement, and the Charpy impact test, which is a blunt notch impact test. These data are conservatively bounded by the K_{IC} curve, which is a lower bound crack initiation fracture toughness curve. In contrast, the master curve method is based on an initiation transition temperature true fracture toughness test technique. The master curve index temperature (T_0) provides a much more accurate measure of the material fracture toughness than RT_{NDT} and K_{IC} [28]. Existing master curve fracture toughness data for A-508 Class 2 type forgings was gathered to establish a generic mean and standard deviation alternate RT_{NDT} for the U.S. PWR inlet and outlet nozzles. This information is used with ASME Section XI Code Case N-629 [29], which has been endorsed by the NRC per Regulatory Guide 1.147 [21] and endorsed by reference in 10 CFR 50.55a [30] as an alternative to RT_{NDT}. As precedent, generic RTT_0 values, as defined in Code Case N-629, have been approved for use for the high copper (Cu) Linde 80 class of materials as an alternate to RT_{NDT} by the NRC [31]. Additionally, NRC Regulatory Issue Summary 2004-04 [32] states the following:

> *Use of NRC approved ASME Code Cases (e.g., N-588, N-640, and N-641) in conjunction with earlier versions of the ASME Code endorsed in 10 CFR 50.55a may also be used for the development of P-T limit curves without the need for an exemption.*

Since Code Case N-629 is endorsed by reference in 10 CFR 50.55a, an exemption is not required for its use by the licensees.

3.1.1 Master Curve Data Search

Master curve data were gathered from the open literature, the EPRI fracture toughness database, and internal Westinghouse references. Thick section A-508 Class 2 or similar forgings that were used in RPV fabrication or are representative of the materials used to construct the U.S. PWR inlet and outlet nozzles are included. Materials that were heat treated specifically to represent embrittled materials were excluded. The intent is to capture all available transition temperature fracture toughness data to establish a generic master curve transition reference temperature for A-508 Class 2 type forgings. The data and variability bound the U.S. RPV A-508 Class 2 forgings. Only quasi-static data were collected.

The nozzle forgings used in the U.S. PWR fleet are all ASME SA-508 Class 2 or ASTM A-508 Class 2 with the following exceptions: Prairie Island Units 1 and 2 nozzles, which are SA-508 Class 3, Palo Verde Units 2 and 3 (which are a combination of SA-508 Classes 2 and 3), and Ginna (which are SA-336). Note that the Ginna nozzles meet the A-508 Class 2 specification requirements per the Ginna Certified Material Test Reports (CMTRs). Substantial master curve data assessed [33] for A-508 Class 3 showed generic RTT_0 of A-508 Class 3 to be better than A-508 Class 2 by 16°C (28°F), therefore the A-508 Class 2 generic RTT_0 developed herein is conservative relative to A-508 Class 3 forgings.

The SA-508 Class 2 and A-508 Class 2 designations are synonymous and are nearly the same as the current ASME SA-508 Grade 2 Class 1 designation, although the specified chemistry limits changed slightly through the years. A-508-64 Class 2 is the ASTM specification and was used prior to ASME adoption of the same specification as SA-508 Class 2. Japanese Industrial Standard (JIS) G 3204 SFVQ2A steel forgings have essentially the same chemistry, tensile and Charpy requirements as SA-508 Class 2 [34]. In addition, the Deutsche Industrie Normen (DIN) 22NiMoCr37 specification is similar to SA-508 Class 2 [35]. Table 3-1 compares chemical and mechanical requirements for 22NiMoCr37, ASTM A-508-64 Class 2, SA-508 Class 2 (1971), and SA-508 Grade 2 Class 1 (2007). The differences in these specification limits are minor, with all being considered the same alloy [36].

The data search included SA-508 Class 2, A-508 Class 2, 22NiMoCr37, and SFVQ2A materials that were commonly used to construct RPVs. In addition, one heat of 20NiMoCr26 was also included, having chemistry and mechanical properties that meet the SA-508 Class 2 specification. The forging specification commonly used for the French RPVs was RCC-M 16MND5, which is similar to SA-508 Class 3 [39]; therefore, data from these materials were not included. Class 2 includes a specified range of Cr (Class 3 limits Cr to a lower level), while Class 3 has a higher Mn content than Class 2 [38]. The EURO forging, for which extensive master curve testing was conducted, appeared to meet neither 22NiMoCr37 or SA-508 Class 3, although it has been claimed as 22NiMoCr37 [40]. For this reason, the EURO forging was not included.

Table 3-1 Specifications for A-508 Class 2 Type Forgings

	Chemical Composition									Mechanical	
Specification	C %	Mn %	P %	S %	Si %	Ni %	Cr %	Mo %	V %	YS[1] ksi	Tensile ksi
22NiMoCr37 [35]	0.17-0.25	0.50-1.00	0.025 max	0.025 max	0.35 max	0.60-1.00	0.30-0.50	0.50-0.80	0.05 max	57 min	81-102
ASTM A-508-64 Class 2 [37]	0.27 max	0.50-0.80	0.025 max	0.025 max	0.15-0.35	0.50-0.90	0.25-0.45	0.55-0.70	0.05 max	50 min	80 min
SA-508 Class 2 (1971) [38]	0.27 max	0.50-0.90	0.025 max	0.025 max	0.15-0.35	0.50-0.90	0.25-0.45	0.55-0.70	0.05 max	50 min	80 min
SA-508 Grade 2 Class 1 (2007) [38]	0.27 max	0.50-1.00	0.025 max	0.025 max	0.40 max	0.50-1.00	0.25-0.45	0.55-0.70	0.05 max	50 min	80-105

Note:
1. YS = Yield Strength

3.1.2 Results from Master Curve Data Search

Transition temperature fracture toughness data sufficient to calculate T_0 or calculated T_0 values were found for 22 distinct forgings. These forgings are, in most cases, the same as were used in commercial PWRs or BWRs. In all cases, the heats selected are representative of the forgings used in commercial PWRs and BWRs. The forgings represent Japanese, Swedish, German, and U.S. RPVs. The references were checked to ensure that all data were collected from unique forgings. Although the production year of each forging with T_0 data could not be confirmed, the majority of the forgings were determined to have been produced in a similar time frame to the nozzle forgings in the U.S. PWR fleet.

One master curve test data set was found for SFVQ2A steel. The bulk of master curve testing was performed on 22NiMoCr37 forgings. Some older K_{IC} data is available for A-508 Class 2 forgings. The results are detailed in Table 3-2. RT_{NDT} for many of the forgings was reported as shown in Table 3-2. The range of RT_{NDT} values in Table 3-2 exceeds the range of the RT_{NDT} values generally observed in U.S. PWR nozzle forgings utilizing NB-2300 criteria, which typically fall between -34°C and -12°C. Additionally, the average RT_{NDT} of the values from Table 3-2 (-11°C) falls above this typical range of RT_{NDT} values observed for U.S. PWR nozzle forgings based on measured data and NB-2300 criteria. Since RTT_0 is an alternate to RT_{NDT}, the developed RTT_0 can be considered conservatively representative of the U.S. PWR fleet forgings.

In some cases, only K_{IC} was reported. The master curve reference temperature can conservatively be developed from K_{IC} values. K_{IC} values are always the same or lower than the

K_{JC} value from the same test, and thus the developed T_0 value would be conservative. Due to the ASTM E399 [41] limitation on ductility, the resulting T_0 from K_{IC} values and K_{JC} values are reasonably close [42]. K_{IC} is defined by ASTM E399 and is K where the load displacement trace deviates from linearity by 5%, whereas K_{JC} is K converted from J at cleavage, as defined in ASTM E1921 [43]. Only data from standard ASTM E1921 specimen geometries were included. Test data from wedge opening loading (WOL) specimen geometry was excluded since it is not an ASTM E1921 standard geometry.

The typical location for removing a test specimen from a forging is at the ¼ or ¾ thickness (¼T or ¾T) location. If reported in the data source, the thickness location of specimen removal is indicated in Table 3-2. The toughness is better near the quenched and tempered forging surfaces. Therefore, it is standard conservative practice to remove specimens at the ¼ thickness location. Specimens related to RPV surveillance programs that comply with ASTM E185 are required to be removed for the ¼ thickness locations [44]. For these reasons, it is assumed that the specimens for which thickness location values were not reported were removed at or between ¼T and ¾T locations.

3.1.2.1 Specimen Geometry Constraint Adjustment

The tested specimen geometries are shown in Table 3-2. Tregoning and Joyce observed a systematic, non-conservative bias toward the Single Edge Notched Bend (SE(B)) specimen of generally 5°C to 10°C relative to the compact tension (CT) specimen geometry due to its lower constraint [45]. The NRC used a 4.7°C bias term for the Kewaunee RPV [46]. The Babcock & Wilcox Owners Group (B&WOG) data showed a varying SE(B) bias averaging 10°C, which was approved by the NRC [31]. More recently, the ASTM committee recognized an average difference between the CT and SE(B) of 10°C, which is included in the E1921 consensus standard [43]. Therefore, a bias of 10°C was added to the SE(B) T_0 values to adjust for the lower constraint SE(B) geometry, as shown in Table 3-2.

Table 3-2 All Available Master Curve Data on A-508 Class 2 Type Forgings

Material Identity	Specification	Measured Value / Standard	Number of Data Points Valid / Total	RT_{NDT} (°C)	T_0 (°C)	Geometry	T_0 (°C) SE(B) Adjusted	Thickness Location	Valid T_0	Orient-ation
JTK15 Japanese K_{IR} Committee [34]	SFVQ2A	K_{IC} & K_{Jc} / E1921-97	6/20	-30	-99	1TCT	-99	¼T	Y	NR
ASME K_{IC} [47, 48] Database[1] RT_{NDT} = 11°C	A-508 Class 2	K_{IC} / E399	7/9	11	-57	2TCT, 4TCT, 6TCT	-57	NR	Y	NR
ASME K_{IC} [47, 48] Database[1] RT_{NDT} = 18°C	A-508 Class 2	K_{IC}/ E399	6/10	18	-21	2TCT, 8TCT	-21	NR	N[2]	NR
SCK-CEN FG2-¼T [49]	A-508 Class 2	K_{Jc} / E1921-08	NR/32	≥-18	-95	SE(B)	-85	¼T & ¾T	Y	TL
JSW4C [50]	A-508 Class 2	NR	6/8	-37	-84	1TCT, 2TCT	-84	NR	Y	NR
CARISMA P7-Klockner [51]	22NiMoCr37	K_{Jc} / E1921-05	NR	-5	-88	SE(B)	-78	NR	Y	TL
CARISMA P147-JSW [51]	22NiMoCr37	K_{Jc} / E1921-05	NR	-17	-112	SE(B)	-102	NR	Y	TL
Atucha I 41.1 [52]	22NiMoCr37	K_{Jc} / E1921-97	NR/12	NR	-42	1TCT	-42	¼T & ¾T	Y	TL
German Nozzle Flange Ring – A [53]	22NiMoCr37	K_{Jc} / E1921-97	NR/8	NR	-75	SE(B)	-65	½T	NR	TL
German Nozzle Flange Ring – B [53]	22NiMoCr37	K_{Jc} / E1921-97	NR/8	NR	<-90	SE(B)	<-80	½T	NR	TL

Table 3-2 All Available Master Curve Data on A-508 Class 2 Type Forgings (cont.)

Material Identity	Specification	Measured Value / Standard	Number of Data Points Valid / Total	RT_{NDT} (°C)	T_0 (°C)	Geometry	T_0 (°C) SE(B) Adjusted	Thickness Location	Valid T_0	Orient-ation
German Nozzle Flange Ring – C [53]	22NiMoCr37	K_{Jc} / E1921-97	NR/8	NR	-17	SE(B)	-7	≥55mm from surface(3)	NR	TL
German Nozzle Flange Ring – D [53]	22NiMoCr37	K_{Jc} / E1921-97	NR/8	NR	-43	SE(B)	-33	≥55mm from surface(3)	NR	TL
KRB-A GEB2 Gundremmingen [54]	20NiMoCr26(4)	K_{Jc} / E813-81	16/18	NR	-53	½TCT	-53	¼T & ½T	Y	TL
CARINA P150-JSW [55, 56, 57]	22NiMoCr37	K_{Jc} / E1921-13	NR	-10	-109	SE(B)	-99	NR	Y	TL
CARINA P151-Klockner [55, 56, 57]	22NiMoCr37	K_{Jc} / E1921-13	NR	-15	-110	SE(B)	-100	NR	Y	TL
Ringhals 4 Lower Shell [56]	SA-508 Class 2	K_{Jc} / E1921-11	NR	-47	-135	SE(B)	-125	¼T	NR	TL
Ringhals 4 Inter. Shell [56]	SA-508 Class 2	K_{Jc} / E1921-11	NR	-47	-123	SE(B)	-113	¼T	NR	TL
Ringhals 3 Lower Shell [56]	SA-508 Class 2	K_{Jc} / E1921-11	NR	44(5)	-79(5)	SE(B)	-69	¼T	NR	TL
Ringhals 3 Inter. Shell [56]	SA-508 Class 2	K_{Jc} / E1921-11	NR	20(5)	-82(5)	SE(B)	-72	¼T	NR	TL
Borssele Ring 3 [36, 58]	22NiMoCr37	K_{Jc} / E1921-05	NR	-10	-106	SE(B)	-96	¼T	NR	TL

Table 3-2 All Available Master Curve Data on A-508 Class 2 Type Forgings (cont.)

Material Identity	Specification	Measured Value / Standard	Number of Data Points Valid / Total	RT_{NDT} (°C)	T_0 (°C)	Geometry	T_0 (°C) SE(B) Adjusted	Thickness Location	Valid T_0	Orient-ation
Borssele Ring 4 [36, 58]	22NiMoCr37	K_{Jc} / E1921-05	NR	-20	-106	SE(B)	-96	¼T	NR	TL
BMWi [59]	22NiMoCr37	K_{Jc} / E1921-02	NR	NR	-65	various	-55	NR	Y	NR

NR = not reported; SE(B) = three point bend specimen; xTCT = x-inch thick compact tension fracture specimen; TL = transverse to the primary working direction

Notes:

1. There is a third heat of A-508 Class 2 that was included in this old dataset, which was used to construct the ASME K_{IC} curve, but it is not included here since the specimen geometry was WOL. The T_0 for this heat is -84°C.
2. While this measurement did not produce a valid T_0 value, it was still included in the analysis, as it is the highest T_0 found and therefore ensures a conservative result.
3. This German nozzle flange ring forging is exceptionally thick at 640mm (25 inches). T_0 was measured through thickness from the surface. The relevant location for U.S. RPV beltline forgings is at ¼T location which is approximately 2 inches (~55 mm) from the surface. Therefore, the T_0 measurement at this depth location is used for the German nozzle flange rings C and D.
4. The measured chemistry and mechanical properties meet the SA-508 Class 2 specification for this forging. This forging is from a decommissioned 250MW BWR which was placed in service in 1966. It had a thinner wall than PWRs (4.7 inches versus 6.5 to 11 inches).
5. These are irradiated to 4.3×10^{19} n/cm^2. The unirradiated T_0 would be significantly lower; therefore, the irradiated T_0 used is conservative. RT_{NDT} is adjusted for irradiation for comparison purposes only.

3.1.2.2 Calculation of Generic Mean Alternate RT_{NDT}

Averaging all the A-508 Class 2 type forging heat adjusted T_0 values in Table 3-2 provides a mean SE(B) adjusted T_0 of -74.1°C (-101.4°F) with a standard deviation of 30.3°C (54.5°F). When the 19.4°C (35°F) is added per ASME Code Case N-629 to T_0, the resultant alternate mean RT_{NDT} (RTT_0) is

$$\text{Alternate generic mean } RT_{NDT} = RTT_0 = -74.1°C + 19.4°C = -54.7°C \ (-66.4°F)$$

This can be substituted for the initial RT_{NDT} in the following equation:

$$ART = \text{Initial } RT_{NDT} + \text{Margin} + \Delta RT_{NDT} \ [60]$$

Where:

$$\text{Margin} = 2 \ (\sigma_I^2 + \sigma_\Delta^2)^{0.5}$$

"σ_I is the standard deviation obtained from the set of data used to establish the mean." [60 and 61] and was determined to be σ_I = 30.3°C (54.5°F) from the 22 measurements reported in Table 3-2.

If there is no ΔRT_{NDT} due to embrittlement then $\sigma_\Delta = 0$ and

$$\text{Margin} = 2 \ \sigma_I = 61°C \ (109°F)$$

The resultant generic alternate ART at the ¼T location is

RTT_0 (with margin) = -54.7°C + 2 * 30.3°C = 6°C (**43°F**).

This value is lower than the NRC approved upper bound of 60°F for forgings [62].

The difference between RT_{NDT} and T_0 can be substantial for most RPV materials as demonstrated in Figure 3-1. This difference has been used to demonstrate margin between RT_{NDT} and RTT_0 [up to 80°C (150°F)]. However, it is material dependent and unknown for any particular material without testing. Figure 3-2 shows the cumulative distribution of the difference between RT_{NDT} and RTT_0 for the A-508 Class 2 type forging data gathered in Table 3-2. This heat-specific data supports the above conclusion that there is an improvement in the generic upper bound value of RTT_0 relative to RT_{NDT} even with the large variation (σ_I) seen in the A-508 type forgings.

The approach of using a generic initial alternate RT_{NDT} for RTT_0 is beneficial because it is based on fracture toughness data and, thus, gives a more realistic representation of the actual toughness of the nozzle forgings. This approach also avoids using RT_{NDT} estimation methods, which are required for many nozzles, and the approach is conservative. The approach taken herein to establish the alternate RTT_0 is conservative because the data used to establish the mean and standard deviation included irradiated materials, K_{IC} data, a material with RT_{NDT} greater than 60°F, and a large diversity of relevant forgings. The relatively large σ_I due to the diversity of forgings assessed ensures conservatism when applied with the margin term.

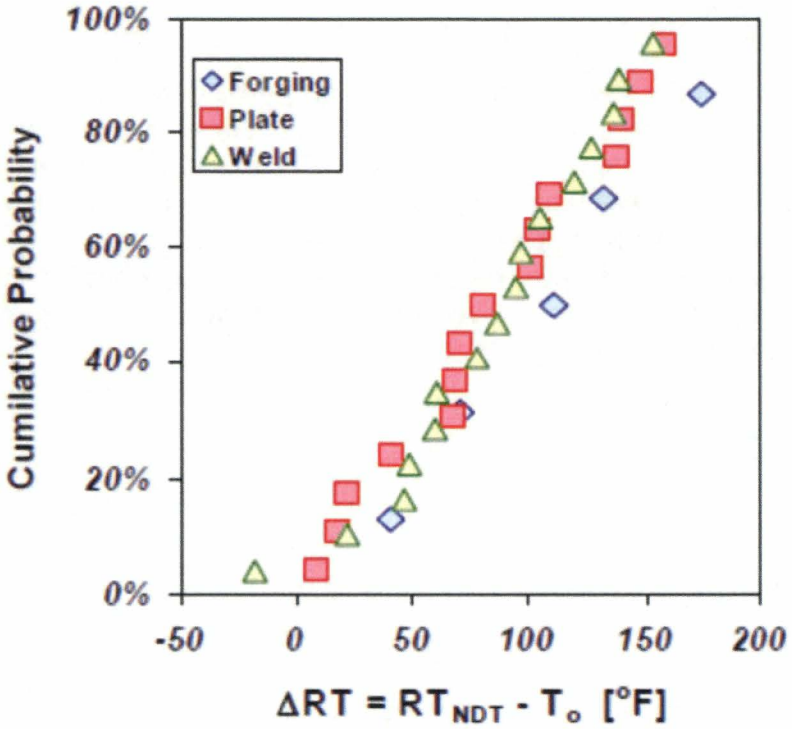

Figure 3-1 Cumulative Distribution Showing the Difference between Unirradiated T_0 and RT_{NDT} [27]

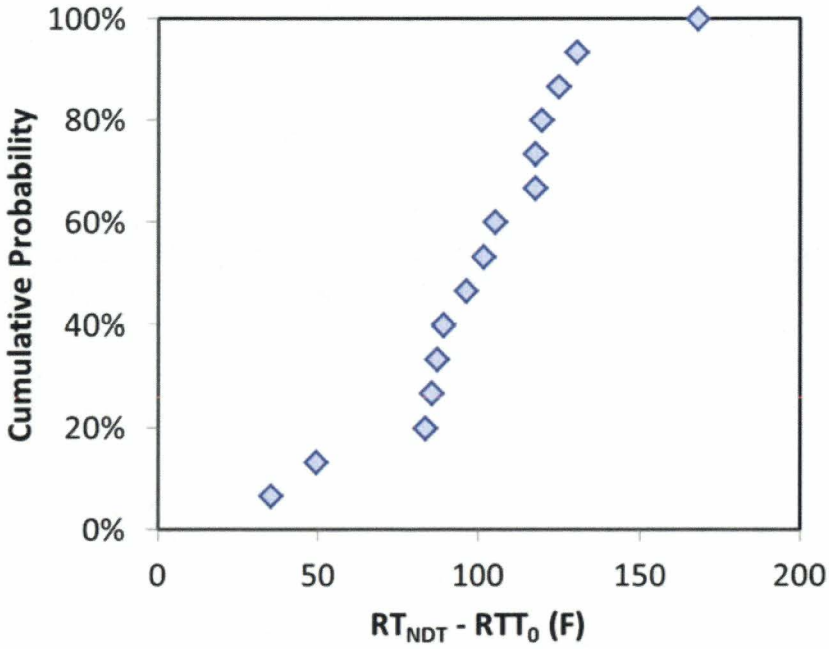

Figure 3-2 A-508 Class 2 Type Forging Cumulative Distribution Showing the Difference between RTT_0 and RT_{NDT}

3.2 SURFACE EFFECT

Since quenching thick forgings results in a faster cooling rate near the surface of the forging, surface mechanical properties are typically superior to internal mechanical properties, as a result of grain size and microstructural differences. An increased cooling rate results in a finer microstructure and, therefore, a better toughness [63]. The critical cooling rate for bainite is lower than martensite [64]. Thus, since the cooling rate is faster at the surface, it is likely that the forging surface will have a smaller carbide phase and more tempered martensite. These differences at the surface result in improved fracture toughness (e.g., Figure 3-3) and better Charpy impact properties (e.g., Figure 3-4).

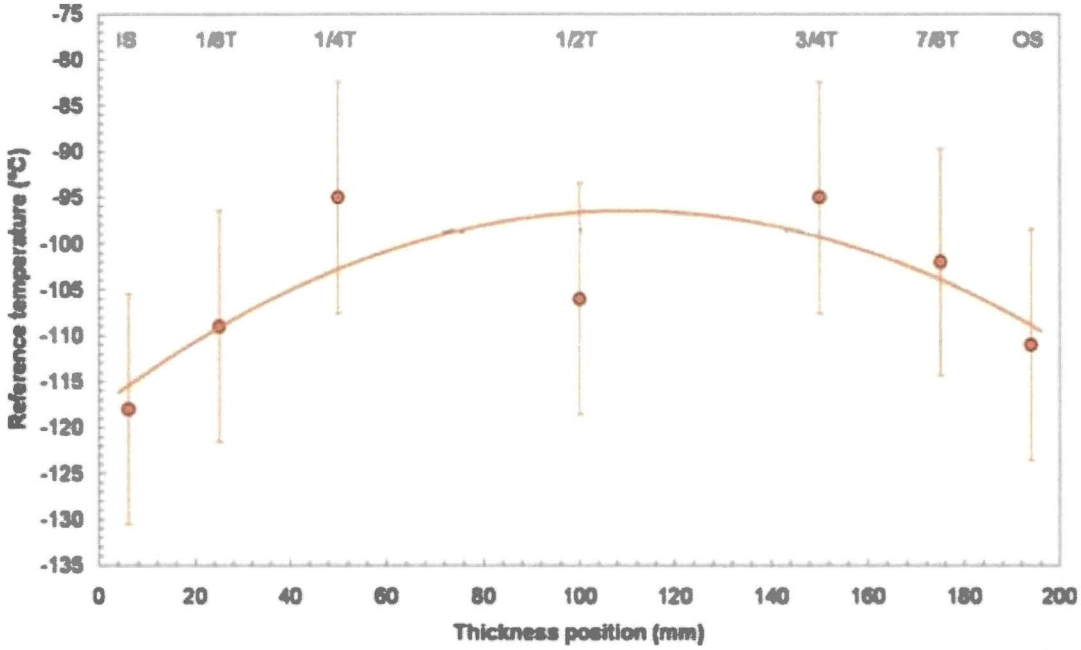

Figure 3-3 Variation of Master Curve Reference Temperature through Thickness for a SA-508 Class 2 Forging [63]

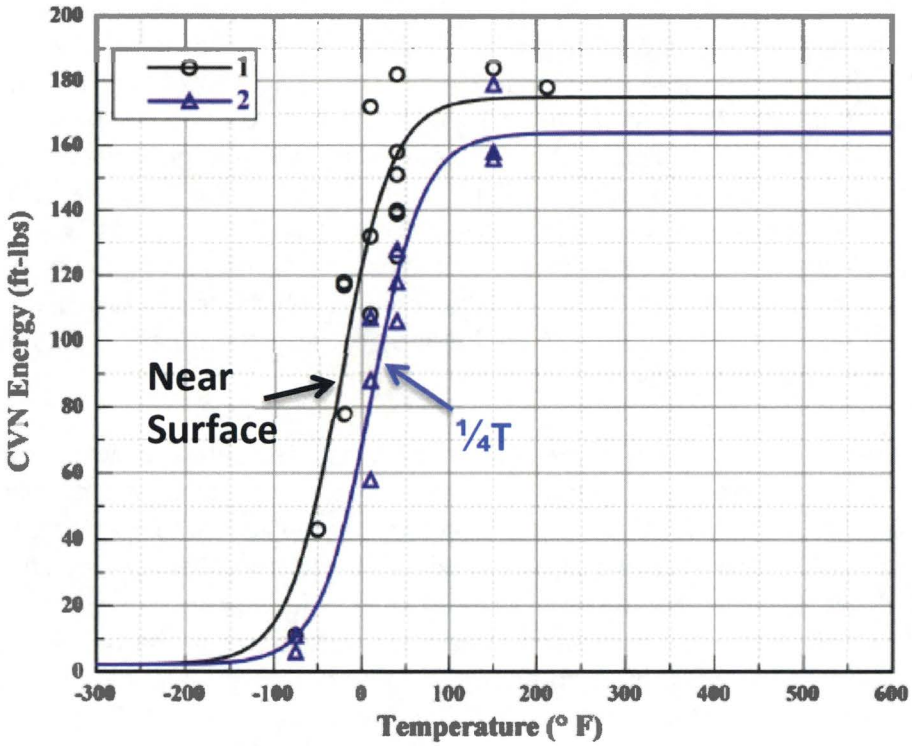

Figure 3-4 Difference of Charpy Impact Energy Near-Surface versus ¼T for a PWR Outlet Nozzle Forging

For very thick and complex forgings, ASME Subparagraph NB-2223.2 [65] requires that the longitudinal axes of the specimens used to determine RT_{NDT} shall not be nearer than ¾ inch to any heat-treated surface. Use of the transition temperature near the surface is, therefore, appropriate since the largest postulated flaw in this evaluation is ½ inch deep into the LAS.

Through thickness variation measurements of ductile-to-brittle transition temperature were gathered for as many applicable ASTM A-508, Class 2 (and similar specification) forgings as possible from the published literature [34, 49, 66, 67, 68 and 69] and internal sources from Westinghouse and Framatome.

In the analysis, the surface transition temperature (as measured by Charpy 30 ft-lb or Master Curve T_0) was compared against the ¼T transition temperature for 24 sets of longitudinal (LT) and seven sets of transverse (TL) data. Note that data without a reported orientation was considered with the LT data. The data is from 24 different forgings. In three cases, measurements were made relative to two surfaces (i.e. inside and outside of the ring forging) on the same forging. In two cases, both TL and LT transition temperatures were measured from the same forging. Five of the measurement sets are from nozzle forgings, while the others are from RPV shell forgings.

While both the LT and TL direction showed an average decrease in transition temperature of the forging surface when compared to the ¼T location, this decrease was more pronounced in the TL direction. The TL direction had an average shift from the surface to the ¼T location of

26.4°C (47.5°F) with a standard deviation of 12.1°C (21.7°F). The shifts of all seven TL datasets considered were positive. Compared to the TL direction, the LT direction had a smaller average shift of 20.3°C (36.5°F) and a larger standard deviation of 16.1°C (28.9°F). Two of the 24 LT datasets considered exhibited a negative shift. Given the average and standard deviation, these negative shifts are not unexpected. Since Charpy testing has a large inherent scatter and the shifts for these two LT data sets [-12.1°C (-21.7°F) and -3.6°C (-6.5°F)] were relatively small, it is likely that these shifts are a result of Charpy data scatter. Both forgings with negative shifts were used by B&W in RPV manufacture. Additionally, one of the forgings with a negative shift had limited data in the vicinity of the 30 ft-lb region. The other forging with negative shift had many measurements in the transition region, but the scatter in the data is substantial compared to the data from the other forgings.

In all cases where the LT and TL difference in transition temperature was measured on the same forging, the TL showed a greater decrease in transition temperature near the surface. Since both directions showed a clear trend, credit can be taken for a decreased transition temperature at the surface of a forging when compared to the ¼T location. The near-surface versus in-depth transition temperature measurements included four separate A-508, Class 2 (3 PWR and 1 BWR) nozzle forgings, and all showed a decrease in the near-surface transition temperature. The results of the through-thickness forging analysis are shown in Figure 3-5 for the LT and unreported orientation specimens. The figure shows the distance from the forging surface to the center of the specimen with the deepest point being approximately the ¼T measurement location. The vertical axis shows the difference in transition temperature between the deeper ¼T depth location with the measurements made closer to the surface. Figure 3-6 shows the same information for the TL-oriented specimens. Note that in some cases more than two measurements were made through thickness. In these cases the trend is generally linear improvement with measurement made closer to the surface. The results are summarized in Table 3-3. For subsequent analysis, the more conservative LT orientation is used, which has the smaller average improvement and larger standard deviation.

It is appropriate to take credit for the difference in properties at the surface, because the measurements that were used to determine the generic RTT_0 were taken at a through-thickness location. Of the measurements that give a fractional through-thickness depth, each of them was at the ¼T or ½T location. For the measurements without a recorded through-thickness depth, it was assumed that the measurement was taken at ¼T or deeper, consistent with accepted industry practice [44]. The ASME Code, Section III specifies that quenched and tempered fracture toughness impact specimens from forgings must have their longitudinal axes at least ¼T from any surface [65].

The LT orientation dataset has a larger amount of data and can conservatively be used since it has a smaller improvement than the TL orientation and a larger standard deviation. For subsequent analysis, the following near-surface toughness improvement will be used:

$$\Delta RT_{NDTsurface} = -36.5°F$$

$$\sigma_{Isurface} = 28.9°F.$$

Table 3-3 Summary of Transition Temperature Shifts for LT and TL Specimens		
	LT[1]	TL
Number of Data Sets Studied	24	7
Average Shift (°F)	36.5	47.5
Standard Deviation (°F)	28.9	21.7
Maximum Shift (°F)	90.6	79.2
Minimum Shift (°F)	-21.7	24.9

Note: 1. The LT grouping included datasets with no reported orientation.

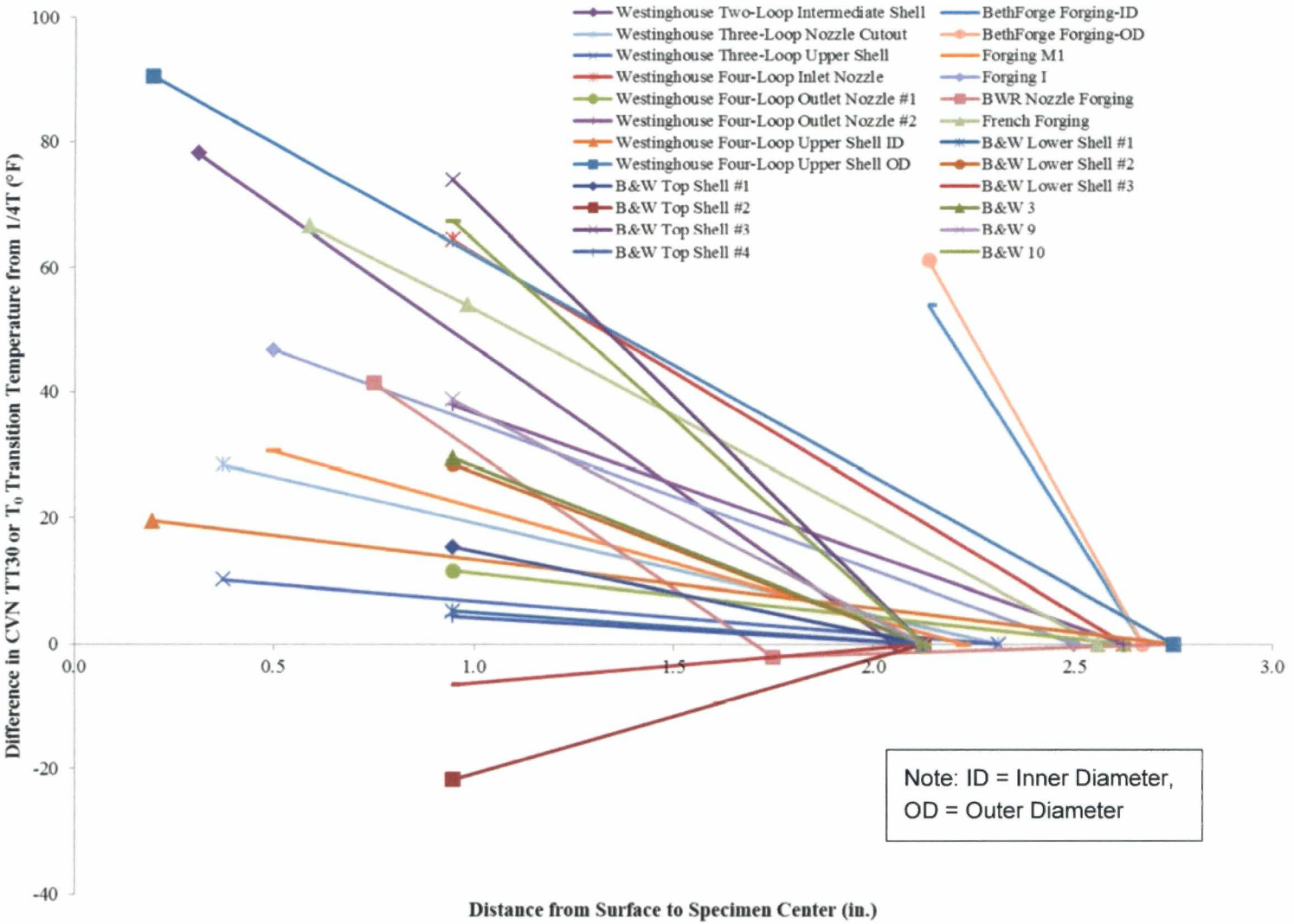

Figure 3-5 Transition Temperature Shifts for LT Specimens

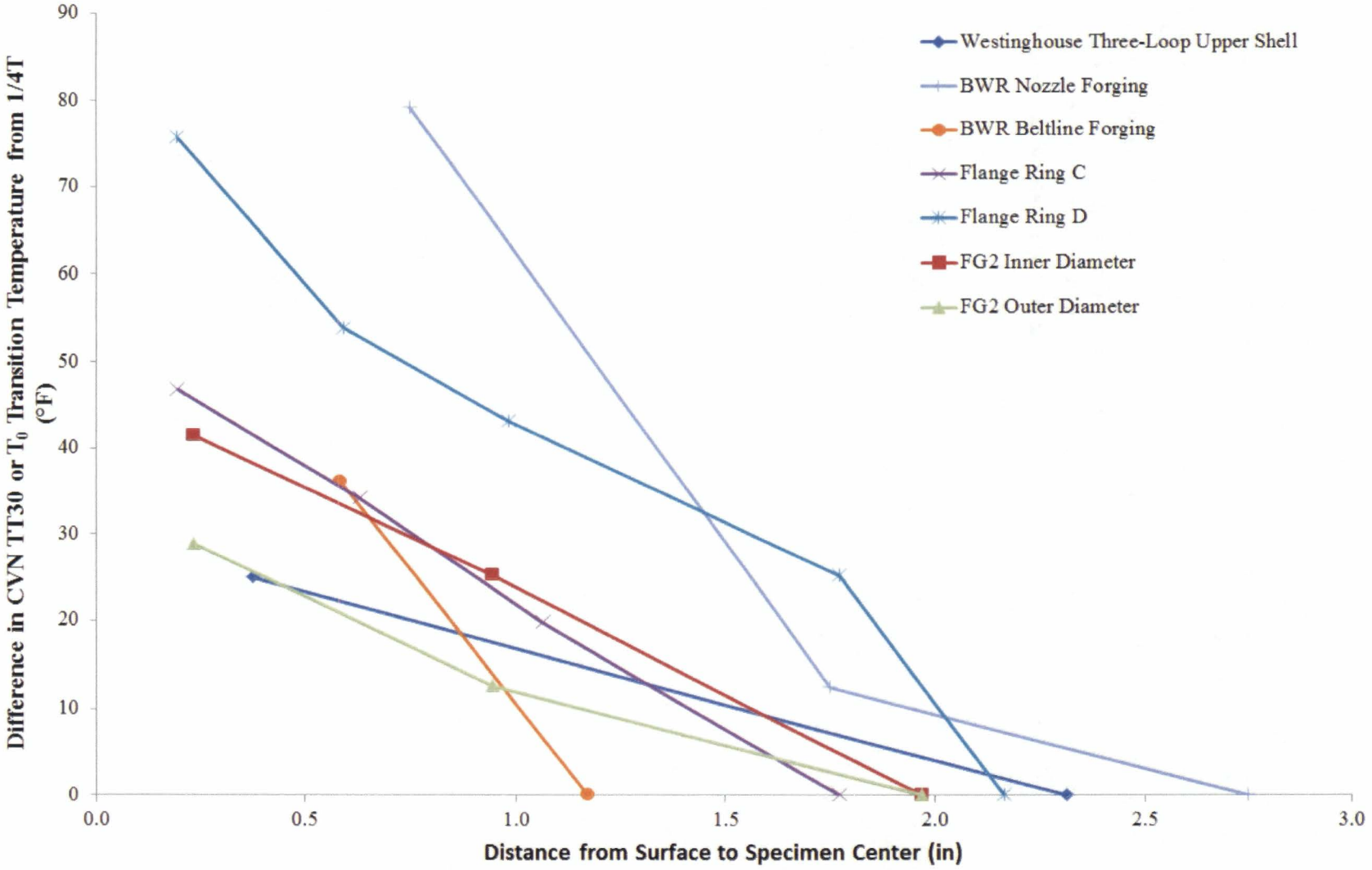

Figure 3-6 Transition Temperature Shifts for TL Specimens

3.3 UNDERCLAD HAZ TOUGHNESS

A significant portion of a small postulated flaw would be in the underclad heat-affected zone (HAZ). Therefore, the properties of the HAZ relative to the adjoining base metal must be considered. ORNL conducted Charpy impact testing on a stainless steel clad plate used to determine the effect of clad on the propagation of small surface flaws. The plate was specifically heat treated to produce a high transition temperature. It was not quenched and only slightly tempered. Charpy impact testing of the plate showed that the clad HAZ had significantly better properties (i.e. lower transition temperature) than the ¼T location in the plate [70]. Since the plate was not quenched, the improved HAZ transition temperature would not be due to a faster cooling rate from quenching, but the tempering of the cladding operation. Another test program tested master curve reference temperature of a clad cylinder HAZ relative to the base metal and found that the T_0 reference temperature was much lower for the clad HAZ [71].

A comprehensive study of U.S. surveillance capsule testing of HAZ 30 ft-lb transition temperature values compared with 30 ft-lb values for companion plate or forging concluded that essentially all the 30 ft-lb values of HAZ were lower than the 30 ft-lb values of the companion plate or forging [72]. Structural welds have many passes, which improves HAZ toughness properties relative to the base metal due to grain refinement, small regions of coarse grains, and tempering of martensite, all of which tend to increase toughness. Underclad HAZ does not experience as many thermal cycles, although the cladding of the nozzle corners is comprised of at least a two layer clad process [73].

In conclusion, the underclad HAZ in the nozzles is as tough, or tougher than, the adjacent forging base metal.

3.4 NEUTRON EMBRITTLEMENT

In 2014, the NRC issued RIS 2014-11 [3], which discussed that all ferritic components within the entire RPV be considered in the development of P-T limit curves. In this RIS, the NRC staff considers materials with a projected neutron fluence greater than 1×10^{17} neutrons per square centimeter (n/cm^2) ($E > 1.0$ MeV) at the end of license (EOL) to experience sufficient neutron damage to be included in the beltline. The effect of neutron damage is dependent on material chemistry and irradiation temperature [60]. Sufficient neutron damage such that it is indistinguishable from data scatter is not apparent at 1×10^{17} n/cm^2 for low Cu RPV steels. Therefore, the NRC provided additional guidance on what is considered sufficient damage such that embrittlement effects must be considered as discussed in NRC Technical Letter Report TLR-RES/DE/CIB-2013-01 [74]:

> *"Embrittlement effects may be neglected for any region of the RPV if either of the following conditions are met:*
>
> *(1) neutron fluence is less than 1×10^{17} n/cm^2 ($E > 1.0$ MeV) at EOL, or*

(2) the mean value of ΔT_{30} estimated using an ETC (embrittlement trend correlation) *acceptable to the staff is less than 25°F at EOL. The estimate of ΔT_{30} at EOL shall be made using best-estimate chemistry values."*

Nozzle fluence values are typically conservatively assumed to be equal to the upper-shell-to-nozzle weld fluence value (below the bottom of the nozzle forging). Even at this conservative location, nozzle forging fluence projections are frequently less than 1×10^{17} n/cm^2. However for some plants, the 60-year fluence projection at this location is greater than 1×10^{17} n/cm^2. Therefore, an estimate of ΔT_{30} at EOL is made using best-estimate chemistry values for PWR nozzle forgings generically to determine the fluence limit where ΔT_{30} reaches 25°F.

Even if the nozzle fluence is projected to be greater than 1×10^{17} n/cm^2, but the calculated ΔT_{30} is less than 25°F using Regulatory Guide 1.99, Revision 2 [60], the embrittlement can be neglected per TLR-RES/DE/CIB-2013-01 [74]. The ΔT_{30} limit of 25°F was used for H. B. Robinson Unit 2 nozzles to justify not adding embrittlement shift and was approved by the NRC in a P-T limit license amendment [11]. The Cu content was not measured for all the nozzles manufactured for the U.S. PWR fleet, however it was measured for a substantial number covering nearly the full range of manufacturing dates and all major fabricators used by the U.S. RPV fabricators. Copper measurements were averaged for 178 inlet and outlet nozzles yielding an average of 0.0947% with a standard deviation of 0.0319%. The definition in Regulatory Guide 1.99, Revision 2 for a generic best-estimate is the mean plus one standard deviation yielding 0.127% for Cu. As precedent, this methodology was approved by the NRC for a plant license renewal application [75 and 76]. For nickel (Ni), the upper limit of the SA-508 Class 2 specification during the fabrication time period is used, which was 0.90%. All U.S. plant nozzles meet A-508 Class 2 or A-508 Class 3 specifications. The Ni limit for A-508 Class 3 is 0.80%. Considering the permitted variation of Ni in the check analysis (0.03%), the chemistry factor tables in Regulatory Guide 1.99, Revision 2 for forgings do not change above 0.80% Ni at this Cu level. Generic properties for U.S. PWR nozzles are shown in Table 3-4.

The BWRVIP-173 [77] report had Cu measurements from 65 A-508 Class 2 forgings, not all of which were nozzle forgings. The best-estimate Ni and Cu contents discussed above and shown in Table 3-4 are appropriate for the U.S. PWR nozzles, since the database was established from Cu measurements from PWR nozzle forgings only.

Using the Regulatory Guide 1.99, Revision 2 and ASTM E900-15 [78] ETCs, the fluence value at which ΔRT_{NDT} (ΔT_{30}) is equal to 25°F was determined. The results are plotted in Figure 3-7.

Using Regulatory Guide 1.99, Revision 2, it can be determined that a shift of 25°F is not predicted to occur at a fluence value less than 4.28×10^{17} n/cm^2. The more recent ASTM E900-15 correlation, which is a function of irradiation temperature, gives a value of 2.73×10^{17} n/cm^2 for a 25°F shift at 528°F. The 528°F value used for E900-15 is conservative because it represents the time-weighted average downcomer temperature of the lowest cold leg temperature plant. The nominal irradiation temperature as defined by Regulatory Guide 1.99, Revision 2 is 550°F. Therefore, it is not surprising that near this temperature (at 550.8°F), the ASTM E900-15 and Regulatory Guide 1.99, Revision 2 ETCs give the same fluence value of 4.28×10^{17} n/cm^2 (E > 1.0 MeV) for a 25°F ΔRT_{NDT}. Approximately 50% of the U.S. PWR fleet

has downcomer temperatures greater than or equal to 550.8°F based on the time-weighted average irradiation temperature of their most recently removed capsule. Outlet nozzle temperatures (T_{hot}) are significantly greater than the inlet temperatures (T_{cold}) and, therefore, are predicted to have less embrittlement than the inlet nozzles. As discussed in Section 5.1.1, the limiting SIF location is at the outlet nozzle corner due to the geometric difference. Given that E900-15 ETC gives a very similar result to the Regulatory Guide 1.99, Revision 2 at a nominal irradiation temperature and the higher temperature outlet nozzles are limiting, it is conservative to use the Regulatory Guide 1.99, Revision 2 fluence value of 4.28×10^{17} n/cm^2 (E > 1.0 MeV) as a screening criterion for the embrittlement of U.S. PWR nozzles.

Table 3-4 Generic Material Properties and T_{cold} for the U.S. PWR Fleet Nozzles

	Generic Value
Cu wt. %	0.127(1)
Ni wt. %	0.90(2)
Mn wt. %	1.11(3)
P wt. %	0.016(3)
T_{cold}(4)	528°F (275.6°C)

Notes:
1. Generic best estimate determined through use of a database of 178 inlet and outlet nozzle forgings.
2. Upper bound value of ASME SA-508, Class 2 specification before the Summer 1975 Addenda [79].
3. Generic value per 10 CFR 50.61a [80].
4. Lowest T_{cold} (normal operation inlet coolant temperature) value for any U.S. PWR most recently removed capsule.

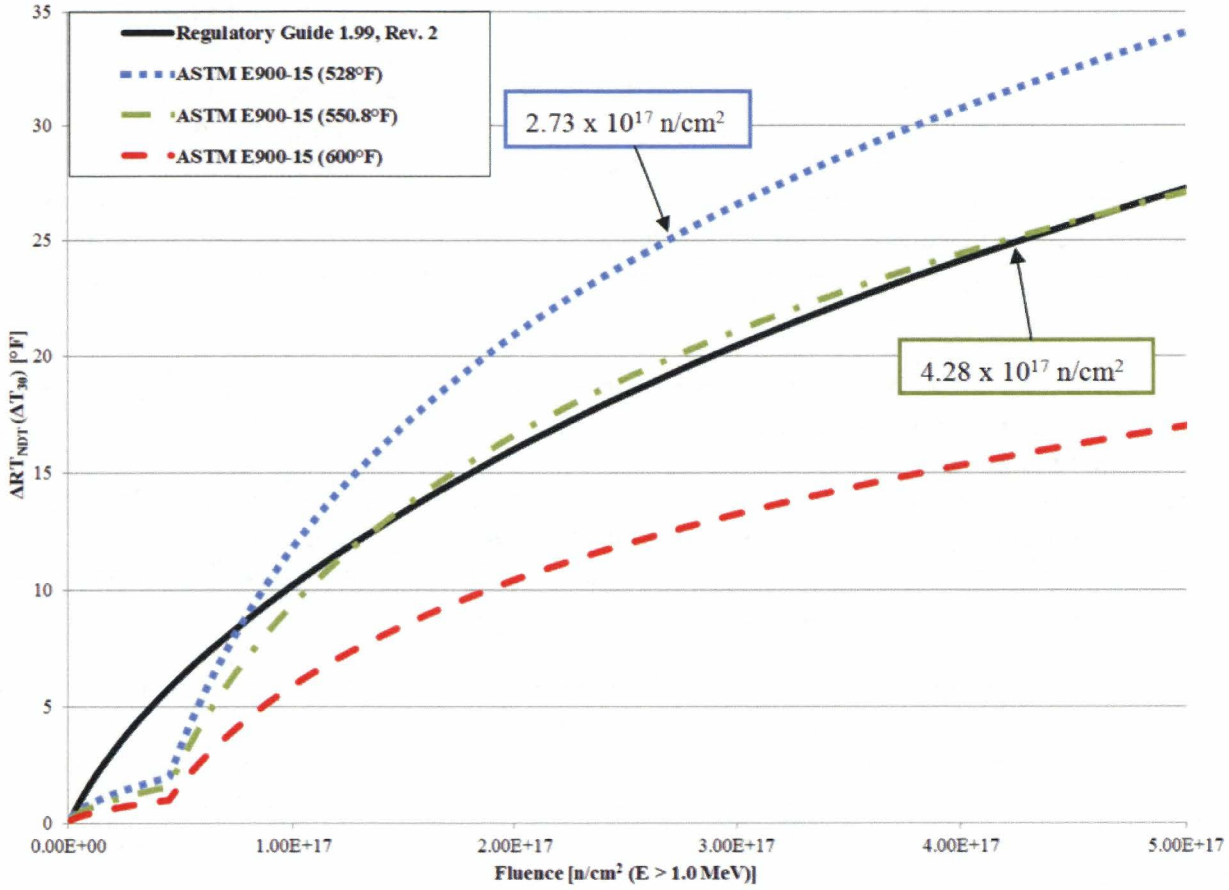

Figure 3-7 Transition Temperature Shift versus Fluence for Best-Estimate Chemistry

A review of the 60-year nozzle fluence data available to Westinghouse indicated that the fluence at the lowest extent of the nozzle forging (or the upper-shell-to-nozzle forging weld location) has been calculated for approximately three-quarters of the 65 operating PWRs. The PWRs analyzed include the B&W, CE, and Westinghouse (2, 3, and 4-loop) plant designs. The only nozzles that exceeded the screening criterion were two Westinghouse 3-loop design inlet nozzles [54 effective full power years (EFPY) at the RPV shell-to-nozzle forging weld] and the CE System-80 outlet nozzles (54 EFPY at the RPV upper-shell-to-nozzle forging weld). These specific higher-fluence nozzles were evaluated using nozzle specific properties. This evaluation showed that these nozzle specific ART values are bounded by the generic ART discussed in Section 3.5.

The PWR fleet nozzle fluence values contain two identified conservatisms: the calculated fluence location relative to the postulated flaw location and the fluence calculational methodology. These conservatisms are documented in the following two sections.

3.4.1 The Calculated Fluence Location Relative to the Postulated Flaw Location

In situations where fluence projections are high enough that embrittlement must be considered, the typical approach that has been used is to more accurately determine the fluence at the postulated flaw location. Nozzle fluence values are typically conservatively assumed to be equal to the RPV upper-shell-to-nozzle forging weld fluence value or the lowest extent of the nozzle forging. Since the current postulated flaws for this assessment are at the nozzle corners, the fluence value of the lowest extent of the nozzle forging or weld is greater than the fluence value of the postulated flaw itself.

During the recent analyses of five Westinghouse 3-loop plants at a 60-year life, the fluence nearer to the postulated flaw location was determined in addition to the lowest extent of the nozzle forging location. Using RPV drawings, an elevation was determined at which the fluence value should be determined which was higher in elevation than the lowest extent of the nozzle but still conservatively lower than the postulated ¼T flaw location. Use of this higher elevation for evaluation of the fluence values reduced the nozzle projected fluence values by greater than 50% for each of the 25 nozzles considered.

The postulated flaws identified in Section 2 are smaller than the ¼T flaw evaluated in the above referenced evaluations. Therefore, the flaw tip is located at a higher elevation, thus resulting in an even larger decrease in the fluence value when the actual flaw fluence value is considered relative to the RPV upper-shell-to-nozzle forging weld location. The fluence at the postulated flaw locations are expected to be considerably lower than the RPV upper shell to nozzle forging weld location.

3.4.2 Fluence Calculational Methodology

The use of new fluence evaluation methods can more accurately determine the nozzle fluence reducing the needed conservatisms. Table 3-5 shows an example of the difference in nozzle fluence values between the previous NRC approved method of fluence evaluation using DORT, and the new TORT and RAPTOR-M3G (RApid Parallel Transport Of Radiation – Multiple 3D Geometries) methods. RAPTOR-M3G has been approved on a plant-specific basis [81], and generic approval for the traditional beltline is currently being pursued [82].

DORT-based calculations use the traditional fluence rate synthesis technique, in which two-dimensional and one-dimensional discrete ordinates models are combined to yield a synthesized three-dimensional solution. This method is effective in the traditional RPV beltline, but introduces conservatism in the nozzle region where three-dimensional effects become more pronounced. TORT uses a three-dimensional discrete ordinates technique to produce a true three-dimensional solution. However, TORT is a single-processor code, and is subject to limitations in the amount of detail that can be modeled in any given problem. RAPTOR-M3G is a parallel-processing Westinghouse code that, like TORT, uses a three-dimensional discrete ordinates technique to produce a true three-dimensional solution. The parallel-processing feature of RAPTOR-M3G allows large, 3D radiation transport calculations to be performed that would otherwise be prohibitively time consuming or cannot be performed with TORT.

As shown in Table 3-5 for a representative 4-loop Westinghouse unit at 54 EFPY, inlet and outlet nozzle weld fluence values were reduced by more than 65% when using the TORT method instead of DORT. The Westinghouse RAPTOR-M3G method is more conservative than TORT, but still reduces the nozzle fluence values by 54% or more. Subsequent investigations by Westinghouse have determined that the reason for the conservatism of the RAPTOR-M3G results relates to choices of solution parameters.

The common practice for fluence calculations is to benchmark calculational methodologies against measured data. For traditional beltline regions, this is typically accomplished by analyzing reactor dosimetry samples included in the reactor in-vessel surveillance program or installed in the reactor cavity as ex-vessel dosimetry. Extensive measurement data exists to qualify fluence calculations in the traditional beltline regions. Measured data available for extended beltline regions of RPVs is limited. To address this lack of data, a partial set of benchmarking data was obtained from surveillance capsule material that was installed in operating PWR reactors which is stored at the Westinghouse Churchill facility.

Material samples were extracted from top support plugs of two recently analyzed surveillance capsules. Top support plugs are stainless steel structural surveillance capsule components that extend between 1 and 2 feet above the top of the core, and are located immediately outside the core barrel. Thus, the top support plugs are ideally located between the core and the materials of interest in the RPV nozzle region. Figure 3-8 shows the relative locations of the active fuel, the top support plugs, and the RPV nozzles. Extracting samples from the top support plugs provided a set of measurement data that are directly applicable to the nozzle corner region.

The measured reaction rates were compared to calculations performed using RAPTOR-M3G. The comparisons demonstrated good agreement, with the calculated reaction rates exceeding the measured reaction rates by 14%. Removal of an apparently outlying measurement improves the agreement to 11%. Since the calculated reaction rates are generally higher than the corresponding measured rates, the fluence values calculated using this method are considered to be conservative. These comparisons provide supporting evidence that the use of 3D methodologies in the extended beltline region can meet the 20% uncertainty criterion in Regulatory Guide 1.190 for neutron fluence calculations.

Table 3-5 Comparison of a Representative Westinghouse 4-Loop Plant 54 EFPY Fluence Values using DORT, TORT, and RAPTOR-M3G[1]

Fluence Value Calculated using DORT (n/cm^2 E>1.0 MeV)		Fluence Value Calculated using TORT (n/cm^2 E>1.0 MeV)		Fluence Value Calculated using RAPTOR-M3G (n/cm^2 E>1.0 MeV)	
Inlet Nozzle	Outlet Nozzle	Inlet Nozzle	Outlet Nozzle	Inlet Nozzle	Outlet Nozzle
1.23×10^{17}	0.667×10^{17}	0.428×10^{17}	0.200×10^{17}	0.567×10^{17}	0.274×10^{17}

Note:

1. The location of the calculated fluence is at the inside surface of lowest extent of the nozzle-forging-to-shell weld.

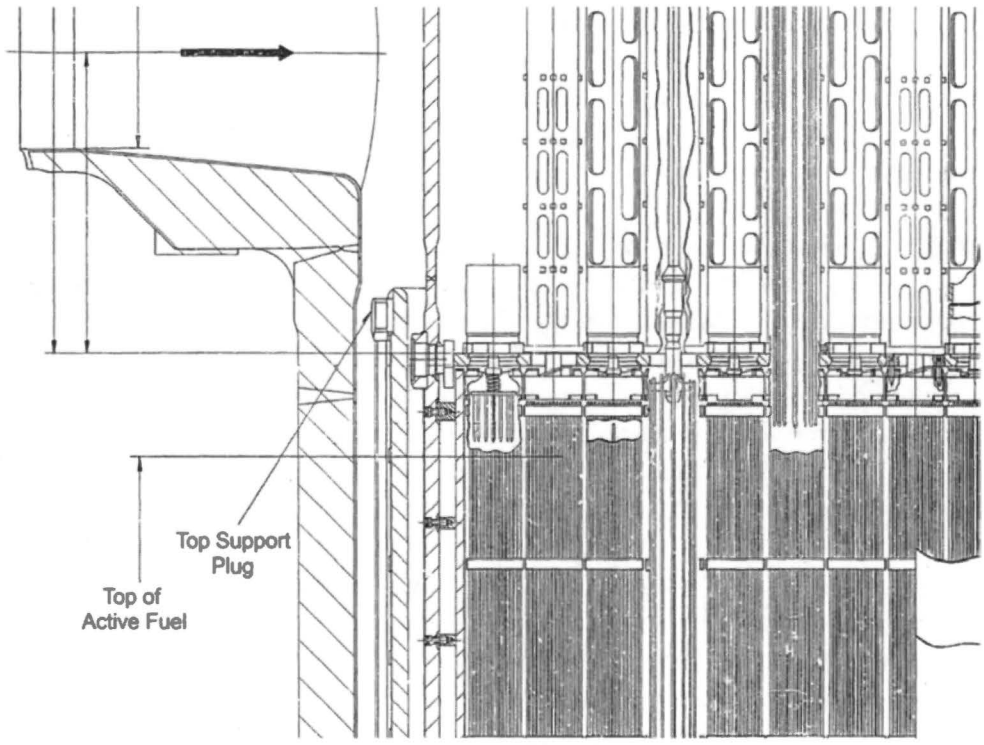

Figure 3-8 Location of the Top Support Plug Relative to the Top of the Active Fuel and the Reactor Vessel Nozzles

3.4.3 Neutron Streaming

It is recognized that there is neutron streaming up the cavity to the nozzle region from the beltline. Because of this, the traditional fluence attenuation equation used in the beltline (Regulatory Guide 1.99, Revision 2) is not appropriate in the nozzle region when only considering fluence calculated at the inside surface. The fluence profile has been calculated along the 45-degree cut from the nozzle corner to the RPV outer diameter [83]. The results show for the Westinghouse 3-loop and 4-loop designs that there is a slightly higher fluence at the location where the shallow flaws are postulated than at the inside surface. Since this increase is relatively small, it is more than compensated for as discussed in Sections 3.4.1 and 3.4.2.

This analysis also showed that the fluence at the outside diameter lowest extent of the nozzles can be significantly higher than the fluence at the lowest extent of the nozzle forging at the RPV inside surface due to cavity neutron streaming [83]. The stresses at the inlet and outlet nozzles both due to pressure and the thermal cooldown transient can be seen in the Section 4.8 figures from the 3D finite element analysis. These figures demonstrate that the stresses at the lowest extent outside diameter of the nozzles are significantly lower than at the nozzle inside corner, and when pressure stress and thermal stress are considered together, the combined stress is

likely compressive. Even if the lowest extent of the nozzles at the outside diameter of the RPV is embrittled more due to the higher fluence than the other locations, a flaw could not propagate since the stress is compressive or very low. As is discussed in Section 4.8, the flaw is postulated at the nozzle inside surface corner at a geometric discontinuity where the highest stresses exist. As a result, the nozzle inside surface corner is the limiting location, and this location is where the fluence is considered for embrittlement.

3.4.4 Nozzle Neutron Embrittlement Conclusion

Although there is not enough data available to generically support quantitative reductions in fluence values based on the fluence value location and fluence evaluation method, the reductions shown in the available data demonstrate that the fluence values used in this assessment are very conservative. The fluence at the location of the postulated flaws is expected to be significantly lower than the screening limit shown in Figure 3-7. Even for the few nozzles which had a fluence higher than the screening limit at the lowest extent of the forging, nozzle specific evaluations demonstrated that they are bounded by the generic ART discussed in Section 3.5. In addition, the limiting SIF location is the outlet nozzle corner due to the geometric difference (See Section 5.1.1). The outlet nozzle temperatures are significantly greater than the inlet temperatures and are predicted to have significantly less embrittlement than predictions at inlet nozzle temperatures. Therefore, embrittlement is not considered to be significant and any embrittlement effects for the nozzle postulated flaw locations can be neglected.

3.4.5 Future Increased Nozzle Fluence Projections

When a licensee applies for SLR or the nozzle fluence projections increase for other reasons, the new projected nozzle fluence values can be compared to the fluence screening criterion established in Section 3.4 (4.28×10^{17} n/cm^2). If the projected nozzle corner fluence remains less than the screening criterion, then this analysis is applicable. If the fluence exceeds the screening criterion, then a shift can be calculated for those nozzles on a plant-specific basis using an NRC approved method; as long as the shift remains below 25°F or the plant-specific nozzle ART values remain below the ART used in this report, then this analysis is applicable.

3.5 ADJUSTED REFERENCE TEMPERATURE

The generic nozzle forging RTT_0 discussed in Section 3.1.2.2 along with the improvement near the surface for the postulated small flaw as described in Section 3.2 is as follows:

- Generic RTT_0

  Alternate generic mean $RT_{NDT} = RTT_0 = -66.4°F$

  Margin = $\sigma_I = 54.5°F$

- Near-Surface Toughness

  $\Delta RT_{NDTsurface} = -36.5°F$

  $\sigma_{Isurface} = 28.9°F$

The surface effect on toughness is statistically independent from the uncertainty in RTT_0; therefore, these uncertainties can be combined using the square root of the sum of the squares as is recommended in Regulatory Guide 1.99, Revision 2:

$$ART = RTT_0 + \Delta RT_{NDTsurface} + 2(\sigma_I^2 + \sigma_{Isurface}^2)^{½}$$

$$ART = -66.4°F - 36.5°F + 2(54.5°F^2 + 28.9°F^2)^{½} = \mathbf{21°F} \text{ (Conservatively rounded up)}$$

Reference [84] demonstrates that the measured near-surface RTT_0 and adjusted near surface RTT_0 data is likely normally distributed using the Anderson-Darling test and that 99% of the data is expected to be bounded by the 21°F near-surface generic alternate RT_{NDT}.

Section 3.4 demonstrated that the embrittlement effects for the nozzle postulated locations can be neglected if the nozzle fluence value is less than 4.28×10^{17} n/cm^2. All U.S. PWR nozzles have a fluence value below this threshold for 60 years or were dispositioned individually. Therefore, no embrittlement shift term or associated uncertainty is required. The conservative generic ART for the nozzle corners that is used in this analysis for the location of the postulated small flaws is 21°F. For deeper postulated flaws, the generic RTT_0 of 43°F is also used (Section 3.1.2.2).

4 STRESS INTENSITY FACTOR CALCULATION

Detailed three-dimensional finite element analyses (3D FEAs) of the RPV inlet and outlet nozzles were performed to derive stresses and stress intensity factors (SIFs) for development of nozzle P-T limit curves.

Nozzle cooldown P-T limit curves were generated using two different methods, which both comply with ASME Section XI, Appendix G:

1. Various small flaw sizes and aspect ratios (Section 2) were explicitly modeled in the 3D FEAs to calculate the SIFs (described in detail in Section 4). The pressure and thermal transient SIFs were then combined to develop nozzle P-T limit curves (Section 5.1.1).

2. A nozzle corner flaw size, comparable to the beltline ¼ thickness flaw (~2.1-inch flaw depth) used in traditional P-T curves, was postulated using stresses from unflawed finite element models (FEMs) with the ASME Section XI, Appendix G SIF solution. This approach using the modeled nozzle geometries is described in Section 5.1.2.

4.1 NOZZLE GEOMETRIES MODELED

The stress and fracture mechanics analyses were initially performed for a Westinghouse designed 4-loop PWR 28-inch diameter inlet nozzle and a 30-inch PWR outlet nozzle (baseline cases). These particular nozzle FEMs are shown in Figure 4-1 and Figure 4-2 for the inlet and outlet nozzles, respectively. The geometry and material used in the development of the FEM for the inlet and outlet nozzles is considered to be representative and useful for identifying the important characteristics that need to be considered to ensure bounding analyses are performed for all the U.S. PWR designs [Westinghouse 2-loop, 3-loop, 4-loop, Combustion Engineering and Babcock and Wilcox (B&W)] based on the consideration of geometry, primary and secondary stresses, and the material specifications.

From the stress analysis perspective, the primary stresses considered in the fracture mechanics are due to the internal pressure within the RPV. The primary stresses are used intrinsically to calculate the SIF for pressure along the postulated crack front. The basis for using a representative RPV design for determining the SIFs is that all of the PWR RPVs were constructed to withstand the design pressure necessary for the plant operation at high pressures. Therefore, the design thickness calculated per ASME Section III was based on the consideration of the primary stress due to high internal design pressures with nozzle reinforcement considerations. The internal hoop and axial pressure stresses are related to the internal pressure based on a ratio of the RPV inside radius (R) to the wall thickness (t). As a result, the R/t ratios for the RPV are similar for the design pressures for all PWRs. Based on a review of the drawings for the various RPV designs at the nozzle shell regions, the R/t ratio is approximately eight, ranging from seven to nine because of variations in reinforcement thickness in the nozzle region. Thus, the primary stresses and the resulting pressure SIF results are similar for all of the PWR RPV designs. However, to ensure that all design variations are bounded, several diverse plant nozzle designs were modeled for the 3D FEA ensuring that the

nozzle shell R/t range extremes were modeled. The different nozzle shell R/t ratios modeled are described in Table 4-1 and are graphically shown in Figure 4-3. The variation in geometry is also important for the consideration of secondary stresses due to the cooldown transient. Thermal stresses are tied to temperature gradients, which are affected by thermal inertial effects due to mass and conduction. For these reasons, variations in both RPV and nozzle geometry can create a range of thermal responses that are important to the development of P-T limit curves.

The models shown in Figure 4-3 are aligned about a common centerline to demonstrate the different sizes and RPV diameters. The important characteristics that affect the nozzle corner stress and SIF were assessed to ensure representative or bounding models were chosen for the whole U.S. PWR fleet. The important characteristics are nozzle shell R/t ratio, clad thickness, nozzle corner geometry, and nozzle diameter. Table 4-1 shows how the chosen plant models either represent or bound the variation of the important characteristics of the operating U.S. PWR fleet. Comparison of modeled baseline and bounding Westinghouse 4-loop nozzle designs are shown in Figure 4-4.

Table 4-1 Model Geometry Comparison

FEM	Description	Nozzle Shell Radius/Thickness Ratio	Clad Thickness
Baseline Westinghouse 4-Loop Design	Representative Westinghouse 4-loop design	7.95 Typical 4-loop	Design maximum
CE System-80	Largest diameter outlet nozzle design; Comparable to the B&W outlet nozzle design	8.1 Higher than the B&W design	Representative of the thicker B&W RPV shell cladding
Bounding Westinghouse 4-Loop Design	Westinghouse 4-loop design	8.9 Largest of the Westinghouse designs	Design maximum
Westinghouse 2-Loop Design	Representative 2-loop Westinghouse design	7.3 Smallest of the Westinghouse designs	Design maximum

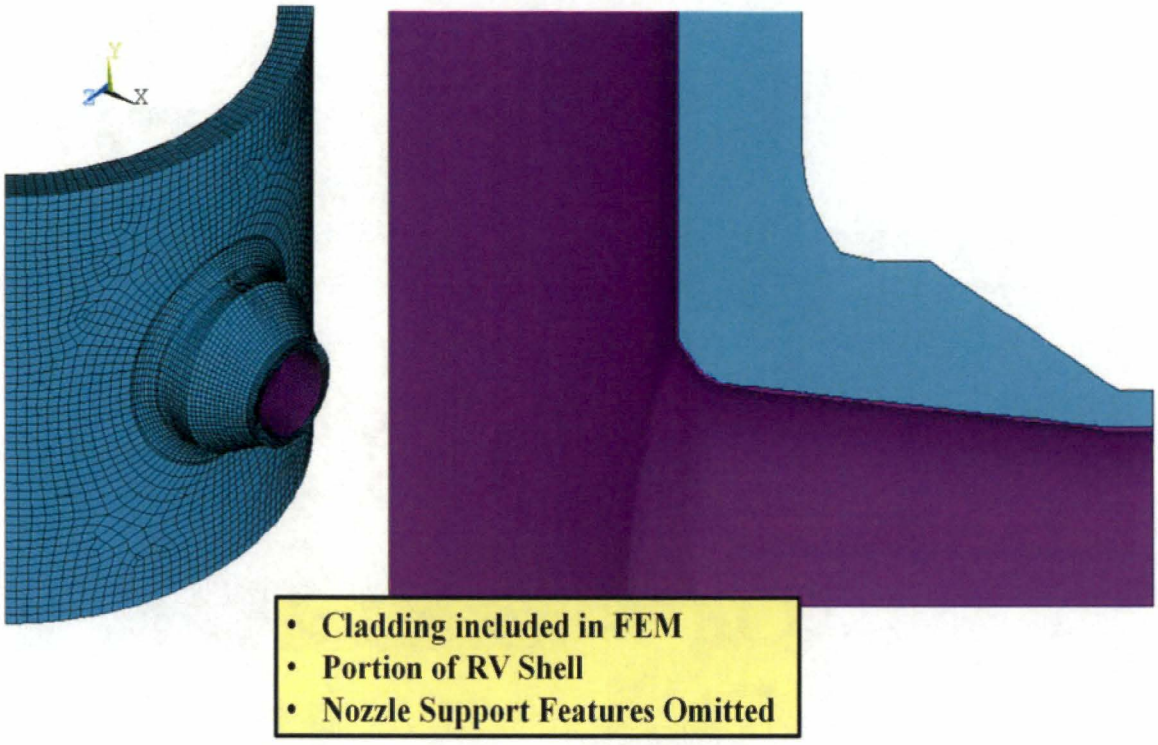

Figure 4-1 FEM with Inlet Nozzle, Shell, and Cladding

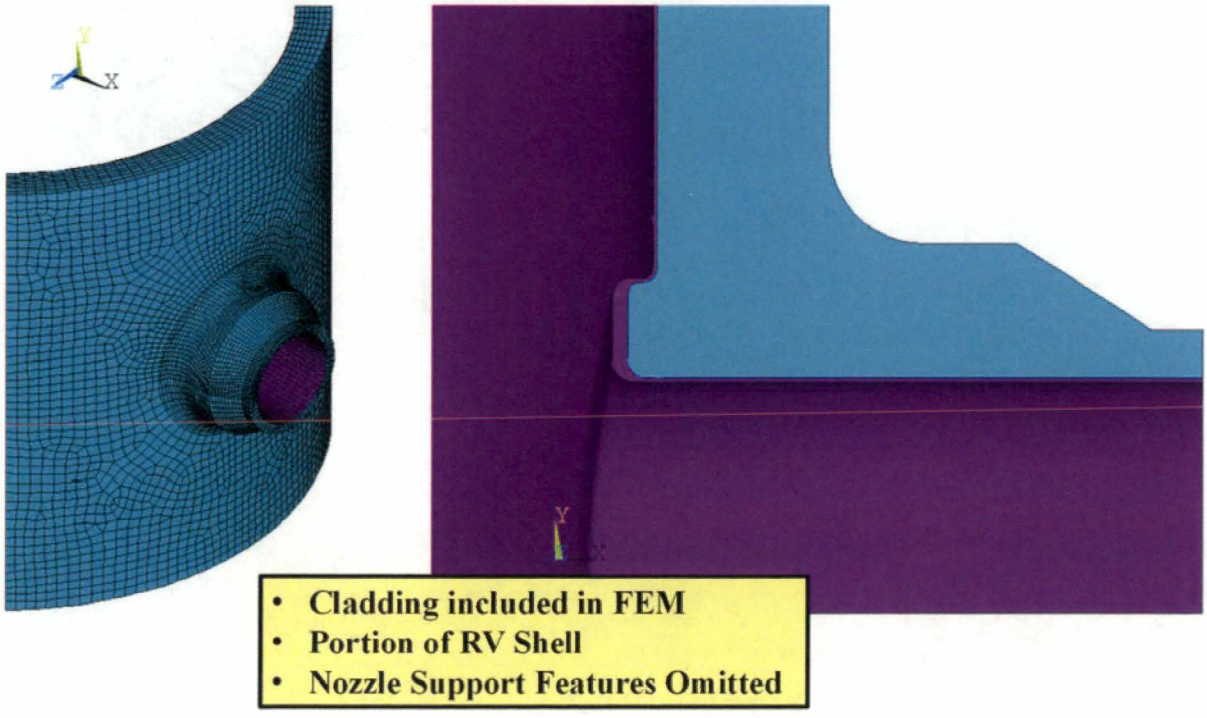

Figure 4-2 FEM with Outlet Nozzle, Shell, and Cladding

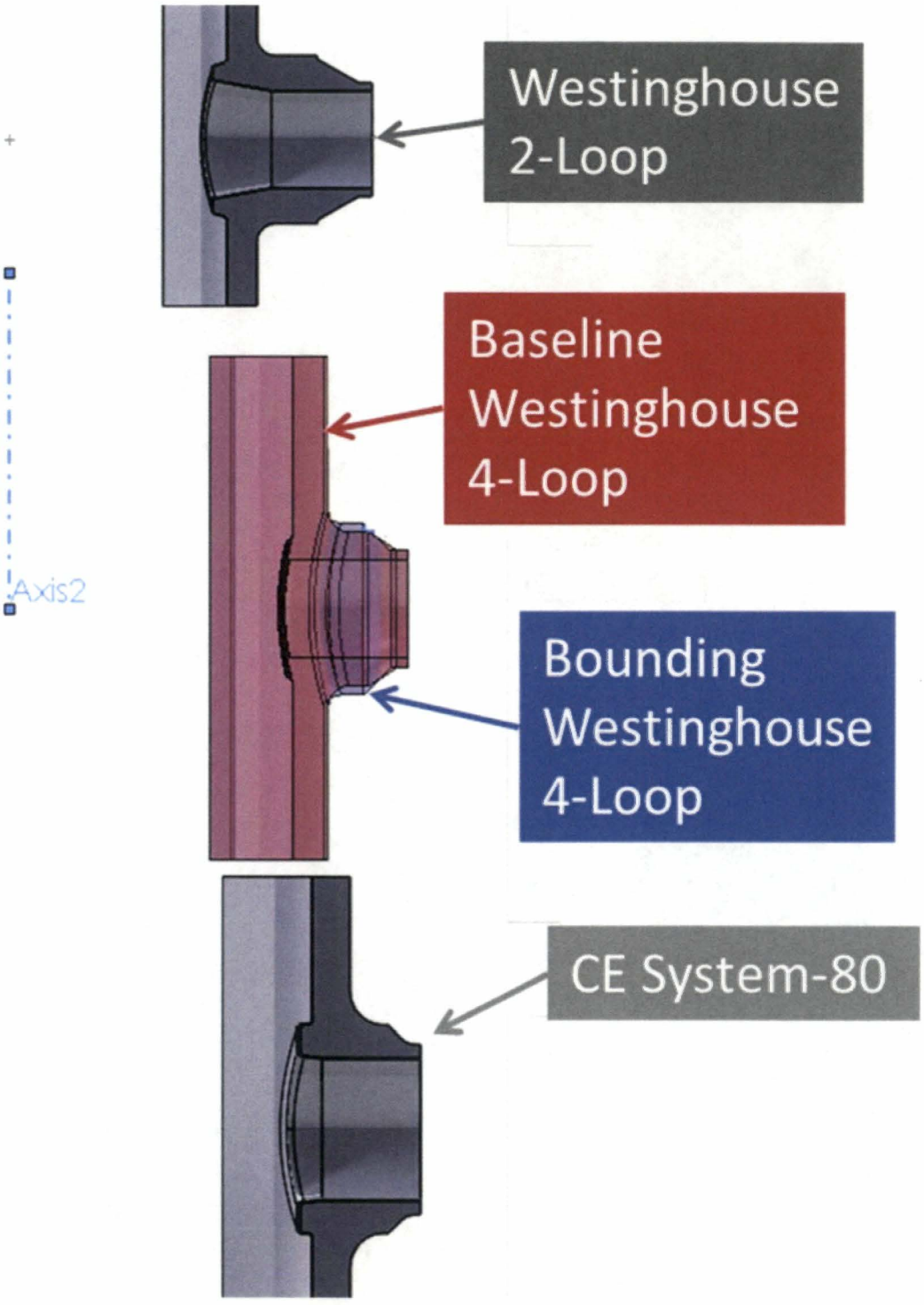

Figure 4-3 Diversity of Nozzle Geometries Modeled

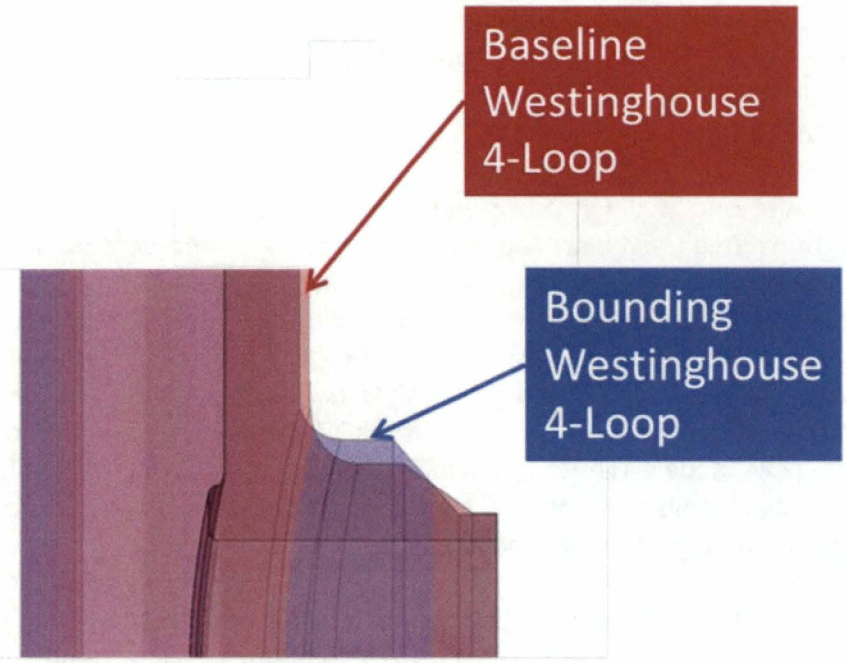

Figure 4-4 Comparison of Modeled Baseline and Bounding Westinghouse 4-Loop Nozzle Designs

For the thermal SIFs and thermal cooldown stresses, the thicknesses used herein for the inlet and outlet nozzles are representative of the other RPV designs based on the geometric configuration of the nozzles and the through-wall thickness at the 45° cut angle where the flaw is postulated. The geometric configurations and the wall thickness used in the fracture mechanics analysis for the inlet and outlet nozzles is representative or bounding for all U.S. PWR RPV designs, as described above. At the low temperature regions (50°F to 80°F transient temperature) of the cooldown curve, the stresses due to the cooldown transient are primarily due to the thickness of the cladding and the residual stresses from the cladding. In the evaluation herein, two cladding thickness cases are considered to cover the various thicknesses of the cladding that are contained in the PWR fleet. The inlet nozzle was modeled with a ¼-inch clad thickness, which is the nominal clad thickness for the corner region for the majority of the PWR designs. The B&W design has a ⅜-inch nominal clad thickness. The modeled CE System-80 outlet nozzle was modeled with ⅜-inch cladding everywhere except the outlet nozzle boss which has thicker cladding. The CE System-80 outlet nozzle design is similar in size to the B&W outlet nozzle, therefore this is an appropriate change that enables the analyses to represent the B&W design. The outlet nozzles were modeled with a thicker clad thickness of 1 inch at the end of the boss. In most cases, during manufacturing the nozzle boss started with a 1 inch minimum clad thickness, which was then reduced to provide the required clearance with the internals mating surface for the 4-loop design. The 3D FEA demonstrated that thicker cladding produced higher SIFs at the crack tip, therefore the modeled 1-inch thickness bounds (or is representative of) the clad thickness of all the operating U.S. PWR designs for the outlet nozzles. The higher SIFs occur at the clad-LAS interface at the thicker clad location (the lower d/D interface location indicated in Section 4.9) for the limiting outlet nozzle case for both the static pressure and thermal cooldown transient cases.

Thus, the diversity of PWR inlet and outlet nozzles considered in the evaluations herein are representative or bounding for all the U.S. PWR RPV designs and configurations.

4.2 MODEL/MESH

3D FEMs of the inlet and outlet nozzles were created using ANSYS® 14.5.7. Flaw sizes of various aspect ratios (e.g., circular and semi-elliptical) are incorporated into the FEMs. A temperature degree of freedom (DOF) model and a displacement DOF model are created for each nozzle and flaw geometry set. The temperature DOF model inputs the conservative cooldown transient described in Section 4.7.3. The temperature DOF generates spatially-varying temperature profiles at discrete time points during the plant cooldown transient. The temperature profiles, RCS pressure transients, and RPV safe-end mechanical loads are input to the displacement DOF models. The displacement DOF models output, spatially-varying stress profiles at discrete time points during the cooldown transient. The stress and displacement results at the flaw tip are further processed to calculate SIFs.

The inlet and outlet nozzle baseline FEMs used various flaw shapes and sizes. The flaw geometries are shown in Table 4-2 and in Figure 2-3. The smallest flaw depths (i.e., cases 1, 2, 5, and 6) are based on a surface breaking flaw extending 0.05 inch into the LAS nozzle forging through the cladding. The dimensions were sized to allow a suitable mesh to be developed without mesh discontinuities affecting the results. Cases 3, 4, 7, and 8 were sized to have 0.5-inch flaw depth into the LAS, which is conservative relative to the NDE detection capability as described in Section 2. The flaw location in the FEM is located on the vertical (x-y) plane because the hoop stress from the RPV shell adds to the hoop stress at the nozzle, which is conservative. The orientation of the nozzle mechanical loads was adjusted to maximize the SIF in the flaw; however, the mechanical SIFs have insignificant impact on the P-T limit curves.

The displacement DOF models used for pressure and thermal stress analyses contain 20-noded hexahedral elements and 10-noded tetrahedral elements. The temperature DOF models were generated by converting the stress elements to thermal hexahedral and tetrahedral elements.

The models include a portion of the RPV shell, with boundaries sufficiently distant from the region of interest as to not affect the results. For the mechanical load models, a portion of main loop piping was added to move the load application point away from the region of interest.

Table 4-2 Flaw Case List

Case	Geometry	Flaw Depth (in) [1]	Flaw Length (in)	Aspect Ratio[2]	Flaw Location Ratio, d/D[3]		
					Deepest Point[4]	LAS[5] Surface 1	LAS[5] Surface 2
1	Inlet	0.3	0.6	2:1 (Circular)	0.500	0.319	0.681
2		0.3	1.8	6:1 (Semi-elliptical)	0.500	0.277	0.723
3		0.75	1.5	2:1 (Circular)	0.500	0.120	0.880
4		0.75	4.5	6:1 (Semi-elliptical)	0.500	0.090	0.910
5	Outlet	0.9	1.8	2:1 (Circular)	0.651	0.439	0.846
6		0.9	5.4	6:1 (Semi-elliptical)	0.662	0.435	0.875
7		1.18	2.36	2:1 (Circular)	0.642	0.367	0.901
8		1.18	7.08	6:1 (Semi-elliptical)	0.639	0.367	0.898

Notes:

1. Flaw depth is the distance from the deepest point at a 45-degree angle to the clad wetted surface. For the outlet nozzle, the clad thickness at this point is in transition from 1 to 0.25 inches (See Section 2).
2. Aspect ratio = L/a, where a is the flaw depth and L is the total flaw length; see Figure 2-2.
3. See Figure 4-21 and Section 4.9.1 for a discussion on flaw location ratio d/D.
4. Deepest point defined at the maximum distance between the flaw tip and the LAS/cladding surface boundary.
5. Location on flaw where LAS and cladding meet.

4.3 FLAW MODELING METHODOLOGY

Nozzle corner flaws of various sizes and aspect ratios were modeled explicitly in the FEMs. The nozzle corner flaws were oriented axially relative to the nozzle geometry. The flaws pass through the cladding into the nozzle forging, as shown in Figure 4-5. Examples of the flaw mesh are shown in Figure 4-6 and Figure 4-7. The model is divided into four regions:

1. Singularity mesh generated by a zero-radius sweep (region 1 in Figure 4-6 and Figure 4-7)
2. Fracture affected zone mesh surrounding the flaw tip mesh (region 2)
3. Transition mesh (region 3)
4. Remote mesh on the nozzle and RPV shell

Regions 1 and 2 are composed of 20-noded hexahedral elements, with wedge elements (i.e., degenerate elements) at the flaw tip. Region 3 is composed of degenerate transition elements at the interface to region 4, and tetrahedral elements in the interior region of the buffer zone. Region 4 is composed of coarser 20-noded hexahedral elements.

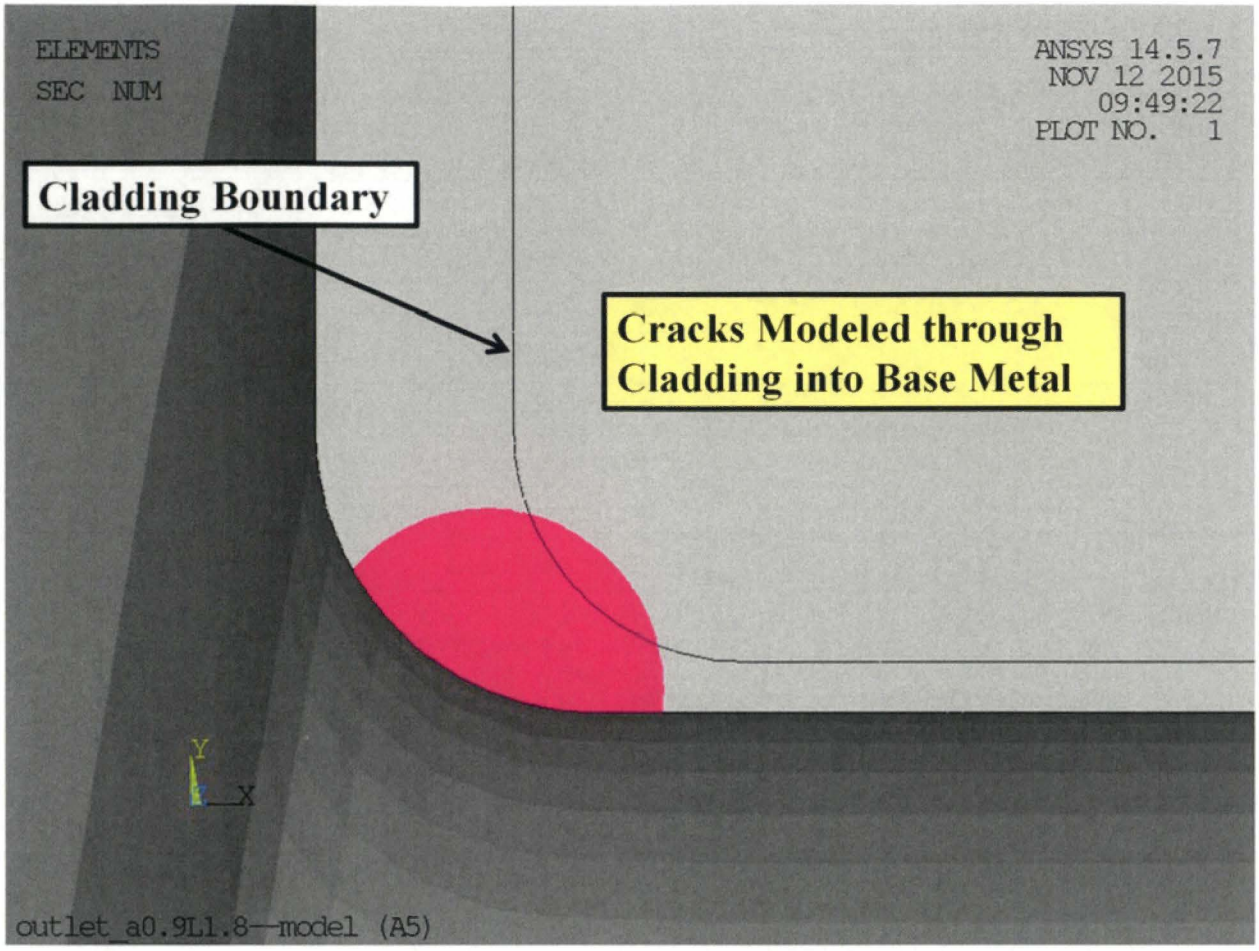

Figure 4-5 Example Cross-section View of Flaw

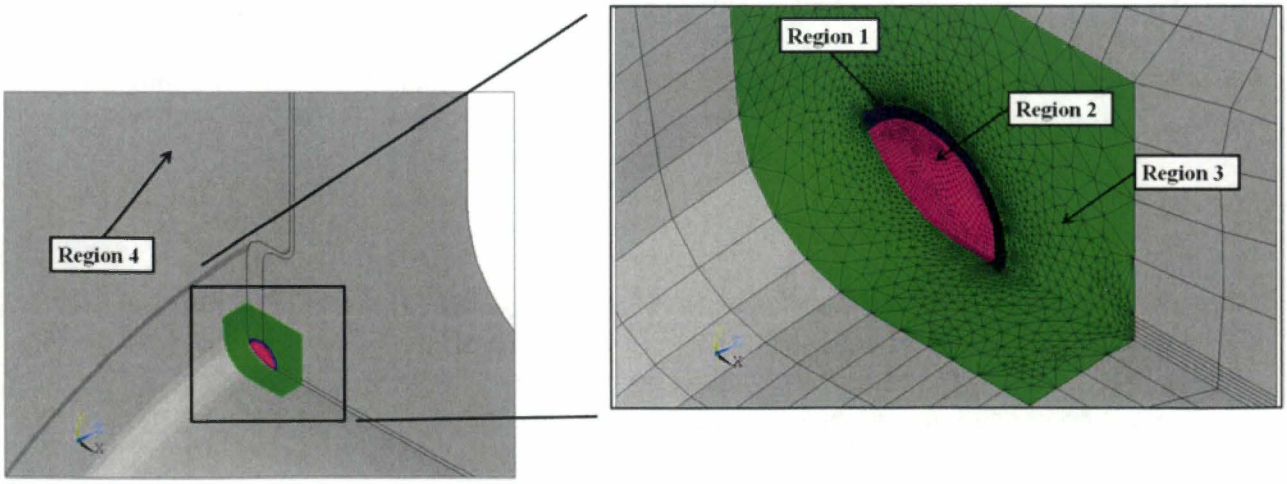

Figure 4-6 Example Flaw Region Mesh

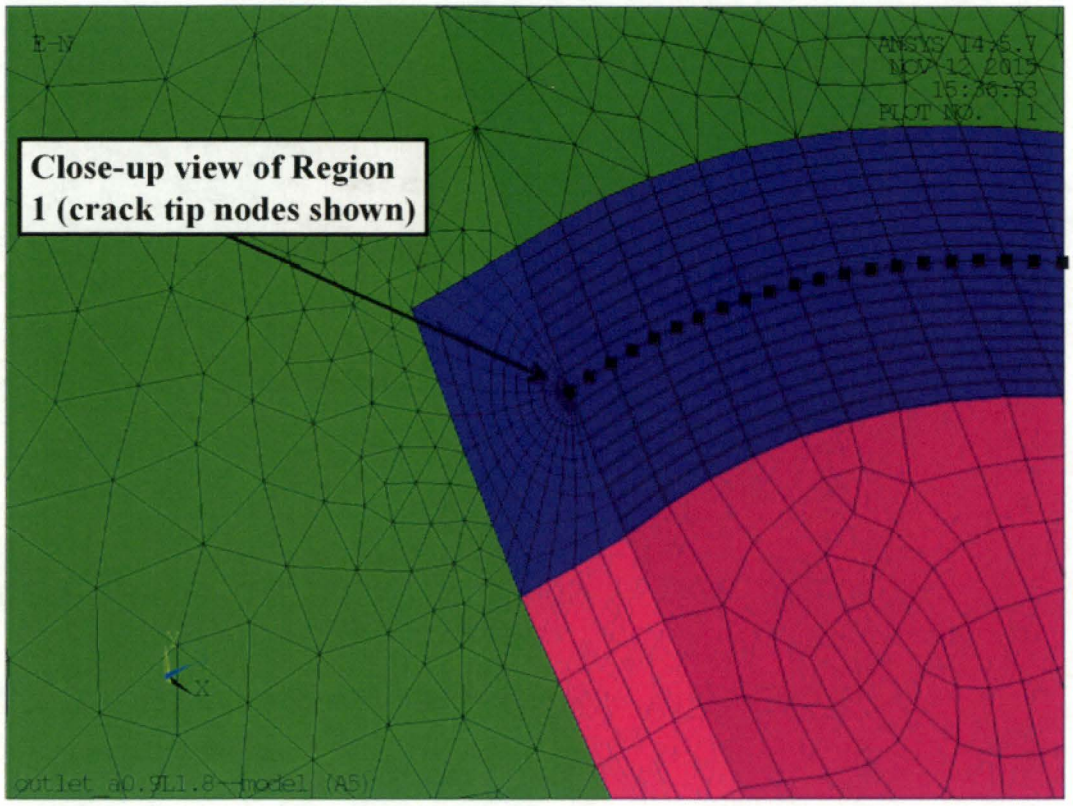

Figure 4-7 Example Flaw Tip Mesh

4.4 THERMAL BOUNDARY CONDITIONS

The surface for temperature application is shown in Figure 4-8. The wetted surface for temperature includes only the inner surface of the RPV shell and nozzle; the flaw gap is assumed to be very small and water in the gap would act as an infinite conductor. This is modeled by coupling the temperatures at the coincident flaw nodes. The RCS flow rate is very large; therefore, it is appropriate to treat the heat transfer coefficient as infinite and directly apply the RCS temperature to the metal surface (i.e., the metal surface temperature is instantaneously equal to the RCS water temperature). The model external surfaces are adiabatic because they are insulated. The sliced surfaces at the top, bottom, and sides of the model are adiabatic because the un-modeled structure would not significantly impact the thermal gradients in the region of interest. The temperature gradients would be radial, which is captured accurately with the adiabatic boundary condition.

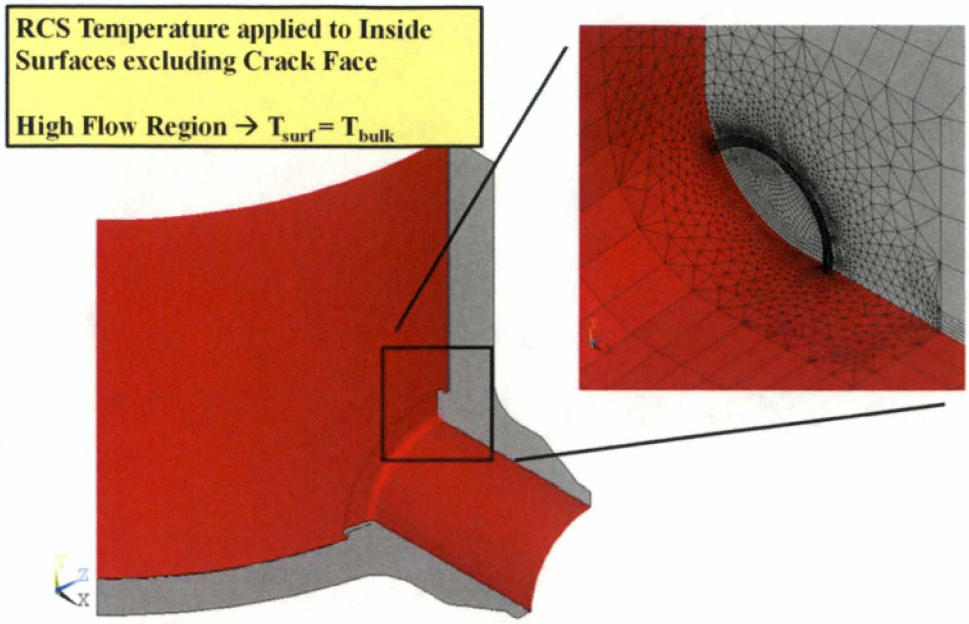

Figure 4-8 Wetted Surface for Bulk Temperature

4.5 STRUCTURAL BOUNDARY CONDITIONS

The boundary conditions consist of displacement restraints, system pressure, mechanical loads and temperature described in the following sections.

4.5.1 Displacement Restraints

The RPV nozzle boundary conditions are shown in Figure 4-9 through Figure 4-11. The bottom and side boundaries to un-modeled portions of the RPV shell are fixed normal to the boundary surface. Therefore, the side boundaries are fixed in the circumferential direction, and the bottom boundary is fixed in the vertical direction. For the quarter-symmetry models used for the outlet nozzle analyses, the bottom boundary is aligned with the centerline of the nozzle, and one of the side boundaries passes through the nozzle centerline, but does not include the flaw face. These conditions are shown in Figure 4-10. For the transient and pressure cases, the top boundary is restrained to remain planar, but allows for upward and radial expansion relative to the centerline of the RPV shell; see Figure 4-11. The fixed displacement boundaries and planar restraint boundary provide appropriate fixity without over-restraining the model for thermal growth. For the mechanical load cases, the top boundary is fixed vertically to distribute the applied load evenly.

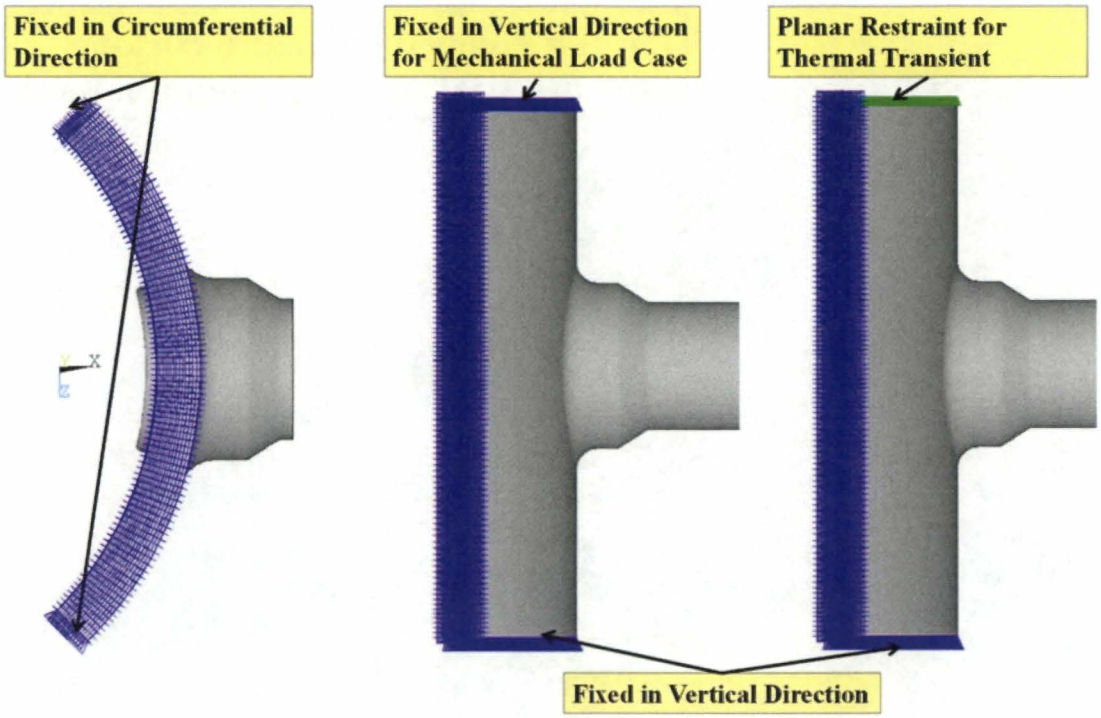

Figure 4-9 Full Model Boundary Conditions

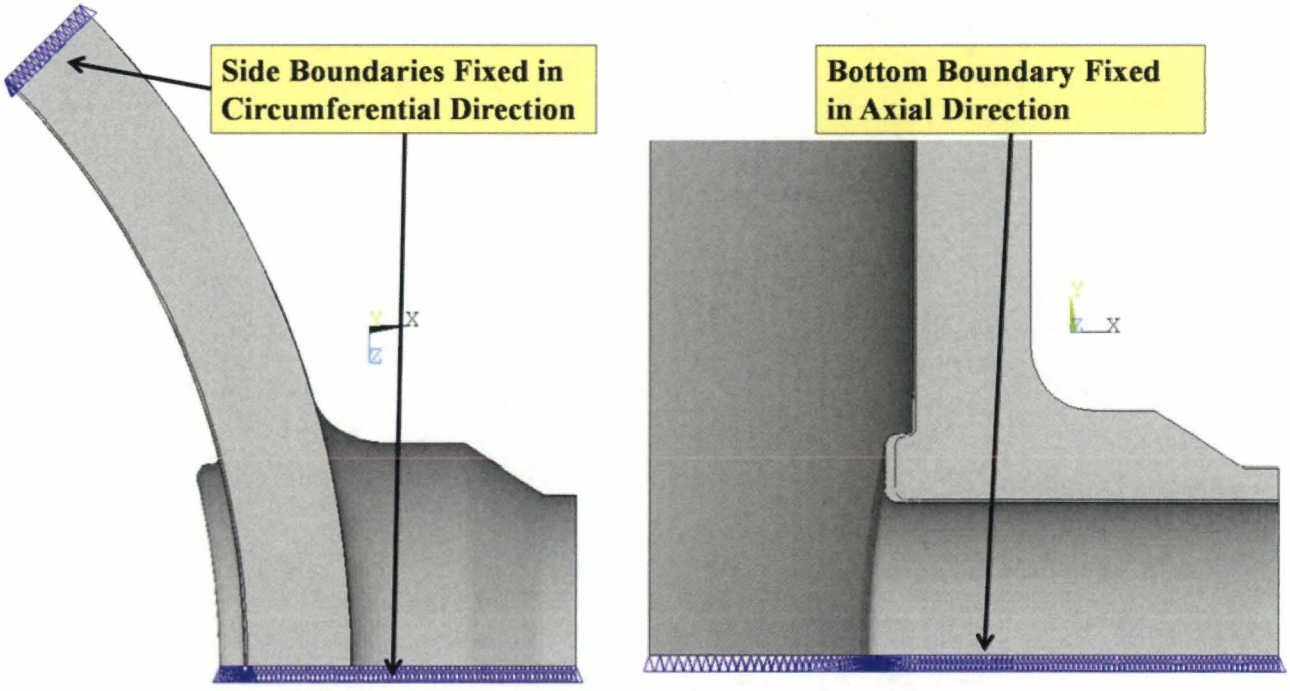

Figure 4-10 Quarter-symmetry Model Boundary Conditions

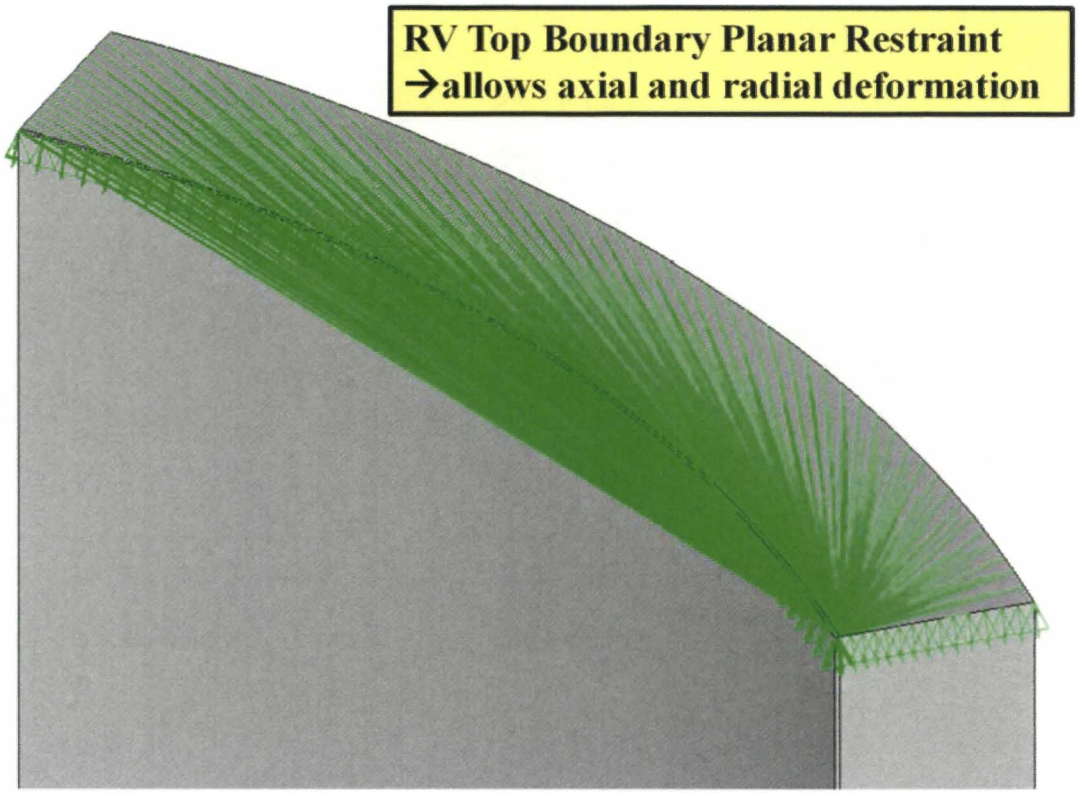

Figure 4-11 Coupled Node Restraint on Top of RPV Shell

4.5.2 System Pressure

A unit RCS pressure of 1,000 psi is applied to all wetted surfaces of the displacement DOF models, including the flaw face, as shown in Figure 4-12. The 1,000 psi is input into the 3D FEM in order to calculate the pressure SIF. The SIF results are combined with the thermal stress, which is then used to calculate the actual limiting pressure (P-T limit curve) using the ASME K_{IC} curve at a given temperature. The pressure stresses and SIF are linearly related for a given geometry. The nozzle safe-end and RPV shell are not capped; therefore, a blowoff pressure is calculated to generate the appropriate tensile load on these components. The blowoff pressure is based on the ratio of the uncapped open area to the cross-section area.

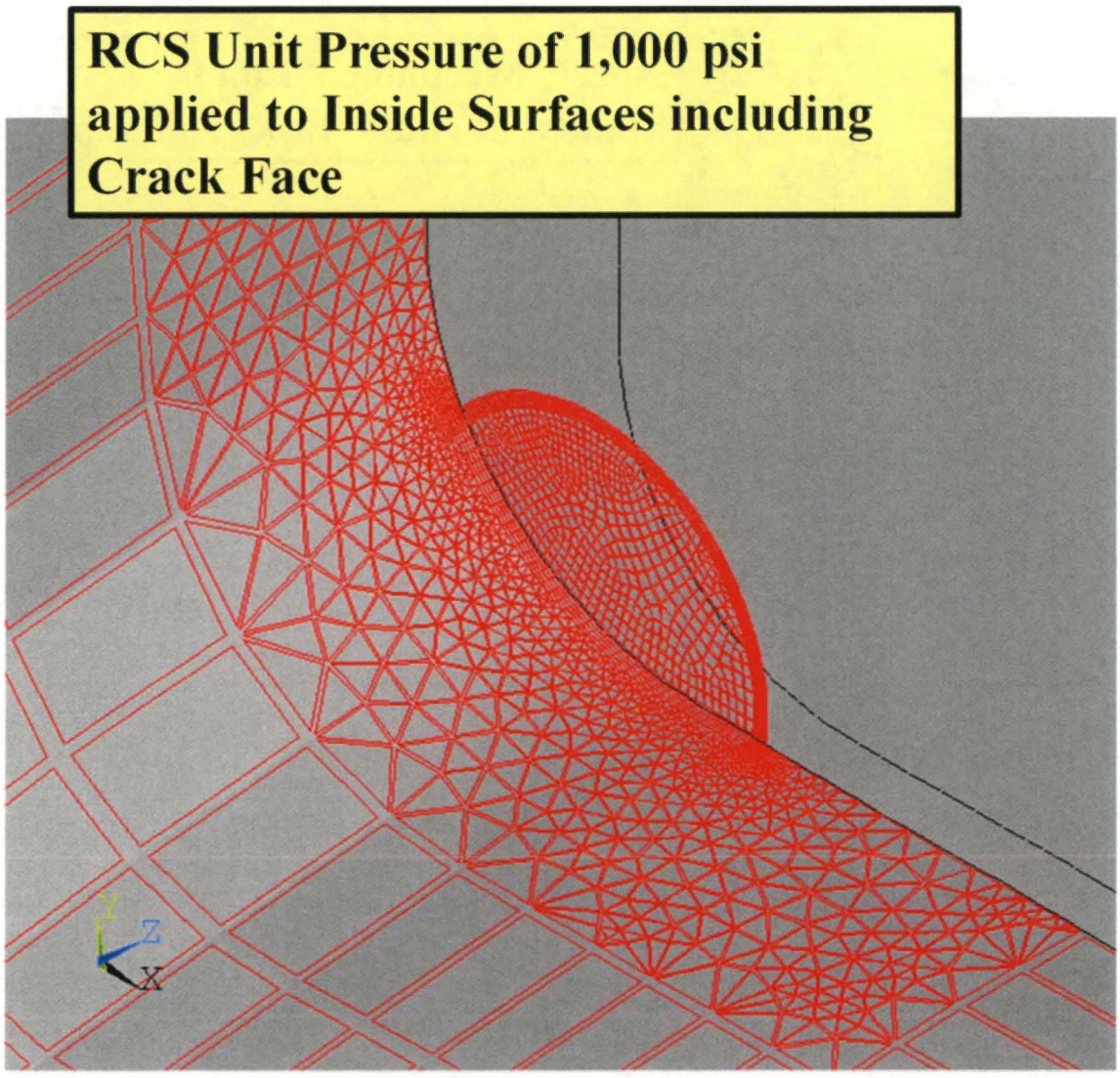

Figure 4-12 Pressure Surface

4.5.3 Nozzle Mechanical Loads

Nozzle loads from the piping are applied to the displacement DOF model. The loads are for the safe-end; however, the loads are applied at the end of a length of pipe to isolate the boundary conditions for load application. The loads are applied to a node that is rigidly connected to the pipe cut surface. This boundary condition is shown in Figure 4-13.

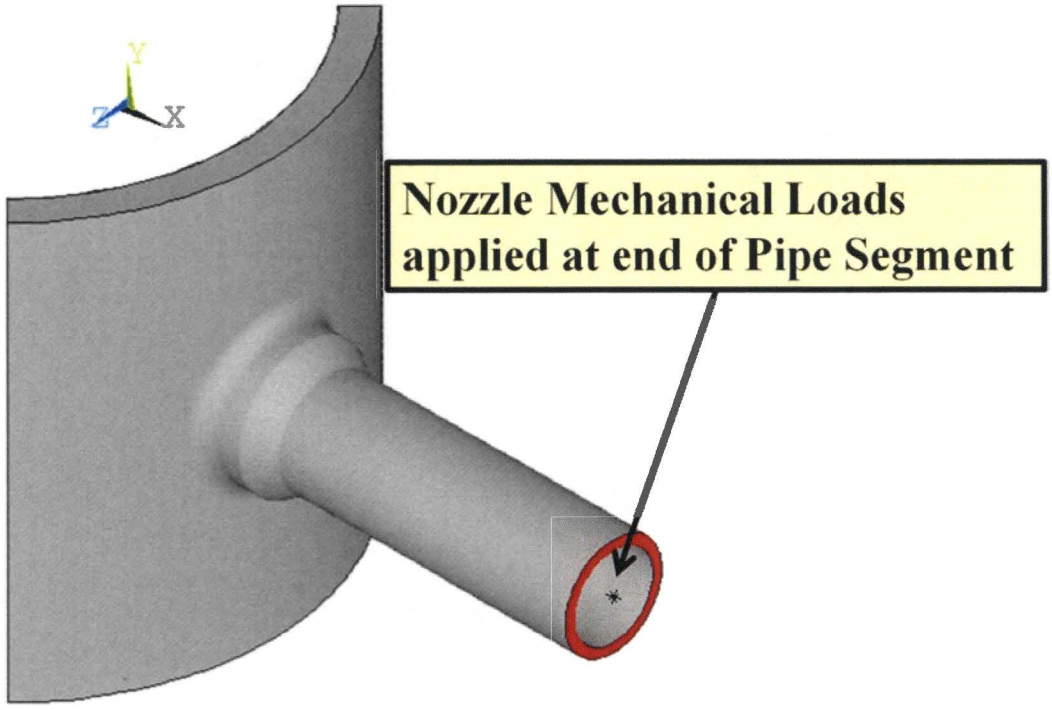

Figure 4-13 Mechanical Load Application Point

4.5.4 Body Temperature

The displacement DOF models input the results of the temperature DOF model. The two types of models are generated from the same mesh; therefore, the temperature contours from the thermal DOF model can be applied directly to the displacement DOF model without interpolation. The temperature contours for each time point in the thermal solution are mapped to every node in the displacement DOF model, which generates only thermal stresses for the cooldown transient.

4.6 MATERIAL PROPERTIES

The 1974 ASME Code [85] was used as the Code year of reference to be representative of PWROG plants. SA-508 Class 2 composition is taken from [86] to determine the elastic modulus. The cladding is assumed to be a typical Type 304 stainless steel. The displacement DOF model inputs are elastic modulus, Poisson's ratio, and coefficient of thermal expansion. The temperature DOF model inputs density, thermal conductivity, and specific heat. Poisson's ratio and density are not listed in the 1974 Code, and are therefore obtained from Table PRD of the 2013 ASME Code, Section II Part D [87]. The ASME Code does not provide specific heat directly; the value is calculated as a function of density, thermal conductivity, and thermal diffusivity.

The linear elastic FEM inputs include elastic modulus, coefficient of thermal expansion, thermal conductivity, and thermal diffusivity. Variations in these properties between different applicable code years for the bounded plants are not expected to significantly change the FEA results.

4.7 LOADS

4.7.1 Clad Residual Stress

The cladding on the inside surfaces of the inlet and outlet nozzle corners is thicker than for the RPV beltline. It consists of at least 2 layers of cladding, and the manual shielded metal arc process was used at the nozzle corners. The cladding thickness on the inlet nozzle corner is approximately ¼ inch thick (⅜ inch for the B&W design), while the cladding on the outlet nozzle corner at the end of the boss could be up to one inch thick. The thicker cladding can have a higher imposed stress in the LAS than a thinner layer simply due to the greater volume of clad thickness. The cladding imposes tensile stress due to the different thermal expansion coefficients of the stainless steel cladding versus the LAS nozzle forging at lower temperatures.

Residual stresses due to the nozzle/shell attachment weld are not considered in the analysis because they were stress relieved and any remaining stresses that that might still exist are remote from the region of interest.

The Swedish Nuclear Power Inspectorate compiled an extensive summary of the cladding effects on structural integrity in which they reviewed a number of measurement programs conducted on clad RPVs [88]. The authors concluded that it is reasonable to assume a peak clad residual stress at room temperature equal to yield stress of the cladding material (approximately 300 MPa [43 ksi]). Some measurements are reported at locations on an inlet and an outlet nozzle for the Lemoniz 2 RPV which show peak clad stresses higher than 300 MPa using the ring core method. Based on the cited reference in this report by Leggat, the ring core technique can produce higher results due to the introduction of excessive plastic strains. In addition, the Lemoniz 2 plant never operated. The measurements performed by Neber and Roth as reported in Reference [88] compared the clad residual stress from an RPV head which had been in operation to a component that had never been in operation. The head peak residual stress measurements were lower, which was attributed to stress relaxation during operation. For these reasons, it is concluded that the peak measurements on the Lemoniz 2

nozzles are higher than the PWROG fleet of nozzles that have been in operation for decades. Measurements were made by Westinghouse using a layer-removal technique for a two layer clad after stress-relief [89 and 90]. These results show a peak stress in the clad of 20 ksi with a compressive stress peaking at -6 ksi to -17 ksi in the LAS at room temperature. The clad stress through thickness averaged approximately 10 ksi.

In another reference, a numerical simulation was performed with a finite element code [91]. The heat source of the model representing the welding process was calibrated against the temperature profiles measured during welding. The temperature-dependent material properties, as well as the transformation behavior of the ferritic LAS, were taken into account. The calculated residual stresses showed tensile stresses in the cladding with significant variation depending on location relative to the clad strip edge in addition to the distance from the surface. This reasonably explains some of the variation seen among the various measurement programs reported in the literature. Other factors which would cause variation would be the heat input, welding speed, clad thickness, and alloy composition. The analysis simulation also showed a significant compressive stress in the LAS that is in agreement with measurements performed with an X-ray diffraction technique and that is needed to counteract for the tensile stress in the clad.

The NESC-IV [92] (and PVP2015-45086 [93]) measurements are more representative of the Ringhals head measurements [88] and scaled down Lemoniz 2 results. These results were determined to be representative of the U.S. PWR operating fleet nozzles and are reproduced in Figure 4-14.

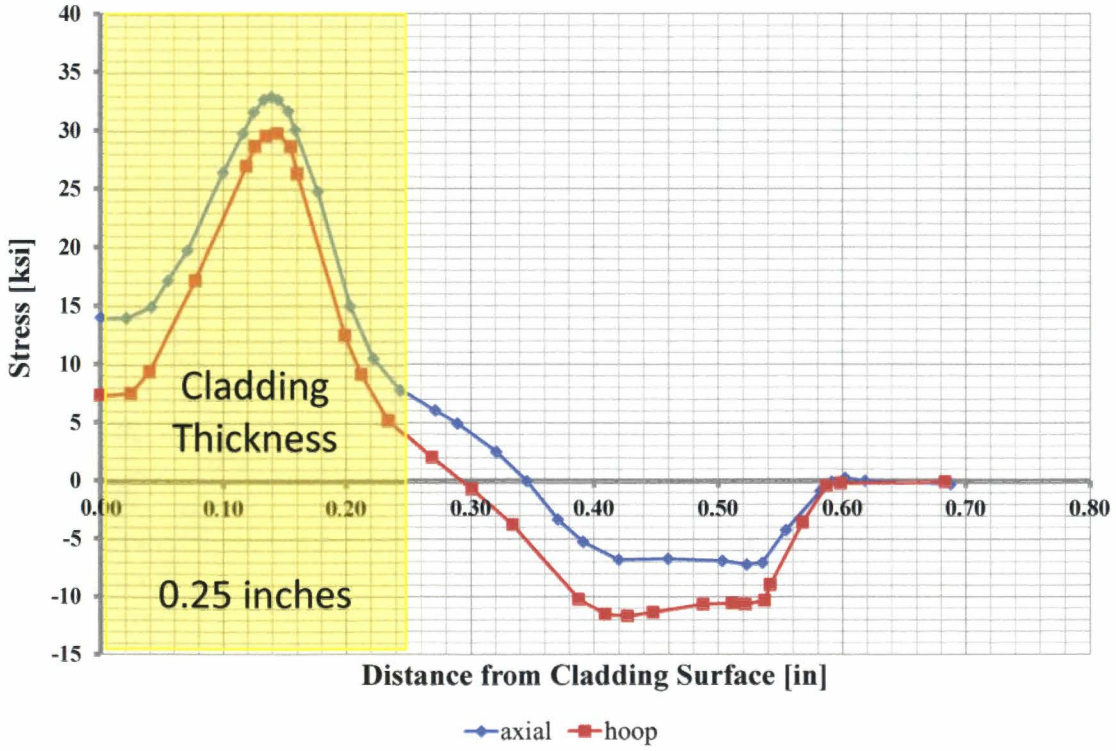

Figure 4-14 Clad Residual Stress Profile through Thickness [92]

For the thermal transient analyses of the nozzle corner flaws discussed in this document, the cladding in the displacement DOF models was provided with an elevated reference temperature for the CTE. This offset generated a tensile stress at room temperature, and was calibrated for each model type (i.e., inlet and outlet) to generate the appropriate average stress in the postulated flaw location. A test analytical model of a representative inlet was created to determine the appropriate average residual stress from the test data. The test model includes an inlet type nozzle on a thick flat plate, which is an approximation of the shell as being locally flat. The through-wall varying residual stress was input directly into the test FEM using table arrays and local coordinate systems. The test model input included only tensile cladding residual stresses because it is conservative to not include the compressive stresses in the LAS, as shown in Figure 4-14. The stresses from Figure 4-14 are based on limiting hoop and axial stresses with respect to the nozzle. The SIF solution was generated along the flaw front, representing the most accurate solution.

The analysis method described in the previous paragraph represents the most accurate solution by utilizing the spatially varying (i.e. through the thickness of the cladding) residual stress profile. However, this methodology is not practical for the wide variation of geometries used in this report for the determination of P-T limit curves, therefore an alternate approach was taken to demonstrate that the thickness varying residual stress profile could be replaced with an average residual stress and produce a similar result at the flaw tip. A series of analyses were made adjusting the cladding CTE reference temperature in the same test model as described in the previous paragraph. The variation of CTE reference temperature is a common approach for developing a pre-stress between two materials. This model was analyzed with the flaw open and with the flaw closed; load step 1 provides the SIF values for the activated flaw for a given reference temperature value and load step 2 provides the average cladding stress for the same reference temperature with the flaw deactivated. The iterations were performed until the SIF result from load step 1 (i.e., flaw open) was similar to the SIF from the explicit residual stress solution described in the preceding paragraph. When this was achieved, the average stress from load step 2 (i.e., flaw closed) was recorded. Figure 4-15 shows the SIF solution using the explicitly-applied data and the SIF solution for a uniform 22 ksi developed using the offset reference temperature method. The two methods show good agreement in the LAS region. The uniform stress value determined through the iterative process is similar to the calculated average of the cladding stress from Figure 4-15. Therefore, it is appropriate to use the analysis-derived uniform stress value of 22 ksi for the detailed inlet and outlet models. For the detailed models used in the analysis in Section 4.2, the cladding reference temperature was adjusted until the desired average cladding stress was achieved; this reference temperature is unique to each nozzle type due to different global stiffness.

In summary, the 3D FEM was designed to match the SIF imposed by the measured residual stress profile at room temperature as shown in Figure 4-14 rather than matching a specific stress-free temperature as was done in the ORNL work [18].

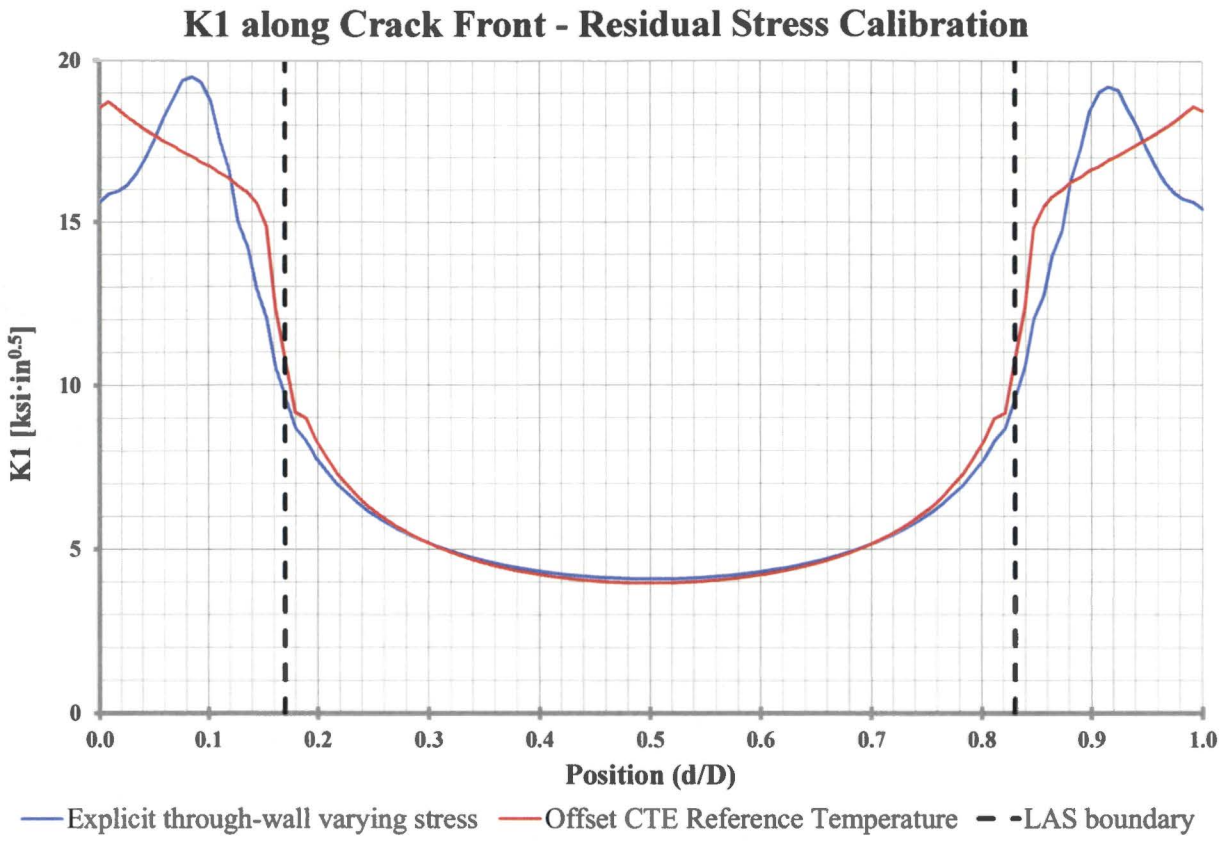

Figure 4-15 SIF Result Comparison for Explicit Method and Reference Temperature Method

4.7.2 Pipe loads

The RPV nozzle mechanical loads included typical deadweight and normal operation (NOp) thermal loads. The loads were applied to the model to maximize the hoop stress at the postulated flaw location. This included combining the magnitude of the deadweight and NOp loads to generate the largest magnitude even when the signs were different. The 3D FEA demonstrated that there was insignificant impact of pipe loads on the nozzle P-T limit curves.

4.7.3 Cooldown Rate

It has been determined that the limiting case is the normal cool-down transient, therefore only the normal cooldown transient was analyzed in this evaluation. The reasons for this determination are:

- Siegele, et al. [20] found that the normal cooldown transient is more severe than the heatup transient for the nozzles,
- Due to the differing thermal expansion of the cladding and the LAS, the warmer cladding relative to the LAS shell during heatup would result in a reduction of stress on a postulated inside surface flaw,

- Due to the temperature gradient during heatup, the thermal stress (excluding the cladding contribution) would produce compressive stress on the postulated inside surface flaw,
- The radii for the inside corners are significantly smaller than for the outside nozzle-to-shell transition making the postulated inside surface corner flaw limiting due to higher stress concentration.

Initially, the following realistic bounding cooldown transient was used (Figure 4-16) for all the cases identified in Table 4-2 for the baseline cases:

- 100°F/hr from operating temperature to 110°F then switch to
- 50°F/hr from 110°F to 100°F then
- 20°F/hr below 100°F.

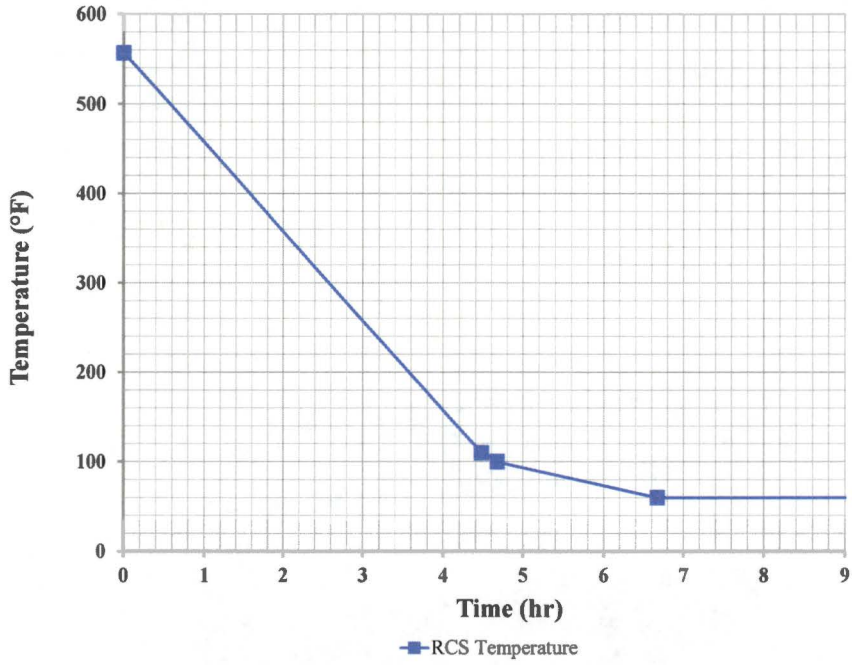

Figure 4-16 Bounding Normal Cooldown Transient

This transient bounds the hypothetical fastest cooldown rate that the residual heat removal (RHR) systems (or shut down cooling systems [SDC]) can achieve under the best circumstances for any U.S. PWR design. In addition, 32 actual cooldown transients were reviewed from the 2, 3, and 4-loop Westinghouse and various CE designs. Based on data pertaining to the 32 cooldown transients from six different plants, it is concluded that:

- The maximum plant cooldown rate averaged from actuation of RHR or SDC system until just prior to shutdown of last RCP was 13°F/hour

- The maximum plant cooldown rate averaged from just prior to shutdown of last RCP until near atmospheric pressure was 11°F/hour

- The lowest temperature at which any significant pressure (> 200 psig) was maintained in the RCS was above 90°F for all cooldowns. At and below this temperature, there was no significant pressure in the RCS. Additionally, the maximum temperature change in any 1-hour increment with all RCPs shut down never exceeded 45°F (above 110°F), with averages throughout the phase never exceeding 11°F/hour

Based on the hypothetical most aggressive case RHR or SDC system capability and operating experience, the above cooldown transient is conservative.

However, since some licensees have allowable cooldown rates of 100°F/hour from operating temperature to 50°F, a 100°F/hour cooldown rate was used in the 3D FEA for the limiting case (outlet nozzle, 6:1 flaw aspect ratio, 0.5-inch deep flaw into LAS) for several nozzle geometries. The 100°F/hour rate from operating temperature to 50°F is very conservative relative to what can be realistically achieved at lower temperatures and is consistent with the U.S. PWR highest allowable cooldown rate.

4.8 STRESSES AT LIMITING LOCATIONS

Figure 4-17 through Figure 4-20 show the stresses in the inlet and outlet models without a flaw at the nozzle corner. These plots demonstrate the nozzle corner is the limiting location for both pressure and thermal gradient induced stresses, which confirms the selection of this region as the location for placing the detailed flaw meshes.

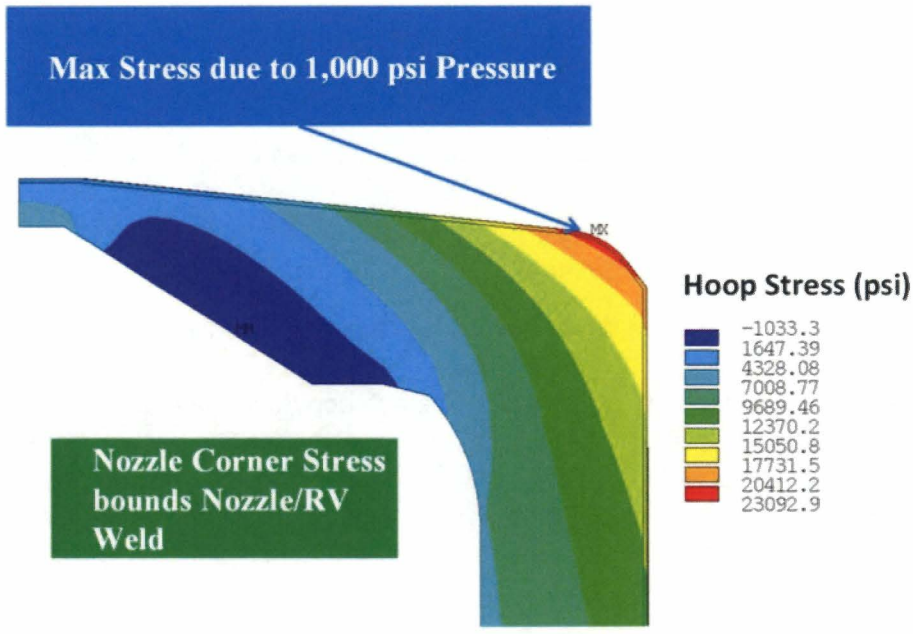

Figure 4-17 Inlet Model without Crack – Stress for 1,000 psi Pressure

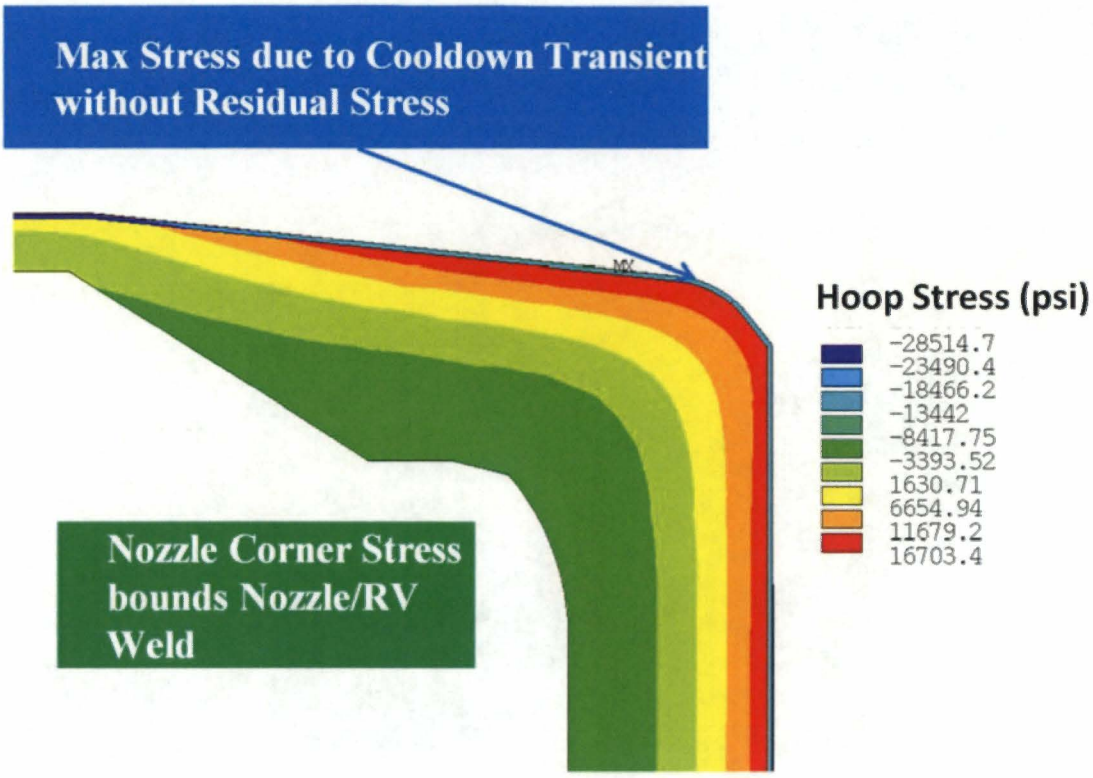

Figure 4-18 Inlet Model without Crack – Maximum Stress during Cooldown

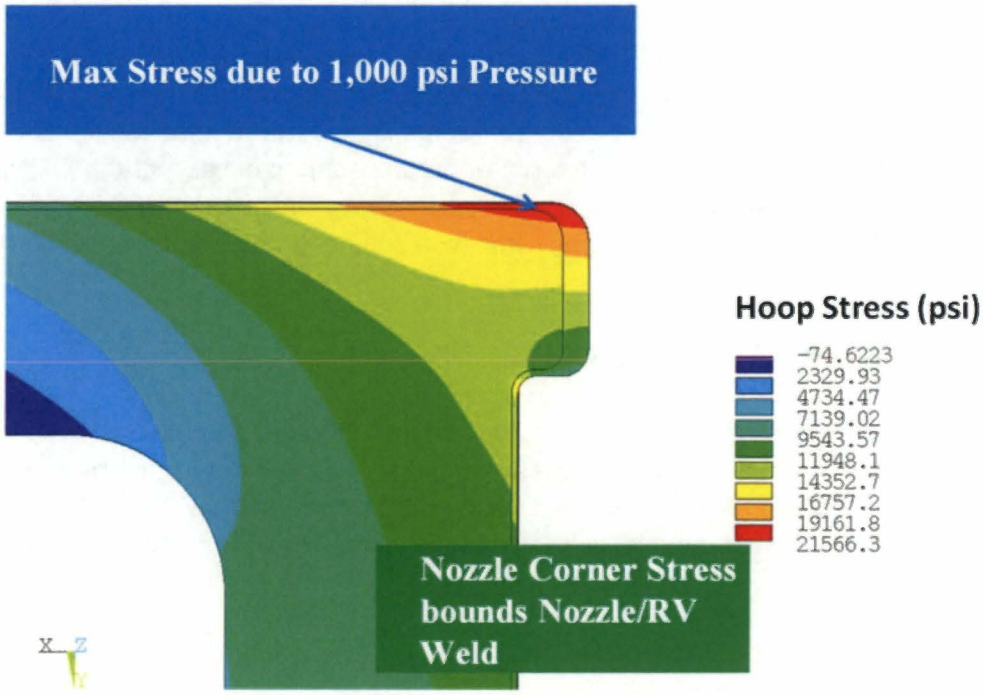

Figure 4-19 Outlet Model without Crack – Stress for 1,000 psi Pressure

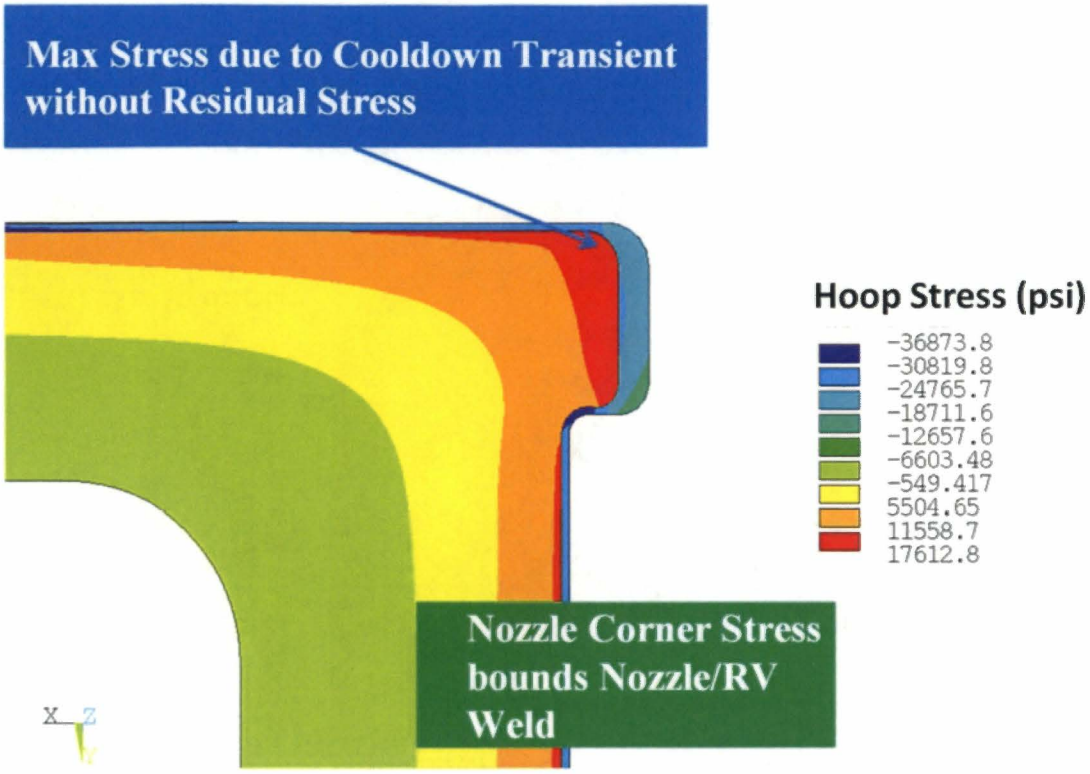

Figure 4-20 Outlet Model without Crack – Maximum Stress during Cooldown

The analyses reported in an ORNL report [18] showed higher stresses for the 1,000 psi unit pressure cases. Close inspection of the figures of the model provided in [18] shows a simpler fillet on the inlet nozzle corner; the top-view in the drawing used for this FEM of the inlet nozzle corner shows a more complicated blend between the conical shaped opening and the RPV inner diameter. This creates a larger effective radius of curvature that lowers the pressure induced stresses. For the outlet nozzle, it is not apparent from inspection of the ORNL model if the significant cladding build-up on the nozzle corner was included; the thicker cladding is present in the FEM included in this report and would tend to reduce stresses for pressure loading.

4.9 STRESS INTENSITY FACTOR RESULTS

In this section, results are presented for the outlet nozzle. Although evaluations were carried out for both inlet and outlet nozzles with the cases identified in Table 4-1, only the results for the limiting case (outlet nozzle, 6:1 flaw aspect ratio, 0.5-inch deep flaw into LAS) are shown. Demonstration that the outlet nozzle is more limiting than the inlet nozzle is contained in Section 5.1.1.

4.9.1 Static Load Cases

A 1,000 psi pressure case and a mechanical load case were performed for the flaw cases from Table 4-2. The "CINT" command in ANSYS was used to calculate the SIF during solution

processing. This command performs contour integration at several distances about the flaw front to generate SIF values, which were extracted for each case. The output for six contours is provided, which show convergence from contours 2 through 6 in Figure 4-22 through Figure 4-24.

Example plots for the outlet nozzle with crack depth, *a*, equal to 1.18 inches and the crack length, *L*, equal to 2.36 inches and 7.08 inches are shown in Figure 4-22 through Figure 4-24. The curves for the pressure case shown in Figure 4-22 and Figure 4-23 demonstrate the difference in the location of the maximum SIF (i.e., inversion of the curve) for circular and semi-elliptical flaws, respectively. The normalized location along the flaw front, d/D, is illustrated in Figure 4-21. Figure 4-24 shows the relatively low SIF for deadweight plus normal operating thermal mechanical loads.

Additional static pressure results for the geometries listed in Table 4-1 are compared to the baseline results in Figure 4-25. The comparison shows that the CE System-80 and the bounding Westinghouse 4-loop geometries are bounding. The three limiting results are included in the evaluation in Section 5.

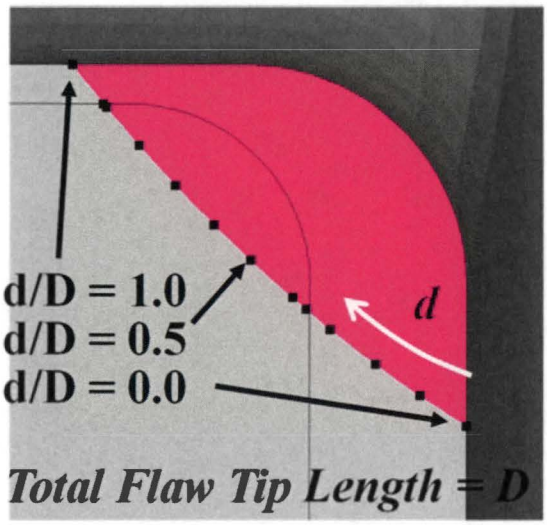

Figure 4-21 SIF Output Location Definition

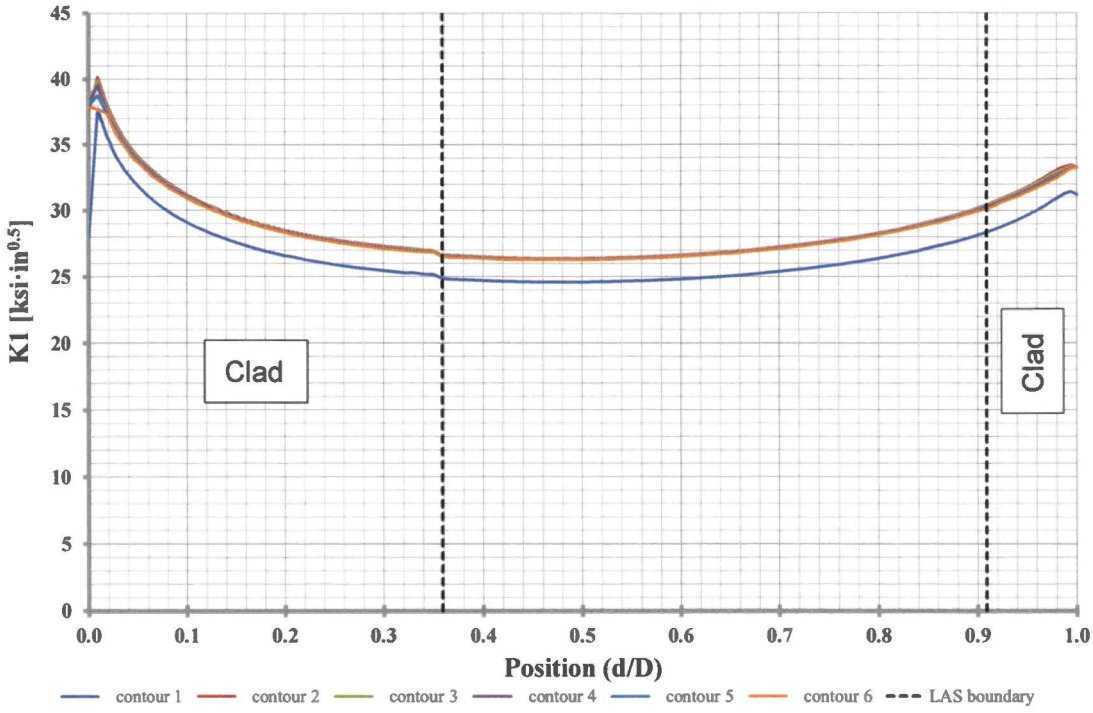

Figure 4-22 Pressure SIF along Crack Front for Baseline Outlet Nozzle with a = 1.18 Inch, L = 2.36 Inch Flaw for 1,000 psi

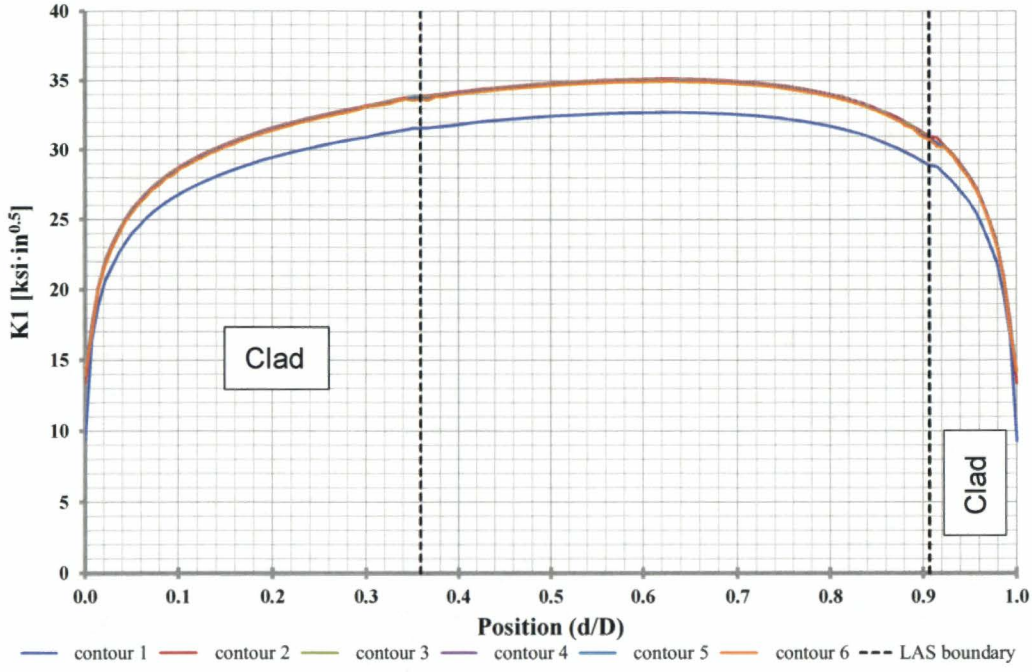

Figure 4-23 Pressure SIF along Crack Front for Baseline Outlet Nozzle with a = 1.18 Inch, L = 7.08 Inch Flaw for 1,000 psi

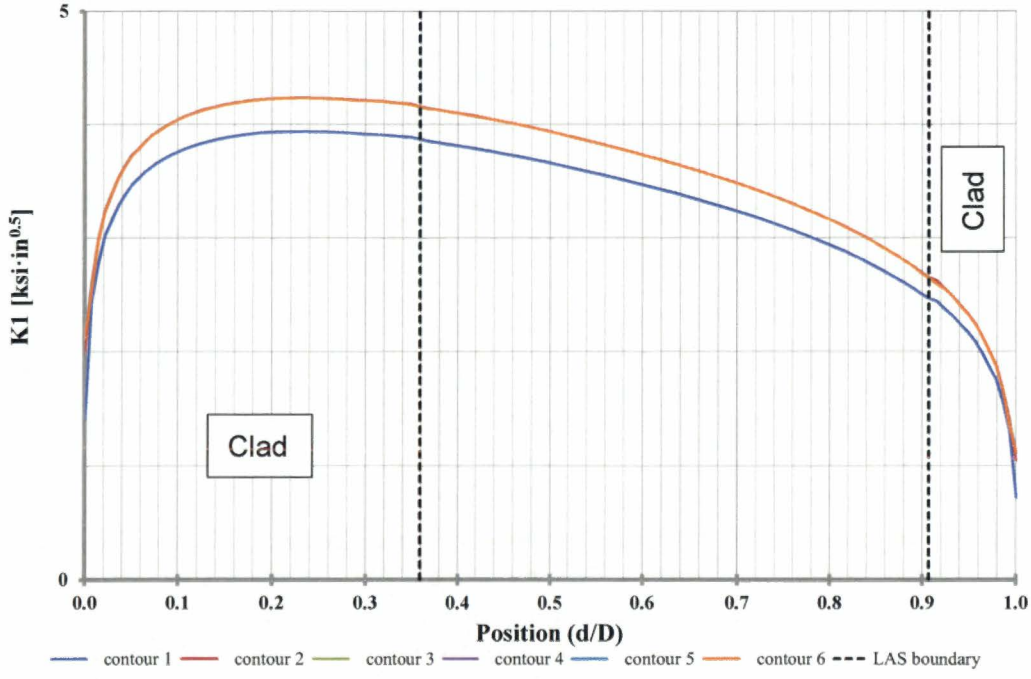

Figure 4-24 SIF for Baseline Outlet Nozzle along Crack Front with a = 1.18 Inch, L = 7.08 Inch Flaw for Deadweight + Normal Operating Thermal Mechanical Load

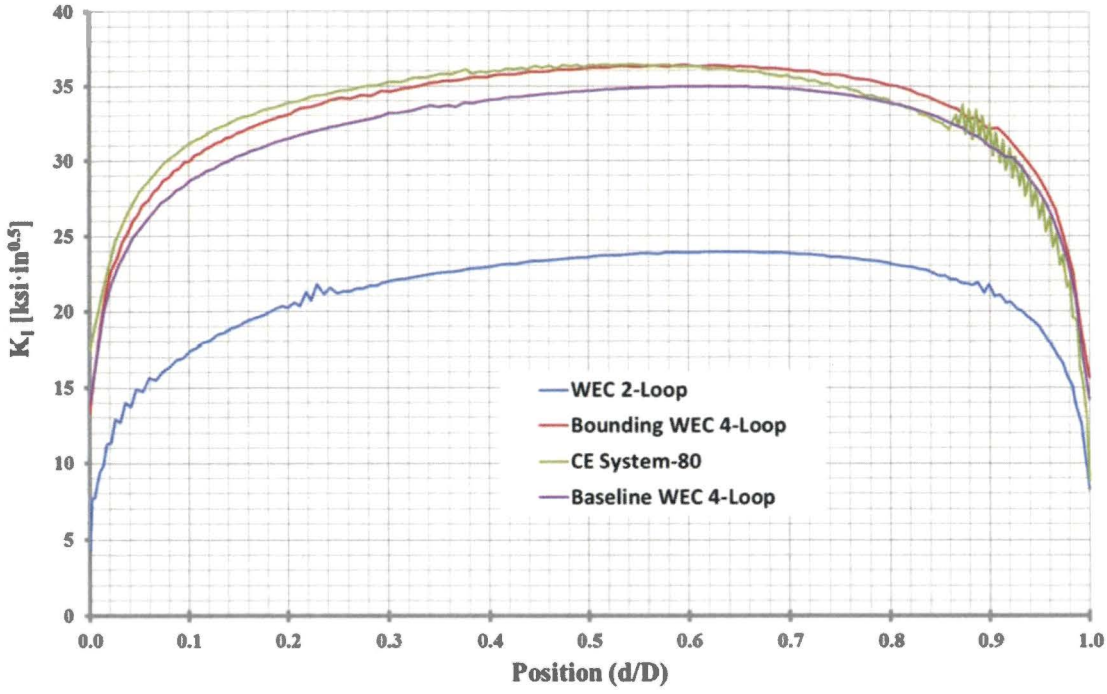

Figure 4-25 Pressure SIF along Crack Front for Outlet Nozzle for Different Modeled Geometries using Limiting LAS Flaw Size of 6:1 Ratio, 0.5-Inch Depth

4.9.2 Cooldown Transient

The flaw cases from Table 4-2 were evaluated with the cooldown transient from Figure 4-16 and the residual stress (Figure 4-14). A time-history of K values for all locations along the crack front was extracted from the model.

Example plots for the outlet nozzle with crack depth, *a*, equal to 1.18 inches and the crack length, *L*, equal to 7.08 inches are shown in Figure 4-26 and Figure 4-27 for the time-history and time point for the maximum SIF, respectively. The time-history plot shows data for locations in the LAS only.

The time-history solution shows that the peak SIF occurs at the end of the 100°F/hour cooldown rate when the nozzle temperature gradient is the largest both for the transient with the constant 100°F/hour to 60°F and the stepped cooldown rate transient. The SIF decreases during the 50°F/hour and 20°F/hour portions of the cooldown transient, and continues to reduce as the gradient settles to a steady-state condition at 60°F (i.e., no temperature gradient).

Additional cooldown results for the geometries listed in Table 4-1 are compared to the baseline results in Figure 4-28. The comparison shows that the CE System-80 design is bounding of the other geometries due to the larger outlet nozzle diameter. These limiting results are included in the evaluation in Section 5. The additional nozzles were analyzed with a constant cooldown

transient of 100°F/hour from operating temperature to 50°F, while the "baseline" cases had the changing cooldown rate shown in Figure 4-16 down to 60°F. The additional cases are very conservative as shown in Figure 4-28 by the higher peak stress at the end of the cooldown when plant systems cannot achieve the 100°F/hour rate. The Westinghouse 2-loop design is not considered in Section 5, since it is not close to limiting in both the static and transient cases as shown in Figure 4-25 and Figure 4-28.

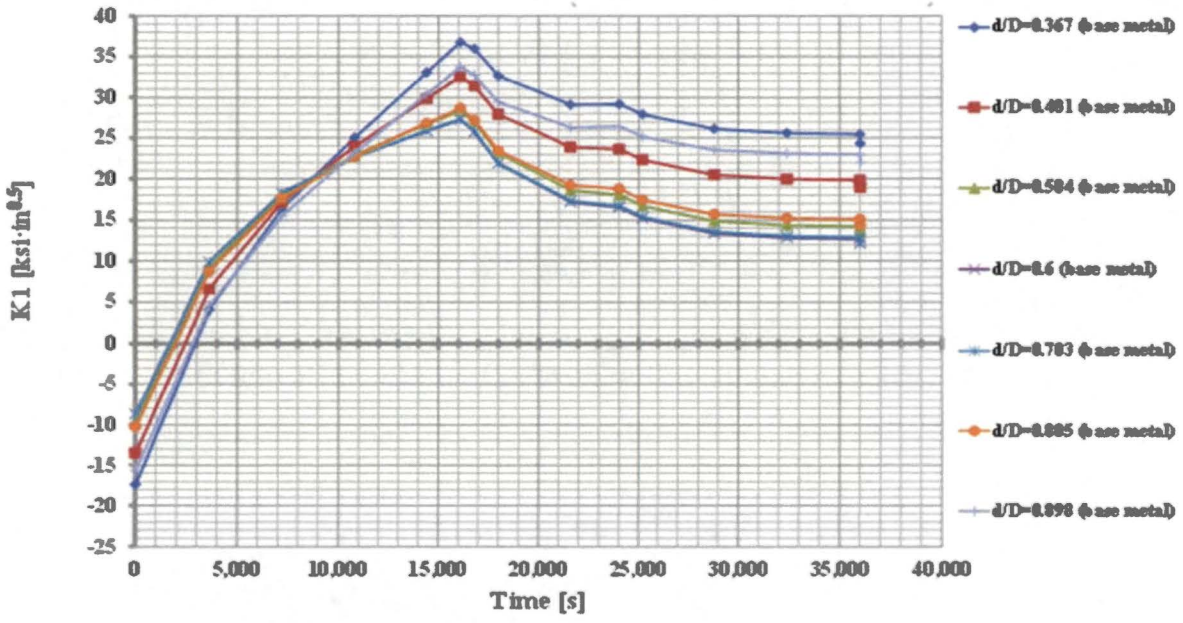

Figure 4-26 SIF Time-history for Baseline Outlet Nozzle with a = 1.18 Inch, L = 7.08 Inch Flaw at Various Locations along the LAS Crack Front during Cooldown (Thermal and Residual)

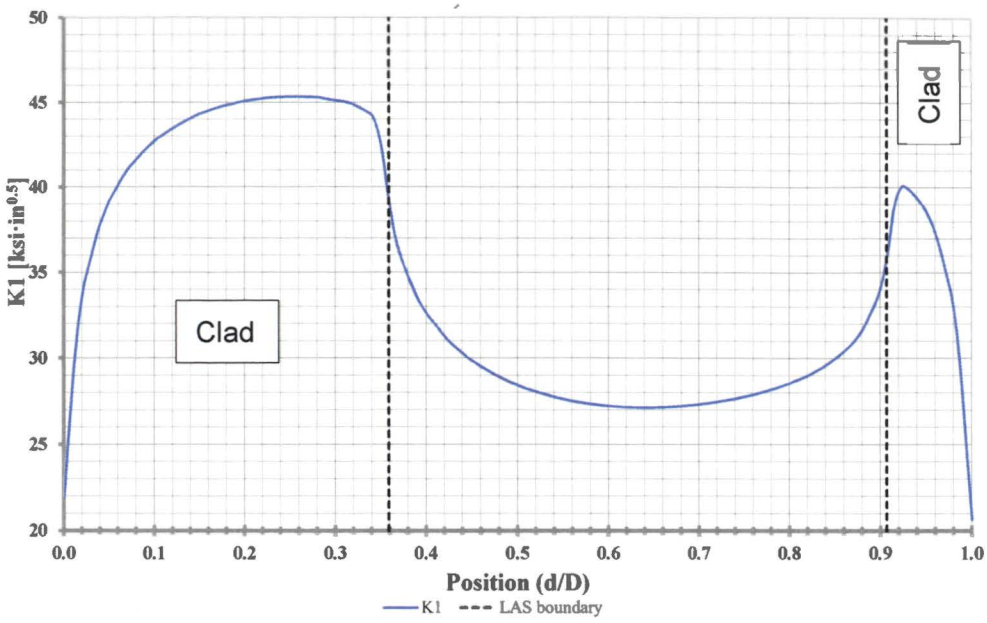

Figure 4-27 SIF for Baseline Outlet Nozzle with a = 1.18 Inch, L = 7.08 Inch Flaw at t = 16,092 Seconds of Cooldown (Thermal and Residual)

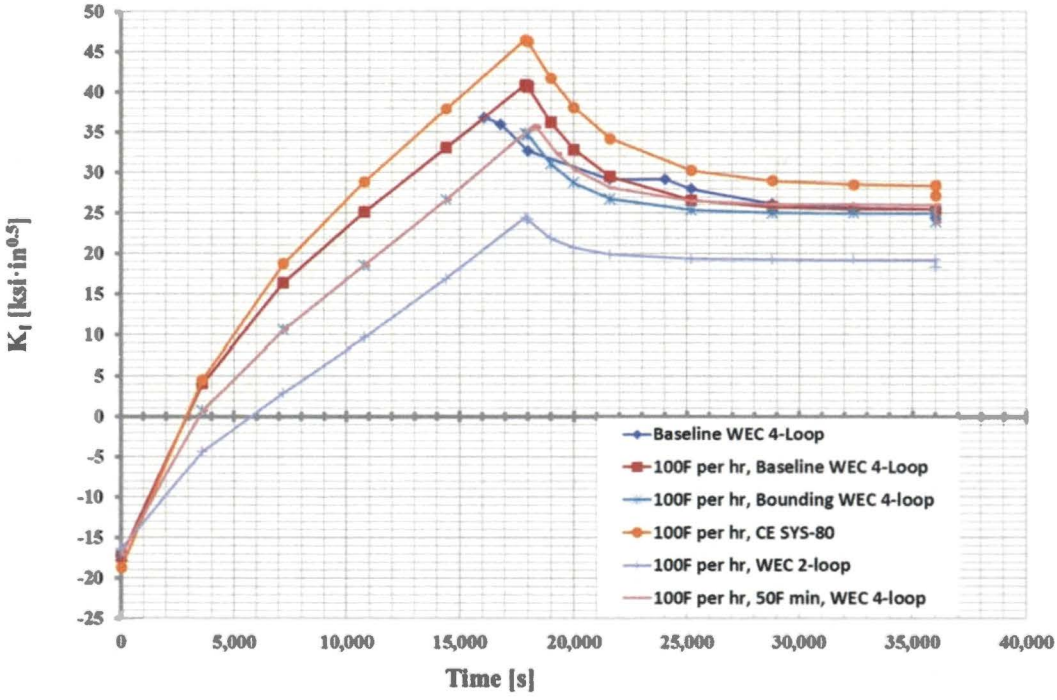

Figure 4-28 SIF Cooldown Time-history for Outlet Nozzle for Different Modeled Geometries using Limiting LAS Flaw Size of 6:1 Ratio, 0.5 Inch Depth

4.10 CONSTRAINT AND CLADDING EFFECT

4.10.1 Constraint

The standard deeply-cracked fracture toughness specimen (CT specimen) has a relatively high constraint condition. This enables testing that produces conservative fracture toughness results. When applying this information to a structure with a postulated flaw, there may be loss of constraint depending on the loading condition and flaw size. There has been an effort in the last two decades to understand and quantify the effect of constraint condition on fracture toughness. The SE(B) specimen has a somewhat lower constraint condition than the CT specimen, which produces lower T_0 values (greater toughness), hence the bias adjustment applied to the SE(B) specimen geometry as discussed in Section 3.1.2.1. There have been a number of methods developed to quantify the constraint condition [94]. The most common is T-stress for application to ductile-brittle fracture toughness of RPVs. T-stress is an elastic parameter that corresponds to the higher order non-singular term in the series expansion of the stress field equation. T-stress is normally expressed in terms of the biaxiality ratio. Details of the T-stress can be found in Wallin's Reference [94]. T-stress is a measure of constraint and is correlated to toughness as expressed in T_0. Wallin provides a correlation for various specimen geometries and T-stress. The standard CT fracture toughness specimen has the highest constraint among various test specimen geometries and produces the highest T_0 (lowest toughness). Thus when this data is applied to a structure with a lower constraint condition, the high constraint toughness is conservative.

A number of analysts have calculated the T-stress for relevant nozzle geometries to assess the amount of conservatism. Siegele et al. evaluated various sized nozzle corner flaws postulated in a German PWR under various loading conditions, including normal cooldown [20 and 95]. They concluded that the nozzle corner flaw had a significant negative T-stress, indicating loss of constraint, resulting in an increase in toughness. The reduction in T_0 for this level of constraint relative to the CT specimen constraint condition was in the range of 40°C to 80°C [95]. The correlation between T-stress and T_0 has been shown by Wallin and others per Figure 4-29.

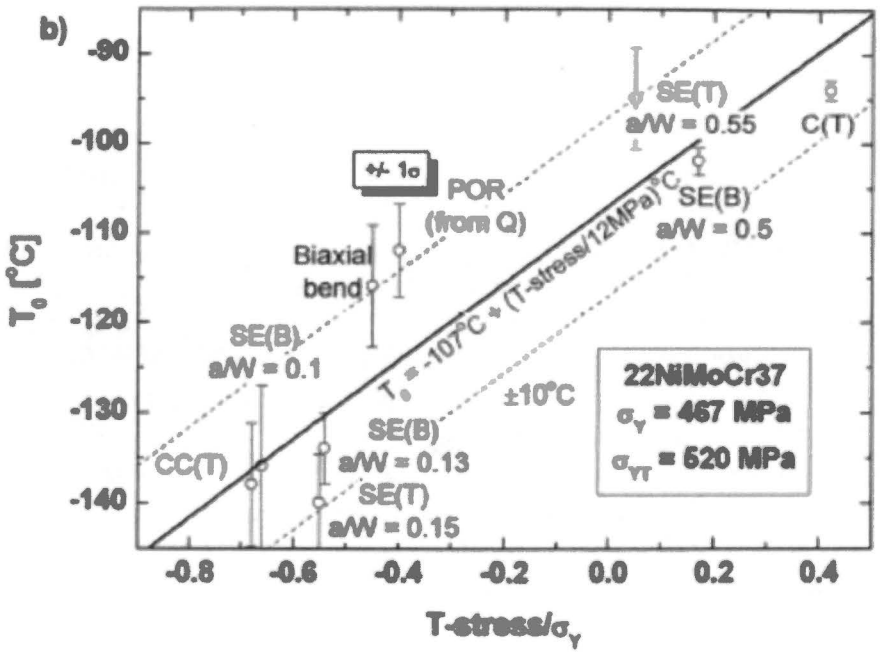

Figure 4-29 T-stress/σ_y versus T_0 Dependency [94]

Corner flaws have also been assessed for T-stress and were determined to have negative T-stress values [96]. Qin et al. evaluated a nozzle corner flaw for a BWR nozzle of varying depth from ¼T and greater [97]. The T-stress was found to be slightly negative considering both pressure and thermal loads on average along the flaw front for a 100°F/hour cooldown transient. The analysis did not include cladding and the ¼T flaw is approximately 2 inches deep (smaller than a PWR RPV nozzle ¼T flaw and larger than the flaws postulated in this assessment).

Two intermediate test vessels with inside nozzle corner flaws were pressurized to failure at ORNL under the Heavy Section Steel Technology (HSST) Program [98]. Vessel V-5 leaked without fracturing and Vessel V-9 failed by fast fracture as expected. The nozzle corner failure strains were considerably greater than the pretest plane-strain estimates. The inside nozzle corner tangential strains were negative, implying transverse contraction along the flaw front. Merkle reassessed these tests considering the constraint condition by using the Irwin beta formula. This is empirical evidence that demonstrates that there is a constraint condition for nozzle corner flaws which demonstrates conservativeness in the approach taken in this report, which does not consider constraint.

Section 5.1.1 demonstrates that the limiting geometry case was the outlet nozzle with the flaw depth and length equal to 1.18 inches and 7.08 inches, respectively. The limiting transient time point shown in Figure 4-26 and the pressure case were performed in ANSYS 16.1 to calculate the T-stress along the flaw tip.

The calculated T-stress is negative for the pressure cases; however, a review of the thermal case shows that the limiting cooldown time point partially negates the pressure effect. The result

shows a small negative T-stress of approximately -2 ksi occuring at the limiting location near the cladding boundary at d/D = 0.359. Relative to the minimum A-508 Class 2 yield stress, it is a ratio slightly less than 0. Comparing this T-stress/σ_y ratio relative to the constraint condition of the CT specimen in Figure 4-29, an expected improvement in T_0 for the constraint condition of the limiting SIF case results in approximately 25°F (14°C).

Other analyses of nozzle corners, the 3D FEA conducted for this report, and empirical evidence show loss of constraint in the nozzle corner region. Loss of constraint is associated with increased toughness. No credit is taken for the increased toughness due to constraint loss of the evaluated nozzles, adding conservatism to the approach used.

4.10.2 Cladding

Cladding has the ability to restrain a flaw from opening due to its superior ductility. A semi-elliptical flaw introduced by fatigue was covered by stainless steel cladding and specimens were tested under biaxial conditions in the ductile-to-brittle transition regime. Test results showed that cladding plays a significant role and contributes to an additional safety margin. In addition, cladding increases the potential for crack arrest [99]. Therefore, one conservativism of this analysis is that it does not credit the potential ability for the ductile cladding to restrain crack growth.

5 PRESSURE-TEMPERATURE LIMIT CURVES

The nozzle P-T limits are determined based on ASME Section XI, Appendix G. The procedures in Appendix G are based on the principles of linear elastic fracture mechanics. Using a postulated flaw, the Mode I SIF, K_I, is calculated based on membrane (and bending for nozzles) stresses due to normal loading conditions. The calculated K_I is compared to a reference value K_{Ic} based on the metal temperature and the material's ART.

5.1 GENERATION OF NOZZLE P-T LIMIT CURVES

Nozzle cooldown P-T limit curves were generated using two different methods, both of which comply with ASME Section XI, Appendix G.

1. The pressure and time-dependent thermal SIFs using FEMs containing the explicit postulated small flaws (Section 2) were determined as described in Section 4 to develop nozzle P-T limit curves. This is described in Section 5.1.1.

2. For the larger postulated flaws, pressure and time-dependent thermal stresses from unflawed FEMs were determined. The closed form SIF solution based on ORNL/TM-2010/246 [18] was used to develop nozzle P-T limit curves with a postulated flaw size comparable to the beltline ¼ thickness flaw used in traditional P-T curves (~2.1 inches). This simpler method using the larger postulated flaw is described in Section 5.1.2.

In Section 5.2 the nozzle P-T limit curves are then compared to current plant traditional NRC approved P-T limit curves to determine if the nozzles are more limiting or are bounded by the traditional P-T limit curves.

5.1.1 Generation of Nozzle P-T Limit Curves with Postulated Small Flaw

In order to determine the nozzle corner P-T limit curves, the allowable pressure has to be calculated for each time step in the cooldown transient. To calculate the allowable pressure, the allowable K_{Im}, membrane SIF, has to be calculated. Based on the ASME Code, Appendix G [1], the K_{Im} is determined as follows:

$$K_{Ic} > 2K_{Im} + K_{It}$$

$$(K_{Ic} - K_{It})/2 > K_{Im}$$

Where:

- $K_{Ic} = 33.2 + 20.734 * e^{(0.02(T-RT_{NDT}))}$ in units of ksi $\sqrt{in}$. This is the fracture toughness calculated based on Section XI, Appendix G.
- T = crack-tip temperature.
- RT_{NDT} = ART = material reference nil-ductility temperature as shown in Section 3.5.
- K_{It} = stress intensity factor calculated for the thermal stress gradient for a cooldown transient based on the methodology in Section 4.9.2.

The allowable pressure ($P_{allowable}$) was determined by taking the ratio of the allowable membrane SIF, K_{Im}, from above and the pressure SIF, K_{Ip}, which is linearly related to the 1,000 psi unit pressure input into the FEM in Section 4.9.1 (P_{FEM}). The pressure SIF (K_{Ip}) was determined based on the FEM that contains the postulated flaw at the nozzle corner cut as shown in Section 4.9.1. The allowable pressure is as follows:

$$P_{allowable} = K_{Im} * P_{FEM} / (K_{Ip})$$

The allowable pressure can be plotted versus temperature for various time steps for the cooldown transient or for the steady-state case to generate the nozzle P-T limit curves.

Figure 5-1 through Figure 5-4 show the inlet and outlet nozzle P-T limits (where the indicated pressure is $P_{allowable}$) developed for the postulated flaws with the Westinghouse 4-loop baseline geometry. The flange-notch requirement which requires a minimum pressure of 621 psig is also shown in Figure 5-1 through Figure 5-4. The flange requirements are based on 10 CFR 50 Appendix G, which requires the allowable pressure to be 20% of pre-service hydrostatic pressure (3,107 psig), which is 621 psig for the PWR design.

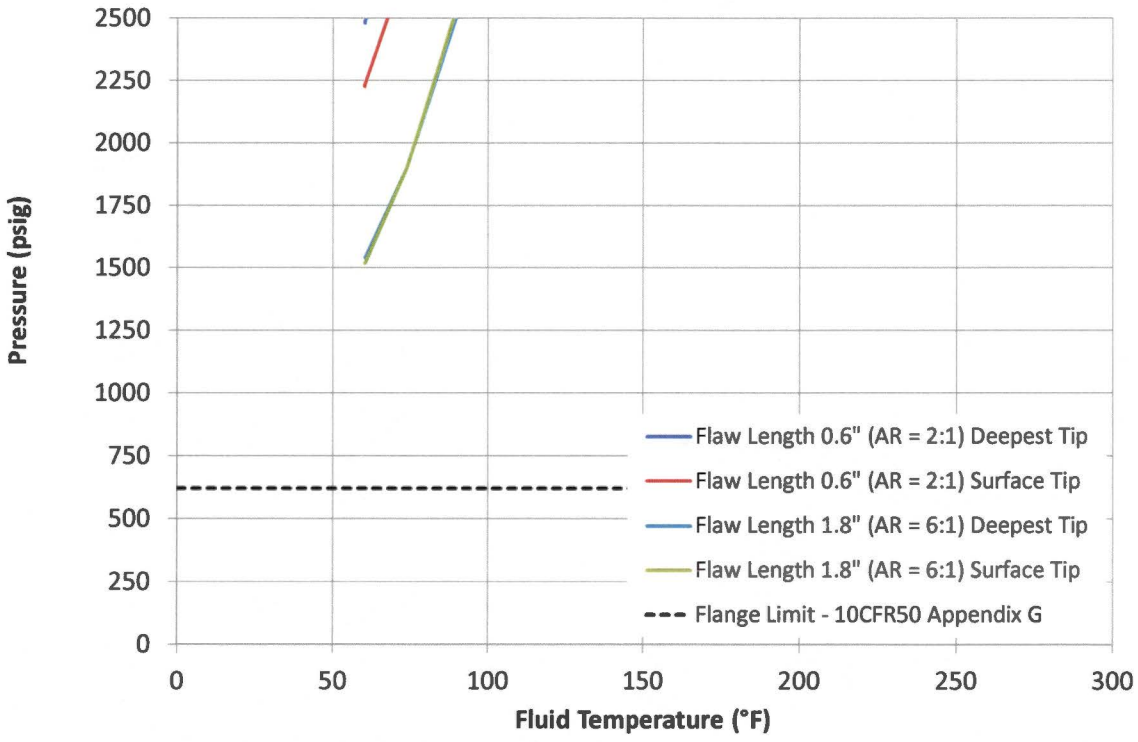

Figure 5-1 Inlet Nozzle Cooldown P-T Limit Curves with Flaw Depth of 0.3 Inch (ART = 21°F)

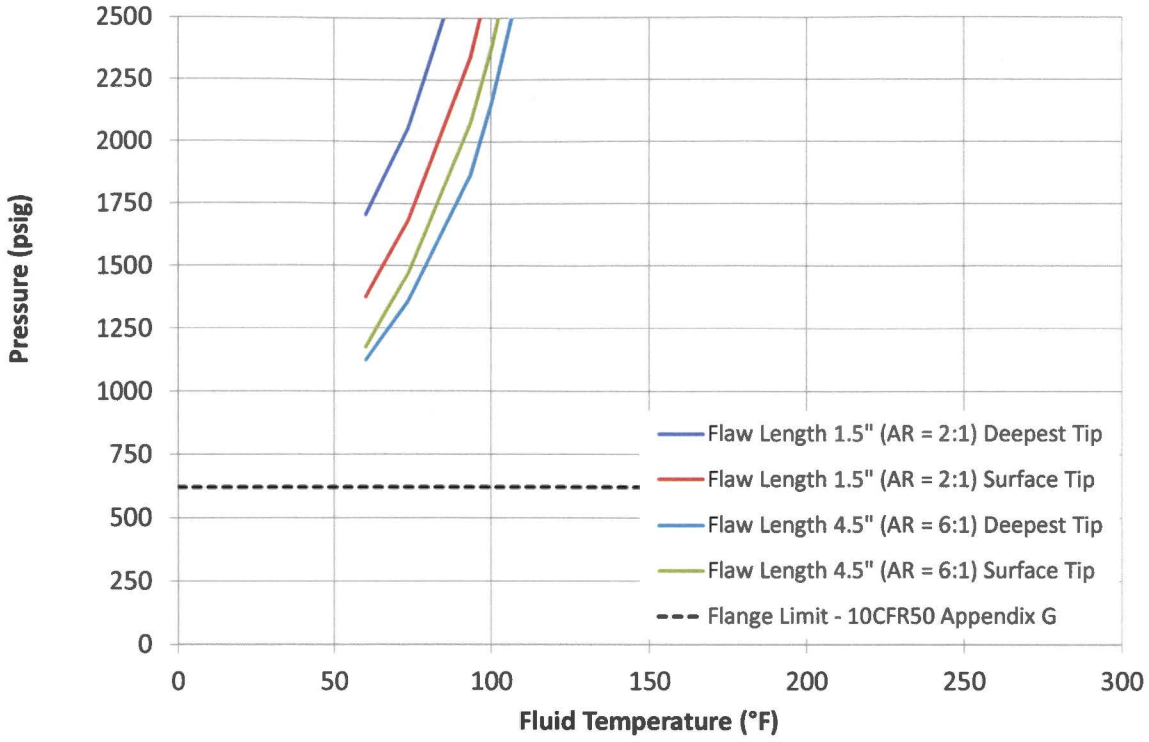

Figure 5-2 Inlet Nozzle Cooldown P-T Limit Curves with Flaw Depth of 0.75 Inch (ART = 21°F)

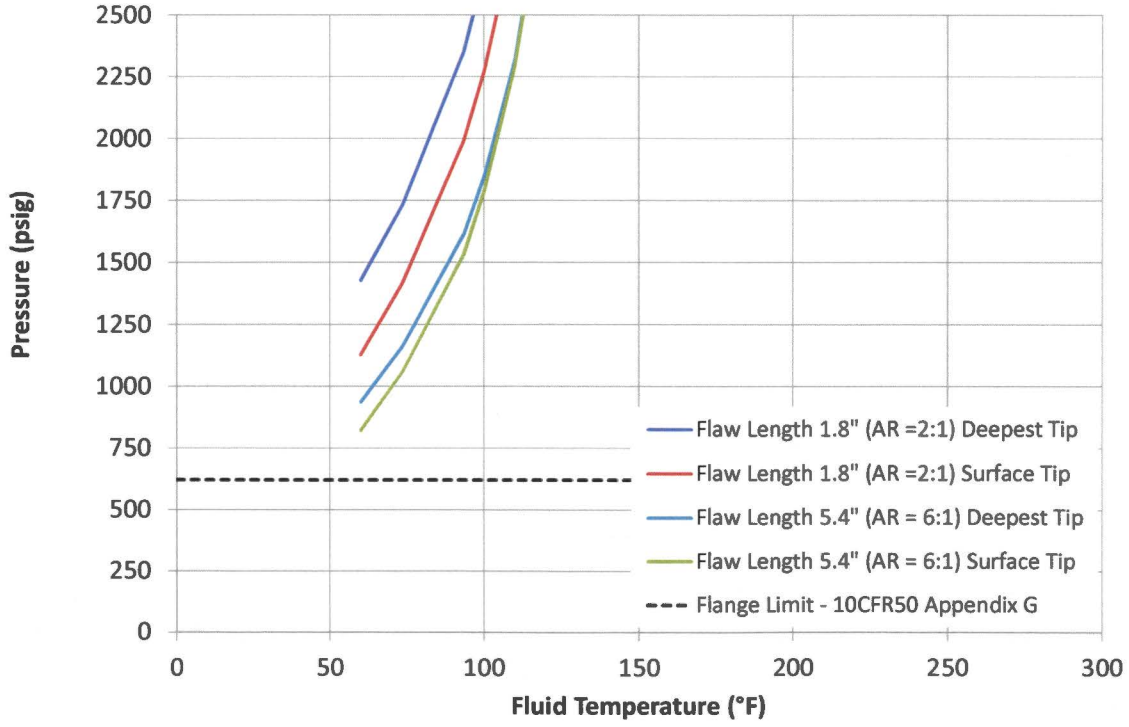

Figure 5-3 Outlet Nozzle Cooldown P-T Limit Curves with Flaw Depth of 0.9 Inch (ART = 21°F)

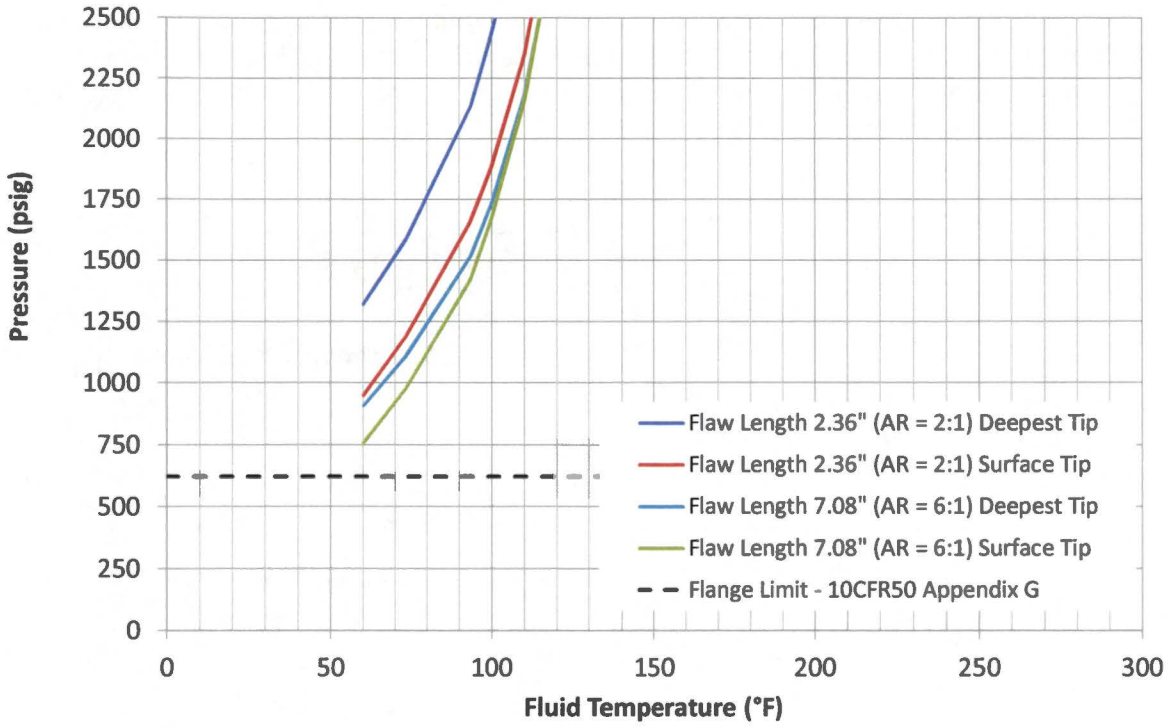

Figure 5-4 Outlet Nozzle Cooldown P-T Limit Curves with Flaw Depth of 1.18 Inch (ART = 21°F)

Based on the results shown in Figure 5-1 through Figure 5-4, the outlet nozzle with a 1.18 inch flaw depth (flaw size of 0.5 inch into the LAS), with a 7.08 inch flaw length (aspect ratio of 6:1) for the surface tip (cladding to LAS forging interface) is the limiting flaw case using the generic ART = 21°F. Similarly, for the inlet nozzle, the limiting nozzle P-T limits using the generic ART = 21°F is for the flaw depth = 0.75 inch (flaw size of 0.5 inch into the LAS), with flaw length = 4.5 inch (aspect ratio = 6:1) for the deepest tip of the postulated flaw.

Therefore, it was concluded that the 0.5-inch flaw size into the low alloy steel is more limiting than the 0.05-inch small flaw size for both the inlet and outlet nozzle. Because, the larger flaw (flaw size of 0.5 inch into the LAS) is the worst case since it has the greater SIF due to the larger flaw and the greater SIF due to clad induced stress at the LAS surface tip. This conclusion is valid for the various geometries and ART values that are evaluated in Section 5.2. The 0.5-inch flaw size is able to be detected as discussed in Section 2, and is an appropriate flaw size for use in the comparison of the nozzle corner P-T limit with the traditional P-T limit curves. The 0.05-inch small flaw size was investigated for the cladding effects on the low alloy steel at the deepest and surface tips of the crack front; and this particular flaw size was demonstrated to be less limiting than the 0.5-inch flaw into the base metal.

The limiting case identified above (outlet nozzle; surface tip; aspect ratio = 6:1, 0.5-inch flaw in LAS) was assessed for the four different limiting geometries, as discussed in Section 4.1, using the 100°F/hour cooldown transient. These P-T limit curves are shown in Figure 5-5.

Based on Figure 5-5, it is concluded that the Westinghouse 4-loop bounding geometry is appropriate for use in comparison with the traditional NRC approved P-T limit curves. At the lower part of the curve, the CE System-80 curve could be limiting so it is compared with the CE and B&W designed plant NRC approved P-T limit curves.

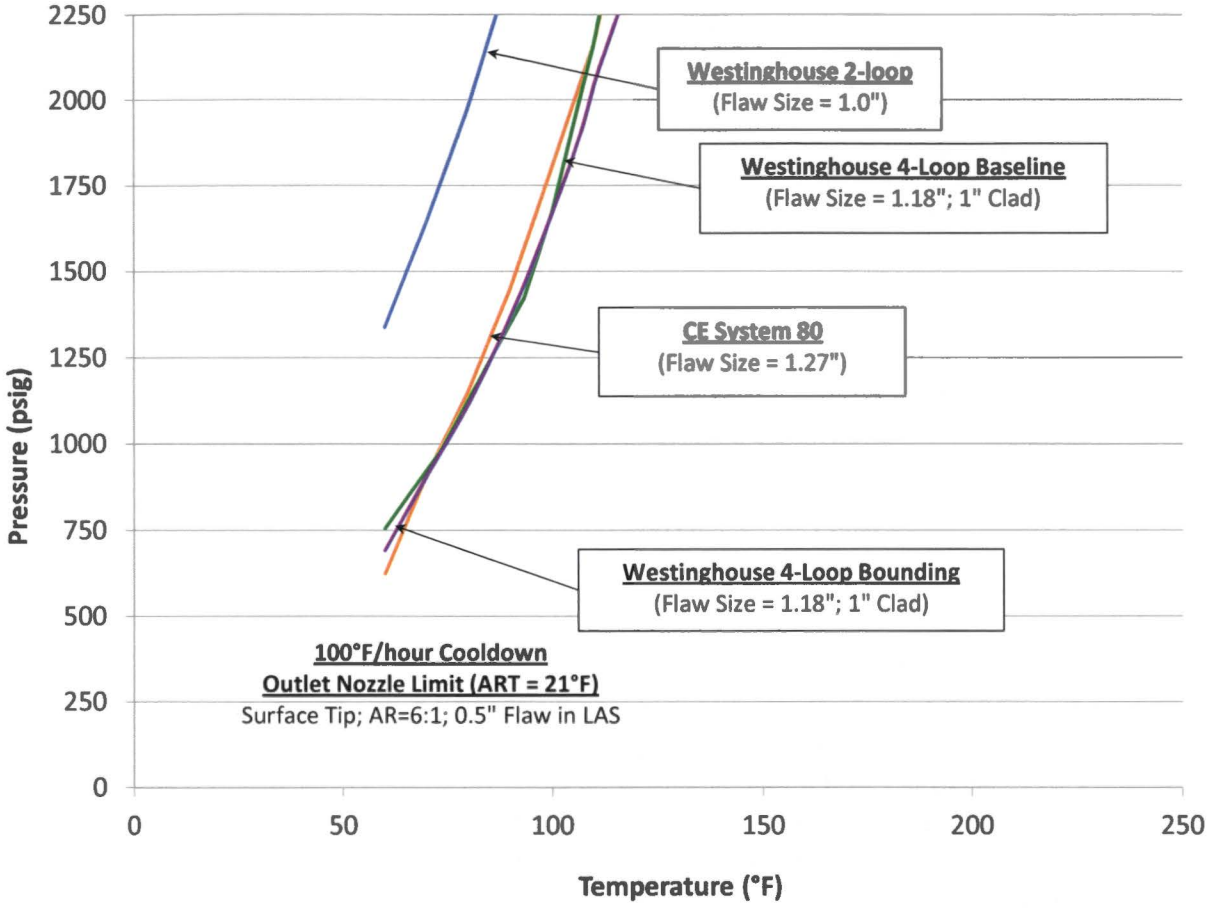

Figure 5-5 Outlet Nozzle 100°F/hour Cooldown P-T Limit Curves Comparing Four Models with Limiting Flaw Geometry/Location (Surface Tip, Aspect Ratio = 6:1, 0.5-Inch Flaw in LAS)

In Section 5.1.2, a larger flaw size comparable to the beltline ¼ thickness is postulated in the nozzle corner using stresses from unflawed FEMs and the ASME Section XI, Appendix G SIF closed form solution.

5.1.2 Generation of Nozzle P-T Limit Curves with Postulated ¼T Beltline Thickness Size Flaw

Postulated nozzle corner flaws with depth on the order of ¼T beltline thickness size flaws were postulated in the outlet nozzle (~2.1 inches for Westinghouse 4-loop and 2.27 inches for CE System-80 models). Unflawed FEM models for three different outlet nozzle designs that bound the fleet were used to generate through-wall pressure and thermal stresses. Due to the large postulated flaw size, the modeled geometries did not need to consider the clad-induced near surface stresses. The SIFs generated for the pressure and thermal gradient were based on the methodology described in ORNL/TM-2010/246 [18]. The stresses taken from the limiting path (1A through 1B) shown in Figure 5-6 from the unflawed model were used to produce P-T nozzle curves for the deepest point of the flaw. A cooldown rate of 100°F/hour from 557°F to 60°F (or 50°F as needed) was used. A few NRC approved P-T limit curves extend to 50°F, so for completeness the cooldown transient was extended to 50°F.

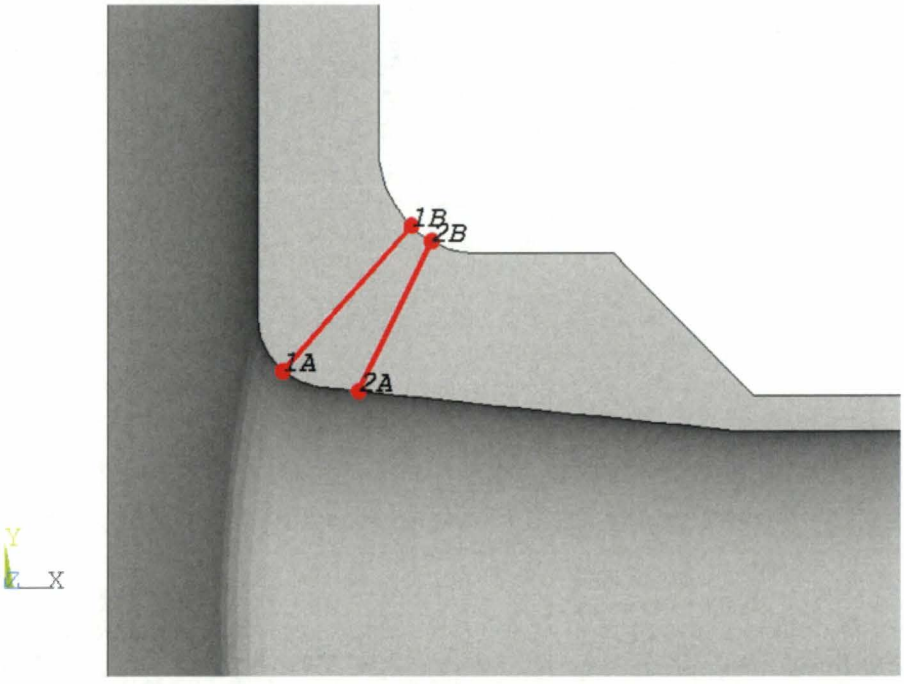

Figure 5-6 Nozzle Corner Stress Path for Pressure and Thermal Stress Analysis (Inlet Nozzle Shown)

The RT_{NDT} = ART = material reference nil-ductility temperature as shown in Section 3.1.2.2 of 43°F (6°C), which is RTT_0 plus 2 σ_I was used. Credit is not taken for better near-surface toughness due to the larger postulated flaw size.

Outlet nozzle P-T curves are generated as shown in Figure 5-7 for the three limiting models. The Westinghouse 2-loop design is not shown since it has much lower SIF (see Figure 4-25 and Figure 4-28) and is not a limiting case for nozzle P-T limits.

Based on Figure 5-7, it is concluded that the Westinghouse 4-loop bounding geometry is appropriate for use in comparison with the traditional NRC approved P-T limit curves. Although,

the CE System-80 curve can be limiting so it is compared with the CE and B&W designed plant NRC approved P-T limit curves.

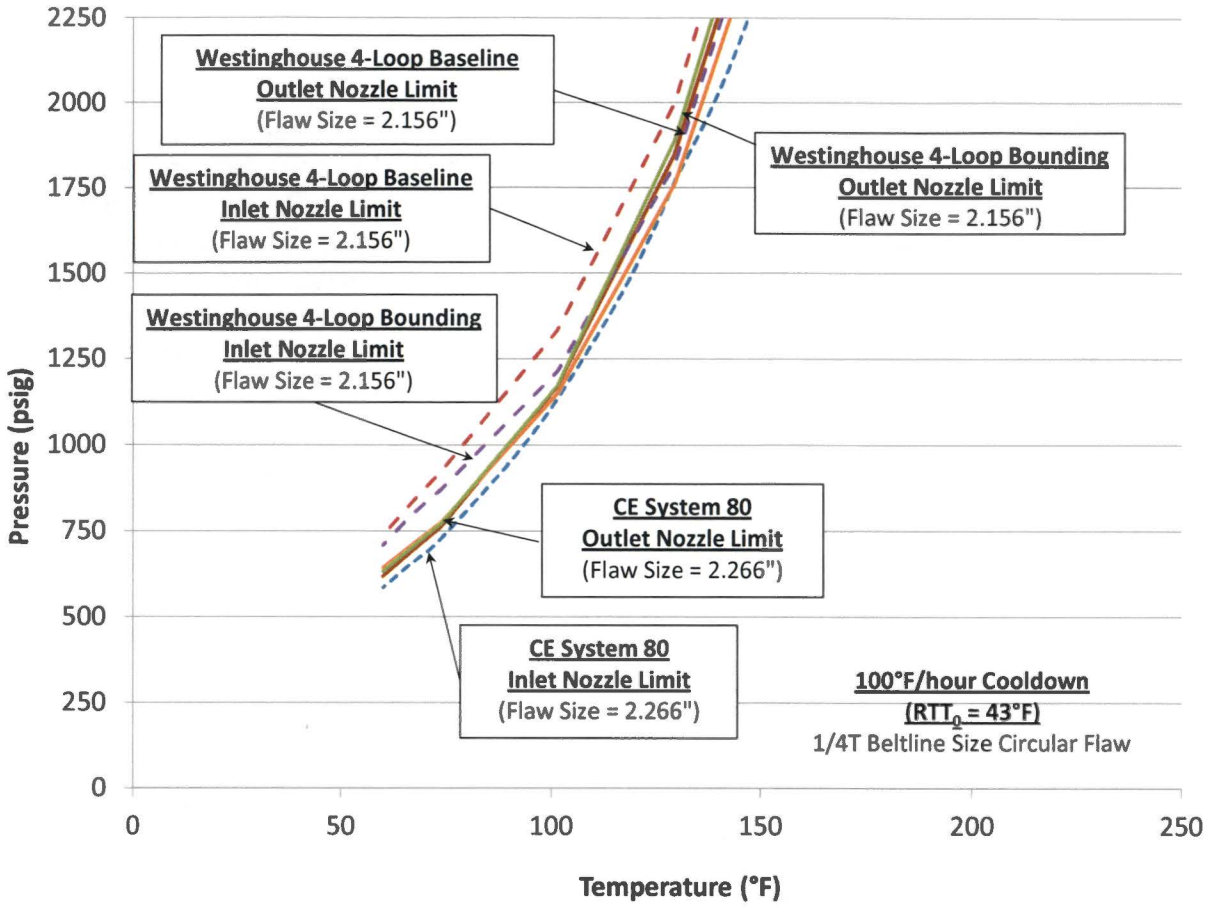

Figure 5-7 Nozzle Cooldown P-T Limit Curves with Flaw Depth Comparable to ¼T Beltline

In Section 5.2, a detailed comparison of the NRC approved plant traditional P-T limit curves is performed with the limiting small flaw nozzle corner P-T limit curve described in Section 5.1.1 and the large flaw postulated from Section 5.1.2.

5.2 COMPARISON OF NOZZLE TO TRADITIONAL NRC APPROVED PRESSURE-TEMPERATURE LIMIT CURVES

All the current U.S. PWR NRC approved Appendix G P-T limit cooldown curves are plotted in Figure 5-8. These NRC approved P-T curves are shown without instrument uncertainty adjustments to readily compare with the unadjusted nozzle curves.

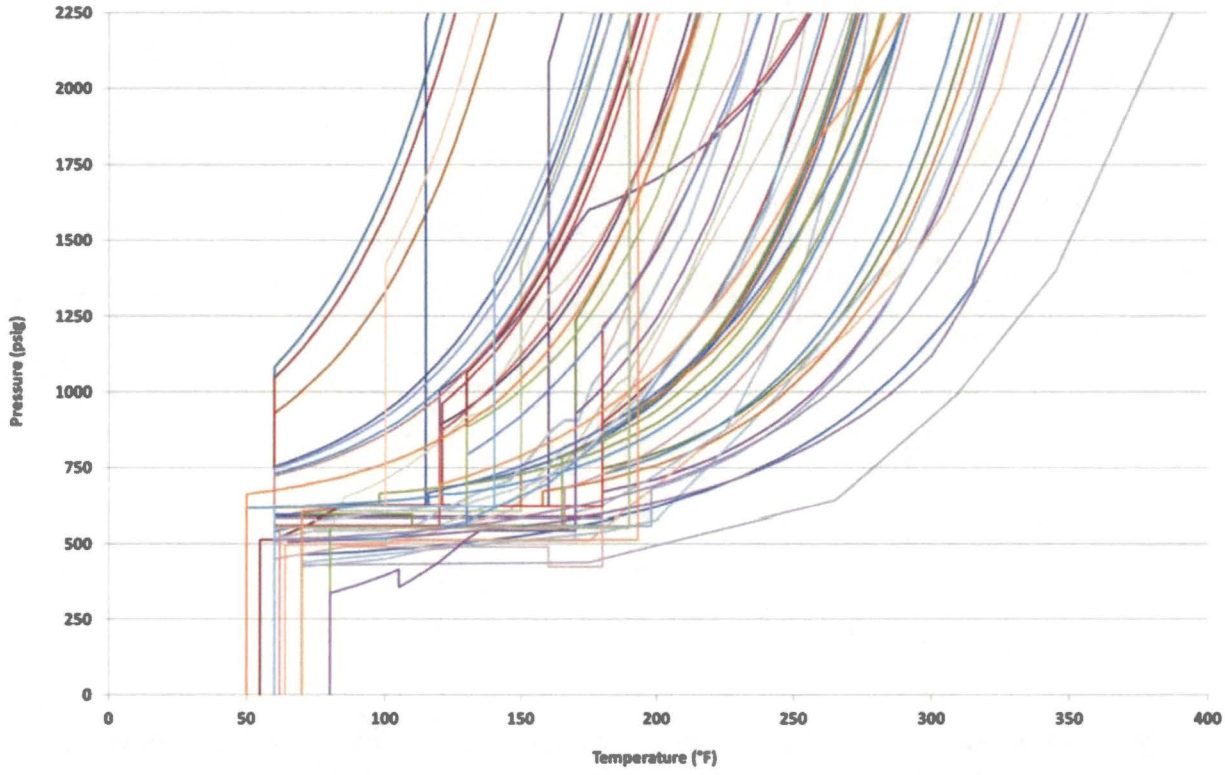

Figure 5-8 U.S. PWR 10 CFR 50 Appendix G NRC Approved P-T Limit Curves

With the exception of eleven plant P-T curves, the NRC approved Appendix G plant cooldown curves bound the limiting 4-loop Westinghouse design nozzle curves (see Figure 5-9) with the generic ART value of 21°F for the explicit small flaw modeled in the nozzles and 43°F for the >2-inch flaw based on the ¼T beltline thickness. The eleven P-T curves that intersect the limiting generic nozzle curves are addressed on a plant-specific basis later in this section, most of which have P-T curves with an exemption to the 10 CFR 50 Appendix G closure flange requirement approved by the NRC. P-T limit curves at low temperatures, i.e. below the closure flange minimum temperature, cannot exceed 20% of the preservice system hydrostatic test pressure. The most limiting, i.e. highest, NRC approved P-T curve is less than 625 psig at temperatures less than the closure flange minimum temperature (except for the plants with an NRC approved flange requirement exemption). The 4-loop Westinghouse design limiting generic nozzle P-T curve remains above 625 psig at 60°F as shown in Figure 5-9.

The traditional beltline P-T limit operating curves are more restrictive than the nozzle P-T limit curves. As plants continue to operate and the P-T curves are updated with higher ART values due to higher fluence, the traditional beltline P-T limit curves will shift downward, moving away from the bounding nozzle corner P-T limit curve increasing the margin. The analyzed nozzle corner P-T limit curves are applicable for a 60-year license and represent the most limiting flaw size and shape postulated from both the inlet and outlet nozzles as discussed in Section 5.1.

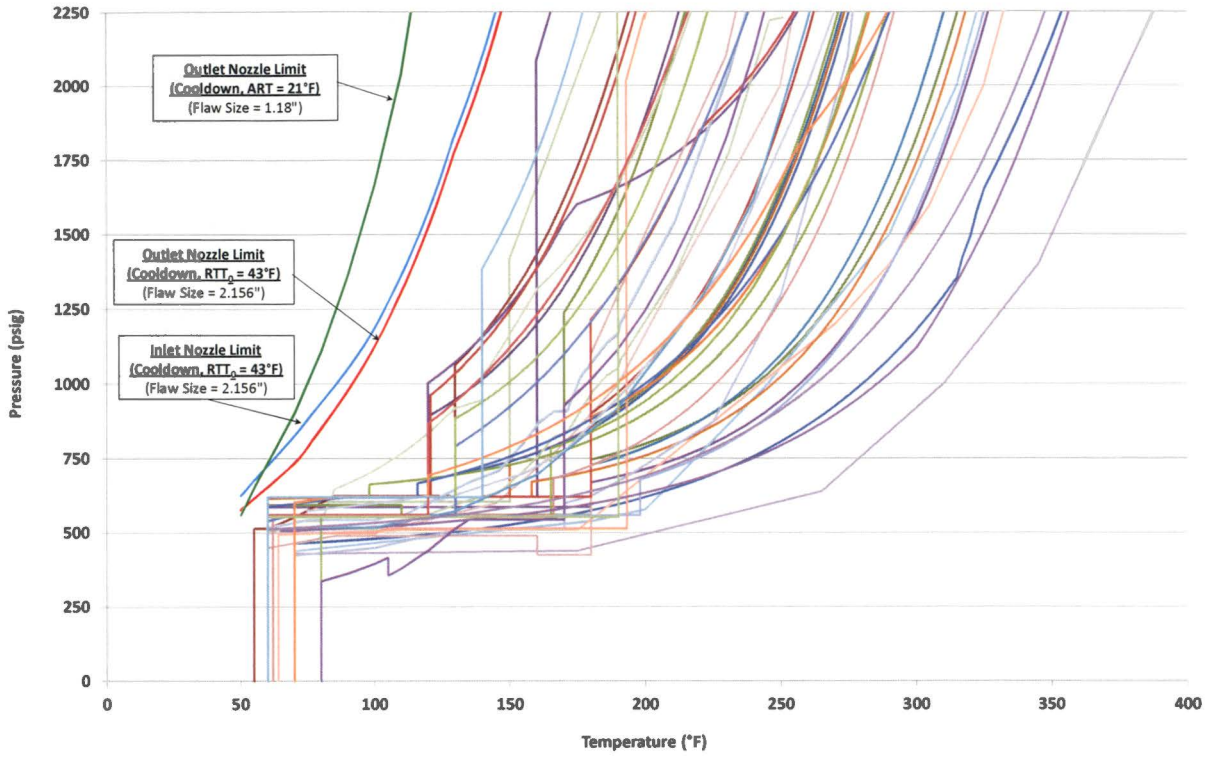

Figure 5-9 Westinghouse 4-Loop Bounding Nozzle P-T Limit Curves Compared to U.S. PWR NRC Approved Appendix G P-T Limit Curves (See Figure 5-10 through Figure 5-14 for Plant-Specific Cases not included)

The U.S. PWR fleet P-T limit curve comparison identified 11 NRC approved P-T curves (identified as A through K) that do not bound the generic bounding nozzle curves (all are of Westinghouse design). Nine of these P-T curves (C through K) use an NRC approved exemption to the 10 CFR 50 Appendix G flange requirement by using a fracture mechanics justification. For plants that have excellent beltline fracture toughness, removal of the flange requirement improves the P-T limit curves significantly. The plant P-T curves which do not bound the generic nozzle curves are evaluated separately in Figure 5-10 through Figure 5-14. Plants C through I had nozzle RT_{NDT} values measured to the requirements of post-1973 ASME Subarticle NB-2300. Since the RT_{NDT} values of these seven plants were all measured to the requirements of NB-2300, the uncertainty associated with an RT_{NDT} estimation method does not affect the RT_{NDT} values shown in Figure 5-10 through Figure 5-13. The limiting RT_{NDT} from the plant nozzles was used instead of the generic RTT_0 value developed in Section 3.5 (and Section 3.1.2.2). For convenience, the plants are grouped together when their highest nozzle RT_{NDT} was the same as shown in Figure 5-11 through Figure 5-13. The plant A nozzle curve had

been calculated in previous work using a very large ¼T nozzle corner flaw. It is compared to the current NRC approved Appendix G P-T curve in Figure 5-14. The plant B traditional P-T limit curves were previously shown to not be impacted by the nozzle curves using the very large ¼T nozzle corner flaw [9]. Since it was shown in Figure 5-7 the CE System 80 nozzles can be more limiting than the Westinghouse 4-loop bounding outlet nozzle limit, the CE System 80 generic nozzles curves are compared to B&W and CE design NRC approved P-T limit curves in Figure 5-15. In every case, the nozzle P-T limit curves are bounded by the traditional NRC approved beltline P-T limit curves.

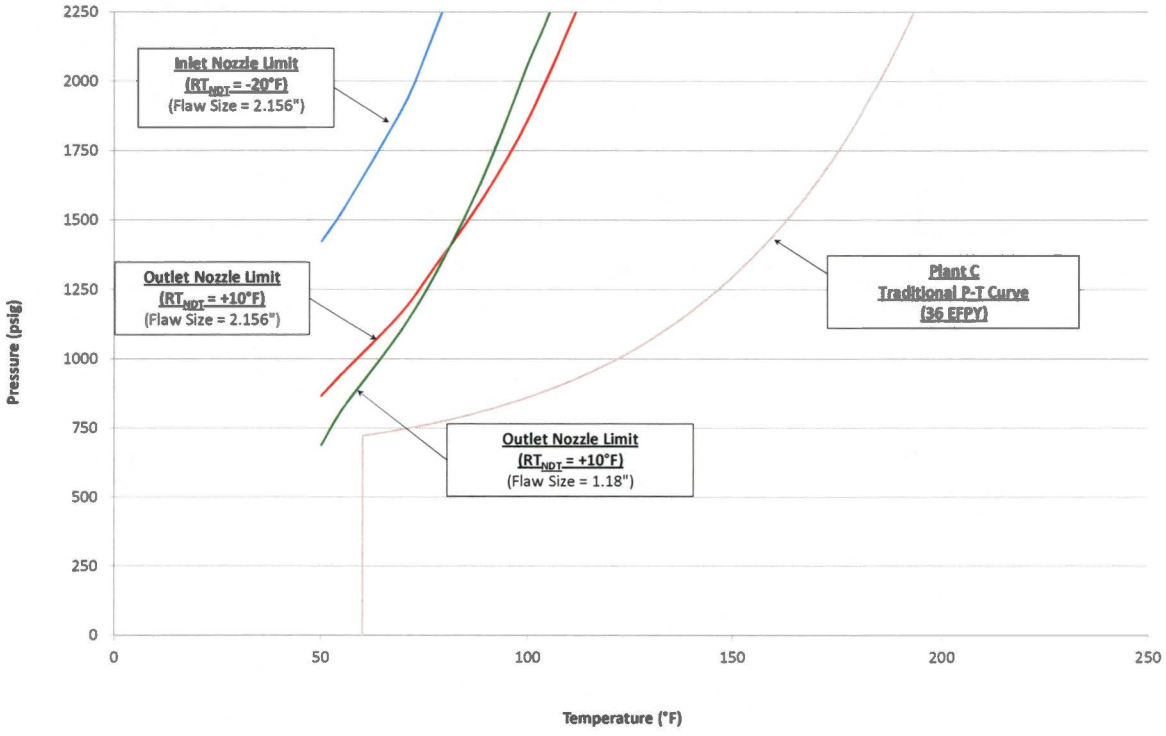

Figure 5-10 Westinghouse 4-Loop Bounding Nozzle P-T Limit Curves Compared to Flange-Exempt Plant C NRC Approved Appendix G P-T Limit Curves

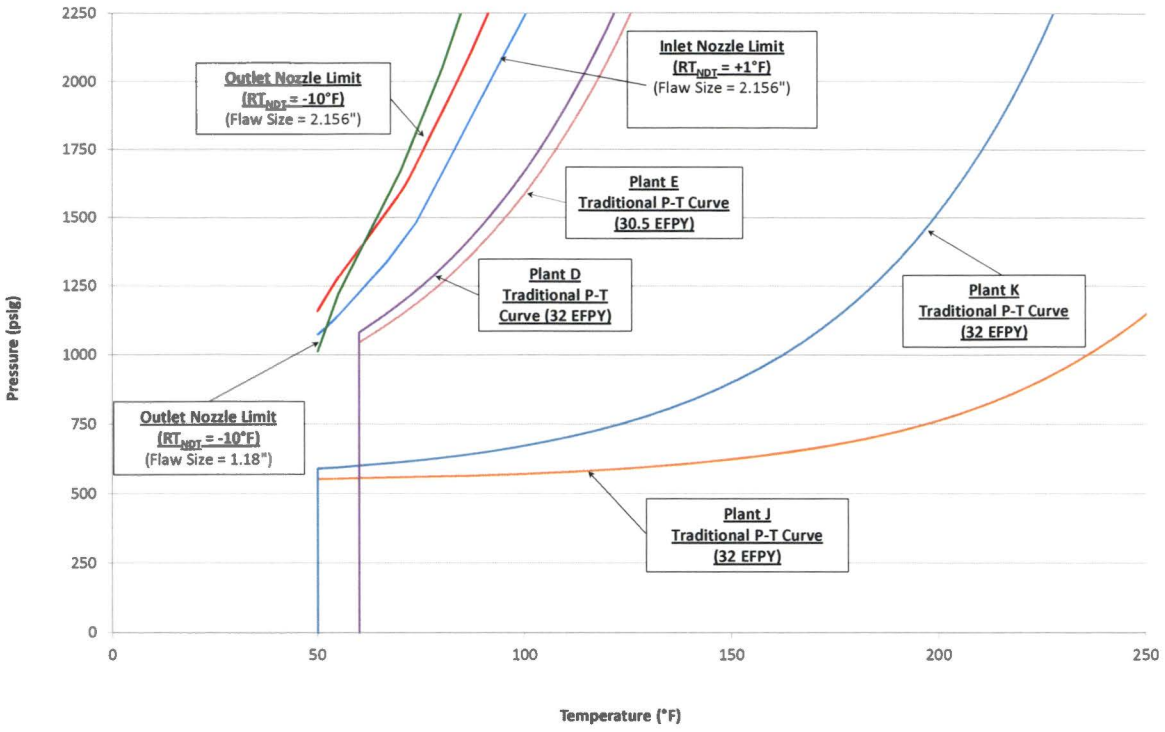

Figure 5-11 Westinghouse 4-Loop Bounding Nozzle P-T Limit Curves Compared to Flange-Exempt Plants D, E, J, and K NRC Approved Appendix G P-T Limit Curves

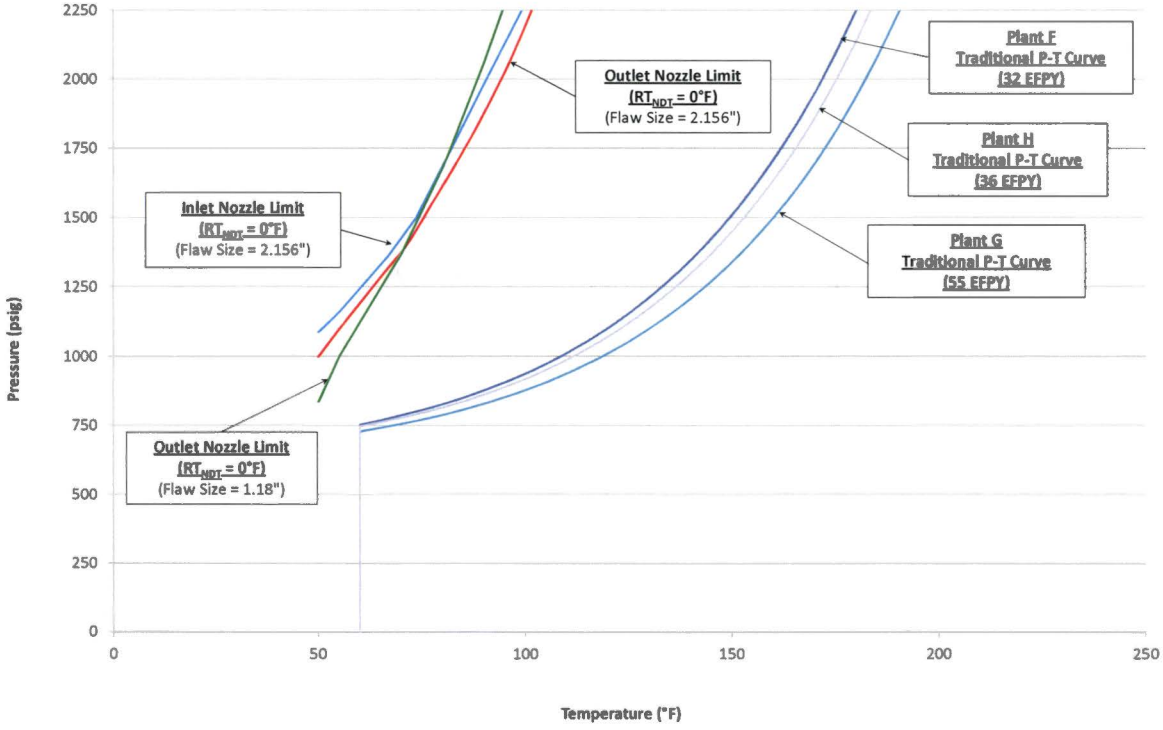

Figure 5-12 Westinghouse 4-Loop Bounding Nozzle P-T Limit Curves Compared to Flange-Exempt Plants F, G and H NRC Approved Appendix G P-T Limit Curves

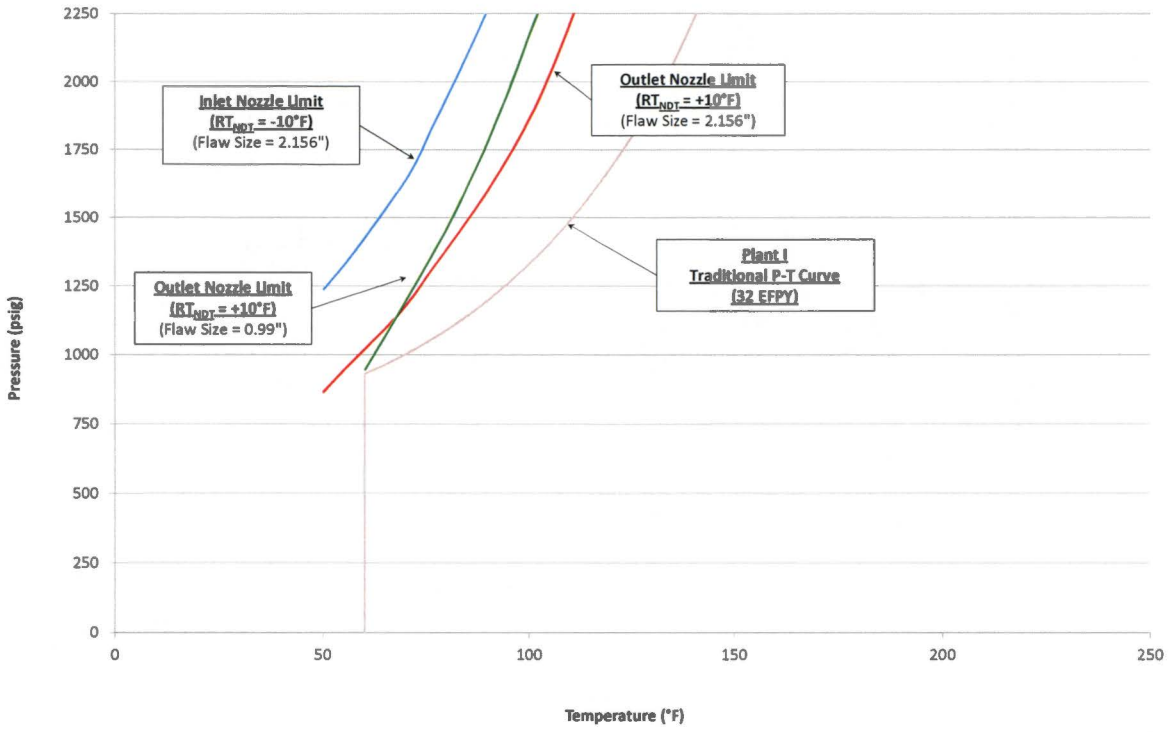

Figure 5-13 Westinghouse 4-Loop Bounding Nozzle P-T Limit Curves Compared to Flange-Exempt Plant I NRC Approved Appendix G P-T Limit Curves

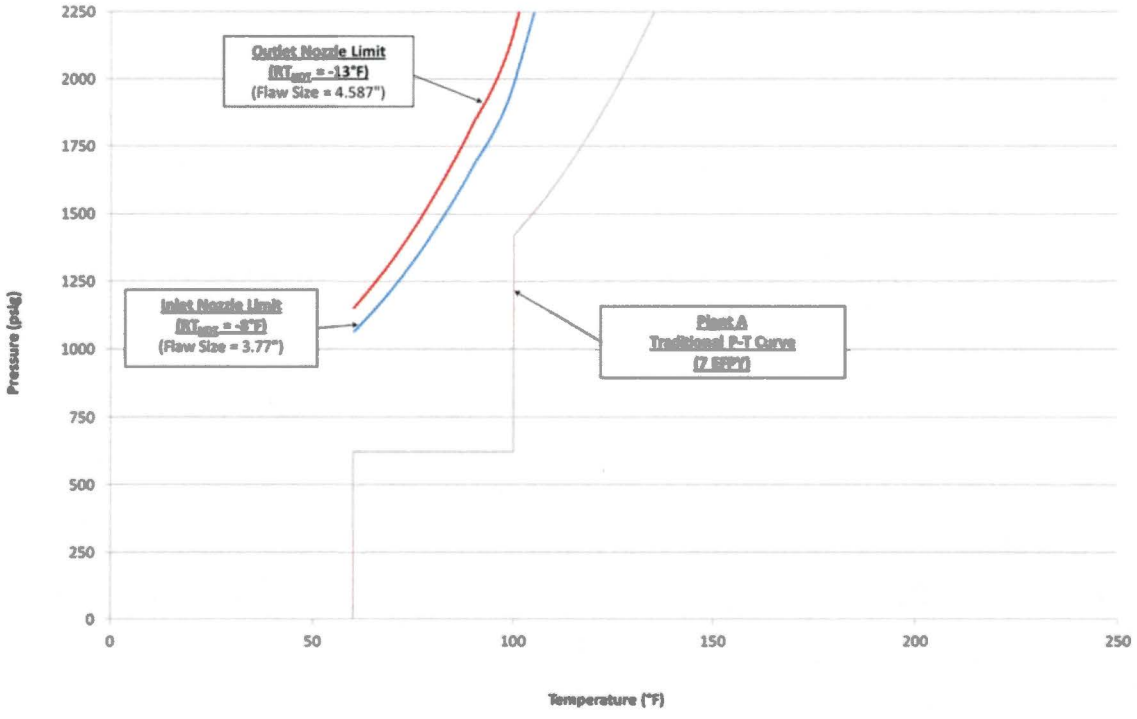

Figure 5-14 Plant-Specific Large Flaw Nozzle P-T Limit Curves Compared to Plant A NRC Approved Appendix G P-T Limit Curves

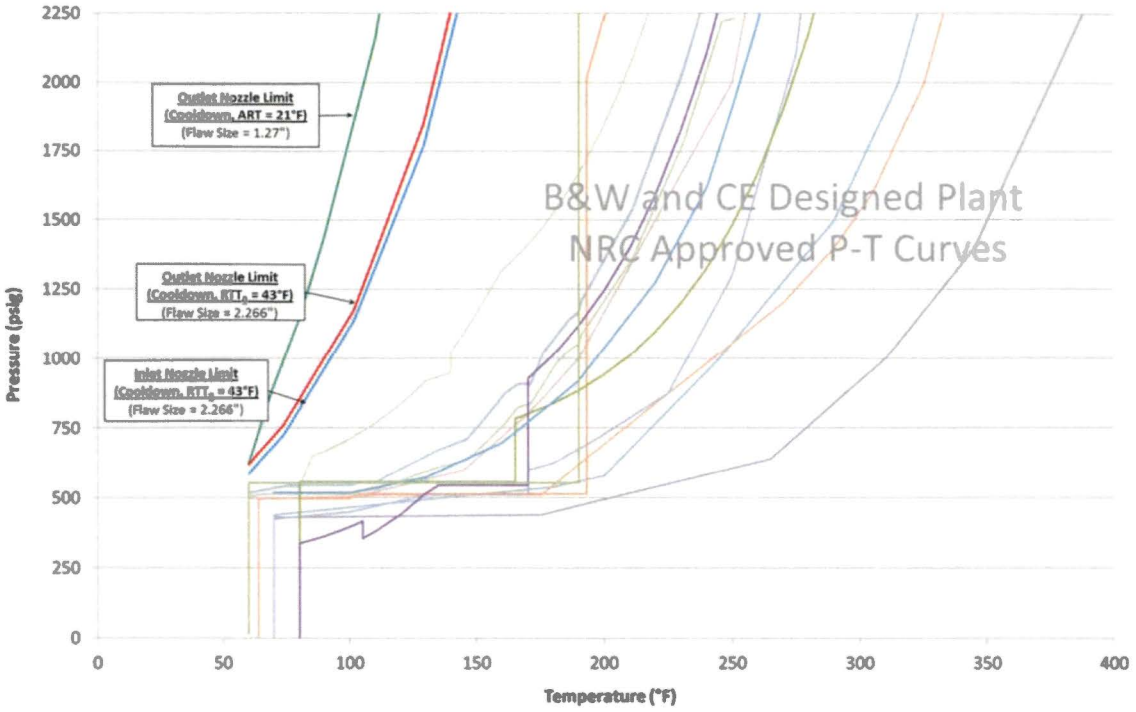

Figure 5-15 CE System-80 Nozzle P-T Limit Curves Compared to U.S. CE and B&W Design NRC Approved Appendix G P-T Limit Curves

6 CONCLUSION

P-T limit curves were developed with postulated ~2.1-inch, 0.5-inch (excluding the clad thickness), and smaller surface breaking flaws in the high stress inlet and outlet nozzle corner regions to assess their impact on the traditional NRC approved 10 CFR 50, Appendix G P-T limit curves.

A generic fracture toughness transition reference temperature was established for the PWR nozzle forgings near the surface at the postulated flaw location as allowed by ASME Section III, Subparagraph NB-2223.2. The fracture toughness was established based on conservative measurements of 22 representative forgings with a margin of two standard deviations, to ensure conservative lower bound toughness using NRC approved ASME Code Case N-629. The near-surface forging toughness was conservatively determined through evaluation of 31 near-surface fracture toughness measurements. The fluence effect at the nozzle corner region was considered and was determined to have an insignificant effect on the fracture toughness at the postulated flaw location.

Detailed three-dimensional finite element analyses of the postulated RPV inlet and outlet nozzles corner flaws for a typical Westinghouse 4-loop plant design were performed to identify the limiting case. The limiting case was then analyzed for four different PWR nozzle designs to ensure that the analyses bound all the U.S. PWR geometrical differences. The analyses were used to generate stresses and stress intensity factors considering typical clad residual stress, pressure, mechanical pipe loads and thermal stress for a bounding normal cooldown transient. In addition, the constraint condition for the postulated flaws was assessed during the cooldown transient. The constraint condition showed additional conservatism in the analysis.

The conservatively-derived generic nozzle Appendix G P-T limit curves were then compared to all the NRC approved P-T limit curves for the U.S. PWR fleet. The results demonstrated that nozzle P-T limit curves were bounded in every case by the NRC approved U.S. PWR P-T limit curves. The nozzle P-T limit curve results are applicable through 60 years of operation. With licensee evaluation of SLR or other operational changes, updated nozzle fluence projections can be compared to the values used in this work for applicability (See Section 3.4.5). If the projected nozzle corner fluence remains less than the screening criterion of 4.28×10^{17} n/cm^2, then this analysis is applicable. If the fluence exceeds the screening criterion, then a shift can be calculated for those nozzles on a plant-specific basis using an NRC approved method; as long as the shift remains below 25°F or the plant-specific nozzle ART values remain below the ART used in this report, then this analysis is applicable. As the plants operate longer, the traditional beltline allowable pressures typically decrease and the curves will become more restrictive; thereby, providing additional margin between the traditional beltline and the nozzle P-T limit curves.

Based on the results of this detailed conservative assessment, the current licensed traditional U.S. PWR P-T limit curves that have used the NRC approved methods of developing P-T limit curves (WCAP-14040-A, Rev. 4, CE NPSD-683-A, Rev. 06 and BAW-10046A, Rev. 2) bound the nozzle P-T limit curves.

7 REFERENCES

1. ASME Boiler and Pressure Vessel Code, 2008 Addenda, Section XI, Division 1, Appendix G "Fracture Toughness Criteria for Protection against Failure," ASME, 2008.

2. U. S. Nuclear Regulatory Commission, Code of Federal Regulations, 10 CFR 50, Appendix G, "Fracture Toughness Requirements," Federal Register, Volume 78, No. 75450, dated December 12, 2013.

3. U. S. Nuclear Regulatory Commission Regulatory Issue Summary 2014-11, "Information on Licensing Applications for Fracture Toughness Requirements for Ferritic Reactor Coolant Pressure Boundary Components," October 2014. [Agencywide Document Access and Management System (ADAMS) Accession Number ML14149A165]

4. U. S. Nuclear Regulatory Commission Letter, "Seabrook Station, Unit No.1 - Issuance of Amendment Re: Revision to the Applicability of the Reactor Coolant System Pressure-Temperature Limits and the Cold Overpressure Protection Setpoints," April 2013. [ADAMS Accession Number ML120820510]

5. U. S. Nuclear Regulatory Commission Letter, "Joseph M. Farley Nuclear Plant, Units 1 and 2, Issuance of Amendments Regarding Technical Specifications Revisions Associated with the Low Temperature Overpressure Protection System and the Pressure and Temperature Limits Report," October 2013. [ADAMS Accession Number ML13249A386]

6. U. S. Nuclear Regulatory Commission Letter, "Indian Point Nuclear Generating Unit No. 2- Issuance of Amendment Re: Pressure-Temperature Limit Curves and Low Temperature Over Pressure Requirements," March 2014. [ADAMS Accession Number ML14045A248]

7. U. S. Nuclear Regulatory Commission Letter, "Indian Point Nuclear Generating Unit No. 3 - Issuance of Amendment Re: Changes to Reactor Vessel Heatup and Cooldown Curves and Low Temperature Overpressure Protection System Requirements," September 2015. [ADAMS Accession Number ML15226A159]

8. U. S. Nuclear Regulatory Commission Letter, "Point Beach Nuclear Plant, Units 1 and 2 – Issuance of Amendment Regarding Change to Technical Specification 5.6.5, Reactor Coolant System (RCS) Pressure And Temperature Limits Report (PTLR)," June 2014. [ADAMS Accession Number ML14126A378]

9. Duke Energy Letter CNS-15-007, "Duke Energy Carolinas, LLC (Duke Energy) Catawba Nuclear Station, Units 1 and 2 Docket Numbers 50-413 and 50-414 License Amendment Request (LAR) for Measurement Uncertainty Recapture (MUR) Power Uprate Response to NRC Requests for Additional Information (RAIs)," January 2015. [ADAMS Accession Number ML15029A417]

10. U. S. Nuclear Regulatory Commission Letter, "McGuire Nuclear Station, Units 1 and 2, Issuance of Amendments Regarding Measurement Uncertainty Recapture Power Uprate," May 2013. [ADAMS Accession Number ML13073A041]

11. U. S. Nuclear Regulatory Commission Letter, "H. B. Robinson Steam Electric Plant, Unit No. 2 - Issuance of Amendment to Revise Reactor Coolant System Pressure and Temperature Limits Applicable for 50 Effective Full Power Years," November 2016. [ADAMS Accession Number ML16285A404]

12. Westinghouse, "Methodology Used to Develop Cold Overpressure Mitigating System Setpoints and RCS Heatup and Cooldown Limit Curves," WCAP-14040-A, Revision 4, May 2004. [ADAMS Accession Number ML050120209]

13. Westinghouse, "Basis for Heatup and Cooldown Limit Curves," WCAP-7924-A, April 1975.

14. Westinghouse, "Development of a RCS Pressure and Temperature Limits Report for the Removal of P-T Limits and LTOP Requirements from the Technical Specifications," Combustion Engineering Owners Group, CE NPSD-683-A, Revision 06, April 2001. [ADAMS Accession Number ML010780017]

15. Framatome (formerly AREVA, Framatome Technologies, and Babcock & Wilcox) "Methods of Compliance with Fracture Toughness and Operational Requirements of 10 CFR 50, Appendix G," B&W Owners Group Document BAW-10046A, Revision 2, June 1986.

16. The Welding Research Council, "PVRC Recommendations on Toughness Requirements for Ferritic Materials," Bulletin WRC-175, August 1972.

17. Framatome (formerly AREVA, Framatome Technologies, and Babcock & Wilcox), "Methods of Compliance with Fracture Toughness and Operational Requirements of 10 CFR 50, Appendix G," B&W Owners Group Document BAW-10046, Revision 4, November 1999. [ADAMS Accession Number ML003673256]

18. Yin, S. and Bass, B., "Stress and Fracture Mechanics Analyses of Boiling Water Reactor and Pressurized Water Reactor Pressure Vessel Nozzles – Revision 1," Oak Ridge National Laboratory, ORNL/TM-2010/246, June 2012. [ADAMS Accession Number ML12181A162]

19. Stevens, G. et al., "Probabilistic Fracture Mechanics Evaluations That Consider Nozzles in the Extended Beltline Region of Reactor Pressure Vessels," Proceedings of the ASME Pressure Vessels and Piping Conference, PVP2015-45065, 2015. [ADAMS Accession Number ML16273A005/ML16273A006]

20. Siegele, Varfolomeyev and Nagel, "Brittle Failure Assessment of a PWR-RPV for Operating Conditions and Loss of Coolant Accident," Journal of Pressure Vessel Technology, Vol. 130, August 2008.

21. U. S. Nuclear Regulatory Commission, "Inservice Inspection Code Case Acceptability, ASME Section XI, Division 1," Regulatory Guide 1.147, Revision 13, June 2003 through Revision 17, August 2014.

22. Bamford, W., et al., "Technical Basis for Elimination of Reactor Vessel Nozzle Inner Radius Inspections," Proceedings of ASME Pressure Vessels and Piping Conference, 2001.

23. BWRVIP-108NP: BWR Vessel and Internals Project, Technical Basis for the Reduction of Inspection Requirements for the Boiling Water Reactor Nozzle-to-Vessel Shell Welds and Nozzle Blend Radii. EPRI, Palo Alto, CA: 2007. 1016123. [ADAMS Accession Number ML073300050]

24. U. S. Nuclear Regulatory Commission Letter from Stuart A. Richards to W. Glenn Warren, Final Safety Evaluation of BWR Owners' Group Alternate Boiling Water Reactor (BWR) Feedwater Nozzle Inspection, "Alternate BWR Feedwater Nozzle Inspection Requirements," GE-NE-523-A71-0594-A, Revision 1, May 2000. [ADAMS Accession Number ML003723265]

25. Long, E., "Material-Orientation Toughness Assessment (MOTA) for the Purposes of Mitigating Branch Technical Position (BTP) 5-3 Uncertainties," PWR Owners Group, PWROG-15003-NP, June 2015. [ADAMS Accession Number ML15268A086]

26. "Application of Master Curve Fracture Toughness Methodology for Ferritic Steels (PWRMRP-01)," PWR Materials Reliability Project (PWRMRP), EPRI Report TR-108390-R1, May 1999 [Publically available at WWW.EPRI.COM].

27. EricksonKirk, M., Bass, B.R., Dickson, T., Pugh, C., Santos, T., Williams, P., "Probabilistic Fracture Mechanics — Models, Parameters, and Uncertainty Treatment Used in FAVOR Version 04.1 (NUREG-1807)," U.S. Nuclear Regulatory Commission, June 2007. [ADAMS Accession Number ML072010411]

28. VanDerSluys, W., et al., "Fracture Toughness Master Curve Development: Application of Master Curve Fracture Toughness Methodology for Ferritic Steels," Welding Research Council Bulletin 458, January 2001.

29. ASME Boiler and Pressure Vessel Code Case, "Use of Fracture Toughness Test Data to Establish Reference Temperature for Pressure Retaining Materials," Section XI, Division 1, Code Case N-629, Approval date: May 7, 1999.

30. U. S. Nuclear Regulatory Commission, 10 Code of Federal Regulations 50.55a, "Codes and Standards," 82 FR 52825, November 15, 2017.

31. Framatome (formerly AREVA, Framatome Technologies and Babcock & Wilcox), "Initial RT_{NDT} of Linde 80 Weld Materials," BAW-2308, Revision 1-A, March 2008. [ADAMS Accession Number ML052070408]

32. U. S. Nuclear Regulatory Commission, Regulatory Issue Summary 2004-04, "Use of Code Cases N-588, N-640, and N-641 in Developing Pressure-Temperature Operating Limits," April 2004. [ADAMS Accession Number ML040920323]

33. Kirk, M., "NRC Review of the Technical Basis for Use of the Master Curve in Evaluation of Reactor Pressure Vessel Integrity," Proceedings of the 28th Water Reactor Safety Meeting, U.S. Nuclear Regulatory Commission, 1999. [ADAMS Accession Number ML010570184 and ML093540004]

34. Yoon, K., et al., "Japanese Fracture Toughness Data Analysis Using Master Curve Method," The 2001 ASME Pressure Vessels and Piping Conference, 2001.

35. Fohl, J., Leitz, Ch., and Anders, D., "Irradiation Experiments in the Testing Nuclear Power Plant VAK," Effects of Radiation on Materials: Eleventh Conference, ASTM STP 782, Brager, H.R., and Perrin, J.S., Eds., ASTM, 1982, pp. 520-527.

36. Framatome (formerly AREVA), "KCB RPV Safety Assessment Assuming 60 Years of Operation," NTCM-G/2009/en/0549, Revision B, 2010.

37. ASTM A-508, "Quenched and Tempered Vacuum-Treated Carbon and Alloy Steel Forgings for Pressure Vessels," ASTM International, 1964.

38. ASME SA-508, "Quenched and Tempered Vacuum-Treated Carbon and Alloy Steel Forgings for Pressure Vessels," ASME Boiler and Pressure Vessel Code, Section II, Part A, ASME International, New York, NY, 1971 and 2007.

39. "Code Comparison Report for Class 1 Nuclear Power Plant Components," STP-NU-051, ASME Standards Technology, January 2012.

40. Joyce, J. A., and Gao. X., "Analysis of Material Inhomogeneity in the European Round Robin Fracture Toughness Data Set," Journal of ASTM International, Vol. 5, No. 9, Paper ID JAI101512, www.astm.org, 2008.

41. ASTM E399, "Standard Test Method for Linear-Elastic Plane-Strain Fracture Toughness K_{IC} of Metallic Materials," ASTM International, 2012.

42. Siegele, D., Keim, E., Nagel, G., "Validation of RT_{T0} for German Reactor Pressure Vessel Steels," Journal of Pressure Vessel Technology, Vol. 130, ASME, 2008.

43. ASTM E1921, "Standard Test Method for Determination of Reference Temperature, T_0, for Ferritic Steels in the Transition Region," ASTM International, 2013.

44. ASTM E185, "Standard Practice for Conducting Surveillance Tests for Light-Water Cooled Nuclear Power Reactor Vessels," ASTM, 1982.

45. Joyce, J. A. and Tregoning, R. L., "Development of the T_0 Reference Temperature from Precracked Charpy Specimens," Engineering Fracture Mechanics 68, Pergamon, Elsevier, 2001, pp. 861-894.

46. U.S. Nuclear Regulatory Commission, "Safety Evaluation by the Office of Nuclear Reactor Regulation Regarding Amendment of the Kewaunee Nuclear Power Plant License to Include the Use of a Master Curve-Based Methodology for Reactor Pressure Vessel Integrity Assessment," May 2001. [ADAMS Accession Number ML011210180]

47. Sokolov, M. A., "Statistical Analysis of the ASME K_{IC} Database," Transactions of the ASME, Vol. 120, February 1998.

48. Marston, T.U., "Flaw Evaluation Procedures, Background and Application of ASME Section XI Appendix A," Report NP-719-SR, EPRI, 1978.

49. Lucon, E., Leenaers, A., Vandermeulen, W., Scibetta, M., "Investigation of Transition Fracture Toughness Variation within the Thickness of Reactor Pressure Vessel Forgings," Journal of ASTM International, Vol. 7, No. 1, 2009.

50. VanDerSluys, W.A., et al., "Fracture Toughness Master Curve Development: Fracture Toughness of Ferritic Steels and ASTM Reference Temperature (T_0)," Welding Research Council Bulletin 457, December 2000.

51. Hein, H., Keim, E., Schnabel, H., Seibert, T., and Gundermann, A., "Final Results from the Crack Initiation and Arrest of Irradiated Steel Materials Project on Fracture Mechanical Assessments of Pre-Irradiated RPV Steels Used in German PWR," Journal of ASTM International, Vol. 6, No. 7, 2009.

52. Chomik E., Liendo, M., and Iorio, A. "Master Curve Testing on 22NiMoCr37 Material," Proceedings of the IAEA Technical Meeting, Master Curve Testing and Results Application, TWG-LMNPP-01/3, 2002, pp. 104.

53. Nagel, G., Blauel, J.G., Siegele, D., "Fracture Toughness Evaluation for a RPV Nozzle using Small Specimens and the Master Curve Approach," Proceedings of the IAEA Technical Meeting, Master Curve Testing and Results Application, TWG-LMNPP-01/3, 2002, p. 238.

54. Hawthorne, J. R. and Hiser, A. L., "Experimental Assessments of Gundremmingen RPV Archive Material for Fluence Rate Effects Studies," NUREG-CR/5201, 1988.

55. Hein, H., Keim, E., Bechler, E., Efsing, P., et al, "CARINA – A Programme for Experimental Investigation of the Irradiation Behaviour of German Reactor Pressure Vessel Materials," VGB PowerTech 5/2013.

56. May, J., Rouden, J., Efsing, P., Valo, M., and Hein, H., "Extended Mechanical Testing of RPV Surveillance Materials Using Reconstitution Technique for Small Sized Specimen to Assist Long Term Operation," Small Specimen Test Techniques: 6th Volume, STP 1576, Sokolov, M. and Lucon, E., Eds., ASTM International, West Conshohocken, PA, 2015.

57. Hein H., Ganswind, J., Gundermann, A., Keim, E. and Schnabel, H., "CARINA: A New Project to Extend the Data Base for Fracture Mechanical Characteristics of Irradiated German RPV Materials at High Neutron Fluences," PVP2009-77035, pp. 613-620, ASME Pressure Vessels and Piping, 2009.

58. Barthelmes, J., Keim, E., Hein, H., and Jong, A., "RPV Testing for Borssele PLEX," Nuclear Engineering Journal, August 2010.

59. Hohe, J., Friedmann, V., Siegele, D., "Reviewing the Master Curve Concept for Evaluation of Brittle Fracture of Ferritic Steels - Application, Limits and Suggestions for Extension," Materialpruefung (2006), 48(5), 239-250.

60. U.S. Nuclear Regulatory Commission, "Radiation Embrittlement of Reactor Vessel Materials," Regulatory Guide 1.99, Revision 2, 1988.

61. Code of Federal Regulations, Title 10, Part 50.61, "Fracture Toughness Requirements for Protection Against Pressurized Thermal Shock Events," 60 Federal Register 65468, Dec. 19, 1995, as amended at 61 FR 39300, July 29, 1996.

62. U.S. Nuclear Regulatory Commission, "Standard Review Plan, Branch Technical Position 5-3," NUREG-0800, Revision 2, March 2007.

63. Lucon, E., et al., "Investigation of Transition Fracture Toughness Variation within the Thickness of Reactor Pressure Vessel Forgings," Journal of ASTM International 7 (2010): JAI102431.

64. U.S. Nuclear Regulatory Commission, "Effect of Welding Conditions on Transformation and Properties of Heat-Affected Zones in LWR Vessel Steels," NUREG/CR-3873, November 1990.

65. ASME Boiler and Pressure Vessel Code, Section III, Division 1, Subarticle NB-2220, "Procedure for Obtaining Test Coupons and Specimens for Quenched and Tempered Material," 2008 Addenda.

66. International Atomic Energy Association Document, TWG-LMNPP-01/3, "Master Curve Testing and Results Application," 2002.

67. U.S. Nuclear Regulatory Commission, "Experimental Assessments of Gundremmingen RPV Archive Material for Fluence Rate Effects Studies," NUREG/CR-5201, October 1988.

68. Nelson, T. D., Bodnar, R. L., and Fielding, J. E., "A Critical Assessment of ASTM A508 Class 2 Steel for Pressure Vessel Applications," 32nd Mechanical Working and Steel Processing, Volume 28, pp. 323-341, 1990.

69. Saillet, S., Rupa, N., and Benhamou, C., "Impact of Large Forging Macrosegregations on the Reactor Pressure Vessel Surveillance Program," SFEN, French Nuclear Energy Society, 2006.

70. U.S. Nuclear Regulatory Commission, "Experimental Results of Tests to Investigate Flaw Behavior of Mechanically Loaded Stainless Steel Clad Plates," NUREG/CR-5785, April 1992.

71. Joint Research Centre, European Commission, "Network for Evaluating Structural Components (NESC-I) Project Overview," EUR 19051EN, 2001.

72. Troyer, G. and Erickson, M., "Empirical Analyses of Effects of the Heat Affected Zone and Post Weld Heat Treatment on Irradiation Embrittlement of Reactor Pressure Vessel Steel," Effects of Radiation on Nuclear Materials: 26th Volume, STP 1572, Mark Kirk and Enrico Lucon, Eds., pp. 163–178, ASTM International, West Conshohocken, PA, 2014

73. Westinghouse, "Summary of RV Vendor Nozzle Clad Practice Survey," PE-RVP-2806, November 1979.

74. U.S. NRC Technical Letter Report TLR-RES/DE/CIB-2013-01, "Evaluation of the Beltline Region for Nuclear Reactor Pressure Vessels," Office of Nuclear Regulatory Research [RES], dated November 14, 2014. [ADAMS Accession Number ML14318A177]

75. U.S. Nuclear Regulatory Commission, "Safety Evaluation Report Related to the License Renewal of Beaver Valley Power Station, Units 1 and 2," NUREG-1929, Vol. 2, October 2009. [ADAMS Accession Number ML093000278]

76. Westinghouse, "Analysis of Capsule Y from Beaver Valley Unit 1 Reactor Vessel Radiation Surveillance Program," WCAP-15571, Supplement 1, Revision 1, April 2008, (Table 2, Note g). [ADAMS Accession Number ML082740205]

77. BWRVIP-173NP-A: BWR Vessel and Internals Project: Evaluation of Chemistry Data for BWR Vessel Nozzle Forging Materials. EPRI, Palo Alto, CA, 2011. 1022835. [ADAMS Accession Number ML12083A268]

78. ASTM E900-15, "Standard Guide for Predicting Radiation-Induced Transition Temperature Shift in Reactor Vessel Materials," ASTM International, 2015.

79. Summer 1975 Addenda of ASME Boiler and Pressure Vessel Code, Section II, "Material specification Part A – Ferrous," dated June 30, 1975.

80. Code of Federal Regulations, 10 CFR Part 50.61a, "Alternate Fracture Toughness Requirements for Protection against Pressurized Thermal Shock Events," U.S. Nuclear Regulatory Commission, Washington D. C., Federal Register, Volume 75, No. 1, dated January 4, 2010, and No. 22 with corrections to part (g) dated February 3, 2010, March 8, 2010, and November 26, 2010.

81. U.S. Nuclear Regulatory Commission Letter, "Catawba Nuclear Station, Units 1 and 2 – Issuance of Amendments Regarding Measurement Uncertainty Recapture Power Uprate (CAC Nos. MF4526 and MF4527)," April 29, 2016. [ADAMS Accession Number ML16081A333]

82. Westinghouse, "Fluence Determination with RAPTOR-M3G and FERRET," WCAP-18124-NP, Revision 0, January 2017. [ADAMS Accession Number ML17030A377]

83. Jones, E., Retzke, K. and Richardson, B., "Evaluation of DPA Profiles in Westinghouse 3-Loop and 4-Loop PWR Inlet and Outlet Nozzle Forgings using the RAMA Fluence Methodology," International Boiling Water Reactor and Pressurized Water Reactor Materials Reliability Conference and Exhibition, EPRI, July 2012.

84. Hall, J., Mays, B., and DeVan, M., "Large SA-508 Class 2 Nozzle Forging Near-Surface Fracture Toughness," ASME Pressure Vessels and Piping Conference, PVP2017-65982, 2017.

85. ASME Boiler and Pressure Vessel Code, Section III, Nuclear Power Plant Components, 1974 without Addenda.

86. ASME Boiler and Pressure Vessel Code, Section II, Part A, "Ferrous Materials," 1974.

87. ASME Boiler and Pressure Vessel Code, Section II, Part D, "Properties," 2013.

88. Swedish Nuclear Power Inspectorate (SKI), Report 2006:23, "Cladding Effects on Structural Integrity of Nuclear Components," ISSN 1104-1374, June 2006.

89. Westinghouse Report, "A Review of Cracking Associated with Weld Deposited Cladding in Operating PWR Plants," WCAP-15338-A, October 2002. [ADAMS Accession Number ML083530289]

90. Bamford, W. and Bush, A., "Effects of Cladding on Fracture Analysis," ASME Pressure Vessels and Piping Conference, PVP Vol. 374, *Fatigue, Environmental Factors, and New Materials*, 1998.

91. Brand M., Hohe, J. and Siegele, D., "Numerical Investigations on the Residual Stress Field in a Cladded Plate Due to the Cladding Process," *Welding In The World*, Vol. 56, 2012.

92. Joint Research Centre, European Commission, "An Investigation of the Transferability of Master Curve Technology to Shallow Flaws Reactor Pressure Vessel Application," NESC-IV Report No. 4 (05), 2005.

93. Kusnick, Joshua, Mark Kirk, B. Richard Bass, Paul Williams, and Terry Dickson, "Effect of Cladding Residual Stress Modeling Technique on Shallow Flaw Stress Intensity Factor in a Reactor Pressure Vessel," ASME Pressure Vessels and Piping Conference, PVP2015-45086, 2015.

94. Wallin, K., "Fracture Toughness of Engineering Materials, Estimation and Application," EMAS Publishing, ISBN: 0-9552994-6-2, 2011, p. 399-415.

95. Siegele, D., Varfolomeyev, I., Hohe, J. and Hardenacke, V., "Integrity Assessment of a German PWR RPV Considering Loss of Constraint," ASME Pressure Vessels and Piping Conference, PVP2010-25615, 2010.

96. Zhoa, L., Tong, J., and Byrne, J., "Stress intensity factor K and the elastic T-stress for corner cracks," International Journal of Fracture 109: 209–225, 2001.

97. Qin, M., et al. "3-Dimensional Finite Element T-Stress Calculation for Reactor Pressure Vessel Nozzle Blend Radius Semi-Elliptical Surface Cracks," ASME Pressure Vessels and Piping Conference, PVP2015-45693, 2015.

98. Merkle, J. G, "An Approximate Method of Elastic-Plastic Fracture Analysis for Nozzle Corner Cracks," Elastic-Plastic Fracture, ASTM STP 668, J. D. Landes, et al. Eds., ASTM International, 1979, 674-702.

99. Scibetta, M., Lucon, E., and Houben, T., "Effect of Cladding on Biaxially Loaded Underclad Part-Through Cracks", Journal of ASTM International, Vol. 7, No. 4, pp. 1-18, 2010.

APPENDIX A

NRC Correspondence

Program Management Office
1000 Westinghouse Drive, Suite 380
Cranberry Township, PA 16066

PWROG-15109-NP, Revision 0
Project Number 99902037

March 27, 2019

OG-19-65

U.S. Nuclear Regulatory Commission
Document Control Desk
11555 Rockville Pike
Rockville, MD 20852

Subject: PWR Owners Group
Transmittal of the Response to Request for Additional Information, RAIs 1-6 Associated with PWROG-15109-NP, Revision 0, "PWR Pressure Vessel Nozzle Appendix G Evaluation," PA-MSC-1091

References:

1. Letter OG-18-55, Transmittal of PWROG-15109-NP, Revision 0, "PWR Pressure Vessel Nozzle Appendix G Evaluation," PA-MSC-1091R4, dated March 5, 2018

2. NRC Acceptance Letter for PWROG-15109-NP, Revision 0, "PWR Pressure Vessel Nozzle Appendix G Evaluation," PA-MSC-1091R4, dated May 9, 2018

3. Email from the NRC (Drake) to the PWROG (Holderbaum), Request for Additional Information, RAIs 1-6, RE: PWROG-15109-NP, Revision 0, "PWR Pressure Vessel Nozzle Appendix G Evaluation," dated October 15, 2018

4 Email from the PWROG (Holderbaum) to the NRC (Drake), DRAFT Response to NRC RAI for the Review of Generic Topical Report No. PWROG-15109-NP, Revision 0, dated January 24, 2019

On March 5, 2018, in accordance with the Nuclear Regulatory Commission (NRC) Topical Report (TR) program for review and acceptance, the Pressurized Water Reactor Owners Group (PWROG) requested formal NRC review and approval of PWROG-15109-NP, Revision 0 for referencing in regulatory actions (Reference 1) The report was accepted for review on May 9, 2018 (Reference 2). The NRC Staff has determined that additional information is needed to complete the review per the email dated October 15, 2018 (Reference 3). Draft responses were provided via email to the NRC on January 24, 2019 (Reference 4).

Enclosure 1 to this letter provides formal responses to NRC RAIs 1-6 (Reference 3) associated with PWROG-15109-NP, Revision 0, "PWR Pressure Vessel Nozzle Appendix G Evaluation".

Correspondence related to this transmittal should be addressed to.

Mr. W Anthony Nowinowski, Executive Director
PWR Owners Group, Program Management Office
Westinghouse Electric Company
1000 Westinghouse Drive
Cranberry Township, PA 16066

If you have any questions, please do not hesitate to contact me at (805) 545-4328 or Mr. W. Anthony Nowinowski, Program Manager of the PWR Owners Group, Program Management Office at (412) 374-6855.

Sincerely yours,

Ken J Schrader

Ken Schrader, COO & Chairman
PWR Owners Group

JKS:am

Enclosure 1: RT-LTR-19-2, Revision 0, RAIs 1-6 Responses for PWROG-15109-NP, Revision 0 (PA-MSC-1091)

cc: PWROG Analysis Committee (Participants of PA-MSC-1091)
PWROG PMO
PWROG Steering and Management Committee
J Drake, US NRC
J. Andrachek, Westinghouse
B. Hall, Westinghouse
B. Mays, Westinghouse
D. Love, Westinghouse

Electronically Approved Records are Authenticated in the Electronic Document Management System

Westinghouse Non-Proprietary Class 3

Westinghouse

To: James P. Molkenthin
cc:

Date: March 22, 2019

From: J. Brian Hall
Ext: 412-342-1916

Our ref: RT-LTR-19-2, Rev. 0

Subject: **Responses to the U.S. NRC Request for Additional Information on PWROG-15109-NP, "PWR Pressure Vessel Nozzle Appendix G Evaluation"**

This letter provides responses to NRC Requests for Additional Information (RAIs) received November 30, 2018 on the subject report If there are any questions, please contact the author

Author: ELECTRONICALLY APPROVED[1]
J. Brian Hall
Churchill Laboratory Services

Verified: ELECTRONICALLY APPROVED[1]
Benjamin E. Mays
Structural Design & Analysis III

Approved ELECTRONICALLY APPROVED[1]
David B. Love, Manager
Churchill Laboratory Services

[1] ***Electronically approved records are authenticated in the electronic document management system.***

Background

By letter dated March 5, 2018 (ADAMS Accession No. ML18067A228), the Pressurized Water Reactor Owners Group (PWROG) submitted to the United States Nuclear Regulatory Commission (NRC) topical report PWROG-15109-NP, "PWR Pressure Vessel Nozzle Appendix G Evaluation," Revision 0 (ADAMS Accession No. ML18067A229, the TR) for review and approval. The TR addresses concerns about the pressure-temperature (P-T) limit curves for inlet or outlet nozzle corners of pressurized water reactors (PWRs) potentially being more limiting than those of the shell (and associated welds) of the traditional beltline region of the reactor pressure vessel (RPV). The PWROG developed the TR to demonstrate that the RPV nozzle corner P-T limits are bounded by the NRC-approved P-T limits of the shell (and associated welds) in the RPV traditional beltline region for PWRs in the United States (U.S.). The NRC staff (the staff) determined it needs additional information to complete its review of the TR.

Regulatory Basis

Title 10 of the Code of Federal Regulations (10 CFR), Part 50, Paragraph 50.60, "Acceptance criteria for fracture prevention measures for light water nuclear power reactors for normal operation," is the governing regulation from which P-T limit curves are developed. 10 CFR 50.60 imposes fracture toughness and material surveillance program requirements, which are set forth in Appendices G, "Fracture Toughness Requirements," and H, "Reactor Vessel Material Surveillance Program Requirements," to 10 CFR Part 50.

Appendix G to 10 CFR Part 50 is the primary basis for a facility's P-T limits for the RPV and requires that P-T limits be at least as conservative as those obtained by analysis methods and safety margins in Appendix G to Section XI of the American Society of Mechanical Engineers Boiler and Pressure Vessel Code (ASME Code). The requirements in Appendix G to 10 CFR Part 50 and the ASME Code, therefore, form the main regulatory bases for the staff's requests for additional (RAIs).

Specifically, Paragraphs III.A and IV.A of Appendix G to 10 CFR Part 50 are the bases for RAIs 1 through 4, which have to do with the TR's approach for establishing a generic fracture toughness for U.S. PWR inlet and outlet nozzle forgings. Paragraph IV.A is the basis for RAI 5, which has to do with the TR's approach for addressing the effects of irradiation on the nozzle forging fracture toughness. Finally, Paragraph IV.A.2.b is the basis for RAI 6, which has to do with the P-T limits developed in the TR.

Request for Additional Information

RAI 1

In Section 3.1.1, "Master Curve Data Search," of the TR, the PWROG described its approach for searching and gathering forging data used to determine the fracture toughness (using the master curve approach) for the nozzle P-T limit evaluation in the TR. Specifically, the PWROG stated the following about the forging data (emphasis added):

- *The data is representative of the materials used to construct U.S. PWR inlet and outlet nozzles.*
- *The intent is to capture all available transition temperature fracture toughness data.*
- *The data and variability bound the fracture toughness data of A-508 Class 2 forgings used in U.S RPVs.*

Based on these statements, it is not clear to the staff the significance of the master curve data presented in the TR and its applicability to U.S. PWR inlet and outlet nozzles. In other words, it's not clear whether, (1) the data bounds the U.S. PWR inlet and outlet nozzles, (2) the data is representative of U.S. PWR inlet and outlet nozzles, or (3) the data is somewhere between bounding and representative of U.S. PWR inlet and outlet nozzles.

Thus, the staff requests the PWROG to discuss and justify the significance of the master curve data presented in the TR and its applicability to U.S. PWR inlet and outlet nozzles.

Response

The data utilized in PWROG-15109-NP is a collection of all available data which is characteristic of the U.S. PWR inlet and outlet nozzles and includes additional data which conservatively represents the U.S. PWR inlet and outlet nozzles. Thus, certain aspects of the master curve data set (and the materials analysed therein) are "representative" of the U.S. PWR inlet and outlet nozzles, while the use of the data set as a whole is "bounding". As a result, the data set is considered to be conservatively representative of the U.S. PWR inlet and outlet nozzles.

The term "representative" is utilized to indicate a similarity in material specification. The forging heats from which master curve data was gathered are representative of the nozzle forgings due to the similarity of the alloy specifications and timeframe of manufacture. Further details on the specific similarities between the materials considered in the master curve data set and U.S. PWR inlet and outlet nozzles are described in PWROG-15109-NP Section 3.1.1 paragraphs 2 and 3, PWROG-15109-NP Subsection 3.1.2 paragraph 1, and the responses to RAIs 2 and 3 following.

As presented in the last two sentences at the bottom of page 3-8, the resulting $RTT_0 + 2\sigma$ is bounding at the mean + 2σ level or better. The inclusion of data from irradiated materials, data based on K_{Ic} data, data from a material with RT_{NDT} greater than 60°F, and data from a large diversity of relevant forgings as evidenced by the large σ value, ensures that the established $RTT_0 + 2\sigma$ is conservative (or

"bounding"). In other words, if the $RTT_0 + 2\sigma$ were calculated for the actual unirradiated U.S. PWR inlet and outlet nozzle materials using K_{Jc}, that $RTT_0 + 2\sigma$ value is expected to be lower than the $RTT_0 + 2\sigma$ value utilized in PWROG-15109-NP.

RAI 2

Table 3-1, "Specification for A-508 Class Type Forgings," of the TR shows a comparison of the chemical composition and mechanical properties of the 22NiMoCr37 forging to those used in U.S. PWR RPV nozzles, A-508 Class 2 or SA-508 Class 2. In Section 3.1.1 of the TR, the PWROG stated that it included two other forging alloys, SFVQ2A and 20NiMoCr26, in the master curve data used in the TR. However, Table 3-1 of the TR does not include the chemical composition and mechanical properties of the other two alloys. Additionally, chemical composition is only one variable affecting the final properties of a material. The material processing (e g., thermomechanical processing, product form thickness, melting/refining process) directly impacts the performance of an alloy. The TR did not discuss/address the processing of the alternate alloys (i.e., 22NiMoCr37, 20NiMoCr26, and SFVQ2A) or its potential impact on mechanical performance, relative to the alloys used in U.S. PWR RPV nozzles.

Thus, the staff requests the following:

a) Provide the chemical composition and mechanical properties of the SFVQ2A and 20NiMoCr26 forgings used in the master curve data.
b) Given that more than just chemistry affects the final properties of a material, provide the technical basis justifying that the alternate alloys (i.e., 22NiMoCr37, 20NiMoCr26, and SFVQ2A) are equivalent/representative to the U.S. alloys from a materials perspective (e.g., thermomechanical processing, product form thickness, melting/refining process) and warrant being included in the master curve data set.

Response

a) The mechanical properties of the SFVQ2A forging included in the evaluation reported a yield stress of 489 MPa (70.9 ksi) and ultimate stress of 637 MPa (92.4 ksi) with a product thickness of 6.3 inches and is considered a SA-508 class 2 forging in [1]. The chemistry for the specific forging is not reported, but it is considered the same alloy per [1] and the specification is almost identical as shown in Table 1 from [2]. The measured chemical composition and mechanical properties for the 20NiMoCr26 forging included in the evaluation are shown in Table 1 as taken from [3].

Table 1 Specifications for A-508 Class 2 Type Forgings

	Chemical Composition									Mechanical		
Specification	C %	Mn %	P %	S %	Si %	Ni %	Cr %	Mo %	V %	Yield ksi	Tensile ksi	Elong. %
22NiMoCr37	0.17-0 25	0.50-1 00	0.025 max	0 025 max	0 35 max	0 60-1 00	0 30-0 50	0 50-0 80	0.05 max	57 min	81-102	19 min
JIS G3204 1988 SFVQ 2A [2]	0 27 max	0 50-1 00	0 030 max	0 030 max	0 40 max	0 50-1 00	0 25-0 45	0 55-0 70	0 05 max	50 min	80-106	16 min
Forging GEB-2 at 1/4T Location [3] (20NiMoCr26)	0.24	0.71	0.015	0.018	0 21	0.79	0 37	0.67	0 031	68[a]	90[a]	40[a]
ASTM A-508-64 Class 2	0.27 max	0 50-0 80	0 025 max	0.025 max	0 15-0 35	0 50-0.90	0 25-0 45	0.55-0 70	0.05 max	50 min	80 min	18 min
SA-508 Class 2 (1971)	0 27 max	0.50-0.90	0.025 max	0.025 max	0 15-0 35	0 50-0 90	0 25-0 45	0 55-0 70	0 05 max	50 min	80 min	18 min
SA-508 Grade 2 Class 1 (2007)	0.27 max	0 50-1 00	0.025 max	0.025 max	0 40 max	0 50-1.00	0 25-0 45	0.55-0 70	0.05 max	50 min	80-105	18 min

Note for Table 1.
(a) Average value measured at the one-quarter thickness (1/4T) location.

b) Each of these forgings was quenched and tempered steel for pressure vessels. The mechanical property requirements are similar including % elongation indicating a similar heat treatment was used to produce the required properties. The master curve data was produced from specimens taken from thick section forgings (6.5" to 11") except for the GEB-2, 20NiMoCr26, forging was thinner at 4.7 inches. It is noted that while the GEB-2 forging is thinner, it is also nuclear pressure vessel material meeting the SA-508 Class 2 requirements, and the consideration of this forging within the dataset is conservative (increases the average RTT_0). Most of the test specimens were taken from actual nuclear reactor pressure vessel forgings. Reference [4] provides discussion of reactor pressure vessel steels around the world, with particular emphasis on 22NiMoCr37 and A508 Class 2, and concludes that "Little basic difference in steel type exists among the vessels of reactors now operating throughout the world."

RAI 3

In Section 3.1.2, "Results from Master Curve Data Search," of the TR, the PWROG stated that the range of the nil-ductility reference temperature (RT_{NDT}) values of the 22 forgings used for the master curve development is higher than those generally observed in U.S. PWR nozzle forgings per the criteria in NB-2300 of Section III of ASME Code, which typically fall between -34 °C and -12 °C. The staff noted that the majority of the data presented in Table 3-2, "All Available Master Curve Data on A-508 Class 2 Type Forgings," of the TR is forgings from foreign countries, not A-508, Class 2 used in U.S RPVs.

To independently assess the master curve data presented in the TR and its applicability to U.S. PWR nozzle forgings, the staff requests the PWROG to provide the data and a description of the evaluation performed to support the statement in Section 3.1.2, regarding RT_{NDT} values generally observed in U.S. PWR nozzle forgings per the NB-2300 criteria. The description should discuss the source of the data and the number of data points.

Response

Some U.S. plant nozzle forgings were procured from overseas suppliers; although many were from suppliers located in the U.S. Table 2 summarizes NB-2300 compliant measured RT_{NDT} values for U.S. PWR nozzles developed from a review of original Certified Material Test Reports (CMTRs). "NB-2300 compliant" means that drop-weight nil-ductility temperature (NDT or T_{NDT}) was measured and Charpy impact energy and lateral expansion data exist for specimens oriented normal to the primary working direction at temperatures appropriate for determination of RT_{NDT} per NB-2300 (e.g., NDT+60°F if the material is T_{NDT} limited). Table 2 is not intended to be a complete list of all U.S. PWR nozzle RT_{NDT} values, but contains those readily available and are representative. The data from Table 2 comes from three different forging suppliers which were the suppliers of approximately half of the U.S. PWR nozzle forgings. NB-2300 compliant RT_{NDT} values were not available in the reviewed CMTRs from the other nozzle forging suppliers. The average is -10.5°F (-23.6°C), which is lower than the average of the reported RT_{NDT} values from PWROG-15109-NP Table 3-2 (-11°C) demonstrating the material used to develop the T_0 used in the topical report is not as tough as the U.S. nozzle material on average.

Table 2 NB-2300 Compliant Unirradiated Nozzle RT_{NDT} Values from U.S. PWR Operating Fleet CMTRs

RT_{NDT}		Number of Occurrences
°C	°F	
-46	-50	1
-40	-40	3
-34	-30	7
-29	-20	36
-23	-10	46
-18	0	22
-12	10	14
-7	20	2

RAI 4

In Section 3.2, "Surface Effect," of the TR, the PWROG discussed improved fracture toughness exhibited near the surface of the material. The PWROG analyzed measured transition temperatures from 24 sets of longitudinal (LT) specimens and seven sets of transverse (TL) specimens. Table 3-3 "Summary of Transition Shifts for LT and TL Specimens" summarizes the fracture toughness improvement exhibited near the surface of the material based on the LT and TL specimens. In addition, the PWROG states "that data without a reported orientation was considered with the LT data," but did not justify why it was appropriate to do so. Thus, the staff requests the following:

a) *Justify that it is appropriate or conservative to consider data without a reported orientation as LT data.*

b) *Discuss the number of data without a reported orientation and justify that their impact to near-surface toughness improvement, including their average and standard deviation, is appropriate or conservative.*

Response

The 10 B&W forgings, the Westinghouse Four-Loop Inlet Nozzle, Westinghouse Four-Loop Outlet Nozzle #1, and Westinghouse Four-Loop Outlet Nozzle #2 certified material test reports are dated 1969 and 1970. Since testing of TL specimens was not required until after the issuance of the Summer 1972 Addenda of the 1971 Edition of the ASME Boiler & Pressure Vessel Code Section III, forgings produced prior to 1972 were likely tested in the strong direction. Thus, the inclusion of these forgings in the LT dataset is appropriate. The orientation was also not reported for the BethForge forging ID, BethForge forging OD, Forging M1, Forging I, and the French forging. However, as described below, inclusion of the unknown orientation forgings with the known LT data is conservative.

Table 3 shows the breakdown of the LT dataset measured transition temperature surface shift between those with a reported LT orientation and those with an assumed LT orientation as described above. The addition of the assumed LT orientation data biases the average shift value in the more conservative direction than the known LT orientation data alone. Thus, using the shift and standard deviation values in PWROG-15109-NP (36.5°F and 28.9°F, respectively) results in a more conservative Adjusted Reference Temperature (ART) compared to the ART value which would be determined using the shift and standard deviation values for the known LT or TL data alone.

Table 3 Summary of Transition Temperature Shifts for the LT Dataset Specimens

	Known LT	Assumed LT
Average Shift (°F)	44 7	33.8
Standard Deviation (°F)	32 7	28.1
Number of Data Sets Studied	6	18

RAI 5

In Section 3.4, "Neutron Embrittlement," of the TR, the PWROG cited NRC Technical Letter Report TLR-RES/DE/CIB-2013-01, "Evaluation of the Beltline Region for Nuclear Reactor Pressure Vessels," Office of Nuclear Regulatory Research [RES], dated November 14, 2014 (ADAMS Accession No. ML14318A177), as a basis for not considering the shift due to irradiation for RPV materials for which the predicted shift in RT_{NDT} (ΔRT_{NDT}) is less than 25 degrees Fahrenheit (°F). The PWROG applied the recommendation in TLR-RES/DE/CIB-2013-01 by not including a shift due to irradiation in its determination of the adjusted reference temperature (ART) in Section 3.5, "Adjusted Reference Temperature," of the TR. Rather the PWROG used the TLR-RES/DE/CIB-2013-01 recommendation in conjunction with Regulatory Guide 1.99, Revision 2, to establish a fluence threshold below which a ΔRT_{NDT} of 25°F is not predicted to occur. The staff notes that the recommendation in TLR-RES/DE/CIB-2013-01 does not provide sufficient justification for neglecting embrittlement if ΔRT_{NDT} is less than 25 °F. Therefore, the staff requests to either:

a) Justify the recommendation in TLR-RES/DE/CIB-2013-01 that the embrittlement shift due to irradiation can be neglected if it is less than 25 °F.

b) Otherwise, revise the P-T limit evaluation in the TR to include the embrittlement shift in accordance with Appendix G to 10 CFR Part 50. Revisions should include, but are not limited to, the determination of ART and the plant-specific P-T limit comparisons in Section 5.2, "Comparison of Nozzle Traditional NRC Approved Pressure-Temperature Limit Curves," of the TR.

Response

Introduction

The Staff's supporting technical basis for their recommendation in TLR-RES/DE/CIB-2013-01 [5] that the embrittlement shift due to irradiation can be neglected if it is less than 25 °F is contained in Section 3 of the TLR. Additional technical justification is provided herein which supports the recommendation in the TLR. The technical justification includes a discussion of the uncertainties associated with the prediction of ΔRT_{NDT} and a comparison of the 25°F threshold value with the 1 x 10^{17} n/cm^2 (E > 1 MeV) threshold value discussed in Regulatory Issue Summary (RIS) 2014-11 [6]. Additionally, justification using 10CFR50, Appendix G [7] and past NRC-approved precedent regarding its use are also provided to confirm that the use of this threshold value is consistent with the requirements of 10CFR50, Appendix G. The PWROG is only interested in applying this TLR recommendation in regions of the reactor vessel not adjacent to the core where the fluence is relatively low.

Technical Justification

To assess the effects of neutron radiation on a component at a specific fluence, a prediction model, also referred to as an embrittlement trend curve (ETC), must be used. Prediction models are based on empirical data with varying amounts of mechanistic understanding included. The empirical data consists of 30 ft-lb index temperature shift measurements (ΔT_{30}) from Charpy V-notch specimens irradiated in light-water reactor (LWR) surveillance program capsules. There is significant scatter in ΔT_{30} because Charpy V-notch testing has inherent scatter as evidenced by the 95% repeatability and reproducibility limits for Charpy testing provided in Section 12 of ASTM E23-18 [8]. Additionally, to determine ΔT_{30}, the Charpy data must be plotted and fit with a curve. The accepted fit for Charpy energy data is the hyperbolic tangent (tanh) curve. Figures 24 and 25 of NUREG/CR-5913 [9] provide sample mean tanh curves and 95% confidence tanh curves for unirradiated and irradiated Charpy V-notch impact energy versus temperature results for two welds. The uncertainty around the mean tanh curve fit at 30 ft-lbs (41 J) at a 95% confidence level is approximately ±12°F. It is important to note that these test results included between 56 and 84 Charpy test specimens, whereas a standard surveillance capsule (which is utilized to provide the majority of irradiated Charpy ΔT_{30} data) contains between 8 and 15 Charpy specimens. Thus, the uncertainty on surveillance capsule data is expected to be higher than that reported in Reference [9]. Since both unirradiated and irradiated tanh fits must be made to determine the neutron radiation damage shift, the uncertainties for each fit must be combined. Combining the unirradiated tanh fit uncertainty with the irradiated tanh fit uncertainty using an uncertainty of 12°F for each fit using the square root of the sum of the squares (SRSS) method, results in an uncertainty of approximately 17°F. Reference [10] provides an additional study of the uncertainty in the evaluation of ΔT at impact energy level of 56 J (41 ft-lbs), including the effect of the number of specimens utilized. This study found a maximum recorded discrepancy between embrittlement shifts for the same material of 36°F (20°C) when varying numbers of specimens (between 8 and 64) were tested.

The uncertainties discussed above only consider the ΔT_{30} measurement (which is assumed to be equal to ΔRT_{NDT}). These uncertainties do not include the uncertainty in the ability of a prediction model to predict ΔRT_{NDT} accurately. Table 4 shows the uncertainty terms for various prediction models (ETCs). Since these models are based on empirical data, the uncertainty terms should implicitly include both the measurement uncertainty and the inaccuracy in the embrittlement model prediction. However, the models are subject to the limitations of the data available, fit technique, and mechanistic insight.

Table 4 Uncertainty in ΔRT_{NDT} for Various Embrittlement Prediction Models

Prediction Model	Weld Standard Deviation (°F)	Forging Standard Deviation (°F)
Reg Guide 1.99, Rev. 2 [11] (assuming no credible capsule data)	28	17
10CFR50 61a [12]	18 6 for Cu ≤ 0 072 wt. % 26 4 for Cu > 0 072 wt. %	18 6 for Cu ≤ 0.072 wt. % 19 6 for Cu > 0.072 wt. %
ASTM E900-15 [13] (assuming ΔRT_{NDT} = 25°F)	22.3	21 2

Figure 6 of TLR-RES/DE/CIB-2013-01 shows the scatter of surveillance program Charpy shift measurements and, based on data shown in Figure 6 of Section 3.3, TLR-RES/DE/CIB-2013-01 determines a standard deviation value of 23°F with a fluence less than 2 x 10^{17} n/cm^2 (E > 1 MeV). The 23°F value does not take into account the effect of chemistry, but chemistry is taken into account in the above Table 4. Figure 1 in this RAI response shows measured ΔT_{30} data from tested surveillance capsules with Regulatory Guide 1.99, Revision 2 predicted shifts less than or equal to 25°F and fluences less than or equal to 4.28 x 10^{17} n/cm^2 (E > 1.0 MeV) consistent with the threshold value developed in PWROG-15109-NP. The data was taken from the database used to develop the ASTM E900 prediction model and includes welds, plates, and forgings [14]. The standard deviation of this data is 18.6°F, which is consistent with the uncertainties of the various prediction models in the above Table 4.

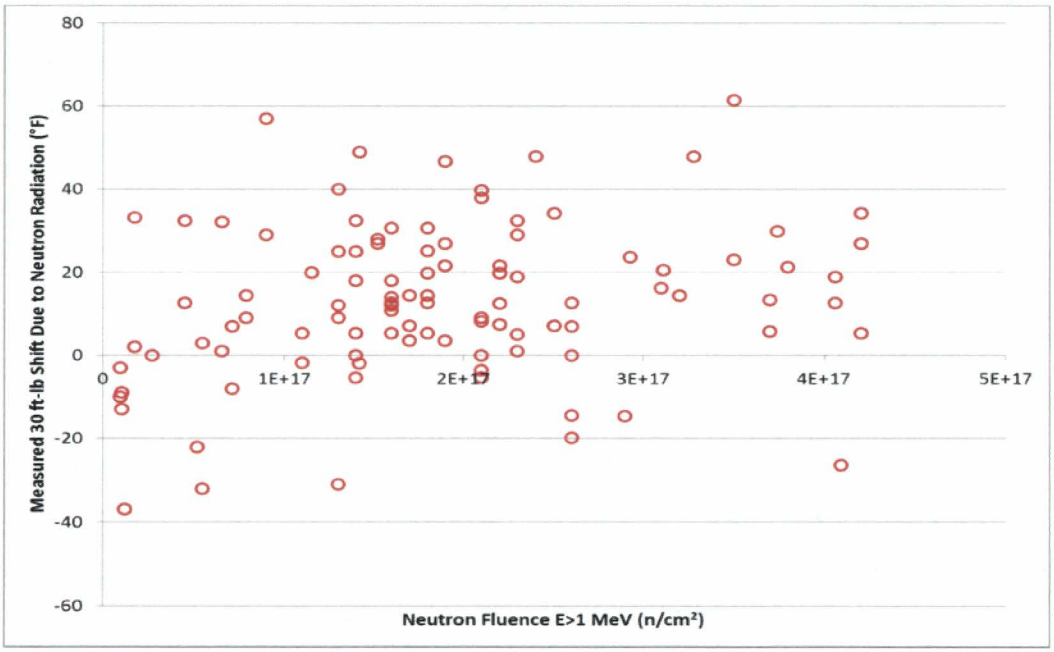

Figure 1 Measured Surveillance Capsule Material ΔT_{30} with Reg. Guide 1.99, Rev. 2 Predicted Shift < 25°F and Fluence < 4.28 x 10^{17} n/cm^2 (E > 1 MeV)

Based on the above discussion, it is concluded that the measurement of ΔT_{30} neutron radiation damage has an inherent uncertainty; furthermore, neutron radiation damage prediction models also have some degree of uncertainty. In reviewing the magnitude of the uncertainties and the typical levels of neutron irradiation damage in a PWR, it is confirmed that a 25°F shift is a reasonable value, using engineering judgement, above which neutron irradiation damage can be considered to be significant. Shifts less than 25°F are within or only slightly larger than the prediction and measurement uncertainty values and would be considered insignificant relative to the uncertainty.

Furthermore, the use of engineering judgement in establishing a threshold for consideration of significant radiation damage is consistent with current practice as summarized in RIS 2014-11 [6], which established a fluence threshold of 1 x 10^{17} n/cm^2 (E > 1.0 MeV).

To further support the use of a 25°F threshold value, comparisons are made below on the use of the 1 x 10^{17} n/cm^2 threshold reported in RIS 2014-11. The RIS 2014-11 threshold neglects the effect of neutron radiation on the material for fluences less than 1 x 10^{17} n/cm^2. As shown in Tables 5 and 6, embrittlement shifts for fluence values slightly less than 1 x 10^{17} n/cm^2 (E > 1.0 MeV) can be similar to the threshold value of 25°F recommended in TLR-RES/DE/CIB-2013-01. Thus, the use of the 25°F threshold is consistent with the 1 x 10^{17} n/cm^2 threshold. Note that the examples provided in Tables 5 and 6 are chosen to demonstrate varying levels of embrittlement.

Table 5 Example Neutron Damage Predictions with Fluence Greater than 1 x 10^{17} n/cm^2

	Chemistry (wt. %)	Fluence (n/cm^2)	FF[(a)]	CF[(a)]	Predicted Shift[(a)] (°F)
Low Cu, high Ni forging	Cu=0.03, Ni=1.00	1.01 x 10^{17}	0.110	20	2.2
Low Cu, high Ni weld	Cu=0.03, Ni=1.00	1.01 x 10^{17}	0.110	41	4.5
Nozzle forging mean Cu [from PWROG-15109-NP] and mean Ni [15]	Cu=0.0947, Ni=0.777	1.01 x 10^{17}	0.110	62.1	6.9
Nozzle forging mean + 1σ Cu, upper A508Cl2 Ni limit used in PWROG 15109-NP	Cu=0.127, Ni=0.90	1.01 x 10^{17}	0.110	93.0	10.3
Nozzle forging mean Cu [from PWROG-15109-NP] and mean Ni [15]	Cu=0.0947, Ni=0.777	4.28 x 10^{17}	0.269	62.1	16.7
Nozzle forging mean + 1σ Cu, upper A508Cl2 Ni limit used in PWROG 15109-NP	Cu=0.127, Ni=0.90	4.28 x 10^{17}	0.269	93.0	25.0

Note for Table 5:
(a) Fluence factor (FF), chemistry factor (CF), and predicted shift are calculated per Regulatory Guide 1.99, Revision 2 [11].

Table 6 Example Neutron Damage Predictions with Fluence Less than 1 x 10^{17} n/cm^2

	Chemistry (wt. %)	Fluence (n/cm^2)	FF[(a)]	CF[(a)]	Predicted Shift[(a)] (°F)
High Cu, high Ni forging	Cu=0.30, Ni=0.80	0.99 x 10^{17}	0.109	225	24.5
High Cu, high Ni forging	Cu=0.28, Ni=1.00	0.99 x 10^{17}	0.109	233	25.4
No chemistry information available[(b)]	Cu=0.35, Ni=1.00	0.99 x 10^{17}	0.109	272	29.6

Notes for Table 6 are contained on the following page.

Notes for Table 6

(a) Fluence factor (FF), chemistry factor (CF), and predicted shift are calculated per Regulatory Guide 1.99, Revision 2 [11]

(b) Regulatory Guide 1.99, Revision 2 [11] indicates "If there is no information available, 0.35% copper and 1.0% nickel should be assumed."

With respect to the PWROG report, there are a number of factors that affect the predicted neutron damage at a nozzle corner. The largest of these are fluence and the Cu and Ni wt. % values. In PWROG-15109-NP, each of these variables are addressed in a conservative manner:

- The majority of nozzle fluence values were calculated using two-dimensional and one-dimensional discrete ordinates models, which have been shown to give more conservative fluence estimates when compared to the more accurate three-dimensional models in the nozzle region. Additionally, fluence values are calculated at locations closer to the core (typically calculated at the lowest extent of the nozzle forging) compared to the location of the postulated flaws evaluated in the report,
- The Cu content used was equal to the mean value plus 1σ, and
- The Ni content used was equal to the material specification maximum value.

It is unlikely for all of these factors to be simultaneously at their maximum values for the same nozzle. However, to consider this likelihood, mean values are often used with uncertainties that have been combined using two times the SRSS, as described in Regulatory Guide 1.99, Revision 2 [11], or uncertainties are combined using the Monte Carlo method. Therefore, since the Cu and Ni wt. % and fluence values were not treated in this manner, the approach utilized in PWROG-15109-NP regarding the assessment of the effect of neutron damage is conservative.

In summary, a predicted shift of less than 25°F is not significantly different than the predicted uncertainty level on that value, a 25°F shift threshold is based on similar engineering judgement used to determine the 1 x 10^{17} n/cm^2 fluence threshold value discussed in RIS 2014-11, and the overall bounding treatment of uncertainties utilized in PWROG-15109-NP is conservative. Thus, neglecting shifts less than 25°F, consistent with the approach taken in PWROG-15109-NP, is technically appropriate, and it is consistent with the recommendation made in TLR-RES/DE/CIB-2013-01.

10CFR50 Appendix G and Precedent

As discussed in the previous section, the 1 x 10^{17} n/cm^2 (E > 1.0 MeV) fluence threshold is technically similar to, and consistent with, an embrittlement shift threshold of 25°F. Furthermore, the implementation of the 25°F shift threshold for reactor vessel materials not adjacent to the core does not represent a change in ideology or a departure from the current regulations, as discussed in the following paragraphs.

10CFR50, Appendix G II.D.(ii) [7] states, "*For the reactor vessel beltline materials, RT_{NDT} must account for the effects* [emphasis added] *of neutron radiation.*" Similarly, 10CFR50, Appendix G II.F

states, " *and adjacent regions of the reactor vessel that are predicted to experience sufficient neutron radiation damage* [emphasis added] *to be considered in the selection of the most limiting material with regard to radiation damage* [emphasis added]." These provisions from 10CFR50, Appendix G require that RT_{NDT} must account for the effects of neutron radiation and sufficient neutron damage. The effect of neutrons depends on temperature, the Cu and Ni wt. % values, and potentially other factors to a lesser extent. Thus, establishing a threshold which is based on the effects of radiation damage (i.e. 25°F shift), is entirely consistent with the regulation in 10CFR50, Appendix G.

Consistent with the requirements of 10CFR50, Appendix G and as discussed in RIS 2014-11, Section 3.4 of PWROG-15109-NP considers the effects of irradiation to the nozzle region. Since the Cu wt. % value in the nozzle forgings is not high, the effect of neutrons on embrittlement damage is not significant even above a fluence of 1×10^{17} n/cm^2. Thus, the effects of radiation are considered, but they are deemed to be negligible.

Furthermore, the utilization of the 25°F shift threshold value recommended in TLR-RES/DE/CIB/-2013-01 was previously used in a license amendment for H. B. Robinson Unit 2. In the Safety Evaluation (SE) [16], the Staff specifically cited the use of TLR-RES/DE/CIB-2013-01 and the 25°F shift recommendation:

> *The licensee re-calculated the ART values for the HBRSEP2 inlet and outlet nozzles and determined the P-T limits curves for the nozzles by postulating a one quarter thickness (defined as the section thickness forty-five degrees from the nozzle corner) inside-surface flaw at the rounded corner (blend radius) of the nozzles. A salient element of the nozzle ART calculations is that if the delta RT_{NDT} (ΔRT_{NDT}) value is less than 25 degrees Fahrenheit (°F), embrittlement effects may be neglected, based on the results of the studies in NRC technical report TLR-RES/DE/CIB-2013-01, "Evaluation of the Beltline Region for Nuclear Reactor Pressure Vessels," dated November 14, 2014 (Reference 22). The NRC staff performed the nozzle ART calculations and confirmed the licensee's values reported in Table 8 of the September 14, 2016, supplemental analysis.*

The foregoing discussion in the SE acknowledges that the use of TLR-RES/DE/CIB-2013-01 is a "salient element" and is appropriate. Therefore, there is precedent regarding the NRC approval of the use of this position, which was also specifically applied to nozzle forging materials.

Summary

PWROG-15109-NP used the NRC's 25°F shift threshold value from TLR-RES/DE/CIB-2013-01 and neglected the effects of neutron radiation due to embrittlement shifts less than this value. The technical basis for the 25°F threshold recommendation is documented in Section 3 of TLR-RES/DE/CIB-2013-01, and additional technical justification confirming this value is provided. Use of the threshold value is also consistent with the requirements of 10CFR50, Appendix G, which requires that RT_{NDT} account for the effects of neutron radiation and sufficient neutron damage. The use of the 25°F threshold value is reasonable and appropriate, given the prediction and measurement

uncertainty of ΔT_{30}, and it is consistent with shifts calculated for fluence values slightly less than the 1 x 10^{17} n/cm^2 fluence threshold discussed in RIS 2014-11. Furthermore, the approach used in PWROG-15109-NP regarding assessment of the effect of neutron damage is conservative.

RAI 6

In Section 5.2 of the TR, the PWROG selected the limiting nozzle P-T limit curves developed in Sections 5.1.1 and 5.1.2 of the TR and compared them to the NRC-approved P-T limits of the shell (and associated welds) in the RPV traditional beltline region. The PWROG determined that 11 NRC-approved P-T limits of Westinghouse plants (identified in the TR as A through K) do not bound the limiting nozzle P-T limits and evaluated them separately in Figures 5-10 through 5-14 of the TR. For these 11 plants, plant-specific nozzle RT_{NDT} values were used instead of the generic nozzle RT_{TO} value developed in the TR, using the P-T limit methodologies in Sections 4 and 5.1.2 of the TR. One of the modeled flaw sizes, 0.99 inch, shown in Figure 5-13 of the TR is not one of the modeled small flaws developed in Section 4 of the TR and there was no discussion of the P-T limit methodology used for this particular case shown in the figure. The PWROG evaluated the P-T limits of Combustion Engineering, and Babcock & Wilson plants in Figure 5-15 of the TR. The PWROG stated that seven of the 11 plants (plants C through I) had nozzle RT_{NDT} values measured to the requirements of post-1973 NB-2300 of Section III of the ASME Code, but did not identify the methodology used to determine RT_{NDT} for plants J and K. For plant A, the PWROG showed in Figure 5-14 that the RPV shell P-T limit bound the nozzle P-T limits, based on previous work that has been performed on a large 1/4T flaw in the nozzle corner. However, the PWROG did not state whether this nozzle corner evaluation for plant A has been approved by the NRC. For plant B, the PWROG cited a previous NRC-approved evaluation that the RPV shell P-T limits were not impacted by the nozzle P-T limits.

Based on the background above, the staff requests the following to complete its evaluation:

a) Describe and justify the P-T limit methodology used for the postulated flaw size of 0.99 inch in Figure 5-13 of the TR.

Response

For this plant-specific case, the actual design dimension of the cladding (5/8" after machining) was utilized which, with the postulated 0.5" deep low alloy steel flaw, yielded a flaw depth of 0.99" from the wetted surface. This 0.99" flaw was modeled in finite element analysis (FEA) to develop the stress intensity factors using the same methodologies that were used for the other FEA-modeled flaws in PWROG-15109-NP.

b) For plants J and K, explain and justify the method used to determine the initial RT_{NDT} for the inlet and outlet nozzles.

Response

Plants J and K initial RT_{NDT} values for the reactor vessel nozzle forging materials were determined using the Branch Technical Position (BTP) 5-3 paragraph 1.1(3)(b) [5] methodology which was found to be acceptable as-written by the NRC in the relevant closure memorandum [18].

It is also noted that the Plants J and K nozzle P-T limit curves in PWROG-15109-NP Figure 5-11 are at a much higher pressure than the Plants J and K beltline P-T curve. Thus, there is large margin.

c) *For plant A, explain and justify the methodology used to develop the nozzle P-T limits. The explanation and justification shall include the methodology used to determine the initial RT_{NDT} for the inlet and outlet nozzles.*

Response

The relevant information for Plant A was submitted to the NRC in WCAP-18191-NP [19]. This WCAP contains a calculation of nozzle P-T limit curves using the standard 1/4T nozzle corner flaw and the standard ORNL/TM-2010/246 [20] method as presented in WCAP-18191-NP, Appendix B. WCAP-18191-NP also contains details of the determination of the initial RT_{NDT} values for the nozzle forgings. The nozzle P-T limit curves in WCAP-18191-NP correspond to end-of-license, but are conservatively applicable to 7 effective full-power years (EFPY), as in PWROG-15109-NP Figure 5-14, as well.

It is noted that the Plant A nozzle P-T limit curves were calculated using a very large 1/4T nozzle corner flaw and still show significant margin (PWROG-15109-NP Figure 5-14).

d) *The requests in a) through c) above presume that the licensee has provided an acceptable justification for neglecting ΔRT_{NDT} of less than 25 °F for the nozzle P-T limits, as the staff requested in RAI 5(a). If the licensee instead chooses to include embrittlement shift for the nozzle P-T limits, as the staff requested in RAI 5(b), then for nozzle P-T limits that are not bounded by the NRC-approved RPV shell P-T limits, provide the following:*

   i. *A description of the P-T limit methodology used.*
   ii. *The method used to determine initial RT_{NDT}.*
   iii. *Fluence, copper, and nickel values used to determine ΔRT_{NDT}.*
   iv. *Determination of ART.*

Response

The recommendation in TLR-RES/DE/CIB-2013-01 that the embrittlement shift due to irradiation can be neglected if it is predicted to be less than 25 °F is justified in the response to RAI 5.

References

[1] Yoon, K , et.al., "Japanese Fracture Toughness Data Analysis Using Master Curve Method," The 2001 ASME Pressure Vessels and Piping Conference, July 23-26, 2001 - Atlanta, Georgia, USA.

[2] Fran Cverna, "Worldwide Guide to Equivalent Irons and Steels," 5th Edition, ASM International, 2006.

[3] Hawthorne, J.R. and Hiser, A.L., "Experimental Assessments of Gundremmingen RPV Archive Material for Fluence Rate Effects Studies," NUREG/CR-5201, 1988.

[4] K. Suzuki, "Reactor Pressure Vessel Materials," The Japan Steel Works, Ltd., date unknown, available at https://inis.iaea.org/collection/NCLCollectionStore/_Public/30/013/30013703.pdf

[5] U. S. NRC Technical Letter Report TLR-RES/DE/CIB-2013-01, "Evaluation of the Beltline Region for Nuclear Reactor Pressure Vessels," Office of Nuclear Regulatory Research [RES], dated November 14, 2014. *[Agencywide Documents Access and Management System (ADAMS) Accession No. ML14318A177]*

[6] U.S. NRC Regulatory Issue Summary 2014-11, "Information on Licensing Applications for Fracture Toughness Requirements for Ferritic Reactor Coolant Pressure Boundary Components," U.S. Nuclear Regulatory Commission, October 2014. *[ADAMS Accession Number ML14149A165]*

[7] Code of Federal Regulations, 10 CFR Part 50, Appendix G, "Fracture Toughness Requirements," U.S. Nuclear Regulatory Commission, Federal Register, Volume 78, No. 75450, dated December 12, 2013.

[8] ASTM E23-18, "Standard Test Methods for Notched Bar Impact Testing of Metallic Materials," ASTM International, 2018.

[9] NUREG/CR-5913, "Irradiation Effects on Fracture Toughness of Two High-Copper Submerged-Arc Welds, HSSI Series 5," Oak Ridge National Laboratory, 1992.

[10] Brillaud, C., Augendre, H., and Bethmont, M., "Uncertainty Evaluation in Transition Temperature Measurements," *Effects of Radiation on Materials: 17th International Symposium, ASTM STP 1270*, ASTM 1996.

[11] U. S. NRC, Office of Nuclear Regulatory Research, Regulatory Guide 1.99, Revision 2, "Radiation Embrittlement of Reactor Vessel Materials," May 1988. *[ADAMS Accession No. ML003740284]*

[12] Code of Federal Regulations, 10 CFR Part 50.61a, "Alternate Fracture Toughness Requirements for Protection Against Pressurized Thermal Shock Events," 75 Federal Register 72653, November 26, 2010.

[13] ASTM E900-15, "Standard Guide for Predicting Radiation-Induced Transition Temperature Shift in Reactor Vessel Materials," ASTM International, 2015.

[14] Adjunct for E900-15, ADJE090015-EA, Plotter Version R8, ASTM International, 2015.

[15] Eason, E.D., et al., "A Physically Based Correlation of Irradiation-Induced Transition Temperature Shifts for RPV Steels," ORNL/TM-2006/530, Oak Ridge National Laboratory, Oak Ridge, TN, November 2007. *[ADAMS Accession No. ML081000630]*

[16] U.S. NRC Safety Evaluation, "Safety Evaluation by the Office of Nuclear Reactor Regulation Related to Amendment No. 248 to Renewed Facility Operating License No. DPR-23 Duke Energy Progress, LLC, H. B. Robinson Steam Electric Plant, Unit No. 2 Docket No. 50-261," November 2016. *[Enclosure 2 of ADAMS Accession No. ML16285A404]*

[17] U. S. NRC Branch Technical Position 5-3, Revision 2, "Fracture Toughness Requirements," Contained in Chapter 5 of Standard Review Plan for the Review of Safety Analysis Reports for Nuclear Power Plants: LWR Edition, NUREG-0800, March 2007. *[ADAMS Accession No. ML070850035]*

[18] U. S. NRC Memorandum, "Closure Memorandum Supporting the Limited Revision of NUREG-0800 Branch Technical Position 5-3, "Fracture Toughness Requirements"," April 2017. *[ADAMS Accession No. ML16364A285]*

[19] Westinghouse Report WCAP-18191-NP, Revision 0, "Watts Bar Unit 2 Heatup and Cooldown Limit Curves for Normal Operation and Supplemental Reactor Vessel Integrity Evaluations," May 2017. *[ADAMS Accession No. ML17289A327]*

[20] Oak Ridge National Laboratory Report ORNL/TM-2010/246, "Stress and Fracture Mechanics Analyses of Boiling Water Reactor and Pressurized Water Reactor Pressure Vessel Nozzles – Revision 1," June 2012. *[ADAMS Accession No. ML110060164]*